University of Tuscia

Department of Agriculture and Forest Sciences (DAFNE)

Ph.D. Course

Animal and Plant Production Sciences (XXXVI)

High polyphenolic wheat genotypes: a study on the role of anthocyanin and flavonoid biosynthetic pathways in Fusarium Head Blight (FHB) resistance

Scientific-disciplinary sector

Plant pathology – AGRI-05/B

Ph.D. candidate:

Linda Felici

Ph.D coordinator:

Prof.ssa Roberta Bernini

Tutor:

Prof. Giorgio Mariano Balestra

Co-tutors:

Prof. Francesco Sestili

Dr. Sara Francesconi

A.Y. 2023/24

Abstract

Fusarium Head Blight (FHB) is one of the most important diseases of cereals. It is caused by various fungal species, including *F. graminearum* and *F. avenaceum*, which reduce yield and contaminate grains with mycotoxins, such as trichothecenes and enniatins. Pigmented cereals are rich in anthocyanins (phenolic compounds) in the pericarp layer (purple pericarp genotypes) or in the aleurone layer (blue aleurone genotypes). It is known that various polyphenols play a role in counteracting abiotic and biotic stress in plants and in reducing the accumulation of mycotoxins. The three-year research activity was structured into four main parts. The aim of the first part was to study, through *in vitro* tests, the antimicrobial and anti-mycotoxigenic activity of four anthocyanin compounds (cyanidin, delphinidin, cyanidin 3-*O*-glucoside or C3G, and delphinidin 3-*O*-glucoside or D3G) using as a model *F. avenaceum*. The results highlighted how the tested compounds lead to a reduction in the production of enniatins from 20-30% (cyanidin and D3G) to 60-80% (delphinidin and C3G). In particular, C3G has a dose-dependent effect: increasing the concentration leads to an increase in biomass and a reduction in enniatins produced. Through differential gene expression analysis, it was highlighted how delphinidin acts by reducing the expression of key genes for the production of enniatins (*ESYN* and *KIVR*) and related to the response to oxidative stress, while treatment with C3G did not result in any difference in expression of the genes considered, suggesting an action at the post-transcriptional level. Additionally, expression of genes related to oxidative stress was also included and the combined effect of C3G and ferulic acid, the most prominent phenolic acid in wheat, were considered. In the second and third part, artificial infection tests with *F. graminearum* were carried out in three durum wheat genotypes: Svevo (susceptible to FHB), DBC-480 (resistant to FHB) and Purple durum (purple pericarp with unknown susceptibility). These genotypes were artificially inoculated with *F. graminearum* spores, in order to evaluate the genotype × infection interaction on parameters describing production traits, metabolite-related traits, and physiological-related traits and correlated them with disease-associated parameters and FHB resistance-associated plant morphological features. The infection affected the difference between the spike temperature and the flag leaf temperature in the resistant and the susceptible control in an opposite way, while the total anthocyanin content (TAC) of the mature spikes was considerably lower in Purple durum subjected to the infection compared to the mock plants, while TAC increased in the infected resistant genotype, suggesting an involvement of flavonoids in the resistance mechanism of DBC-480. The polyphenol biosynthetic pathway was also studied in depth in the three varieties mentioned above in an early phase (2 day post infection, DPI) and a late phase (21 DPI) of the infection, analyzing the expression of key genes and the quantification of the main metabolites. While in the early phase there is a greater activation of the entire pathway in the DBC-480 resistant genotype, in the late phase there is an over-expression of the phenyl-alanine ammonia lyase (*PAL*) and cinnamate-4-hydroxylase (*C4H*) genes in Svevo, and the genes encoding chalcone synthase (CHS) and "purple pericarp MYB 1" (Ppm1) in Purple durum. This last gene encodes a transcription factor essential for the purple coloration of the grains and its activation is confirmed by a greater quantity of anthocyanins accumulated in the late phase by Purple durum in response to the infection, in particular malvidin 3-*O*-glucoside (oenin). In the fourth and last part, the resistance/susceptibility of 5 pigmented genotypes of common wheat was characterized: 3 purple (Vanilnoir, Indigo and Rosso) and 2 blue varieties (Skorpion and Purendo), compared with a susceptible control (Rebelde) and a resistant one (Sumai 3). From the results, Vanilnoir is resistant and Rosso is very susceptible, therefore they are chosen for subsequent transcriptomic analysis. Vanilnoir showed type II resistance, most likely thanks to the reinforcement of cell wall, supported by the upregulation of pathways and function related to the accumulation of lignin and hydroxycinnamic acid amides. The susceptible genotypes showed a growth–defense trade-off unbalanced towards growth, stimulated by the upregulation of cytokines biosynthetic pathway. Noteworthy, flavonoids biosynthesis was boosted in the resistant genotypes compared to the susceptible ones, but in the purple pigmented genotypes it was more stimulated by the infection than in the yellow pigmented lines. More in detail, while in Sumai3 and Rosso the production of flavan-3-ols was favored to the detriment of anthocyanins, in infected Vanilnoir the simultaneous production of anthocyanins and flavones was stimulated, both potentially involved in its resistance mechanism. Furthermore, ten LRR receptor-like protein kinases (LRR-RLKs) were exclusively up-regulated in the FHB-resistant genotypes together with two genes from the MAPK signaling. Further investigation on these genes can provide valuable information about the specific cross-talk between wheat and *F. graminearum*.

Riassunto

La fusariosi della spiga (Fusarium Head Blight o FHB) è una delle più importanti malattie dei cereali. È causata da varie specie fungine, tra cui *F. graminearum* e *F. avenaceum*, che riducono la resa e contaminano le cariossidi con micotossine, come tricoteceni ed enniatine. I cereali pigmentati sono ricchi di antociani (composti fenolici) nel pericarpo (genotipi a pericarpo viola) o nell'aleurone (genotipi ad aleurone blu). È noto che diversi polifenoli svolgono un ruolo nel contrastare lo stress abiotico e biotico delle piante e nel ridurre l'accumulo di micotossine. L'attività di ricerca triennale è stata strutturata in quattro parti principali. Lo scopo della prima parte è stato quello di studiare, attraverso test *in vitro*, la diretta attività antimicrobica e antimicotossigena di quattro composti antocianici (cianidina, delfinidina, cianidina 3-*O*-glucoside o C3G e delfinidina 3-*O*-glucoside o D3G) utilizzando come modello *F. avenaceum*. I risultati hanno evidenziato come i composti testati portino ad una riduzione della produzione di enniatine dal 20-30% (cianidina e D3G) al 60-80% (delfinidina e C3G). In particolare, il C3G ha un effetto dose-dipendente: aumentando la concentrazione si ottiene un aumento della biomassa e una riduzione delle enniatine prodotte. Attraverso l'analisi dell'espressione genica differenziale, è stato evidenziato come la delfinidina agisca riducendo l'espressione di geni chiave per la produzione delle enniatine (*ESYN* e *KIVR*), mentre il trattamento con C3G non ha comportato alcuna differenza di espressione dei geni considerati, suggerendo un'azione a livello post-trascrizionale. Inoltre, è stata inclusa l'analisi dell'espressione di geni legati allo stress ossidativo ed è stato considerato l'effetto combinato di C3G e acido ferulico, l'acido fenolico più abbondante nel frumento. Nella seconda e terza parte, sono stati condotti test di infezione artificiale con *F. graminearum* in tre genotipi di frumento duro: Svevo (sensibile a FHB), DBC-480 (resistente a FHB) e Purple durum (pericarpo viola con suscettibilità sconosciuta). Questi genotipi sono stati inoculati artificialmente con spore di *F. graminearum*, al fine di valutare l'interazione genotipo × infezione sui parametri che descrivono i caratteri di produzione, i caratteri correlati ai metaboliti, i caratteri fisiologici e correlarli con parametri associati alla malattia e parametri morfologici della pianta associati alla resistenza alla fusariosi. L'infezione ha influenzato la differenza tra la temperatura della spiga e la temperatura della foglia a bandiera nel controllo resistente e su quello suscettibile in modo opposto, mentre il contenuto totale di antociani (TAC) delle spighe mature è stato notevolmente più basso in Purple durum sottoposto all'infezione rispetto a quello nelle piante sane, mentre la TAC è aumentata nel genotipo resistente infetto, suggerendo un coinvolgimento dei flavonoidi nel meccanismo di resistenza di DBC-480. Nelle tre varietà sopra citate è stata inoltre studiata approfonditamente la via biosintetica dei polifenoli in una fase precoce (2 days post infection, DPI) ed in una fase tardiva (21 DPI) dell'infezione, analizzando l'espressione di geni chiave e la quantificazione dei principali metaboliti. Mentre nella fase iniziale si è verificata una maggiore attivazione dell'intera via nel genotipo resistente DBC-480, nella fase tardiva si è verificata una sovraespressione della fenil-alanina ammoniaca liasi (*PAL*) e della cinnamato-4-idrossilasi (*C4H*) in Svevo, e dei geni che codificano per la calcone sintasi (CHS) e il "purple pericarp MYB 1" (*Ppm1*) in Purple durum. Quest'ultimo gene codifica un fattore di trascrizione essenziale per la colorazione viola della cariosside e la sua attivazione è stata confermata da una maggiore quantità di antociani accumulati in fase tardiva da Purple durum in risposta all'infezione, in particolare malvidina 3-*O*-glucoside. Nella quarta ed ultima parte, è stata caratterizzata la resistenza/suscettibilità di 5 genotipi pigmentati di frumento tenero: 3 varietà porpora (Vanilnoir, Indigo e Rosso) e 2 blu (Skorpion e Purendo), confrontate con un controllo suscettibile (Rebelde) e uno resistente (Sumai3). I risultati indicano che Vanilnoir è resistente mentre Rosso è molto suscettibile, pertanto sono stati scelti per la successiva analisi trascrittomica. Vanilnoir ha mostrato una resistenza di tipo II, molto probabilmente grazie al rinforzo della parete cellulare, supportato dalla sovraregolazione dei pathway e delle funzioni legate all'accumulo di lignina e delle ammidi degli acidi idrossicinnamici. I genotipi sensibili hanno mostrato un trade-off crescita-difesa sbilanciato verso la crescita, stimolato dalla sovraregolazione della via biosintetica delle citochinine. È interessante notare che la biosintesi dei flavonoidi è stata potenziata nei genotipi resistenti rispetto a quelli suscettibili, ma nei genotipi pigmentati è stata più stimolata dall'infezione che nelle linee non pigmentate. Più nel dettaglio, mentre in Sumai3 e Rosso la produzione di flavan-3-oli è stata favorita a scapito degli antociani, in Vanilnoir infetto è stata stimolata la produzione simultanea di antociani e flavoni, entrambi potenzialmente coinvolti nel suo meccanismo di resistenza. Inoltre, dieci proteine chinasi recettoriali LRR (LRR-RLKs) sono state sovraregolate esclusivamente nei genotipi resistenti a FHB insieme a due geni della segnalazione MAPK. Ulteriori indagini su questi geni possono fornire preziose informazioni sulla specifica comunicazione tra frumento e *F. graminearum*.

List of Figures

List of tables

Funding and Acknowledgement

This dissertation is the results of a three years long work carried out within the PhD course in Plant and Animal Production Sciences (Department of Agricultural and Forest Sciences, DAFNE University of Tuscia, Viterbo, Italy). This research was supported by the project *Valorizzazione Multifunzionale di Frumenti Pigmentati per la realizzazione di Alimenti Funzionali e di NanoAgrofarmaci Green per la Protezione del Frumento* acronym MULTIFRU funded by POR FESR Lazio 2014-2020 action 1.2.1 and by Departments of Excellence MUR Law 232/2016 (SafeMed Project), and the research was carried out in the framework of the National program for "Departments of Excellence 2023-2027" of MUR (DiVerSo Project) at DAFNE, University of Tuscia.

I wish to acknowledge my supervisors, Prof. Giorgio Mariano Balestra, Dr. Sara Francesconi and Prof. Francesco Sestili, and all the researchers who helped me in this work. Thank you to Dr. Florence Richard-Forget (Mycology and Food Safety, MycSA, INRAE Bordeaux-Aquitaine), and to the whole team she leads, for hosting me in MycSA laboratory for seven months and allowing me to carry forward the work presented in chapter 2. I wish to acknowledge Dr. Federica Castellani and Prof. Matteo Vitali (Department of Public Health and Infectious Diseases, University of Rome La Sapienza) for the help in metabolites and mycotoxins analysis in chapter 4 and 5. Thank you to Dr. Cecilia Miccoli (University of Tuscia, Department of Agricultural and Forest Sciences) who put great effort into the success of the MULTIFRU project and to Dr. Silvia Turco (University of Tuscia, Department of Agricultural and Forest Sciences) for the support in bioinformatics analysis.

Summary

1. General introduction

1.1. Overview

Wheat is a pivotal crop for food security and it is the staple crop for an estimated 35% of the world population (Grote et al. 2021). Furthermore, FAO projects staple cereals to continue to play a critical role for food security till 2050, contributing nearly half of both daily calories and protein intake in low- and middle-income countries (FAO, IFAD, UNICEF 2023). After sugarcane and maize, wheat is the third most produced commodities in the world, cultivated in more than 219 million ha (FAO 2024). Asia was the main wheat producer in 2021-2022 (43.2% of world production), followed by Europe (34.9%) and Americas (13.8%) (FAO 2024). Together, cereals provide 45% of the caloric and almost 40% of the protein intake in the human diet. While only around 12% of maize is used for food (the residue is used as animal feed or for industrial purposes), 77% of the rice and 65% of the wheat crop is used for human diet (Langridge et al. 2022). The importance of wheat for food security was recognized by the policy makers who endorsed the establishment of Expert Working Groups and trans-national collaborative research programs, such as Wheat Initiative, promoted by Chief Agricultural Scientists of the G20 group of countries (Langridge et al. 2022), or the Wheat Yield Consortium (WYC) led by International Maize and Wheat Improvement Centre (CIMMYT) (Reynolds et al. 2011).

Wheat yield tripled from 1960 (when around 222 million tons of wheat were produced in the world) to 2022 (more than 808 million tons produced) (FAO 2024). Yield increase was achieved thanks to several changes of agricultural practices and to dedicated breeding efforts. Agriculture modernization included the development and adoption of technology, the mechanization, high-input farming based on the use of chemical fertilizers, pesticides and irrigation and farm consolidation, allowing to take advantage of economies of scale (Shewry 2009; Jetté-Nantel et al. 2020). Furthermore, since the 1940s–60s, the Green Revolution led to the development of high-yielding plant varieties, especially of wheat and rice, that increased food supplies and staved off widespread starvation in developing countries (Phillips 2014). High-yielding varieties, such as the new dwarf varieties of wheat, have a high Harvest Index, which means that they put more of their energy resources into seeds rather than leaves, stems, and other plant structures (Gellatly and Dennis 2011). Yield in wheat is a complex, polygenic trait, with multiple genes contributing to yield potential and many more to how much of that potential is realized when the crop is challenged by particular abiotic and biotic stresses (Marcussen et al. 2014). Improvement of yield potential was achieved through morphology and physiology empowerment such as increasing spike fertility, altering sinks that compete with spike fertility, increasing photosynthetic capacity, improving biomass and radiation use efficiency (Rauf et al. 2015).

The occurrence of one or more stresses may reduce the yield from yield potential to the actual yield, creating a yield gap. Indeed, despite the increase in yields, several threats still endanger wheat production, and thus food security, around the world. Abiotic stress, such as drought, salinity, and high temperature adversely affect different growth and developmental stages of wheat (Dutta et al. 2023). Moreover, the ongoing climate change risks worsening the situation, considering that extreme weather events (such as frost and heat shock) are predicted to increase under future climate scenarios (Chakraborty and Newton 2011; Barlow et al. 2015; Bajwa et al. 2020).

Biotic stresses are a major impediment to the production and quality of important food stuffs. In particular, fungal diseases of wheat (such as stem ruts, wheat blast or fusarium head blight) could be particularly catastrophic, causing crop failures and grain contamination with dangerous mycotoxins (Singh et al. 2008; Chakraborty and Newton 2011; Lidwell-Durnin and Lapthorn 2020; Islam et al. 2020). Since the Green Revolution, crop losses to diseases have been

greatly reduced through campaigns to breed resistant varieties and the development of fungicides. However, the success of the Green Revolution had unintentional consequences on genetic diversity in wheat, narrowing the genetic base of germplasm used to develop varieties for cultivation (Lidwell-Durnin and Lapthorn 2020; Balfourier et al. 2024). Furthermore, pathogens change quickly evolving fungicide resistance (Pintye et al. 2024), and there is increasing evidence that the use of harmful pesticides in agriculture has significant impacts on non-target organisms and biodiversity, also endangering human health (Finger et al. 2024). Therefore, efforts to find new solutions must increase and plant resistance continues to play a key role in the search for a more sustainable agricultural system.

But this is not enough. Indeed, staple foods are not only required to provide carbohydrates for sustenance, through sustainable agricultural practices and ensuring high yields, but also to be a source of other essential nutrients. This is why many efforts has been made to develop biofortified food, increasing levels of essential vitamins and minerals in edible parts of cereals (Kamble et al. 2022; Zubair et al. 2023) or other staple crops (Agrawal et al. 2024). Biofortified food not only may counteract the widespread issue of micronutrient malnutrition, but can respond to the growing demand for healthy food. Colored wheat, rich in anthocyanins, showed antioxidant and anti-inflammatory activity, protecting from metabolic syndromes like obesity, diabetes, hypertension, and possessed desirable product-making and commercial utilization features (Garg et al. 2022). Furthermore, plant secondary metabolites are known to play active role in plant defense (Anjali et al. 2023), but the role of anthocyanins in wheat-fungal disease interaction was poorly investigated.

In the following paragraphs the main characteristics of wheat (bread wheat, *Triticum aestivum*, and durum wheat, *Triticum turgidum* subsp. *durum*) are summarized, with a particular focus on colored wheat and the potential of using genotypes rich in polyphenols in combating plant diseases, especially in response to fusarium head blight.

1.2. Wheat

1.2.1. Origin and evolution of polyploid *Triticum* wheats under cultivation

Cultivated wheats and their close wild relatives belong to the genus *Triticum* L., a member of the tribe *Triticeae*, which contains ≈300 species (Clayton and Renvoize 1986). The wheat genus *Triticum* has a relatively small number of species (six species) with wild taxa occurring in the Middle East and Transcaucasus region (Gaut 2002). Nowadays, *Triticum* genus include: *Triticum monococcum* L. (AA genome); *Triticum urartu* Tumanian ex Gandilyan (AA genome); *Triticum turgidum* L. (AABB genome); *Triticum aestivum* L. (AABBDD genome) (Matsuoka 2011). Bread wheat (*Triticum aestivum* L., 2n = 6x = 42, BBAADD), also known as common wheat, is a predominantly autogamous allohexaploid species. It was subjected to a complex evolutionary history, involving distant hybridization, polyploidization, adaptation, domestication, selection and breeding, profoundly impacting the formation of current wheat (Wang et al. 2023). The first hybridization (Fig. 1.1) occurred approximately 0.8 million years ago between *Triticum urartu* (AA) and a diploid species closely related to *Aegilops speltoides* (BB, maternal), giving rise to the allotetraploid wild emmer wheat (*Triticum dicoccoides*, BBAA) (Marcussen et al. 2014). Allohexaploid wheat originated through allopolyploidization from the second hybridization event between cultivated domesticated tetraploids (*Triticum dicoccon*, BBAA, maternal) and *Aegilops tauschii* (DD) (Matsuoka 2011; Wang et al. 2023).

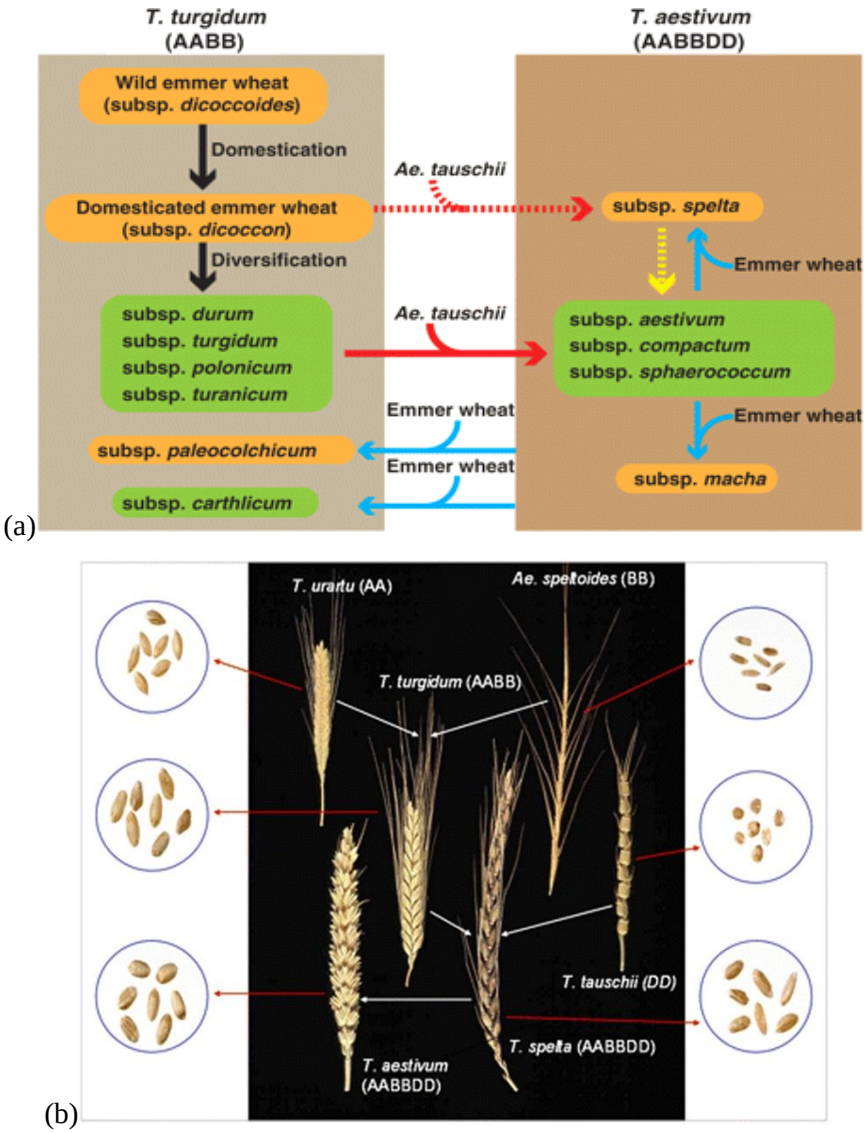

Fig 1.1: (a) Evolution of the *T. turgidum–T. aestivum* complex (Matsuoka 2011); (b) The evolutionary and genome relationships between cultivated bread and durum wheat and related wild diploid grasses, showing examples of spikes and grain (Khalid et al. 2023)

1.2.2. Wheat morphology, physiology and phenology

The description that follows is based largely on studies of common or bread wheat (*Triticum aestivum* L.), which share many morphological characteristics with *Triticum durum* subsp. *durum*. Differences are highlighted.

The wheat shoot is a short rhizome bearing several axillary leafy culms (tillers) that may grow to about a meter in height. The number of culms varies with cultivar, planting depth and density, and external conditions (Shang et al. 2021). Each culm has five to seven nodes. Only three or four foliage leaves develop. The uppermost, or flag leaf, subtends the inflorescence. Flag leaf is a major source of photosynthate for the developing grain and its size contributes to interplant competition both in durum wheat (Spagnoletti et al. 1990) and in bread wheat (Khaliq et al. 2008). Each culm produces an inflorescence, which is a thick, condensed branch system. The diffuse root system consists of adventitious roots (including the so-called seminal embryo roots). Some roots extend horizontally for 30 to 35 cm just

below the surface; others grow diagonally downward within the top 30 cm of soil. Below 30 cm, however, fewer and less branched roots extend vertically to 150 cm or deeper (Thorup-Kristensen et al. 2009).

The spikes, or ears, contain the wheat grains. The major axis, called the rachis, bears two rows of spikelets in alternating order, in the case of wheat (Fig. 1.2a), while rows number of spikelets may vary in other cereals. The basic unit of the spike is the spikelet, within which are borne the specialized flowers (florets) typical of grasses (Lersten 1987). The rachilla is the axis of a spikelet. It is also branched alternately, bearing a pair of empty (or nonflowering) glumes at the base and a series of up to six florets in the spikelet. Each floret consists of a pair of pales (flowering glumes), the lower or outer lemma and the upper or inner palea, enclosing the ovary and later the caryopsis (Fig. 1.2b). Floret size decreases from the base upward, and the largest grains are usually in the basal or second florets. Spikelet differentiation starts in the middle of the spike and proceeds toward the base and the tip (Bechtel et al. 2009).

Caryopsis (or grain or kernel), is a single-seeded fruit in which the ripened ovary wall is fused with or closely connected to the seed (Fig. 1.2c). Wheat grain is made of several layers having different functions. From the outside to the inside, pericarp, testa and aleurone form the protective or outer coating layer which is removed during the milling process, forming the bran, rich in fibre, essential fatty acid, starch and protein (Wrigley 2017). Aleurone frame consists of one layer in most cereals. The endosperm constitutes the largest part of whole grain (80–85%) rich in starch and energy-producing carbohydrates. By milling of bread wheat, flour is obtained, while semolina is the product of durum wheat milled grains. Durum and bread wheat are characterized by a few distinct quality and technological properties and have traditionally been used for different end-use products, pasta or couscous, and bread, respectively. However, these end-products do not represent the exclusive application, because bread made with durum wheat semolina and pasta made with bread wheat flour also exist (Martínez et al. 2016; Mastrangelo and Cattivelli 2021). The germ, the smallest part of whole grain, represents around 3% of the grain, on average, and reflects the living part of the grain because, when seeded, it can grow into a new plant (Iji 2019).

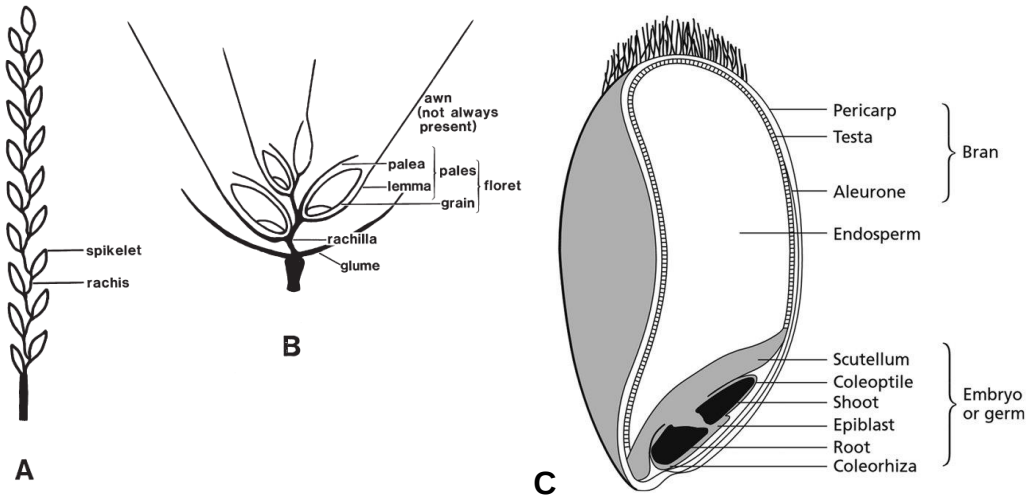

Fig. 1.2: The relationship among parts of the wheat spike or ear. (A), spikelets arranged alternately on the main axis or rachis. (B), the structure of the mature spikelet. Its axis, or rachilla, bears (sterile) glumes at its base and florets arranged alternately along its length. In each floret, a grain is enclosed between two pales or fertile glumes (Bechtel et al. 2009). (C) Cross-sectional structure of wheat grain (McDonald et al. 2011).

Wheat is a widely adapted crop. It is grown from temperate, irrigated to dry and high-rain-fall areas and from warm, humid to dry, cold environments. Undoubtedly, this wide adaptation has been possible due to the complex nature of the plant's genome, which provides great plasticity to the crop (Hyles et al. 2020). Wheat is a C3 plant and, as such, it thrives in cool environments (Maurino et al. 1997). Germination may occur between 4° and 37°C, optimal temperature being from 12° to 25°C. Wheat development can be divided into vegetative and reproductive periods. During the vegetative period, the repeated production of tillers determines the number of heads produced. Tillering has great agronomic importance in cereals since it may partially or totally compensate the differences in plant number after crop establishment and may allow crop recovery from early frosts (Shang et al. 2021). Following vegetative development, some tillers enter the reproductive period, generating spikes at their tops that bear spikelets that give rise to kernels. Wheats, which are responsive to vernalization, flower after the completion of a cold period (Milec et al. 2023). After vernalization is completed, genotypes, which are sensitive to photoperiod, require a certain day-length to flower. Most cultivated wheats, however, are quantitative long-day plants (Pérez-Gianmarco et al. 2020). Wheat plants have from four to eight leaves in the main shoot when the growing apex changes from the vegetative to the reproductive stage. The length of the apex at this time is approximately 0.5 mm. The glume and lemma primordium stages follow. The floret primordia are found in the axil of each lemma. Temperatures above 30°C during floret formation cause complete sterility (Emebiri et al. 2024).

Different developmental scales describe wheat phenology (Fig. 1.3) (Hyles et al. 2020). Feekes developed a scale (stages 1–11) classifying the wheat lifecycle from tillering, stem elongation, heading and flowering, through to ripening (Feekes 1941). The "Zadoks scale" comprises 100 stages describing development of the wheat plant (Z1 to Z100) (Zadoks et al. 1974).

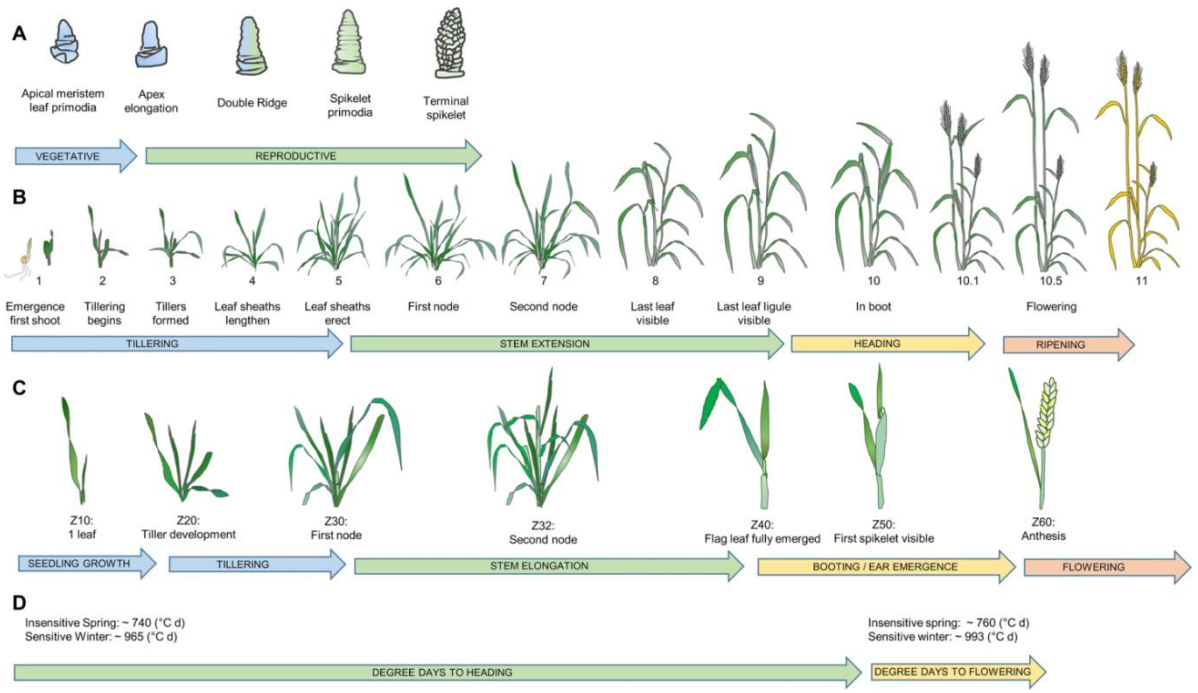

(caption in the next page)

Fig. 1.3: (a) Apex morphology, vegetative to reproductive. (b) Feekes Scale, stage 1–11. (c) Zadoks Decimal Scale, score 0–100. (d) Example of cumulative degree-days from emergence to heading and emergence to flowering for near-isogenic lines (NIL)s with differing vernalization or photoperiod requirements grown in inductive conditions (Hyles et al. 2020).

1.3. The colors of wheat: focus on purple and blue pigmented genotypes

The development of biofortified colored wheat (black, purple, and blue) adds nutritional and functional health benefits to the energy-rich wheat. Anthocyanin compounds have proven to have numerous health benefits, most of which are associated with their antioxidant properties (Lachman et al. 2017), thus colored wheat lines with high anthocyanin, iron, and zinc contents showed antioxidant and anti-inflammatory activity and possessed desirable product-making and commercial utilization features (Garg et al. 2022). Purple wheat is currently processed into a variety of foods with potent antioxidant properties (Gamel et al. 2023). Despite this, their diffusion is currently restricted, potentially due to consumers' acceptability and preference. Indeed, especially for durum wheat, the yellow-amber color of semolina has become an important quality trait for durum wheat end products, commercially identified as the yellow index (Ficco et al. 2014a). However, a recent investigation proved that pigmented pastas were well accepted by consumers, due to its peculiar color and more complex aromatic profile that triggered consumers' interest (Suo et al. 2023), suggesting that better promotion can encourage the diffusion of these pigmented healthy products.

1.3.1. Definition, origin and composition

During caryopsis development, different pigments may accumulate in the external layers, which later become the ripe seed coat. Ripe wheat caryopses usually vary from light buff or yellow to red-brown according to the absence or presence of red pigmentation in this external layer (Bechtel et al. 2009). In colored grains genotypes, a purple, blue or black pigmentation in the seed coat has been found. Varied concentration of pigments, such as, carotenoids, anthocyanins, phenolics, xanthophylls can be found in bran layers, producing different colored grains (red, yellow, white, purple, blue, and black) (Saini et al. 2020). In purple, blue and black genotypes, the pigments accumulated are mainly anthocyanins, water-soluble natural pigments, produced as secondary metabolites in plants and belonging to the flavonoid family. In this dissertation, the terms "pigmented" and "colored" grains are used as synonyms. Even if carotenoids are pigments and can give yellow color to grains (especially durum wheat grains), the terms "pigmented" and "colored" refer to purple, blue or black pigmentation, conferred by anthocyanins.

The anthocyanins composition strongly depends on the genotypes, but it is also influenced by the genetic architecture, agro-environmental conditions and processing techniques. Beleggia et al. (2021) showed that delayed sowing time favor anthocyanins accumulation. Anthocyanin content of grains in purple wheat is affected by grain position and magnesium fertilization and early harvesting increased anthocyanin content and concentration by 65 and 39% (Bustos et al. 2012). Furthermore, light is essential for purple pigments accumulation in the grains (Jiang et al. 2023). The main anthocyanins detected and quantified in pigmented wheat were revised by different authors (Saini et al. 2020; Garg et al. 2022). According to LC-MS analyses, blue and purple wheat contain 19 and 26 anthocyanins, respectively, with the total anthocyanin content being between 9.26 mg/kg and 13.23 mg/kg in the purple lines (Garg et al. 2016). Table 1.1 summarize the most relevant compounds present in purple, blue and black grains.

Table 1.1: Main anthocyanins present in pigmented grains

Anthocyanin (characteristic color)	Derivatives	Chemical formula	Wheat type	Amount (mg/kg)	References
Cyanidin (Orange-red)	Cyanidin-3-arabinoside	$C_{20}H_{19}ClO_{10}$	Purple	23.2–25.1	Hosseinian et al. 2008
	Cyanidin-3-galactoside	$C_{21}H_{21}O_{11}$+	Purple	0.98–72	Abdel-Aal and Hucl 2003
	Cyanidin-3-glucoside	$C_{21}H_{20}O_{11}$	Blue	1.17–29.14	Abdel-Aal et al. 2006; Garg et al. 2016; Ficco et al. 2016; Gamel et al. 2020
			Purple	0.63–116.2	
Delphinidin (Blue-red)	Delphinidin-3-arabinoside	$C_{20}H_{19}ClO_{11}$	Purple	15.1–16.7	Hosseinian et al. 2008
	Delphinidin-3-galactoside	$C_{21}H_{21}ClO_{12}$	Purple	38.3–36.4	Garg et al. 2016
	Delphinidin-3-glucoside	$C_{21}H_{20}O_{12}$	Blue	0.52–56.5	Abdel-Aal et al. 2006
Malvidin (Blue-red)	Malvidin-3-glucoside	$C_{23}H_{24}O_{12}$	Blue	10.26–13.8	Garg et al. 2016
			Purple	0.17–60.03	Hosseinian et al. 2008; Abdel-Aal and Hucl 2003
	Malvidin-3-rutinoside	$C_{29}H_{34}O_{16}$	Red	0.06–0.43	Abdel-Aal and Rabalski 2008; Ficco et al. 2014; Abdel-Aal et al. 2018
			Blue	2	Garg et al. 2016
			Purple	2.6	Abdel-Aal et al. 2006
Pelargonidin (Orange-red)	Pelargonidin-3-arabinoside	$C_{20}H_{19}O_9$ +	Purple	9.3–11.3	Lachman et al. 2017
	Pelargonidin-3-galactoside	$C_{21}H_{21}ClO_{10}$	Purple	22.1–26.1	Hosseinian et al. 2008
	Pelargonidin-3-glucoside	$C_{21}H_{20}O_{10}$	Purple	2.185–29.3	Garg et al. 2016
Peonidin (Orange-red)	Peonidin-3-arabinoside	$C_{21}H_{21}ClO_{10}$	Blue	0.95–3.49	Ficco et al. 2014b
			Purple	28.4–29.3	Hosseinian et al. 2008
	Peonidin-3-glucoside	$C_{22}H_{22}O_{11}$	Blue	0.76 - 0.99	Gamel et al. 2020
			Purple	2.7–17.5	Garg et al. 2016
Petunidin (Blue-red)	Petunidin-3-galactoside	$C_{22}H_{23}O_{12}$+	Purple	38.3–40.4	Hosseinian et al. 2008

Pigments may accumulate in the aleurone layer, giving blue pigmentation (Fig. 1.4b), or in the pericarp layer leading to a purple appearance (Fig. 1.4c). When pigments are present at the same time in aleurone and in the pericarp layers, a black-grained line is obtained (Fig. 1.4d).

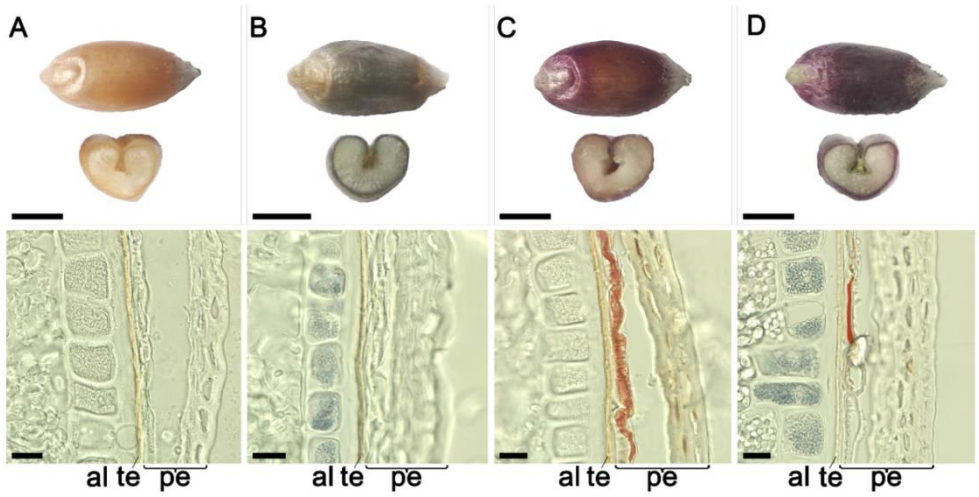

Fig. 1.4: Grains showing different pigmentation, from Gordeeva et al. (2022). (A) Cultivar "Saratovskaya 29", the aleurone, seed coat (or testa), and pericarp were clearly visible, but except for a brown strip that we identified as a testa, no pigments in the grain layers were detectable; (B) a blue-grained substitution line in which many blue small inclusions in the cells of the aleurone were observed within organelles similar to vacuoles; (C) brown-red pigmented structures identified as anthocyanins were found in the pericarp of a purple-grained line; (D) black-grained line showing both blue and brownish-red pigmented structures similar to vacuoles with anthocyanins were visible in the aleurone and pericarp layer. al: aleurone layer, te: testa, pe: pericarp. The scale bars for the seeds are 2.5 mm, and for the micrographs, 25 µm.

Origin of purple pigmentation most likely derives from Ethiopian regions 2400 m above sea level. With increased altitude, there is an associated waterlogging stress at earlier developmental stages of the wheat plant. Purple wheats are better equipped with favorable adaptive traits to highland growth conditions (Tesemma et al. 1993). Indeed, these varieties show different adapted traits, like earlier maturity, shorter height, higher fertility, tillering capacity and harvest index (Belay et al. 1995), and the frequency of the purple seed color increases with increasing altitude (Kebebew et al. 2001). These evidences suggest that this trait results from a natural selection. Most likely also a human selection occurred, but it may be difficult to distinguish whether the earliest wheat farmers selected for the purple seed-color *per se*, due to cultural or social reasons, or for the adaptive traits which eventually led to a correlated high frequency (Belay et al. 1995).

Origin of blue pigmentation is more controversial. In hexaploid wheat, it was hypothesized that blue aleurone derives from the introgression of chromosomal segments from wild relatives and behaves as a single dominant blue aleurone (Ba1) locus (Keppenne and Baenziger 1990). Jia et al. (2020) suggested blue aleurone as a recently evolved trait resulting from environmental adaptation and identified a *Pooideae*-specific flavonoid 3′,5′-hydroxylase (F3′5′H) lineage, demonstrating a scenario of convergent evolution. The blue aleurone color expression is influenced by xenia effect (Zeven 1991; Gordeeva et al. 2019).

From these original landraces, many varieties and breeding lines were obtained through introgression of pigmented grain traits into commercial cultivars. According to Padhy et al. (2024) currently, for bread wheat, there are 15 blue

aleurone genotypes, counting 3 released variety, 12 purple pericarp genotypes, including 6 released variety and 13 released black variety.

1.3.2. Phenolic compounds and anthocyanins

Phenolic compounds (or phenylpropanoids) are commonly found in almost all plants, occurring in various parts (roots, flowers, leaves, fruits or seeds), comprise a large group of more than 8000 different compounds with the phenolic hydroxyl groups being the common structural feature (Stockley et al. 2012).

Polyphenols are commonly categorized as flavonoids, characterized by a C6-C3-C6 structure, and non-flavonoids (Fig. 1.5). Non-flavonoids include phenolic acids, in particular, hydroxybenzoic acids (i.e., vanillic and gallic acids), and cinnamic acids (i.e., ferulic and caffeic acids). All of these molecules have proven to have biological activities (Teng and Chen 2019; Di Lorenzo et al. 2021). Furthermore, these compounds are essential components of wheat cell wall, reinforcing external cell barrier against the attack of pathogens (Saulnier et al. 2012; Liu et al. 2022).

Flavonoids generally present in plants are anthocyanins, flavonols, flavan-3-ols, flavones, isoflavones, flavanones, and stilbenes (Fig. 1.5). The anthocyanidins (or aglycons) are the basic structures of the anthocyanins and consist of an aromatic ring bonded to a heterocyclic ring that contains oxygen, which is also bonded by a carbon–carbon bond to a third aromatic ring (Castañeda-Ovando et al. 2009) (Fig. 1.6). When the anthocyanidins are found in their glycoside form (bonded to a sugar moiety) they are known as anthocyanins.

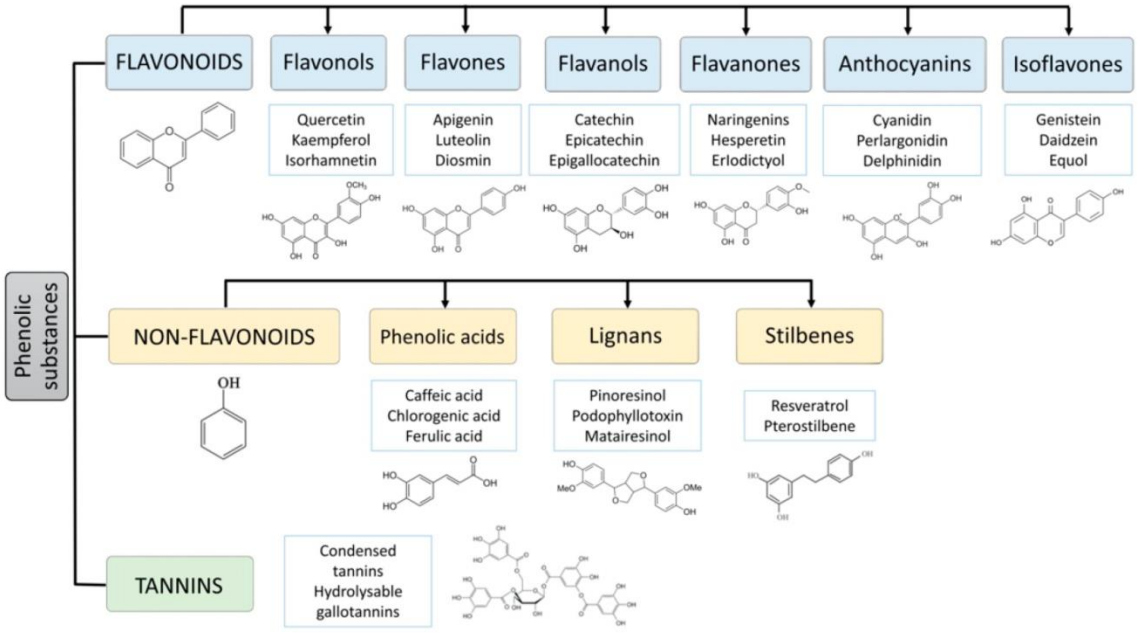

Fig 1.5: Main classes of polyphenols: flavonoids, non-flavonoids (phenolic acids, lignans, and stilbenes) and tannins (Serra et al. 2021).

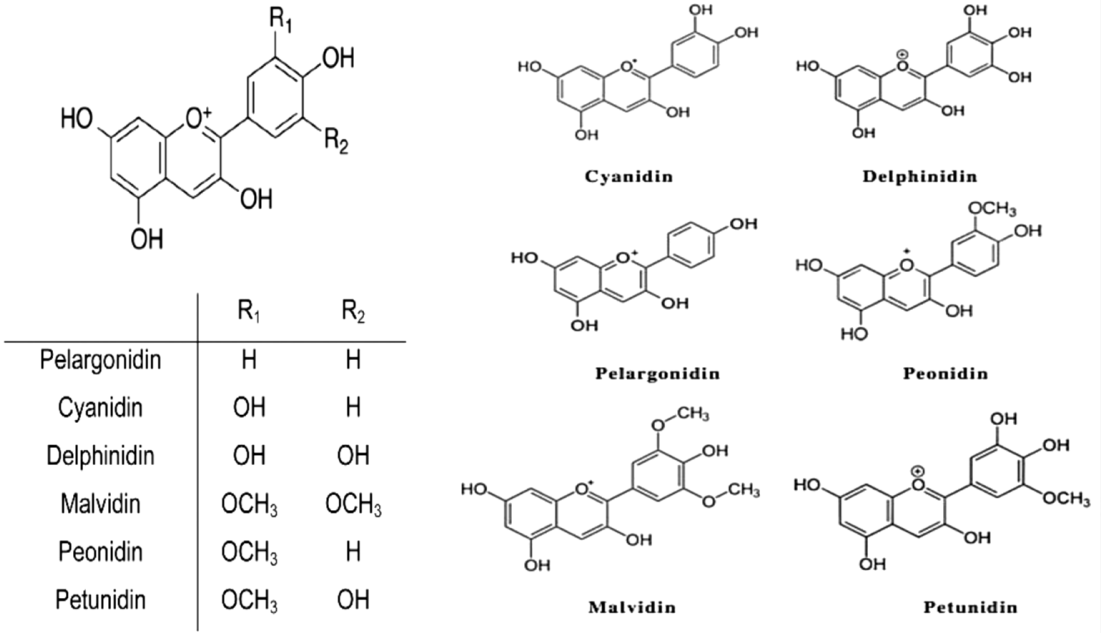

	R_1	R_2
Pelargonidin	H	H
Cyanidin	OH	H
Delphinidin	OH	OH
Malvidin	OCH_3	OCH_3
Peonidin	OCH_3	H
Petunidin	OCH_3	OH

Fig 1.6: Structure of major anthocyanidins in colored wheat (Saini et al. 2020).

Into the plant, anthocyanins are sequestrated into the vacuoles through transporter, like glutathione-S-transferase (GST) and MATE-type transporters, named anthoMATEs (Irani and Grotewold 2005; Gomez et al. 2011). The isolated anthocyanins are highly instable and very susceptible to degradation (Enaru et al. 2021). Their stability is affected by several factors such as pH, temperature, chemical structure, concentration, light, oxygen, solvents, the presence of enzymes, flavonoids, proteins and metallic ions (Castañeda-Ovando et al. 2009). Anthocyanins can be found in different chemical forms, which depend on the pH of the solution (Fig. 1.7) (Abdel-Aal and Hucl 2003; Rosales and Fabi 2022). At pH 1, the flavylium cation (red color) is the predominant species and contributes to purple and red colors. At pH values between 2 and 4, the quinoidal blue species are predominant. At pH values between 5 and 6 only two colorless species can be observed, which are a carbinol pseudobase and a chalcone, respectively. At pH values higher than 7, the anthocyanins are degraded depending on their substituent groups. In contrast with aglycons, monoglycosides, and mostly, diglycosides derivatives are more stable in neutral pH conditions (Jing et al. 2020). This behavior is explained because the sugar molecules avoid the degradation of instable intermediaries into phenolic acid and aldehyde compounds.

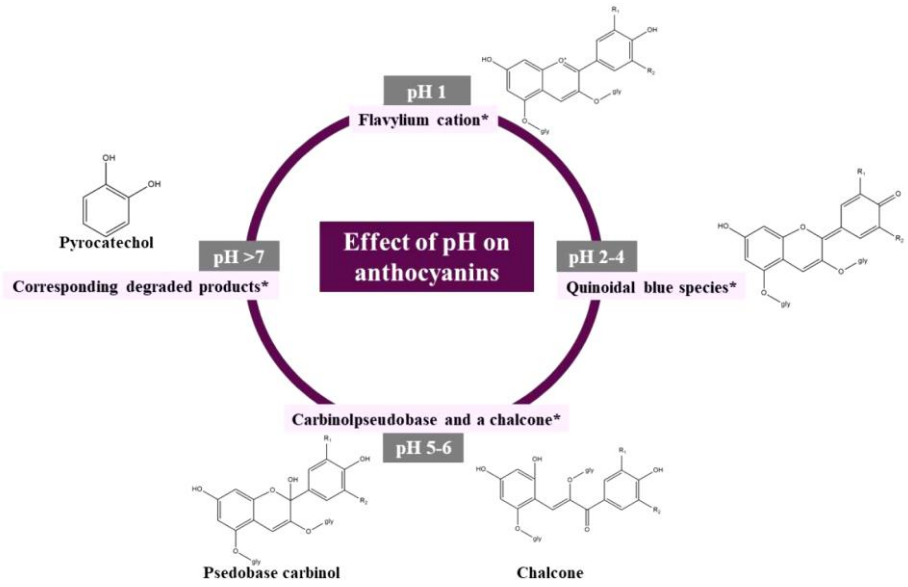

Fig 1.7: Anthocyanins at different pH values, * predominant chemical form (Enaru et al. 2021)

1.3.3. Anthocyanins biosynthetic pathway

Phenylpropanoid biosynthesis in plants has been studied in-depth (Fig. 1.8) (Ma et al. 2021). It begins with the deamination of L-phenylalanine by L-phenylalanine ammonia-lyase (PAL), followed by reactions catalyzed by 4CL (4-coumarate-coenzyme A ligase, which catalyzes the formation of CoA thioesters of hydroxycinnamic acids) and C4H (cinnamate-4-hydroxylase, which leads to the hydroxylation at the C4 position of the aromatic ring). The pathway then branches out into several routes. The 3′-hydroxylation of coumaroyl quinate/shikimate, followed by the reactions catalyzed by ferulate 5-hydroxylase (F5H) and caffeic acid O-methyltransferase (COMT), lead to the production of lignin monomers and then lignin (Goujon et al. 2003). The production of naringenin chalcone from p-coumaroyl-CoA and malonyl-CoA molecules by CHS (chalcone synthase) starts the flavonoid branch of the pathway. This branch continues through reactions catalyzed by chalcone isomerase (CHI) to form trihydroxyflavanones, further hydroxylated by flavanone-3-hydroxylase (F3H) to form dihydroflavanols. Dihydroflavanols are then reduced by dihydroflavonol reductase (DFR) to produce colorless anthocyanin glycosides, which are subsequently catalyzed by anthocyanidin synthase (ANS) to produce colored anthocyanins (Sunil and Shetty 2022). Dihydroflavanols can be the substrate of other enzymes, such as the FLS (flavonol synthase) producing flavones like kaempferol or quercetin (Gebhardt et al. 2007). The genes involved in phenylpropanoid biosynthesis can be divided into structural genes (functional genes, which encode for the above-mentioned enzymes) and regulatory genes. The expression of structural genes during anthocyanin biosynthesis is directly regulated by the MYB-bHLH-WDR complex (Liu et al. 2021), which varies in the different plant species.

Recently, different studies revealed key genes for anthocyanins accumulation in pigmented wheat. Kapoor et al. (2023) putatively identified eight structural genes in the anthocyanin biosynthesis pathway, and, in developing seeds from colored wheats, identified differential expressions in 97 isoforms. In particular, *F3H* on chromosomes 2 and *F3'5'H* on 1D chromosomes could be significant influencers in purple and blue color development, respectively. According to Wang et al. (2021) *TaBZ1* (homologous enzyme encoded by the maize Bronze-1 locus) may be a core gene in anthocyanin biosynthesis and *TaCHS* and *TaANS* were considered critical structural genes in the anthocyanin biosynthesis pathway. Furthermore, Sgaramella et al. (2023) mapped two QTL for total anthocyanins content regulation

and the candidate genes *Pp-A3*, *Pp-B1*, *R-A1*, and *R-B1* involved in flavonoid biosynthetic pathways encode for transcription factors bHLH (*Myc-1*) and MYB (*Mpc1*, *Myb10*).

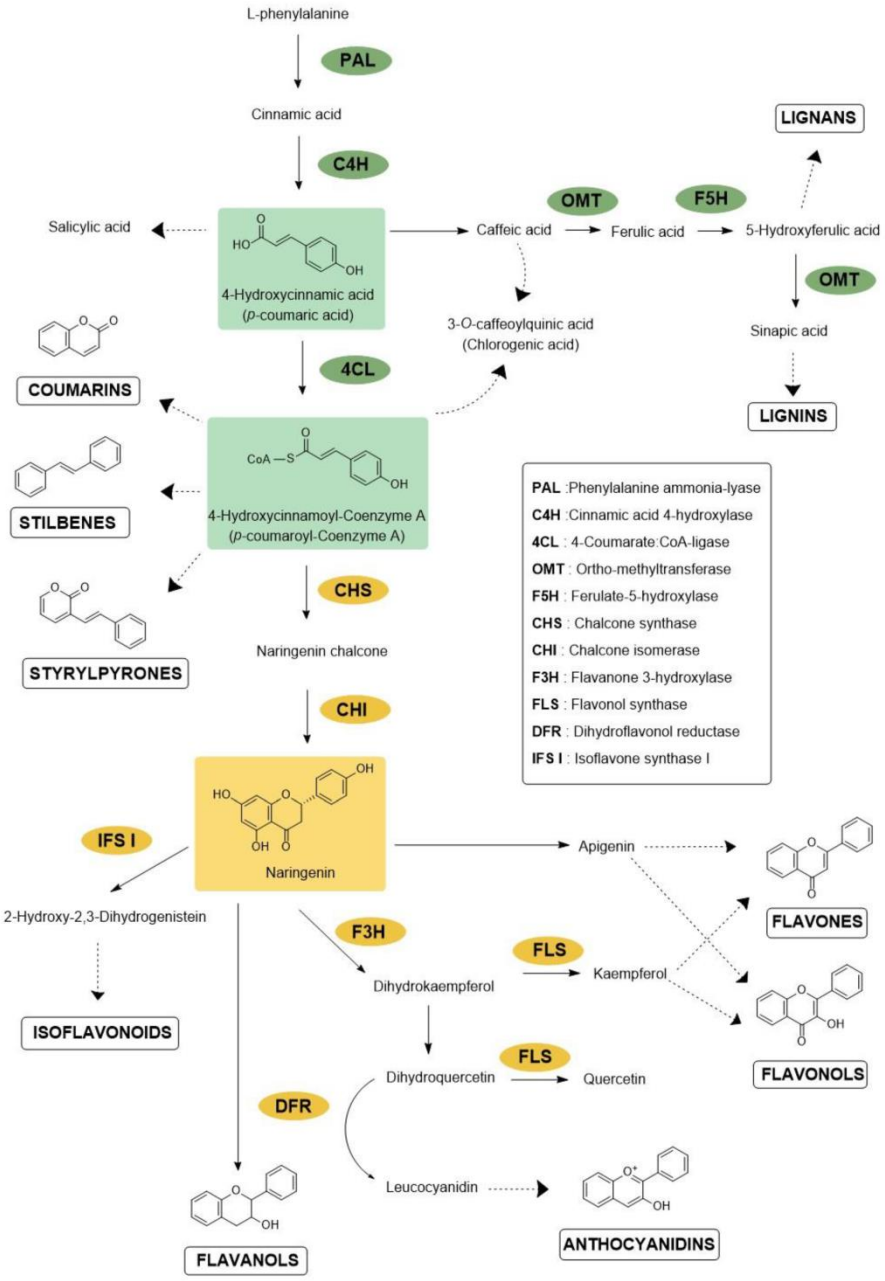

Fig. 1.8: Main steps of the phenylpropanoid and flavonoid pathways. Enzymes are shown in green and yellow for central phenylpropanoid pathways and flavonoid biosynthesis, respectively. Complete arrows refer to one step in the biosynthetic pathway, whereas dashed arrows represent undetailed pathways leading to one molecule or molecule subfamilies (Ramaroson et al. 2022).

1.3.4. Antimicrobial effect of flavonoids and anthocyanins

Secondary metabolites are defined as not essential for plant growth and development. Nevertheless, recent researches are rehabilitating secondary metabolites, recognizing to them a key role in plant life, and some authors rather refer to

them as “specialized” metabolites, while “central” is used for primary metabolites (Pott et al. 2019). Surely, essential is the role of phenylpropanoids in plant defense against abiotic and biotic stresses. Focusing on biotic stress, phenylpropanoids and flavonoids may act as antimicrobial agents, directly contrasting pathogens, or may indirectly counteract the infection by straitening plant defense. Antimicrobial effect is presented in this paragraph, while role in plant defense is discussed in paragraph 1.4.3.

Phenylpropanoids may have a direct effect against pathogens, showing antimicrobial effects. Phenylpropanoids like phenolic acids, stilbenes, lignans, coumarins, flavonoids (including anthocyanins) and tannins may affect bacterial cells thought destruction of the structure and function of cell membrane, oxidative stress, inhibition of macromolecules synthesis and disturbance of energy metabolism, interference with quorum sensing system and alteration of biofilm formation (Chen et al. 2024). The antifungal activity exerted by phenylpropanoids and flavonoids has been investigated, corroborating the metabolomic and functional genomic-driven hypothesis on their link to disease resistance. Flavonol glycosides (such as myricetin 3-*O*-rhamnoside, quercetin-7-*O*-rhamnoside, quercetin-7-*O*-rutinoside, and trimeric form of kaempferol) were responsible for antifungal activity against *Botrytis cinerea*, inhibiting mycelial growth and conidia germination (Rguez et al. 2022). These compounds may exert their antifungal activity alone or may interact with others, such as the glycoalkaloids (Sánchez-Maldonado et al. 2016). Other flavonoids, such as eriodictyol, homoeriodictyol, dihydroquercetin, and luteolin isolated from *Ficus sarmentosa*, var. *henryi*, were effective against pathogenic fungi, e.g., *Fusarium graminearum* and *Septoria zeicola* (Wang et al. 2010). Flavan-3-ols were reported as strong antifungals against wheat rusts (Ullah et al. 2017). Furthermore, several researches report the effect of plant extracts rich in flavonoids as strong antifungals (Salhi et al. 2017; Nguyen et al. 2024). However, despite all these investigations on biosynthesis and targets, little is known about the mode of action involved in the described fungicidal activities. Phenylpropanoids may alter cellular permeability and induce structural and practical disintegration of casing proteins, resulting in pH interruption, ATP generation, substrate consumption, and membrane bound enzymes (Anjali et al. 2023).

1.4. Fusarium head blight

1.4.1. Relevance, life cycle and management

Fusarium Head Blight (FHB) is among the most dangerous fungal disease of cereals. This disease was first described in England in 1884 (Goswami and Kistler 2004). From 1993 to 2001, there was a loss of $7.6 billion due to an FHB epidemic in the United States (McMullen et al. 2012). After the spread in the USA and Canada between 1991 and 1996, many publications report the spread of the disease to other regions of the world, including Europe and China (Elias et al. 2005; Oliver et al. 2007; Giroux et al. 2016). In China, yield losses of 5-10% are commonly due to FHB, and yield loss can reach 100% in some years and affect 7 million ha (Zhang et al. 2011). In Europe, Africa and Brazil, *Fusarium* epidemics occur approximately every 4 to 5 years (Figueroa et al. 2018; Khan et al. 2020). In Italy, wheat has been affected by FHB practically every year since 1995, at different levels of incidence and severity depending on the year, the region and the wheat variety (Pancaldi et al. 2010). The disease is reported mainly in the Central-Northern regions and the incidence and severity increase from the Southern to the Northern regions, mainly due to a more humid climate in the Northern regions of the Country (Covarelli et al. 2015).

FHB is caused by a community of fungal species, mostly belonging to the genus *Fusarium*. This community of species is often referred to as Fusarium Head Blight species complex (FHB species complex) and includes at least 17 species (Parry et al. 1995), among which the most important (and therefore considered as the main causal agents) are: *F. graminearum* Schwabe (Fig. 1.9a), *F. culmorum* (W. G. Smith) Sacc., *F. aveanaceum* (Fr.) Sacc. and *F. poae* (Peck) Woll (Xu et al. 2008). In Italy, research carried out in particular on wheat, shows that *F. graminearum* sensu strictu is the main causal agent of fusarium wilt and that *F. avenaceum*, *F. poae* and *F. culmorum* are other important components of the FHB species complex (Pancaldi et al. 2010). While the above-mentioned species are considered the most incidental as they are cosmopolitan, other pathogens belonging to the *Fusarium* genus have been found on infected plants with a variable incidence, depending on the climatic conditions of the area; these are *F. sporotrichioides*, *F. langsethiae*, *F. tricinctum*, *F. acuminatum* and members of the *Fusarium incarnatum-equiseti* species complex (FIESC) (Beccari et al. 2018). The establishment of individual species depends on climatic conditions, mainly on temperature and humidity conditions during flowering (Mielniczuk and Skwaryło-Bednarz 2020), but also on the previous crop (Schöneberg et al. 2016). The co-presence of different species within the same field is frequent (Xu and Nicholson 2009). The etiology of the disease contributes to making it complex and maintaining the risk of infection high over different years due to the different climatic needs of the species which can, individually or in association, infect the ears of the host plants during the growing season, also causing the co-presence of different mycotoxins (Beccari et al. 2017).

In wheat, the symptoms of the infection become visible between heading and the milky-waxy maturation phase (Fig. 1.9b). Main symptoms are necrotic lesions of different colors (brown, dark purple or black) on the external surface of the spikelets and glumes (Goswami and Kistler 2004). Only a few spikelets may be affected, which appear discolored and dry out quickly, or even the entire spike, which may appear necrotic. After a few days after infection, during periods of persistent high relative humidity and mild temperatures, mycelial clusters and pink or salmon-colored sporodochia may appear on the infected glumes (Mielniczuk and Skwaryło-Bednarz 2020). The rachis immediately below the inflorescence can turn to brown/purple color; this browning, which inhibits the development of the kernels, is associated with the death of the tissue of the symptomatic spikelets, resulting in a lower number of seeds per spike. Furthermore, the remaining caryopses are generally smaller, greyish and shriveled, lose consistency and are often covered with sporodochia and mycelium (Kheiri, Moosawi Jorf, and Malihipour 2019).

1. (b)

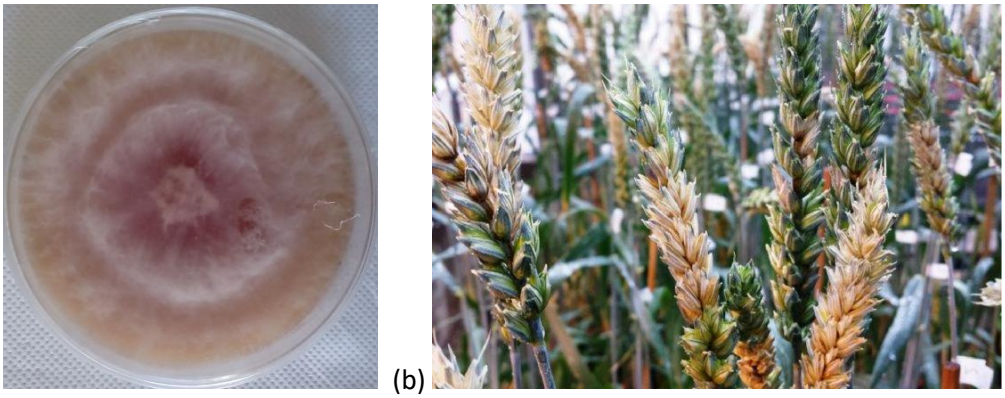

Fig. 1.9: (a) Fungal colony of *F. graminearum* on potato dextrose agar; (b) Severe symptoms of Fusarium Head Blight in wheat (Mahlein et al. 2019).

Fig. 1.10 summarizes the life cycle of FHB and the main management strategies.

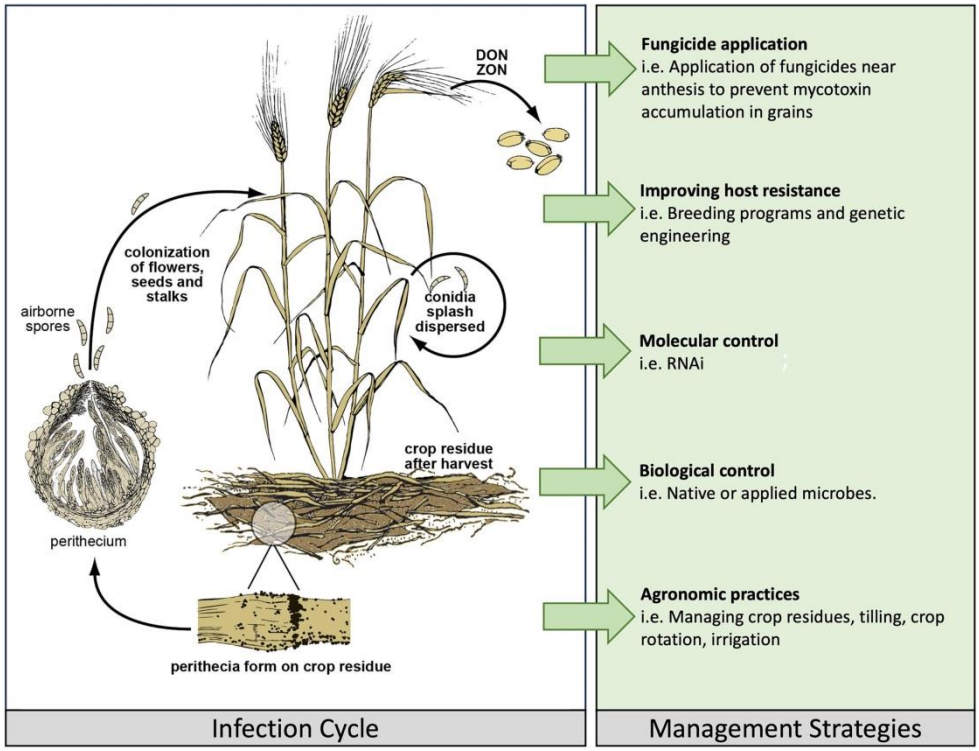

Fig. 1.10: FHB infection cycle and management strategies (Moonjely et al. 2023).

F. graminearum is a homothallic, facultative parasite of wheat that normally overwinters as a saprophyte in the plant debris of small grains and corn which serves as a reservoir for primary inoculum the next season (Dweba et al. 2017). Most *Fusarium* species are distributed in the environment in the form of conidia, *via* transport through wind and water (Paul et al. 2004). During anthesis and the first stages of development of the caryopses, the conidia or ascospores can infect the ears, causing FHB. Dispersal via the "splash effect" allows reaching limited heights: for example, both *F. culmorum* and *F. poae* have demonstrated a maximum dispersal height of 60 cm in the laboratory (Mirjani Hörberg 2002), so only one part of the conidia present in the residues on the ground reaches the ears in a single passage. Asymptomatic infections on leaves (e.g. flag leaf) can represent an important bridge between ground debris and ears (Xu and Nicholson 2009). The pathogen has a brief biotrophic phase until it colonizes the living tissue to maintain the necrotrophic relationship with its host (Goswami and Kistler 2004). The fungus colonizes wheat anthers and eventually the middle rachis blocking the vascular cambium; thus, the portion of the wheat head above the affected area stops growing and exhibits a typical premature bleaching symptom. It is also common to observe black-colored overwintering perithecia and sporodochia on matured wheat spikes, as well as corn debris, which serve as primary inoculum for next season continuing the disease cycle (McMullen et al. 2012).

Main management strategies include agricultural practices, such as crop rotation, management of crop residues using tillage and irrigation, which have proven successful in mitigating the incidence and spread of FHB (Wegulo et al. 2015). Fungicides are still a primary means for controlling FHB in the world. In wheat, fungicides are applied during a short window of time, coinciding approximately with anthesis, when the fungus initiates infection that will result in grain contamination (Moonjely et al. 2023). Rainy season usually complicate the fungicide application, reducing the efficacy. Innovative strategies include the use of natural compounds, such as chitosan (Francesconi et al. 2020) or the application

of precision agriculture strategies, including remote sensing and applying efficient disease forecasting models and decision support system (Francesconi et al. 2021). Host resistance is discussed in paragraph 1.5.3.

1.4.2. Mycotoxins

In addition to reducing yield, FHB is of particular concern because of its direct impacts on human and animal health. Indeed, mycotoxins and pesticide residues in food are among the top food safety concerns associated with a changing climate in Europe (Chakraborty and Newton 2011). Mycotoxin contamination is a global risk to food crops, including cereals, and according to Mesterházy et al. (2020), contamination with mycotoxins is responsible for the wastage of approximately 1.3 billion metric tons of food annually, equivalent to one-third of global food production. Mycotoxins can also cause cancer, allergies, and organ toxicity (Alshannaq and Yu 2017).

Trichothecenes are cyclic sesquiterpenes synthesized by various fungi, including *Fusarium*, *Trichothecia*, and *Stachybotrys* (Marin et al. 2013). Trichothecenes can be classified into four types (type A, B, C, and D) according to chemical structure. The most widespread are the type B trichothecenes, which mainly include deoxynivalenol (DON, also called "vomitoxin", due to the symptoms it causes) and nivalenol (NIV), produced by different species (*F. graminearum*, *F. poae*, *F culmorum*). Some type A trichothecenes (including T-2 toxin, HT-2 toxin, diacetoxyscirpenol, neosolaniol) and type B trichothecenes (such as DON and NIV) are extremely common in food and feed (Gab-Allah et al. 2021). DON is non-carcinogenic for humans, but induces harmful effects on the upper intestine after being absorbed. Acute exposure to DON causes vomiting and anorexia, while chronic exposure is linked to intestinal lesions, inflammation, and immune modulation (Khan et al. 2024).

Other important mycotoxins produced by *Fusarium* spp. are the fumonisins (produced by *F. moniliforme*, *F. verticillioides*, and *F. oxysporum*, having carcinogenic effects) (Marin et al. 2013; De Ruyck et al. 2015) and zearalenone (produced by *F. moniliforme*, *F. verticillioides*, *F. oxysporum*, and *F. equiseti*) (R. Khan, Anwar, and Ghazali 2024).

Moreover, some Fusarium species, such as *F. avenaceum*, may produce the so called "emerging mycotoxins". Enniatins (ENNs), beauvericin (BEA), fusaproliferin (FUSA) and moniliformin (MON) belong to this group, which are neither routinely determined, nor legislatively regulated. However, the evidence of their incidence is rapidly increasing in terms of frequency of occurrence and level of contamination. Indeed, NIV, BEA and ENNs were found to be the most prevalent, sometimes at exceedingly high concentrations (Vaclavikova et al. 2013; Kolawole et al. 2024).

1.4.3. Wheat resistance to FHB and role of phenylpropanoids

Host plant resistance is defined as the intentional use of resistant crop cultivars to reduce the negative impacts of pests or diseases on crop production systems (Stout et al. 2024). Different levels of resistance to FHB were described. Type I resistance is defined as the plant ability to avoid initial penetration (studied by spray inoculation), while type II resistance describes the spread of head blight from the ovary to the other parts of the head, after artificial tip inoculation (Schroeder and Christensen 1963). Despite types I and II are the most studied and described, also types III, IV and V have been proposed: type III refers to variations of DON accumulation in different genotypes (Miller, Young, and Sampson 1985), type IV is related to lower kernel infection rate (analyzed measuring Fusarium Damaged Kernel %), while type V for host tolerance is indicated as preservation of grain yield (Mesterházy 1995). None of them is feasible alone to draw a conclusion on FHB susceptibility/resistance, since they could not be correlated (Mesterhazy 2020). This

is because FHB resistance is a complex quantitative trait, with more than 500 QTL reported in previous studies and mapped on all the wheat chromosomes, except on 7D (Buerstmayr et al. 2009). Among these QTLs, *Fhb1* (on chromosome 3B) was the first sequenced FHB resistance locus in wheat and, together with 6B (QTL-Fhb2) and 2D (QTL-2DL), confer rachis resistance, while *Qfhs.ifa-5A* (Steiner et al. 2017) and QTL-Fhb4 (McCartney et al. 2007) are major contributor to spikelets resistance (Dhokane et al. 2016). However, the casual genes behind many QTLs remain unclear.

Although none of the wheat varieties is completely immune, selection for resistant lines were more successful in hexaploid wheat, whereas *Triticum durum* still remains one of the most susceptible cereals to *Fusarium* infection (Prat et al. 2017) due to a narrow genetic variation. Indeed, compared to hexaploid wheat with the addition of the D genomes, durum wheat has limited genetic variations and allelic combinations, resulting in narrow adaptability to different photoperiods, vernalization, soil conditions, and stresses (Yang et al. 2022). Additionally, cell wall traits were associated to the susceptibility of durum wheat. Significant differences in lignin monolignols composition, arabinoxylan substitutions and pectin methylesterification were found between FHB-resistant bread wheat and FHB-susceptible durum wheat (Lionetti et al. 2015), while other authors tried to transfer of cell wall features from common into durum wheat to improve FHB resistance (Giancaspro et al. 2018).

Indeed, resistance to disease involves a combination of preformed and inducible mechanisms. Preformed mechanisms include all the barriers which impede or create an obstacle to pathogen penetration. Plant cell wall is the foremost barrier that fungal pathogens encounters and need to overcome when infect plant tissues. The combination of cell wall composition and lignification were found to plays a role in the mechanism of type II host resistance to FHB (Lahlali et al. 2016). However, cell wall fortification may also be actively induced by the infection, through the stimulation of phenylpropanoids pathway, in particular by the stimulation of key flavonoid and hydroxycinnamic acid amides (HCAAs) biosynthetic genes (Karre et al. 2019) or by an increase in total lignin content in rachis (Soni et al. 2021) driven by different transcription factors.

Inducible mechanisms are activated by recognition of the pathogen, which activate the PAMP-triggered immunity (PTI) and effector-triggered immunity (ETI) (Jones and Dangl 2006). The pathogen secretes proteins (Avr), known as effectors, in plant cells to facilitate infection and they are directly or indirectly detected by the host's resistance (R) proteins (Flor 1971). Rapid progress in the discovery and functional genomics of disease resistance genes in plants, including wheat, has revealed wide diversity in the type and their mechanisms of action, far exceeding the typical R-Avr interaction (Sinha et al. 2022). Examples of such atypical resistance genes include receptor-like kinases (RLKs), transmembrane cell surface immune receptors. While different RLKs for pathogen recognition was already been described for other wheat pathogens (such as *Zymoseptoria tritici*, *Blumeria graminis* f. sp. *tritici* or *Puccinia graminis* f. sp. *tritici*), less is known for FHB (Sinha et al. 2022).

Moreover to local resistance (PTI and ETI), systemic acquired resistance (SAR) is a defense mechanism in plants that can be triggered by microbial attacks in a part of the plant and provides the whole plant with a boosted resistance. This response is mediated by signaling molecules which activate uninfected systemic (distal) organs in response to a prior (primary) infection elsewhere in the plant, enhancing resistance to later pathogen infection within several days (Shah and Zeier 2013). Several authors underlined the essential role of SAR in FHB response (Francesconi et al. 2020; Wang et al. 2018; Zhang et al. 2021).

In pigmented wheat genotypes, a few research works have speculated the activation of broad spectrum stress-responsive genes, acting against both abiotic and biotic stresses (Li et al. 2020). Phenolic compounds, including anthocyanins, are secondary metabolites activated during stress responses. Interestingly, the prompt biosynthesis of phenolic compounds is described as one of the major mechanisms of resistance against FHB in Sumai3, the bread wheat resistant genotype harboring *Fhb1* (Hao et al. 2020). Indeed, in Sumai3, an early activation of the phenylpropanoid and flavonoid metabolites, due to the up-regulation of *PAL*, leads to the production of antimicrobial compounds and cell wall thickening resulting in type II FHB resistance (Wu et al. 2022). For such reasons, purple pericarp and blue aleurone wheat varieties could be potentially a great source of resistance against FHB for breeding programs. Despite that, a few research works reported contradictory data regarding the employment of pigmented wheat varieties for FHB management. For instance, Spanic et al. (2020) reported that the activation of antioxidant metabolites, such as anthocyanins, plays an important role against FHB, but the timing and type of antioxidant enzymes expressed may result in different levels of resistance. Moreover, Martin et al. (2017) found no relationship with anthocyanin levels in wheat varieties with reduction of FHB symptoms, which were affected more by environmental conditions. Chrpová et al. (2021) investigated the ability of a barley mutant (over-accumulating dihydroquercetin) against *F. graminearum* and *F. culmorum* and reported an inhibition in hyphal penetration thanks to the overexpression of dihydroflavonol reductase. Also Karre et al. (2019) investigated the role of HvWRKY23 trasncription factor in barley in response to FHB, demonstrating that the silencing of *HvWRKY23* increased susceptibility to FHB, leading to the reduction of accumulated secondary metabolites, including anthocyanins. On the contrary, it is also known that pigmented wheat varieties susceptible to FHB are present, such as the blue aleurone Skorpion (Martinek et al. 2013). This was also confirmed by a recent study conducted by Gozzi et al. (2023), who investigated against FHB twelve pigmented bread wheat varieties in open field over two consecutive years and they observed that purple pericarp wheat varieties had significantly lower DON content compared to the blue aleurone ones.

1.5 Aim and scope

In this framework, this research aims to investigate the role of flavonoids, and in particular of anthocyanins, in the bread wheat and durum wheat resistance mechanism against FHB, using pigmented genotypes as a model. The main hypothesis is that pigmented genotypes may be more resistant due to the enrichment in flavonoids and/or for a more activated phenylpropanoid and flavonoid pathways.

Direct effect of anthocyanins on FHB causal agents during initial penetration is unlikely, because the initial penetration occurs at flowering, when grains and also the majority of flavonoids are not present yet. Nevertheless, investigations on the influence of anthocyanins on *Fusarium* spp is currently missing. The impact of four anthocyanins (using *F. avenaceum* as a model) were investigated, analyzing the effects on fungal growth and on mycotoxins accumulation.

Investigations using durum wheat involved three genotypes differing for their grains pigmentation (a purple pericarp line was included) and for their resistance to FHB (the resistant line DBC-480 was considered). These genotypes were used for a morphological and physiological evaluation of traits related to resistance and for a time course analysis of gene expression and metabolites accumulation during the infection. Expression of structural genes related to both phenylpropanoid and flavonoid pathways were examined and a transcription factor (*Ppm1*) was also considered.

Finally, five bread wheat pigmented genotypes were evaluated for their FHB tolerance. Then, the most resistant and the most susceptible were chosen to investigate the resistance mechanism through transcriptomic analysis, with a particular focus on flavonoid and anthocyanin biosynthetic pathways.

1.6 References

Abdel-Aal, E.-S. M., and Rabalski, I. (2008). Bioactive Compounds and their Antioxidant Capacity in Selected Primitive and Modern Wheat Species. *The Open Agriculture Journal*, *2*(1), 7–14. https://doi.org/10.2174/1874331500802010007

Abdel-Aal, E. S. M., and Hucl, P. (2003). Composition and stability of anthocyanins in blue-grained wheat. *Journal of Agricultural and Food Chemistry*, *51*(8), 2174–2180. https://doi.org/10.1021/jf021043x

Abdel-Aal, E. S. M., Hucl, P., and Rabalski, I. (2018). Compositional and antioxidant properties of anthocyanin-rich products prepared from purple wheat. *Food Chemistry*, *254*(February), 13–19. https://doi.org/10.1016/j.foodchem.2018.01.170

Abdel-Aal, E. S. M., Young, J. C., and Rabalski, I. (2006). Anthocyanin composition in black, blue, pink, purple, and red cereal grains. *Journal of Agricultural and Food Chemistry*, *54*(13), 4696–4704. https://doi.org/10.1021/jf0606609

Agrawal, S., Kumar, A., Gupta, Y., and Trivedi, A. (2024). Potato Biofortification: A Systematic Literature Review on Biotechnological Innovations of Potato for Enhanced Nutrition. In *Horticulturae* (Vol. 10, Issue 3). https://doi.org/10.3390/horticulturae10030292

Alshannaq, A., and Yu, J.-H. (2017). Occurrence, Toxicity, and Analysis of Major Mycotoxins in Food. In *International Journal of Environmental Research and Public Health* (Vol. 14, Issue 6). https://doi.org/10.3390/ijerph14060632

Anjali, Kumar, S., Korra, T., Thakur, R., Arutselvan, R., Kashyap, A. S., Nehela, Y., Chaplygin, V., Minkina, T., and Keswani, C. (2023). Role of plant secondary metabolites in defence and transcriptional regulation in response to biotic stress. *Plant Stress*, *8*(April), 100154. https://doi.org/10.1016/j.stress.2023.100154

Bajwa, A. A., Farooq, M., Al-Sadi, A. M., Nawaz, A., Jabran, K., and Siddique, K. H. M. (2020). Impact of climate change on biology and management of wheat pests. *Crop Protection*, *137*, 105304. https://doi.org/10.1016/j.cropro.2020.105304

Balfourier, F., Bouchet, S., Robert, S., De Oliveira, R., Rimbert, H., Kitt, J., Choulet, F., Consortium, I. W. G. S., Consortium, B., and Paux, E. (2024). Worldwide phylogeography and history of wheat genetic diversity. *Science Advances*, *5*(5), eaav0536. https://doi.org/10.1126/sciadv.aav0536

Barlow, K. M., Christy, B. P., O'Leary, G. J., Riffkin, P. A., and Nuttall, J. G. (2015). Simulating the impact of extreme heat and frost events on wheat crop production: A review. *Field Crops Research*, *171*, 109–119. https://doi.org/10.1016/j.fcr.2014.11.010

Beccari, G., Colasante, V., Tini, F., Senatore, M. T., Prodi, A., Sulyok, M., and Covarelli, L. (2018). Causal agents of Fusarium head blight of durum wheat (*Triticum durum* Desf.) in central Italy and their in vitro biosynthesis of secondary metabolites. *Food Microbiology*, *70*, 17–27. https://doi.org/10.1016/j.fm.2017.08.016

Beccari, Giovanni, Prodi, A., Tini, F., Bonciarelli, U., Onofri, A., Oueslati, S., Limayma, M., and Covarelli, L. (2017). Changes in the Fusarium head blight complex of malting barley in a three-year field experiment in Italy. *Toxins*, *9*(4), 2011–2013. https://doi.org/10.3390/toxins9040120

Bechtel, D. B., Abecassis, J., Shewry, P. R., and Evers, A. D. (2009). Chapter 3: Development, Structure, and Mechanical Properties of the Wheat Grain. In *WHEAT: Chemistry and Technology*, *Fourth Edition* (pp. 51–95). hhttps://doi.org/10.1094/9781891127557.003

Belay, G., Tesemma, T., Bechere, E., and Mitiku, D. (1995). Natural and human selection for purple-grain tetraploid wheats in the Ethiopian highlands. *Genetic Resources and Crop Evolution*, *42*(4), 387–391. https://doi.org/10.1007/BF02432143

Beleggia, R., Ficco, D. B. M., Pecorella, I., De Vita, P., Nigro, F. M., Giovanniello, V., and Colecchia, S. A. (2021). Effect of sowing date on bioactive compounds and grain morphology of three pigmented cereal species. *Agronomy*, *11*(3). https://doi.org/10.3390/agronomy11030591

Buerstmayr, H., Ban, T., and Anderson, J. A. (2009). QTL mapping and marker-assisted selection for Fusarium head blight resistance in wheat: a review. *Plant Breeding*, *128*(1), 1–26. https://doi.org/10.1111/j.1439-

0523.2008.01550.x

Bustos, D. V., Riegel, R., and Calderini, D. F. (2012). Anthocyanin content of grains in purple wheat is affected by grain position, assimilate availability and agronomic management. *Journal of Cereal Science*, *55*(3), 257–264. https://doi.org/10.1016/j.jcs.2011.12.001

Castañeda-Ovando, A., Pacheco-Hernández, M. de L., Páez-Hernández, M. E., Rodríguez, J. A., and Galán-Vidal, C. A. (2009). Chemical studies of anthocyanins: A review. *Food Chemistry*, *113*(4), 859–871. https://doi.org/10.1016/j.foodchem.2008.09.001

Chakraborty, S., and Newton, A. C. (2011). Climate change, plant diseases and food security: an overview. *Plant Pathology*, *60*(1), 2–14. https://doi.org/10.1111/j.1365-3059.2010.02411.x

Chen, X., Lan, W., and Xie, J. (2024). Natural phenolic compounds: Antimicrobial properties, antimicrobial mechanisms, and potential utilization in the preservation of aquatic products. *Food Chemistry*, *440*, 138198. https://doi.org/10.1016/j.foodchem.2023.138198

Chrpová, J., Orsák, M., Martinek, P., Lachman, J., & Trávníčková, M. (2021). Potential Role and Involvement of Antioxidants and Other Secondary Metabolites of Wheat in the Infection Process and Resistance to Fusarium spp. In *Agronomy* (Vol. 11, Issue 11). https://doi.org/10.3390/agronomy11112235

Clayton, W. D., and Renvoize, S. A. (1986). Genera graminum. Grasses of the World. *Kew Bulletin Additional Series*, *13*, 389pp.

Covarelli, L., Beccari, G., Prodi, A., Generotti, S., Etruschi, F., Juan, C., Ferrer, E., and Mañes, J. (2015). *Fusarium* species, chemotype characterisation and trichothecene contamination of durum and soft wheat in an area of central Italy. *Journal of the Science of Food and Agriculture*, *95*(3), 540–551. https://doi.org/10.1002/jsfa.6772

De Ruyck, K., De Boevre, M., Huybrechts, I., and De Saeger, S. (2015). Dietary mycotoxins, co-exposure, and carcinogenesis in humans: Short review. *Mutation Research/Reviews in Mutation Research*, *766*, 32–41. https://doi.org/10.1016/j.mrrev.2015.07.003

Dhokane, D., Karre, S., Kushalappa, A. C., and McCartney, C. (2016). Integrated metabolo-transcriptomics reveals Fusarium head blight candidate resistance genes in wheat QTL-Fhb2. *PLoS ONE*, *11*(5), 1–27. https://doi.org/10.1371/journal.pone.0155851

Di Lorenzo, C., Colombo, F., Biella, S., Stockley, C., and Restani, P. (2021). Polyphenols and Human Health: The Role of Bioavailability. In *Nutrients* (Vol. 13, Issue 1). https://doi.org/10.3390/nu13010273

Dutta, D., Karmakar, S., Hossain, A., Sadhukhan, R., Atta, K., and Pramanick, S. (2023). *Chapter 1 - Wheat and abiotic stress challenges: An overview* (M. K. Khan, A. Pandey, M. Hamurcu, O. P. Gupta, and S. B. T.-A. S. in W. Gezgin (eds.); pp. 1–13). Academic Press. https://doi.org/10.1016/B978-0-323-95368-9.00006-0

Dweba, C. C., Figlan, S., Shimelis, H. A., Motaung, T. E., Sydenham, S., Mwadzingeni, L., and Tsilo, T. J. (2017). Fusarium head blight of wheat: Pathogenesis and control strategies. *Crop Protection*, *91*(November), 114–122. https://doi.org/10.1016/j.cropro.2016.10.002

Elias, E. M., Manthey, F. A., Stack, R. W., and Kianian, S. F. (2005). Breeding Efforts to Develop Fusarium Head Blight Resistant Durum Wheat in North Dakota. *Proceedings of the 2005 National Fusarium Head Blight Forum*, 31. https://doi.org/10.1007/s00122-007-0577-2

Enaru, B., Drețcanu, G., Pop, T. D., Stănilă, A., and Diaconeasa, Z. (2021). Anthocyanins: Factors Affecting Their Stability and Degradation. *Antioxidants (Basel, Switzerland)*, *10*(12). https://doi.org/10.3390/antiox10121967

FAO, IFAD, UNICEF, W. and W. (2023). The State of Food Security and Nutrition in the World 2023. In *The State of Food Security and Nutrition in the World 2023*. https://doi.org/10.4060/cc3017en

FAO. (2024). *Production / Crops and livestock products - Metadata - Food and Agriculture Organization of the United Nations (FAO)*. https://www.fao.org/faostat/en/#data/QCL/metadata

Feekes, W. (1941). De tarwe en haar milieu. *Vers XVII Tech. Tarwe. Comm., Groningen, 1941*.

Ficco, B. D. M., De Simone, V., De Leonardis, A. M., Giovanniello, V., Del Nobile, A. M., Padalino, L., Lecce, L.,

Borrelli, G. M., and De Vita, P. (2016). Use of purple durum wheat to produce naturally functional fresh and dry pasta Running title. Purple durum wheat: a natural ingredient for functional pasta. *Food Chemistry*, *205*, 187–195. https://doi.org/10.1016/j.foodchem.2016.03.014

Ficco, D. B. M., Mastrangelo, A. M., Trono, D., Borrelli, G. M., De Vita, P., Fares, C., Beleggia, R., Platani, C., and Papa, R. (2014). The colours of durum wheat: A review. *Crop and Pasture Science*, *65*(1), 1–15. https://doi.org/10.1016/j.foodchem.2016.03.014

Ficco, D., De Simone, V., Colecchia, S. A., Pecorella, I., Platani, C., Nigro, F., Finocchiaro, F., Papa, R., and De Vita, P. (2014). Genetic variability in anthocyanin composition and nutritional properties of blue, purple, and red bread (*Triticum aestivum* L.) and durum (*Triticum turgidum* L. ssp. *turgidum* convar. *durum*) wheats. *Journal of Agricultural and Food Chemistry*, *62*(34), 8686–8695. https://doi.org/10.1021/jf5003683

Figueroa, M., Hammond-kosack, K. I. M. E., and Solomon, P. S. (2018). A review of wheat diseases — a field perspective. *Molecular Plant Pathology*, *9*(6), 1523–1536. https://doi.org/10.1111/mpp.12618

Finger, R., Schneider, K., Candel, J., and Möhring, N. (2024). Europe needs better pesticide policies to reduce impacts on biodiversity. *Food Policy*, *125*, 102632. https://doi.org/10.1016/j.foodpol.2024.102632

Flor, H. H. (1971). Current Status of the Gene-For-Gene Concept. *Annual Review of Phytopathology*, *9*(Volume 9, 1971), 275–296. https://doi.org/10.1146/annurev.py.09.090171.001423

Francesconi, S., Harfouche, A., Maesano, M., and Balestra, G. M. (2021). UAV-Based Thermal , RGB Imaging and Gene Expression Analysis Allowed Detection of Fusarium Head Blight and Gave New Insights Into the Physiological Responses to the Disease in Durum Wheat. *Frontiers in Plant Science*, 12(April), 1–19. https://doi.org/10.3389/fpls.2021.628575

Francesconi, S., Steiner, B., Buerstmayr, H., Lemmens, M., Sulyok, M., and Balestra, G. M. (2020). Chitosan Hydrochloride Decreases *Fusarium graminearum* Growth and Virulence and Boosts Growth, Development and Systemic Acquired Resistance in Two Durum Wheat Genotypes. *Molecules*, 1–29. https://doi.org/10.3390/molecules25204752

Gab-Allah, M. A., Mekete, K. G., Choi, K., and Kim, B. (2021). Occurrence of major type-B trichothecenes and deoxynivalenol-3-glucoside in cereal-based products from Korea. *Journal of Food Composition and Analysis*, *99*, 103851. https://doi.org/10.1016/j.jfca.2021.103851

Gamel, T. H., Saeed, S. M., Ali, R., and Abdel-Aal, E.-S. M. (2023). Purple Wheat: Food Development, Anthocyanin Stability, and Potential Health Benefits. In *Foods* (Vol. 12, Issue 7). https://doi.org/10.3390/foods12071358

Gamel, T. H., Wright, A. J., Pickard, M., and Abdel-Aal, E.-S. M. (2020). Characterization of anthocyanin-containing purple wheat prototype products as functional foods with potential health benefits. *Cereal Chemistry*, *97*(1), 34–38. https://doi.org/10.1002/cche.10190

Garg, M., Chawla, M., Chunduri, V., Kumar, R., Sharma, S., Sharma, N. K., Kaur, N., Kumar, A., Mundey, J. K., Saini, M. K., and Singh, S. P. (2016). Transfer of grain colors to elite wheat cultivars and their characterization. *Journal of Cereal Science*, *71*(September 2018), 138–144. https://doi.org/10.1016/j.jcs.2016.08.004

Garg, M., Kaur, S., Sharma, A., Kumari, A., Tiwari, V., Sharma, S., Kapoor, P., Sheoran, B., Goyal, A., and Krishania, M. (2022). Rising Demand for Healthy Foods-Anthocyanin Biofortified Colored Wheat Is a New Research Trend. *Frontiers in Nutrition*, *9*. https://doi.org/10.3389/fnut.2022.878221

Gaut, B. S. (2002). Evolutionary dynamics of grass genomes. *New Phytologist*, *154*(1), 15–28. https://doi.org/10.1046/j.1469-8137.2002.00352.x

Gebhardt, Y. H., Witte, S., Steuber, H., Matern, U., and Martens, S. (2007). Evolution of flavone synthase I from parsley flavanone 3beta-hydroxylase by site-directed mutagenesis. *Plant Physiology*, *144*(3), 1442–1454. https://doi.org/10.1104/pp.107.098392

Gellatly, K., and Dennis, D. T. (2011). *4.02 - Plant Biotechnology and GMOs* (M. B. T.-C. B. (Second E. Moo-Young (ed.); pp. 9–22). Academic Press. https://doi.org/10.1016/B978-0-08-088504-9.00272-5

Giancaspro, A., Lionetti, V., Giove, S. L., Zito, D., Fabri, E., Reem, N., Zabotina, O. A., De Angelis, E., Monaci, L., Bellincampi, D., & Gadaleta, A. (2018). Cell wall features transferred from common into durum wheat to

improve Fusarium Head Blight resistance. *Plant Science*, *274*, 121–128. https://doi.org/10.1016/j.plantsci.2018.05.016

Giroux, M. E., Bourgeois, G., Dion, Y., Rioux, S., Pageau, D., Zoghlami, S., Parent, C., Vachon, E., and Vanasse, A. (2016). Evaluation of forecasting models for fusarium head blight of wheat under growing conditions of Quebec, Canada. *Plant Disease*, *100*(6), 1192–1201. https://doi.org/10.1094/PDIS-04-15-0404-RE

Gomez, C., Conejero, G., Torregrosa, L., Cheynier, V., Terrier, N., and Ageorges, A. (2011). In vivo grapevine anthocyanin transport involves vesicle-mediated trafficking and the contribution of anthoMATE transporters and GST. *The Plant Journal*, *67*(6), 960–970. https://doi.org/10.1111/j.1365-313X.2011.04648.x

Gordeeva, E., Badaeva, E., Yudina, R., Shchukina, L., Shoeva, O., and Khlestkina, E. (2019). Marker-Assisted Development of a Blue-Grained Substitution Line Carrying the Thinopyrum ponticum Chromosome 4Th(4D) in the Spring Bread Wheat Saratovskaya 29 Background. In *Agronomy* (Vol. 9, Issue 11). https://doi.org/10.3390/agronomy9110723

Gordeeva, E., Shoeva, O., Mursalimov, S., Adonina, I., and Khlestkina, E. (2022). Fine Points of Marker-Assisted Pyramiding of Anthocyanin Biosynthesis Regulatory Genes for the Creation of Black-Grained Bread Wheat (*Triticum aestivum* L.) Lines. In *Agronomy* (Vol. 12, Issue 12). https://doi.org/10.3390/agronomy12122934

Goswami, R. S., and Kistler, H. C. (2004). Heading for disaster: *Fusarium graminearum* on cereal crops. *Molecular Plant Pathology*, *5*(6), 515–525. https://doi.org/10.1111/J.1364-3703.2004.00252.X

Goujon, T., Sibout, R., Eudes, A., MacKay, J., and Jouanin, L. (2003). Genes involved in the biosynthesis of lignin precursors in Arabidopsis thaliana. *Plant Physiology and Biochemistry*, *41*(8), 677–687. https://doi.org/10.1016/S0981-9428(03)00095-0

Gozzi, M., Blandino, M., Dall'Asta, C., Martinek, P., Bruni, R., & Righetti, L. (2023). Anthocyanin Content and *Fusarium* Mycotoxins in Pigmented Wheat (*Triticum aestivum* L. spp. *aestivum*): An Open Field Evaluation. *Plants*, *12*(4). https://doi.org/10.3390/plants12040693

Grote, U., Fasse, A., Nguyen, T. T., and Erenstein, O. (2021). Food Security and the Dynamics of Wheat and Maize Value Chains in Africa and Asia. *Frontiers in Sustainable Food Systems*, *4*. https://doi.org/10.3389/fsufs.2020.617009

Hao, Y., Rasheed, A., Zhu, Z., Wulff, B. B. H., & He, Z. (2020). Harnessing Wheat *Fhb1* for Fusarium Resistance. *Trends in Plant Science*, *25*(1), 1–3. https://doi.org/10.1016/j.tplants.2019.10.006

Hosseinian, F. S., Li, W., and Beta, T. (2008). Measurement of anthocyanins and other phytochemicals in purple wheat. *Food Chemistry*, *109*(4), 916–924. https://doi.org/10.1016/j.foodchem.2007.12.083

Hyles, J., Bloom, M. T., Hunt, J. R., Trethowan, R. M., and Trevaskis, B. (2020). Phenology and related traits for wheat adaptation. *Heredity*. https://doi.org/10.1038/s41437-020-0320-1

Iji, P. (2019). The role of specific cereal grain dietary components in poultry gut function. In *Improving gut health in poultry* (pp. 1–22). https://doi.org/10.19103/AS.2019.0059.23

Irani, N. G., and Grotewold, E. (2005). Light-induced morphological alteration in anthocyanin-accumulating vacuoles of maize cells. *BMC Plant Biology*, *5*(1), 7. https://doi.org/10.1186/1471-2229-5-7

Islam, M. T., Gupta, D. R., Hossain, A., Roy, K. K., He, X., Kabir, M. R., Singh, P. K., Khan, M. A. R., Rahman, M., and Wang, G.-L. (2020). Wheat blast: a new threat to food security. *Phytopathology Research*, *2*(1), 28. https://doi.org/10.1186/s42483-020-00067-6

Jetté-Nantel, S., Hu, W., and Liu, Y. (2020). Economies of scale and mechanization in Chinese corn and wheat production. *Applied Economics*, *52*(25), 2751–2765. https://doi.org/10.1080/00036846.2019.1696933

Jia, Y., Selva, C., Zhang, Y., Li, B., McFawn, L. A., Broughton, S., Zhang, X., Westcott, S., Wang, P., Tan, C., Angessa, T., Xu, Y., Whitford, R., and Li, C. (2020). Uncovering the evolutionary origin of blue anthocyanins in cereal grains. *The Plant Journal*, *101*(5), 1057–1074. https://doi.org/10.1111/tpj.14557

Jiang, Q., Jiang, W., Hu, N., Tang, R., Dong, Y., Wu, H., Liu, T., Guan, L., Zhang, H., Hou, J., Chai, G., and Wang, Z. (2023). Light-Induced TaHY5-7A and TaBBX-3B Physically Interact to Promote PURPLE PERICARP-MYB 1

Expression in Purple-Grained Wheat. *Plants*, *12*(16). https://doi.org/10.3390/plants12162996

Jing, N., Song, J., Liu, Z., Wang, L., and Jiang, G. (2020). Glycosylation of anthocyanins enhances the apoptosis of colon cancer cells by handicapping energy metabolism. *BMC Complementary Medicine and Therapies*, *20*(1), 1–13. https://doi.org/10.1186/s12906-020-03096-y

Jones, J. D. G., & Dangl, J. L. (2006). The plant immune system. *Nature*, *444*(7117), 323–329. https://doi.org/10.1038/nature05286

Kamble, U., Mishra, C. N., Govindan, V., Sharma, A. K., Pawar, S., Kumar, S., Krishnappa, G., Gupta, O. P., Singh, G. P., and Singh, G. (2022). Ensuring Nutritional Security in India through Wheat Biofortification: A Review. In *Genes* (Vol. 13, Issue 12). https://doi.org/10.3390/genes13122298

Kapoor, P., Sharma, S., Tiwari, A., Kaur, S., Kumari, A., Sonah, H., Goyal, A., Krishania, M., and Garg, M. (2023). Genome–Transcriptome Transition Approaches to Characterize Anthocyanin Biosynthesis Pathway Genes in Blue, Black and Purple Wheat. In *Genes* (Vol. 14, Issue 4). https://doi.org/10.3390/genes14040809

Karre, S., Kumar, A., Yogendra, K., Kage, U., Kushalappa, A., & Charron, J. B. (2019). HvWRKY23 regulates flavonoid glycoside and hydroxycinnamic acid amide biosynthetic genes in barley to combat Fusarium head blight. *Plant Molecular Biology*, *100*(6), 591–605. https://doi.org/10.1007/s11103-019-00882-2

Kebebew, F., Tsehaye, Y., and McNeilly, T. (2001). Diversity of durum wheat (*Triticum durum* Desf.) at in situ conservation sites in North Shewa and Bale, Ethiopia. *Journal of Agricultural Science*, *136*(4), 383–392. https://doi.org/10.1017/S0021859601008887

Keppenne, V. D., and Baenziger, P. S. (1990). Inheritance of the blue aleurone trait in diverse wheat crosses. *Genome*, *33*(4), 525–529. https://doi.org/10.1139/g90-078

Khalid, A., Hameed, A., and Tahir, M. F. (2023). Wheat quality: A review on chemical composition, nutritional attributes, grain anatomy, types, classification, and function of seed storage proteins in bread making quality. *Frontiers in Nutrition*, *10*. https://doi.org/10.3389/fnut.2023.1053196

Khaliq, I., Irshad, A., and Ahsan, M. (2008). Awns and flag leaf contribution towards grain yield in spring wheat (Triticum aestivum L.). *Cereal Research Communications*, *36*(1), 65–76. https://doi.org/10.1556/crc.36.2008.1.7

Khan, M. K., Pandey, A., Athar, T., Choudhary, S., Deval, R., Gezgin, S., Hamurcu, M., Topal, A., Atmaca, E., Santos, P. A., Omay, M. R., Suslu, H., Gulcan, K., Inanc, M., Akkaya, M. S., Kahraman, A., and Thomas, G. (2020). Fusarium head blight in wheat: contemporary status and molecular approaches. *3 Biotech*, *10*(4), 1–17. https://doi.org/10.1007/s13205-020-2158-x

Khan, R., Anwar, F., and Ghazali, F. M. (2024). A comprehensive review of mycotoxins: Toxicology, detection, and effective mitigation approaches. *Heliyon*, *10*(8), e28361. https://doi.org/10.1016/j.heliyon.2024.e28361

Kheiri, A., Moosawi Jorf, S. A., and Malihipour, A. (2019). Infection process and wheat response to Fusarium head blight caused by *Fusarium graminearum*. *European Journal of Plant Pathology*, *153*(2), 489–502. https://doi.org/10.1007/s10658-018-1576-7

Kolawole, O., Siri-Anusornsak, W., Petchkongkaew, A., and Elliott, C. (2024). A systematic review of global occurrence of emerging mycotoxins in crops and animal feeds, and their toxicity in livestock. *Emerging Contaminants*, *10*(3), 100305. https://doi.org/10.1016/j.emcon.2024.100305

Lachman, J., Martinek, P., Kotíková, Z., Orsák, M., and Šulc, M. (2017). Genetics and chemistry of pigments in wheat grain – A review. *Journal of Cereal Science*, *74*, 145–154. https://doi.org/10.1016/j.jcs.2017.02.007

Lahlali, R., Kumar, S., Wang, L., Forseille, L., Sylvain, N., Korbas, M., Muir, D., Swerhone, G., Lawrence, J. R., Fobert, P. R., Peng, G., and Karunakaran, C. (2016). Cell Wall Biomolecular Composition Plays a Potential Role in the Host Type II Resistance to Fusarium Head Blight in Wheat. *Frontiers in Microbiology*, *7*. https://doi.org/10.3389/fmicb.2016.00910

Langridge, P., Alaux, M., Almeida, N. F., Ammar, K., Baum, M., Bekkaoui, F., Bentley, A. R., Beres, B. L., Berger, B., Braun, H.-J., Brown-Guedira, G., Burt, C. J., Caccamo, M. J., Cattivelli, L., Charmet, G., Civáň, P., Cloutier, S., Cohan, J.-P., Devaux, P. J., … Zhang, X. (2022). Meeting the Challenges Facing Wheat Production: The Strategic Research Agenda of the Global Wheat Initiative. In *Agronomy* (Vol. 12, Issue 11).

https://doi.org/10.3390/agronomy12112767

Lersten, N. R. (1987). Morphology and Anatomy of the Wheat Plant. In *Wheat and Wheat Improvement* (pp. 33–75). https://doi.org/10.2134/agronmonogr13.2ed.c2

Li, X. Lan, Lü, X., Wang, X. Hong, Peng, Q., Zhang, M. Sheng, And Ren, M. Jian. (2020). Biotic and abiotic stress-responsive genes are stimulated to resist drought stress in purple wheat. *Journal of Integrative Agriculture*, *19*(1), 33–50. https://doi.org/10.1016/S2095-3119(19)62659-6

Lidwell-Durnin, J., and Lapthorn, A. (2020). The threat to global food security from wheat rust: ethical and historical issues in fighting crop diseases and preserving genetic diversity. *Global Food Security*, *26*, 100446. https://doi.org/10.1016/j.gfs.2020.100446

Lionetti, V., Giancaspro, A., Fabri, E., Giove, S. L., Reem, N., Zabotina, O. A., Blanco, A., Gadaleta, A., and Bellincampi, D. (2015). Cell wall traits as potential resources to improve resistance of durum wheat against Fusarium graminearum. *BMC Plant Biology*, *15*(1), 6. https://doi.org/10.1186/s12870-014-0369-1

Liu, H., Liu, Z., Wu, Y., Zheng, L., and Zhang, G. (2021). Regulatory Mechanisms of Anthocyanin Biosynthesis in Apple and Pear. In *International Journal of Molecular Sciences* (Vol. 22, Issue 16). https://doi.org/10.3390/ijms22168441

Liu, S., Jiang, J., Ma, Z., Xiao, M., Yang, L., Tian, B., Yu, Y., Bi, C., Fang, A., and Yang, Y. (2022). The Role of Hydroxycinnamic Acid Amide Pathway in Plant Immunity. *Frontiers in Plant Science*, *13*. https://doi.org/10.3389/fpls.2022.922119

Ma, Y., Ma, X., Gao, X., Wu, W., and Zhou, B. (2021). Light Induced Regulation Pathway of Anthocyanin Biosynthesis in Plants. In *International Journal of Molecular Sciences* (Vol. 22, Issue 20). https://doi.org/10.3390/ijms222011116

Mahlein, A., Alisaac, E., Masri, A. Al, Behmann, J., Dehne, H., and Oerke, E. (2019). Comparison and Combination of Thermal, Fluorescence, and Hyperspectral Imaging for Monitoring Fusarium Head Blight of Wheat on Spikelet Scale. *Sensors* 19(10):2281. https://doi.org/10.3390/s19102281

Marcussen, T., Sandve, S. R., Heier, L., Spannagl, M., Pfeifer, M., The International Wheat Genome Sequencing Consortium, Jakobsen, K. S., Wulff, B. B. H., Steuernagel, B., Mayer, K. F. X., Olsen, O.-A., Rogers, J., Doležel, J., Pozniak, C., Eversole, K., Feuillet, C., Gill, B., Friebe, B., Lukaszewski, A. J., … Praud, S. (2014). Ancient hybridizations among the ancestral genomes of bread wheat. *Science*, *345*(6194), 1250092. https://doi.org/10.1126/science.1250092

Marin, S., Ramos, A. J., Cano-Sancho, G., and Sanchis, V. (2013). Mycotoxins: Occurrence, toxicology, and exposure assessment. *Food and Chemical Toxicology*, *60*, 218–237. https://doi.org/10.1016/j.fct.2013.07.047

Martin, C., Schöneberg, T., Vogelgsang, S., Bertossa, M., Mauch-mani, B., Mascher, F., Mauch-mani, B., Mascher, F., Martin, C., Schöneberg, T., Vogelgsang, S., Vincenti, J., & Bertossa, M. (2017). Factors of wheat grain resistance to Fusarium head blight. *Phytopathologia Mediterranea*. https://doi.org/10.14601/Phytopathol_Mediterr-20292

Martinek, P., Škorpík, M., Chrpová, J., Fučík, P., & Schweiger, J. (2013). Development of the new winter wheat variety Skorpion with blue grain. *Czech Journal of Genetics and Plant Breeding*, *49*(2), 90–94. https://doi.org/10.17221/7/2013-cjgpb

Martínez, C. S., Bustos, M. C., and León, A. E. (2016). *Production of Pastas with Bread Wheat Flour BT - Modernization of Traditional Food Processes and Products* (A. McElhatton and M. M. El Idrissi (eds.); pp. 75–89). Springer US. https://doi.org/10.1007/978-1-4899-7671-0_8

Mastrangelo, A. M., and Cattivelli, L. (2021). What Makes Bread and Durum Wheat Different? *Trends in Plant Science*, *26*(7), 677–684. https://doi.org/10.1016/j.tplants.2021.01.004

Matsuoka, Y. (2011). Evolution of Polyploid Triticum Wheats under Cultivation: The Role of Domestication, Natural Hybridization and Allopolyploid Speciation in their Diversification. *Plant and Cell Physiology*, *52*(5), 750–764. https://doi.org/10.1093/pcp/pcr018

Maurino, V. G., Drincovich, M. F., Casati, P., Andreo, C. S., Edwards, G. E., Ku, M. S. B., Gupta, S. K., and Franceschi, V. R. (1997). NADP-malic enzyme: immunolocalization in different tissues34 plant maize and the C3

plant wheat. *Journal of Experimental Botany*, *48*(3), 799–811. https://doi.org/10.1093/jxb/48.3.799

McCartney, C. A., Somers, D. J., Fedak, G., DePauw, R. M., Thomas, J., Fox, S. L., Humphreys, D. G., Lukow, O., Savard, M. E., McCallum, B. D., Gilbert, J., and Cao, W. (2007). The evaluation of FHB resistance QTLs introgressed into elite Canadian spring wheat germplasm. *Molecular Breeding*, *20*(3), 209–221. https://doi.org/10.1007/s11032-007-9084-z

McDonald, P., Morgan, C. A., Sinclair, L. A., and Wilkinson, R. G. (2011). *Animal Nutrition (7th edn.)*.

McMullen, M., Bergstrom, G., De Wolf, E., Dill-Macky, R., Hershman, D., Shaner, G., and Van Sanford, D. (2012). A Unified Effort to Fight an Enemy of Wheat and Barley: Fusarium Head Blight. *Plant Disease*, *96*(12), 1712–1728. https://doi.org/10.1094/PDIS-03-12-0291-FE

Mesterhazy, A. (2020). Updating the breeding philosophy of wheat to fusarium head blight (Fhb): Resistance components, qtl identification, and phenotyping—a review. In *Plants* (Vol. 9, Issue 12). https://doi.org/10.3390/plants9121702

Mesterházy, A. (1995). Types and components of resistance to Fusarium head blight of wheat. *Plant Breeding*, *114*(5), 377–386. https://doi.org/10.1111/j.1439-0523.1995.tb00816.x

Mesterházy, Á., Oláh, J., and Popp, J. (2020). Losses in the Grain Supply Chain: Causes and Solutions. In *Sustainability* (Vol. 12, Issue 6). https://doi.org/10.3390/su12062342

Mielniczuk, E., and Skwaryło-Bednarz, B. (2020). Fusarium head blight, mycotoxins and strategies for their reduction. In *Agronomy* (Vol. 10, Issue 4). MDPI AG. https://doi.org/10.3390/agronomy10040509

Milec, Z., Strejčková, B., and Šafář, J. (2023). Contemplation on wheat vernalization. *Frontiers in Plant Science*, *13*. https://doi.org/10.3389/fpls.2022.1093792

Miller, J. D., Young, J. C., and Sampson, D. R. (1985). Deoxynivalenol and Fusarium Head Blight Resistance in Spring Cereals. *Journal of Phytopathology*, *113*(4), 359–367. https://doi.org/10.1111/j.1439-0434.1985.tb04837.x

Mirjani Hörberg, H. (2002). Patterns of splash dispersed conidia of *Fusarium poae* and *Fusarium culmorum*. *European Journal of Plant Pathology*, *108*, 73–80. http://link.springer.com/article/10.1023/A:1013936624884

Moonjely, S., Ebert, M., Paton-Glassbrook, D., Noel, Z. A., Roze, L., Shay, R., Watkins, T., and Trail, F. (2023). Update on the state of research to manage Fusarium head blight. *Fungal Genetics and Biology*, *169*, 103829. https://doi.org/10.1016/j.fgb.2023.103829

Nguyen, V. D. H., Nguyen, T. T. T., Huynh, T. N. P., Ho, H. H., Nguyen, A. T. V, and Trinh, L. T. P. (2024). Effective control of Fusarium wilt on tomatoes using a combination of phenolic-rich plant extracts. *European Journal of Plant Pathology*. https://doi.org/10.1007/s10658-024-02830-3

Oliver, R. E., Stack, R. W., Miller, J. D., and Cai, X. (2007). Reaction of wild emmer wheat accessions to fusarium head blight. *Crop Science*, *47*(2), 893–899. https://doi.org/10.2135/cropsci2006.08.0531

Padhy, A. K., Kaur, P., Singh, S., Kashyap, L., and Sharma, A. (2024). Colored wheat and derived products: key to global nutritional security. *Critical Reviews in Food Science and Nutrition*, *64*(7), 1894–1910. https://doi.org/10.1080/10408398.2022.2119366

Pancaldi, D., Tonti, S., Prodi, A., Salomoni, D., Dal Prà, M., Nipoti, P., Alberti, I., and Pisi, A. (2010). Survey of the main causal agents of fusarium head blight of durum wheat around Bologna, northern Italy. *Phytopathologia Mediterranea*, *49*(2), 258–266. https://doi.org/10.14601/Phytopathol_Mediterr-3442

Parry, D. W., Jenkinson, P., and McLeod, L. (1995). Fusarium ear blight (scab) in small grain cereals—a review. *Plant Pathology*, *44*(2), 207–238. https://doi.org/10.1111/j.1365-3059.1995.tb02773.x

Paul, P. A., Lipps, P. E., and Madden, L. V. (2004). Rain Splash Dispersal of *Gibberella zeae* Within Wheat Canopies in Ohio. *Phytopathology*, *94*, 1342–1349. https://doi.org/10.1094/PHYTO.2004.94.12.1342

Pérez-Gianmarco, T. I., Severini, A. D., and González, F. G. (2020). Photoperiod-sensitivity genes (Ppd-1): quantifying their effect on the photoperiod response model in wheat. *Journal of Experimental Botany*, *71*(3), 1185–1198. https://doi.org/10.1093/jxb/erz483

Phillips, R. L. (2014). *Green Revolution: Past, Present, and Future* (N. K. B. T.-E. of A. and F. S. Van Alfen (ed.); pp. 529–538). Academic Press. https://doi.org/10.1016/B978-0-444-52512-3.00208-4

Pintye, A., Bacsó, R., and Kovács, G. M. (2024). Trans-kingdom fungal pathogens infecting both plants and humans, and the problem of azole fungicide resistance. *Frontiers in Microbiology*, *15*. https://doi.org/10.3389/fmicb.2024.1354757

Pott, D. M., Osorio, S., and Vallarino, J. G. (2019). From Central to Specialized Metabolism: An Overview of Some Secondary Compounds Derived From the Primary Metabolism for Their Role in Conferring Nutritional and Organoleptic Characteristics to Fruit. *Frontiers in Plant Science*, *10*. https://doi.org/10.3389/fpls.2019.00835

Prat, N., Guilbert, C., Prah, U., Wachter, E., Steiner, B., Langin, T., Robert, O., and Buerstmayr, H. (2017). QTL mapping of Fusarium head blight resistance in three related durum wheat populations. *Theoretical and Applied Genetics*, *130*(1), 13–27. https://doi.org/10.1007/s00122-016-2785-0

Ramaroson, M.-L., Koutouan, C., Helesbeux, J.-J., Le Clerc, V., Hamama, L., Geoffriau, E., and Briard, M. (2022). Role of Phenylpropanoids and Flavonoids in Plant Resistance to Pests and Diseases. In *Molecules* (Vol. 27, Issue 23). https://doi.org/10.3390/molecules27238371

Rauf, S., Zaharieva, M., Warburton, M. L., Zhang, P., AL-Sadi, A. M., Khalil, F., Kozak, M., and Tariq, S. A. (2015). Breaking wheat yield barriers requires integrated efforts in developing countries. *Journal of Integrative Agriculture*, *14*(8), 1447–1474. https://doi.org/10.1016/S2095-3119(15)61035-8

Reynolds, M., Bonnett, D., Chapman, S. C., Furbank, R. T., Manès, Y., Mather, D. E., and Parry, M. A. J. (2011). Raising yield potential of wheat. I. Overview of a consortium approach and breeding strategies. *Journal of Experimental Botany*, *62*(2), 439–452. https://doi.org/10.1093/jxb/erq311

Rguez, S., Papetti, A., Bourguou, S., Msaada, K., Hammami, M., Mkadmini Hammi, K., and Hamrouni Sellami, I. (2022). Antifungal and antioxidant effects of phenolic acids and flavonol glycosides from Tetraclinis articulata . *Archives of Phytopathology and Plant Protection*, *55*(3), 284–302. https://doi.org/10.1080/03235408.2021.2015888

Rosales, T. K. O., and Fabi, J. P. (2022). Nanoencapsulated anthocyanin as a functional ingredient: Technological application and future perspectives. *Colloids and Surfaces B: Biointerfaces*, *218*(April). https://doi.org/10.1016/j.colsurfb.2022.112707

Saini, P., Kumar, N., Kumar, S., Mwaurah, P. W., Panghal, A., Attkan, A. K., Singh, V. K., Garg, M. K., and Singh, V. (2020). Bioactive compounds, nutritional benefits and food applications of colored wheat: a comprehensive review. *Critical Reviews in Food Science and Nutrition*, *0*(0), 1–14. https://doi.org/10.1080/10408398.2020.1793727

Salhi, N., Mohammed Saghir, S. A., Terzi, V., Brahmi, I., Ghedairi, N., and Bissati, S. (2017). Antifungal Activity of Aqueous Extracts of Some Dominant Algerian Medicinal Plants. *BioMed Research International*, *2017*. https://doi.org/10.1155/2017/7526291

Sánchez-Maldonado, A. F., Schieber, A., and Gänzle, M. G. (2016). Antifungal activity of secondary plant metabolites from potatoes (Solanum tuberosum L.): Glycoalkaloids and phenolic acids show synergistic effects. *Journal of Applied Microbiology*, *120*(4), 955–965. https://doi.org/10.1111/jam.13056

Saulnier, L., Guillon, F., and Chateigner-Boutin, A. L. (2012). Cell wall deposition and metabolism in wheat grain. *Journal of Cereal Science*, *56*(1), 91–108. https://doi.org/10.1016/j.jcs.2012.02.010

Schöneberg, T., Martin, C., Wettstein, F. E., Bucheli, T. D., Mascher, F., Bertossa, M., Musa, T., Keller, B., Schöneberg, T., Martin, C., Wettstein, F. E., Bucheli, T. D., Mascher, F., Bertossa, M., Musa, T., Keller, B., and Fusarium, S. V. (2016). Food Additives and Contaminants : Part A *Fusarium* and mycotoxin spectra in Swiss barley are affected by various cropping techniques. *Food Additives and Contaminants: Part A*, *33*(10), 1608–1619. https://doi.org/10.1080/19440049.2016.1219071

Schroeder, H. W., and Christensen, J. J. (1963). Factors affecting resistance of wheat to scab caused by *Gibberella zeae*. *Phytopathology*, *53*(7, 1), 831–838.

Serra, V., Salvatori, G., and Pastorelli, G. (2021). Dietary Polyphenol Supplementation in Food Producing Animals: Effects on the Quality of Derived Products. In *Animals* (Vol. 11, Issue 2). https://doi.org/10.3390/ani11020401

Sgaramella, N., Nigro, D., Pasqualone, A., Signorile, M. A., Laddomada, B., Sonnante, G., Blanco, E., Simeone, R., and Blanco, A. (2023). Genetic Mapping of Flavonoid Grain Pigments in Durum Wheat. In *Plants* (Vol. 12, Issue 8). https://doi.org/10.3390/plants12081674

Shah, J., & Zeier, J. (2013). Long-distance communication and signal amplification in systemic acquired resistance. *Frontiers in Plant Science*, *4*. https://doi.org/10.3389/fpls.2013.00030

Shang, Q., Wang, Y., Tang, H., Sui, N., Zhang, X., and Wang, F. (2021). Genetic, hormonal, and environmental control of tillering in wheat. *The Crop Journal*, *9*(5), 986–991. https://doi.org/10.1016/j.cj.2021.03.002

Shewry, P. R. (2009). Wheat. *Journal of Experimental Botany*, *60*(6), 1537–1553. https://doi.org/10.1093/jxb/erp058

Sinha, A., Singh, L., & Rawat, N. (2022). Current understanding of atypical resistance against fungal pathogens in wheat. *Current Opinion in Plant Biology*, *68*, 102247. https://doi.org/10.1016/j.pbi.2022.102247

Singh, R. P., Hodson, D. P., Huerta-Espino, J., Jin, Y., Njau, P., Wanyera, R., Herrera-Foessel, S. A., and Ward, R. W. B. T.-A. in A. (2008). *Will Stem Rust Destroy the World's Wheat Crop?* (Vol. 98, pp. 271–309). Academic Press. https://doi.org/10.1016/S0065-2113(08)00205-8

Soni, N., Altartouri, B., Hegde, N., Duggavathi, R., Nazarian-Firouzabadi, F., & Kushalappa, A. C. (2021). TaNAC032 transcription factor regulates lignin-biosynthetic genes to combat Fusarium head blight in wheat. *Plant Science*, *304*, 110820. https://doi.org/10.1016/j.plantsci.2021.110820

Spagnoletti Zeuli, P. L., and Qualset, C. O. (1990). Flag Leaf Variation and the Analysis of Diversity in Durum Wheat. *Plant Breeding*, *105*(3), 189–202. https://doi.org/10.1111/j.1439-0523.1990.tb01196.x

Spanic, V., Vuletic, M. V., Horvat, D., Sarkanj, B., Drezner, G., & Zdunic, Z. (2020). Changes in antioxidant system during grain development of wheat (*Triticum aestivum* L.) and relationship with protein composition under FHB stress. *Pathogens*, *9*(1), 1–15. https://doi.org/10.3390/pathogens9010017

Steiner, B., Buerstmayr, M., Michel, S., Schweiger, W., Lemmens, M., and Buerstmayr, H. (2017). Breeding strategies and advances in line selection for Fusarium head blight resistance in wheat. *Tropical Plant Pathology*, *42*(3), 165–174. https://doi.org/10.1007/s40858-017-0127-7

Stockley, C., Teissedre, P.-L., Boban, M., Di Lorenzo, C., and Restani, P. (2012). Bioavailability of wine-derived phenolic compounds in humans: a review. *Food and Function*, *3*(10), 995–1007. https://doi.org/10.1039/C2FO10208K

Stout, M. J., Bernaola, L., and Acevedo, F. (2024). Recent history and future trends in host–plant resistance. *Annals of the Entomological Society of America*, saae006. https://doi.org/10.1093/aesa/saae006

Sunil, L., and Shetty, N. P. (2022). Biosynthesis and regulation of anthocyanin pathway genes. *Applied Microbiology and Biotechnology*, *106*(5), 1783–1798. https://doi.org/10.1007/s00253-022-11835-z

Suo, X., Pompei, F., Bonfini, M., Mustafa, A. M., Sagratini, G., Wang, Z., and Vittadini, E. (2023). Quality of wholemeal pasta made with pigmented and ancient wheats. *International Journal of Gastronomy and Food Science*, *31*, 100665. https://doi.org/10.1016/j.ijgfs.2023.100665

Teng, H., and Chen, L. (2019). Polyphenols and bioavailability: an update. *Critical Reviews in Food Science and Nutrition*, *59*(13), 2040–2051. https://doi.org/10.1080/10408398.2018.1437023

Tesemma, T., Becker, H. C., Belay, G., Mitiku, D., Bechere, E., and Tsegaye, S. (1993). Performance of Ethiopian tetraploid wheat landraces at their collection sites. *Euphytica*, *71*(3), 221–230. https://doi.org/10.1007/BF00040411

Thorup-Kristensen, K., Salmerón Cortasa, M., and Loges, R. (2009). Winter wheat roots grow twice as deep as spring wheat roots, is this important for N uptake and N leaching losses? *Plant and Soil*, *322*(1), 101–114. https://doi.org/10.1007/s11104-009-9898-z

Ullah, C., Unsicker, S. B., Fellenberg, C., Constabel, C. P., Schmidt, A., Gershenzon, J., and Hammerbacher, A. (2017). Flavan-3-ols Are an Effective Chemical Defense against Rust Infection . *Plant Physiology*, *175*(4), 1560–1578. https://doi.org/10.1104/pp.17.00842

Vaclavikova, M., Malachova, A., Veprikova, Z., Dzuman, Z., Zachariasova, M., and Hajslova, J. (2013). 'Emerging' mycotoxins in cereals processing chains: Changes of enniatins during beer and bread making. *Food Chemistry*, *136*(2), 750–757. https://doi.org/10.1016/j.foodchem.2012.08.031

Wang, F., Ji, G., Xu, Z., Feng, B., Zhou, Q., Fan, X., and Wang, T. (2021). Metabolomics and Transcriptomics Provide Insights into Anthocyanin Biosynthesis in the Developing Grains of Purple Wheat (Triticum aestivum L.). *Journal of Agricultural and Food Chemistry*, *69*(38), 11171–11184. https://doi.org/10.1021/acs.jafc.1c01719

Wang, X., Wei, X., Tian, Y., Shen, L., and XU, H. (2010). Antifungal Flavonoids from *Ficus sarmentosa* var. henryi (King) Corner. *Agricultural Sciences in China*, *9*(5), 690–694. https://doi.org/10.1016/S1671-2927(09)60144-9

Wang, X., Bi, W., Gao, J., Yu, X., Wang, H., & Liu, D. (2018). Systemic acquired resistance, NPR1, and pathogenesis-related genes in wheat and barley. *Journal of Integrative Agriculture*, *17*(11), 2468–2477. https://doi.org/10.1016/S2095-3119(17)61852-5

Wang, Z., Miao, L., Chen, Y., Peng, H., Ni, Z., Sun, Q., and Guo, W. (2023). Deciphering the evolution and complexity of wheat germplasm from a genomic perspective. *Journal of Genetics and Genomics*, *50*(11), 846–860. https://doi.org/10.1016/j.jgg.2023.08.002

Wegulo, S. N., Baenziger, P. S., Hernandez Nopsa, J., Bockus, W. W., and Hallen-Adams, H. (2015). Management of Fusarium head blight of wheat and barley. *Crop Protection*, *73*, 100–107. https://doi.org/10.1016/j.cropro.2015.02.025

Wrigley, C. (2017). Chapter 4 - Cereal-Grain Morphology and Composition. In C. Wrigley, I. Batey, and D. B. T.-C. G. (Second E. Miskelly (Eds.), *Woodhead Publishing Series in Food Science, Technology and Nutrition* (pp. 55–87). Woodhead Publishing. https://doi.org/10.1016/B978-0-08-100719-8.00004-8

Wu, F., Zhou, Y., Shen, Y., Sun, Z., Li, L., and Li, T. (2022). Linking Multi-Omics to Wheat Resistance Types to Fusarium Head Blight to Reveal the Underlying Mechanisms. *International Journal of Molecular Sciences*, *23*(4). https://doi.org/10.3390/ijms23042280

Xu, M., Nicholson, P., Thomsett, M. A., Simpson, D., Cooke, B. M., Doohan, F. M., Brennan, J., Monaghan, S., Moretti, A., Mule, G., Hornok, L., Beki, E., Tatnell, J., Ritieni, A., and Edwards, S. G. (2008). Relationship between the fungal complex causing Fusarium head blight of wheat and environmental conditions. *Phytopathology*, *98*(1), 69–78. https://doi.org/10.1094/PHYTO-98-1-0069

Xu, X., and Nicholson, P. (2009). Community ecology of fungal pathogens causing wheat head blight. *Annual Review of Phytopathology*, *47*, 83–103. https://doi.org/10.1146/annurev-phyto-080508-081737

Yang, F., Zhang, J., Liu, Q., Liu, H., Zhou, Y., Yang, W., and Ma, W. (2022). Improvement and Re-Evolution of Tetraploid Wheat for Global Environmental Challenge and Diversity Consumption Demand. In *International Journal of Molecular Sciences* (Vol. 23, Issue 4). https://doi.org/10.3390/ijms23042206

Zadoks, J. C., Chang, T. T., and Konzak, C. F. (1974). A decimal code for the growth of cereals. *Weed Research*, *14*, 415–421. https://doi.org/10.1111/j.1365-3180.1974.tb01084.x

Zeven, A. C. (1991). Wheats with purple and blue grains: a review. *Euphytica*, *56*(3), 243–258. https://doi.org/10.1007/BF00042371

Zhang, L., Luo, P., Ren, Z., and Zhang, H. (2011). Controlling fusarium head blight of wheat (*Triticum aestivum* L.) with genetics. *Advances in Bioscience and Biotechnology*, *02*(04), 263–270. https://doi.org/10.4236/abb.2011.24038

Zhang, E. T., Zhang, H., and Tang, W. (2021). Transcriptomic Analysis of Wheat Seedling Responses to the Systemic Acquired Resistance Inducer N-Hydroxypipecolic Acid. *Frontiers in Microbiology*, *12*(February), 1–12. https://doi.org/10.3389/fmicb.2021.621336

Zubair, A., Zaib, S., Ul Ghani, N. N., and Mehboob, S. (2023). Zinc-Fortified Rice: Approach to Improve Dietary Zinc Consumption and Effect on Human Health. *ACS Agricultural Science and Technology*, *3*(11), 926–938. https://doi.org/10.1021/acsagscitech.3c00140

2. Effect of cyanidin 3-*O*-glucoside and other anthocyanins on the production of mycotoxins by *Fusarium avenaceum*

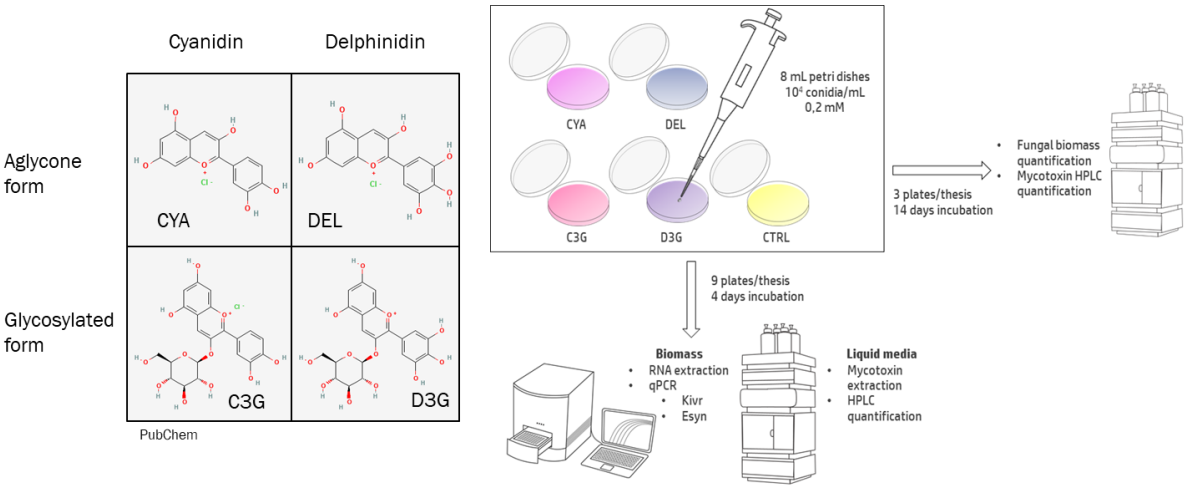

Abstract: Anthocyanins, such as cyanidin 3-*O*-glucoside (C3G) and delphinidin 3-*O*-glucoside (D3G), are among the compounds responsible for the pigmentation in colored wheat grains. The effects of anthocyanins on one of the main causal agents of Fusarium Head Blight have been investigated in this chapter. Different *in vitro* cultures of *Fusarium avenaceum* were treated using four compounds (two anthocyanidins and two anthocyanins). Fungal growth, enniatins production, and the relative expression of enniatin-related (*Esyn* and *Kivr*) and oxidative stress-related genes were evaluated, with a particular focus on C3G. The anthocyanidins, delphinidin and cyanidin, initially (after 6 hours of incubation) reduced conidial germination but not during the entire incubation trial, since, at the end of the incubation period (14 days) no effect on fungal growth was recorded. Conversely, the two anthocyanidins had a diverse effect on mycotoxins reduction and gene expression level. Indeed, delphinidin reduced enniatins accumulation by the downregulation of *Esyn* and *Kivr*, while cyanidin did not affect mycotoxins accumulation as well as gene expression. On the other hand, the two glucosides (C3G and D3G) did not show any fungistatic effect (considering conidial germination after 6 h), but rather they induced a significant increase (45.72% and 25.37% respectively) in fungal biomass accumulation. C3G treatment, in particular, showed a positive dose-dependent effect on fungal biomass. Mycotoxins accumulation was affected by both the glucosides, but while the enniatins reduction due to D3G treatment (-90.4% Enn B1) may be explained by the downregulation of *Esyn* and *Kivr*, the strong and dose-dependent reduction of mycotoxins accumulation due to C3G treatments (-97.8% Enn B) was not caused by *Esyn* and *Kivr* downregulation. A putative explanation of these different behaviors is discussed in the chapter.

Publications:
Selected oral presentation: **L. Felici**, V. Atanasova, N. Ponts, C. Ducos, F. Richard-Forget, S. Francesconi, G. M. Balestra, F. Sestili. *Effect of anthocyanins on the production of mycotoxins by Fusarium spp*. EFS16 16th European Fusarium Seminar, Sapienza University of Rome, Jun 2023, Rome, Italy. hal-04179098f

2.1. Introduction

Fusarium Head Blight (FHB) is among the most widespread worldwide and devastating fungal diseases in wheat and other cereals. It ends in spikelets bleaching and kernels shriveling, resulting in yield and quality losses and grains contamination with fungal mycotoxins (Wegulo et al. 2015). High attention and extensive researches were dedicated for the investigation of toxigenic potential and the occurrence of mycotoxins like zearalenone (ZEA), type B trichothecenes (including deoxynivalenol, DON, and nivalenol, NIV), mainly produced by *Fusarium* species like *F. graminearum* and *F. culmorum*, and fumonisins, mainly produced by *F. verticillioides* and *F. proliferatum* (Perochon and Doohan 2024). *Fusarium avenaceum* (Corda) Saccardo is among the most important causal agents of FHB in barley (Senatore et al. 2021; Nielsen et al. 2014; Garmendia et al. 2018), durum wheat (Beccari et al. 2018), sorghum (Szabó et al. 2023) and oat (Sohlberg et al. 2022). *F. avenaceum* is one of the main producers of enniatins (Enns), cyclic hexadepsipeptides belonging to the category of the so-called "emerging mycotoxins", which include all the mycotoxins neither routinely investigated nor legislatively regulated (Gautier et al. 2020). In 2014, EFSA concluded that acute exposure of enniatins does not indicate concern for human health, but there might be a concern with respect to chronic exposure (EFSA 2014). There is increasing evidence that at least some of emerging mycotoxins have relevant effects on health (Polano et al. 2024). Recent studies on Enns toxicity on animal and human cells founds decrease in cell viability (Hasuda and Bracarense 2024), impact on the cholesterol biosynthesis pathway (Coulet et al. 2024), and bioaccumulation in the human body in liver and fat samples (Castell et al. 2024). Furthermore, the co-occurrence of Enns and other mycotoxins and their combined effect in human and animal body was not investigated. Similarly, the ecological role of Enns is controversial. Enns may have a role in virulence (Eranthodi et al. 2020) or a role in the interaction with bacteria and with other *Fusarium* species, thanks to antibiotic (Meca et al. 2011; Sy-Cordero et al. 2012) and antifungal properties (Ederli et al. 2021). In the last decades, many studies were focused on strategies to counteract FHB and mycotoxin accumulation, focusing on plant resistance (Mandalà et al. 2021) or on sustainable crop protection products (Kumar and Pruthi 2014; Rossetti et al. 2017). In both cases plant secondary metabolites and phenylpropanoids in particular, seems to have a crucial part (Treutter 2006). Several authors studied the effect of natural occurring plant secondary metabolites on fungal growth and mycotoxins accumulation (Atanasova-Penichon et al. 2016). Numerous researches demonstrated that phenolic acids and plant extract rich in phenolic acids can reduce trichothecenes production in vitro (Boutigny et al. 2009; Boutigny et al. 2010; Aristimuño Ficoseco et al. 2014; Gauthier et al. 2016; Shirai and Tanaka 2024). Many efforts were also dedicated in study the anti-mycotoxins effect of plant extracts or pure phenylpropanoids on *F. verticilloides* or other fumonisins producers (Dambolena et al. 2011; Aristimuño Ficoseco et al. 2014; Martínez-Fraca et al. 2022; Lalak-Kańczugowska et al. 2023). Gautier et al. (2020) investigated the efficiency of hydroxycinnamic acids on the production of Enns by *F. avenaceum*. The mode of action of these compounds usually involves the regulation of gene expression (Gautier et al. 2020; Boutigny et al. 2010) and the alteration of the oxidative balance (Savignac et al. 2023). The plant secondary metabolites more investigated were phenolic acids (mainly caffeic acid, *p*-coumaric acid, ferulic acid, sinapic acid, vanillic acids, and syringic acid), carotenoids (zeaxanthin), and some flavonoids (rutin, quercetin, narigenin, chlorogenic acid). The role and the effect of many others flavonoids have not been investigated so far. Anthocyanins are pigmented phenylpropanoids with different important roles in plants life (Wagay et al. 2020; Li and Ahammed 2023). These pigments are stable at acid pH conditions (Enaru et al. 2021) and naturally occur in several cereals in the outer grains layer, particularly in colored grains (Beta et al. 2020). The most abundant anthocyanins in pigmented grains are cyanidin 3-*O*-glucoside (C3G) and delphinidin 3-*O*-glucoside (D3G), ranging from 3 to 150 µg/g in the bran of pigmented genotypes (Abdel-Aal et al. 2018). Other studies showed as the alteration in phenylpropanoids biosynthetic pathway affect resistance response to bacterial (Wegener and Jansen 2007;

Lei et al. 2018) and fungal pathogens (Flachowsky et al. 2010; Zhang et al. 2013; Sivankalyani et al. 2016), but a direct investigation on anthocyanin effect on *Fusarium* species is currently lacking.

The purpose of this investigation was to explore the influence of anthocyanins on *F. avenaceum* growth and Enns production. *F. avenaceum* was chosen considering its leading role in causing FHB and because of its ability to produce mycotoxins at lower pH starting condition (pH 4), important to maintain anthocyanins activity and stability, than other *Fusarium* species (for instance, *F. graminearum* require a starting pH of 6 for trichothecenes production). The impact of four anthocyanins was examined: cyanidin, delphinidin, cyanidin 3-*O*-glucoside (C3G) and delphinidin 3-*O*-glucoside (D3G). Different anthocyanins supplemented liquid culture assays were used in order to assess: (I) the effect on fungal growth; (II) the effect on mycotoxins accumulation, considering the main Enns produced by *F. avenaceum*: A, A1, B, B1; (III) the effect on the expression of genes related to mycotoxins production and oxidative stress; (IV) the combined effect with other phenolic acids with known anti-mycotoxin effect (ferulic acid). A particular focus was dedicated to C3G, the most abundant pigment in purple pericarp wheat genotypes.

2.2. Materials and Methods

2.2.1.Chemicals

For HPLC/DAD analysis, LC-grade acetonitrile and methanol were purchased from VWR (Fontenay-Sous-Bois, France). Enniatin A, enniatin A1, enniatin B, and enniatin B1 and ferulic acid were purchased from Sigma-Aldrich (Saint-Quentin-Fallavier, France). The following anthocyanins were purchased from Extrasynthese (Lyon, France): cyanidin chloride (syn. 3,3',4',5,7-Pentahydroxyflavylium chloride; CAS: 528-58-5; molecular weight: 322.7 g/mol), cyanidin-3-*O*-glucoside chloride (syn. kuromanin chloride; CAS: 7084-24-4; molecular weight: 484.82 g/mol), delphinidin chloride (syn. 3,3',4',5,5',7-Hexahydroxyflavylium chloride; CAS: 528-53-0; molecular weight: 338.7 g/mol), and delphinidin-3-*O*-glucoside chloride (syn. myrtillin chloride; CAS 6906-38-3; molecular weight: 500.9 g/mol).

2.2.2.Fungal material and inoculum preparation

The strain *Fusarium avanceum* I612 (isolated in 2010 in Scotland from wheat) was provided by INRAE-MycSa. I612 is an Enns producing strain and it can produce about 3000 $\mu g \cdot g^{-1}$ (sum of enniatin A, enniatin A1, enniatin B and enniatin B1 after 10 days of culture in Fusarium defined medium, FDM) (Gautier et al. 2020; Fanelli et al. 2014). Stock cultures were maintained at 4 °C on Potato Dextrose Agar (PDA) slants under mineral oil. When inoculum was required, the *F. avenaceum* I612 was grown on PDA plates at 25 °C in the dark for 5 days, and spore suspensions were prepared in carboxymethyl cellulose (CMC) liquid medium (15 g CMC, 1 g Yeast extract, 0.5 $MgSO_4$ 7 H_2O, 1 g NH_4NO_3, 1 g KH_2PO_4, for 1 L medium) and incubated in darkness at 25 °C and at 180 rpm in a Multitron incubator shaker (INFORS AG, Bottmingen, Switzerland). After 3 days, the conidia were recovered using centrifugation (2300× *g* for 10 min), counted in a Thoma chamber to assess the conidial concentration used for the following assays.

2.2.3.Effect on fungal growth: supplemented liquid culture experiment (Assay 1)

Liquid culture experiments were performed in FDM medium (Fanelli et al. 2014). FDM was supplemented or not with anthocyanins at the optimal concentration for their solubility: 0.17 mM for cyanidin and cyanidin-3-*O*-glucoside chloride, 0.2 mM for delphinidin and delphinidin-3-*O*-glucoside. To improve anthocyanins solubility, the FDM solutions were sonicated for 15 minutes in an ultrasound bath. For each condition, cultures were made in quadruplicate.

Sterile 6-multiwell plates containing 5 mL of liquid medium in each well were inoculated in order to obtain a final concentration of 10^4 spores mL^{-1}. Fungal liquid cultures were incubated statically at 25 °C in the dark for 14 days. After incubation, the cultures were centrifuged at 4 °C and at 5000x *g* for 10 min. Fungal biomass was measured by weighing the mycelial pellet after 48 hours of freeze-drying (Cryotec®, Saint Gely du Fesc, France). Results were expressed as % of growth reduction/improvement, calculated for each tested substance by using the following equation

$$\% \text{ of reduction/improvement} = 100 \times (\text{Treated-Mock mean/Mock mean})$$

2.2.4.Effect on fungal growth: pre-incubation assays (Assay 2)

To verify if a limited exposure to anthocyanins can affect mycelium growth, 1 mL of FDM media supplemented or not with anthocyanins, prepared as mentioned above, was inoculated with *F. avenaceum* I612 conidia (final concentration $8{\cdot}10^5$ spores mL^{-1}) and pre-incubated for 6 hours in the dark at 25°C. After 6 hours, conidial germination was checked and 100 µL of the conidial suspension pre-incubated with anthocyanins were transferred into 8 mL plates containing fresh FDM not supplemented with anthocyanins (final concentration 10^4 spores mL^{-1}) and incubated at 24 °C in the dark for 14 days. After incubation, the cultures were centrifuged at 4 °C at 5000x *g* for 10 minutes. Fungal biomass was measured as mentioned above. Results were expressed as % of growth reduction/improvement, calculated for each tested substance by using the equation mentioned above. For conidial germination after 6 hours of pre-incubation, 100 spores for each biological replicate were visually examined under a microscope and results were reported as germination rate. A summary of assay 1 and assay 2 is presented in Fig. 2.1.

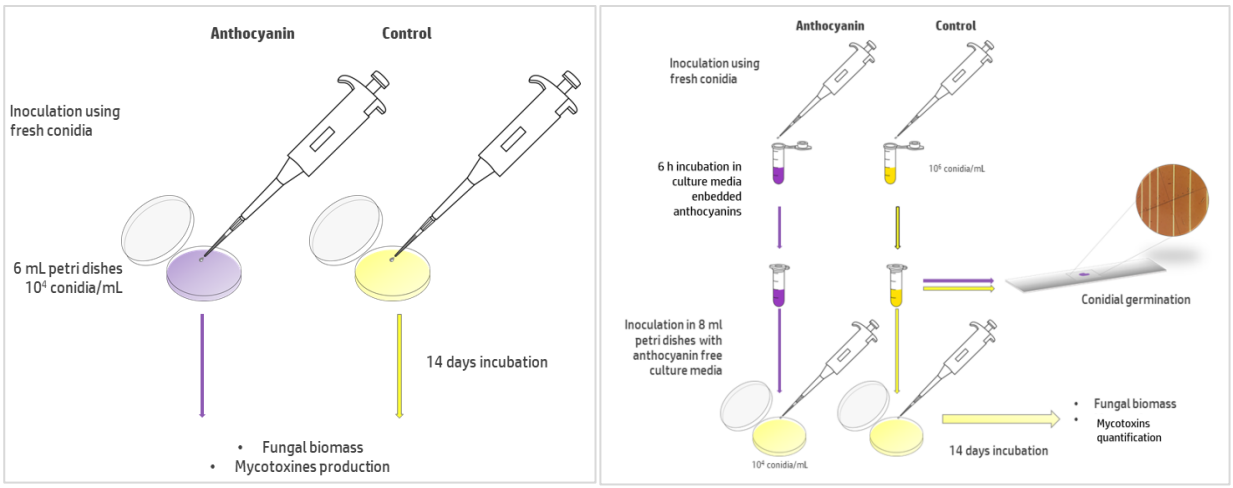

Fig 2.1: Experimental design of assay 1 (left) and assay 2 (right).

2.2.5.Effect on mycotoxins accumulation and differential gene expression analysis

2.2.5.1. Mycotoxins and RNA extraction

F. avenaceum I612 was cultivated in 8 mL plates containing FDM media supplemented or not with 0.2 mM of each compound (cyanidin and cyanidin-3-*O*-glucoside, delphinidin or delphinidin-3-*O*-glucoside), by inoculating a spore concentration of 10^4 spores mL^{-1}. RNA was extracted from 4-days old mycelium. In order to obtain a sufficient quantity of mycelium, after 4 days of incubation (24°C in the dark), each biological replicate was obtained by pooling 3 plates with 8 mL $plate^{-1}$. Three additional plates for each condition were incubated until 14 days after inoculation and used for mycotoxins quantification at the end point. After 4 and 14 days, liquid media and mycelium were separated by

centrifugation. The liquid medium was used for mycotoxin extraction and HPLC/DAD quantification (described below), while mycelium from 4 days after inoculation was immediately frozen in liquid nitrogen and stored at -80°C until total RNA extraction. For mycotoxins extraction (Gautier et al. 2020), 16 mL (after 4 days) or 6 mL (after 14 days) of culture media were subjected to extraction with 2 volumes of ethyl acetate. The organic phases were evaporated to dryness and dried extracts were dissolved in 200 µL of methanol/water 1:1, v/v and filtered (0.2 µm). Frozen mycelia (50 mg) for RNA extraction were freeze-dried and immediately ground (Precellys Evolution and Cryolis, Montigny Le Bretonneux, France) with glass beads in 1 mL of lysis buffer (TRIzol™ Reagent, Thermo Fischer Scientific, Vantaa, Finland) for 2 cycles of 25 seconds at 30 Hz. After that, 200 µL of chloroform were added to the homogenate, shacked vigorously for 15 seconds and then centrifuged for 15 minutes at 12000x *g* at 4°C. The upper aqueous phase was used for total RNA extraction following the instruction of miRNeasy Kit (Qiagen, Courtaboeuf, France). In order to completely remove flavonoids, total RNA was purified using the RNeasy MinElute Cleanup Kit (Qiagen, Courtaboeuf, France). The quality of the prepared RNA was evaluated by agarose gel electrophoresis. The RNA was quantified by spectrometry (DeNovix DS-11 FX+, Wilmington, DE, United States).

2.2.5.2. Primer design

Primers used in this study are reported in Table 2.1. Housekeeping genes and genes related to the modulation of Enns production were obtained from literature (Pinson-Gadais et al. 2008; Fanelli et al. 2014). The primer pairs for analysis of oxidative stress in *F. avenaceum* were designed and verified on known sequences of *F. avenaceum* genome. Primer design was performed using the National Center for Biotechnology Information (NCBI) tool Primer-blast (https://blast.ncbi.nlm.nih.gov/Blast.cgi), using sequences available in NCBI (https://www.ncbi.nlm.nih.gov/) belonging to the *Fusarium avenaceum* strain Fa05001 Fave_05001_scaffold21.1, whole genome shotgun sequence (Lysøe et al. 2014) and *Fusarium avenaceum* strain MPI-SDFR-AT-0044 DER45scaffold_2, whole genome shotgun sequence (Mesny et al. 2021). Primers were designed inside the exonic regions.

2.2.5.3. RT-qPCR

Reverse transcription was performed with the SuperSript™ IV First-Strand Synthesis System kit (Invitrogen, Vilnius, Lithuania) according to the supplier's protocol. The cDNA samples were stored at −20 °C until their use for PCR analysis. qPCR analyses were performed with a QuantStudio5™ (ThermoFisher Scientific, Vantaa, Finland) using 1 µL of cDNA (10 ng of reverse transcribed RNA) mixed with 9 µL of reaction mix prepared using the Power Track SYBR® Green Master Mix (Applied Biosystems, Vilnius, Lithuania). The forward and reverse primers used for the genes targeted in the study are reported in Table 2.1. The PCR cycling conditions were set at 95 °C for 20 s, 40 × [95 °C for 3 s, 60 °C for 20 s]. The melting curves were acquired by heating the samples to 95 °C for 1 s, cooling to 60 °C for 20 s and then slowly increasing the temperature from 60 °C to 95 °C at the rate of 0.15 °C s^{-1}, with a continuous measurement of the fluorescence. Amplification and melting curve data were generated and analyzed using the QuantStudioTM Design and Analysis Software v1.5.1 (ThermoFisher Scientific, Vantaa, Finland). For each gene, the efficiency was evaluated using serial dilutions of cDNA samples. The expression levels of the genes studied were normalized with the expression of the reference genes *ef1α* (Elongation factor 1-alpha), *rpb2* (RNA Polymerase II Gene), *β-tubuline*, *citrate synthase* and *histone h3*. The calculation of normalization factor based on the identified reference gene, the calculation of normalized expression for each gene of interest, and the rescaling of the normalized expression across biological replicates were computed using the web tool SATqPCR (Rancurel et al. 2019).

Table 2.1: Primer pairs used in this study (continue in the next page)

Gene	Primer name	Primers 5'-3'	PCR product (bp)	Accession n.	Ref
β-tubuline	β-tubuline 261F	GGTAACCAAATCGGTGCTGCTTTC	248	Donaldson et al. 1995	INRAE - mycsa
	β-tubuline 536R	GATTGACCGAAAACGAAGTTG		Pinson-Gadais et al.2008	
Citrate synthase	FACIT.F	GCAGTGCTCTCAGCTCTCCT	171	*F. avenaceum FaLH27:* JQGD01000010.1	
	FACIT.R	GGGTGGACCAGAGGTAGTCA			
EF1α	FAEF1αF	ACTTCCCCTCCAGGATGTCT	232	*F. avenaceum FaLH03:* JQGD01000010.1	
	FAEF1αR	GTTACCACGTCGGATGTCCT			
Histone 3	HistH3FaveF	GAGATTCGACGATACCAGAAG	120	*F. avenaceum Fa05001: JPYM01000013,1*	
	HistH3FaveR	GATAGCGGAAGACTGGAATC		*F. avenaceum FaLH03: JQGD01000007.1*	
				F. avenaceum 12.56.2016: MK547655,1	
RPB2	RPB2FaveF	CCGAGGATCTCGAACTTTAC	105	*F. avenaceum MRC 1413: MH582082,1*	
				F. avenaceum p12,56,2016: MK560856,1	
				F. avenaceum YNSF16-66: MK185026,1	
				F. avenaceum YNSF16-68: MK185027.1	
	RPB2FaveR	GATAGCGGAAGACTGGAATC		*F. avenaceum CML3545: MK572784.1*	
Enniatin synthase (esyn1)	Esyn-F	GAGTCCTCTCCCAAGTTC	102	*G. avenaceum* 2562: AF351597,2	
				G. avenaceum 262: AF351594.2	
	Esyn-R	AGTTGAAGACCACGAGAT		*F. sporotrichioides CBS178,64: EF029064,1*	
Keto isovalerate reductase	KIVR-Fave-F1	CGGAGACTAGACCACAGTAT	151	*F. avenaceum* Fa05001; JPYM0100012,1:136516…960415	
	KIVR-Fave-R1	GCAAAGACGACAGAACTACA			
catalase 21.1	Fa.CAT21 F	GCTTGGATGGTGAGGACGAT	106	JPYM01000021.1:602392-601201; JAGMVH010000002.1:1395027-1396218	This study

	Fa.CAT21 R	AGACACCCGAAGACAAGCAG			
catalase 1	Fa.CAT1 F	AAGGCTATCCAGCTGCCC	90	JPYM01000012.1_cds_KIL89103.1_1 (505864.507620,507717..507957,508020..508238); JAGMVH010000002.1_cds_KAH6964439.1_1 (5334532..5336288,5336391..5336631,5336696..5336914)	This study
	Fa.CAT1 R	AGCATTCTTCAGGGTCACAACA			
catalase P3	Fa.CATP3 F	ATGCCCAGTACCATCGCATT	143	JPYM01000012.1 (354970...357050); JAGMVH010000002.1 (5183377...5185456)	This study
	Fa.CATP3 R	GGGGGCGTATTGCTTGTTTC			
catalase-peroxidase	Fa.CATP F	TGGCTTCTGCTTCTTGGAGG	118	JPYM01000017.1 (cds: 559075..559410,559466..559862,559934..561390,561454..561486); JAGMVH010000002.1 (cds: 573510-575921)	This study
	Fa.CATP R	CCTCTTCCAGTTCGAGTGGG			
catalase-peroxidase 2	Fa.CATP2 F	TTCTTTCCGCCCTCAAGACC	75	JPYM01000003.1:728272-730820; JAGMVH010000006.1: 782469-785018	This study
	Fa.CATP2 R	GATCAGCCAGAGAGACCTGC			
superoxide dismutase	Fa.SOD F	GCTTCCTCTGGCTCGTCAAG	150	JAGMVH010000002.1:3801107-3802065 (3801107.3801735,3801852..3802065); JPYM01000031.1:258264-259222 (258264..258477,258594..259222)	This study
	Fa.SOD R	TCATAAAGGTGCGGGCAGAG			
Manganese/iron superoxide dismutase	Fa.MnSOD 2 F	CAAGACCTACTCCGCCGCTA	81	JPYM01000009.1 (589803..589925,589979..590446,590522..590716); JAGMVH010000007.1 (1505357..1505479,1505533..1506000,1506076..1506270)	This study
	Fa.MnSOD 2 R	CCGCCGTTGAACTTGATGGC			

2.2.6. 24-multiwell assay

In order to focus the attention on the most representative pigment in colored grains (cyanidin-3-*O*-glucoside, C3G) the effect of this flavonoid on fungal growth and Enns production were analyzed, alone and in combination with the most representative phenolic acid in cereals, ferulic acid (FA). Different concentrations of cyanidin-3-*O*-glucoside (0.2 mM, 0.02 mM, 0.002 mM), ferulic acid (0.5 mM, 0.05 mM, 0.005 mM) and their combination (C3G:FA 0.2:0.5 mM; 0.02:0.05 mM; 0.002:0.005 mM) were considered. The assay was performed in 24-multiwell plates (2 mL $well^{-1}$), using 5 biological replicates. The assay was repeated twice. Phenols were weighted and directly dissolved in FDM media to prepare the supplemented media having the highest concentration and the other concentrations were prepared by dilutions using fresh FDM. Thus, 2 mL of FDM supplemented or not with phenols were distributed in each well and fresh *F. avenaceum* conidia were used for inoculation (final concentration 10^4 spores mL^{-1}). Plates were incubated statically in the dark for 14 days at 24°C. During the incubation, every 3 days, absorbance at 520 nm of each well was measured using a multiwall plate reader (Infinite 200 Pro, Tecan Switzerland). After incubation, culture media and mycelium were separated as mentioned above to extract Enns (2 mL of culture medium were extracted with 4 mL of ethyl acetate; 3.5 mL of the organic phase were evaporated to dryness; dried samples were dissolved in 200 µL of methanol/water 1:1, v/v and filtered 0.2 µm) and to measure fungal biomass. Enns were quantified using HPLC/DAD as described below.

2.2.7. Mycotoxins quantification

Quantification of A, A1, B and B1 Enns was performed on a 1100 Series HPLC system (Agilent, France) equipped with an autosampler system, an Agilent photodiode array detector and the ChemStation chromatography manager software (Agilent, France). Separation was achieved on a Kinetex 2,6U XB-C18—100 Å column (150 × 4.6 mm; 2.6 µm) (Phenomenex, Le Pecq, France) maintained at 45 °C. The mobile phase consisted of water (solvent A) and acetonitrile (solvent B). The following gradient was used for elution: 70% B for 5 min, 70-90% B in 10 min, 90% B for 5 min, 90–70% B in 1 min, and 5 minutes post-run equilibration with initial conditions (Gautier et al. 2020; Gauthier et al. 2016). The flow was kept at 1 mL min^{-1}. The injection volume was 10 µL. UV-visible spectra were recorded from 190 to 450 nm and peak areas were measured at 205 nm (1–100 µg mL^{-1}). Quantification was performed using external calibration with standard solutions. The limit of detection was 1 µg mL^{-1}. The retention time of Enns were 15.7 minutes for B, 16.1 minutes for B1, 16.5 minutes for A1, and 16.8 minutes for A.

2.2.8. Data analysis

Results of liquid culture experiment, conidial germination, 24-multiwell assay (fungal biomass, mg, and mycotoxin accumulation, µg/g) were subjected to one-way analysis of variance (ANOVA). Conidial germination % were transformed using arcsin transformation before analysis. Two levels of significance ($p<0.05$; $p<0.01$) were computed to assess the significance of the F values. A pairwise analysis was carried out using the Tukey Honestly Significant Difference test (Tukey test) at the 0.95 or 0.99 confidence levels. Linear correlation analyses among the considered variables were computed considering Pearson's *r* coefficient. ANOVA and correlation analysis were performed using PAST ver. 4.05 (University of Oslo) (Hammer et al. 2005). For relative gene expression data, the classical method of pairwise t-tests with a pooled standard deviation was computed using SATqPCR (Rancurel et al. 2019).

2.3. Results

2.3.1.Anthocyanins stimulate fungal growth while anthocyanidins slow down conidial germination

To assess the effect of the four considered anthocyanins (cyanidin and delphinidin, C3G and D3G) on *F. avenaceum* growth, two in-broth culture assays were performed. Supplemented liquid culture (assay 1) was performed in 6-well multiwell plate (5 mL well^{-1}) and the mycelium grew within the supplemented anthocyanins for 14 days. FDM culture media had a starting pH equal to 4.5, and *F. avenaceum* (in all the conditions) increased the pH up to 5 after 48h, reached pH 7 after 6 days and at the end point (14 dpi) pH was equal to 9. Fig. 2.2a shows the color of the different well at 14 dpi, highlighting a visible degradation of the anthocyanidins (cyanidin and delphinidin), while the samples containing the anthocyanins (C3G and D3G) maintained a bright color. The mycelium treated with C3G and D3G had a gelatinous appearance. In the pre-incubation assay (assay 2) conidia were incubated in supplemented or not FDM media for 6 hours and then transferred in 8 mL petri dishes with fresh FDM. Fig. 2.2b shows fungal growth in liquid culture at the end of the assay: a normal mycelium appearance is visible.

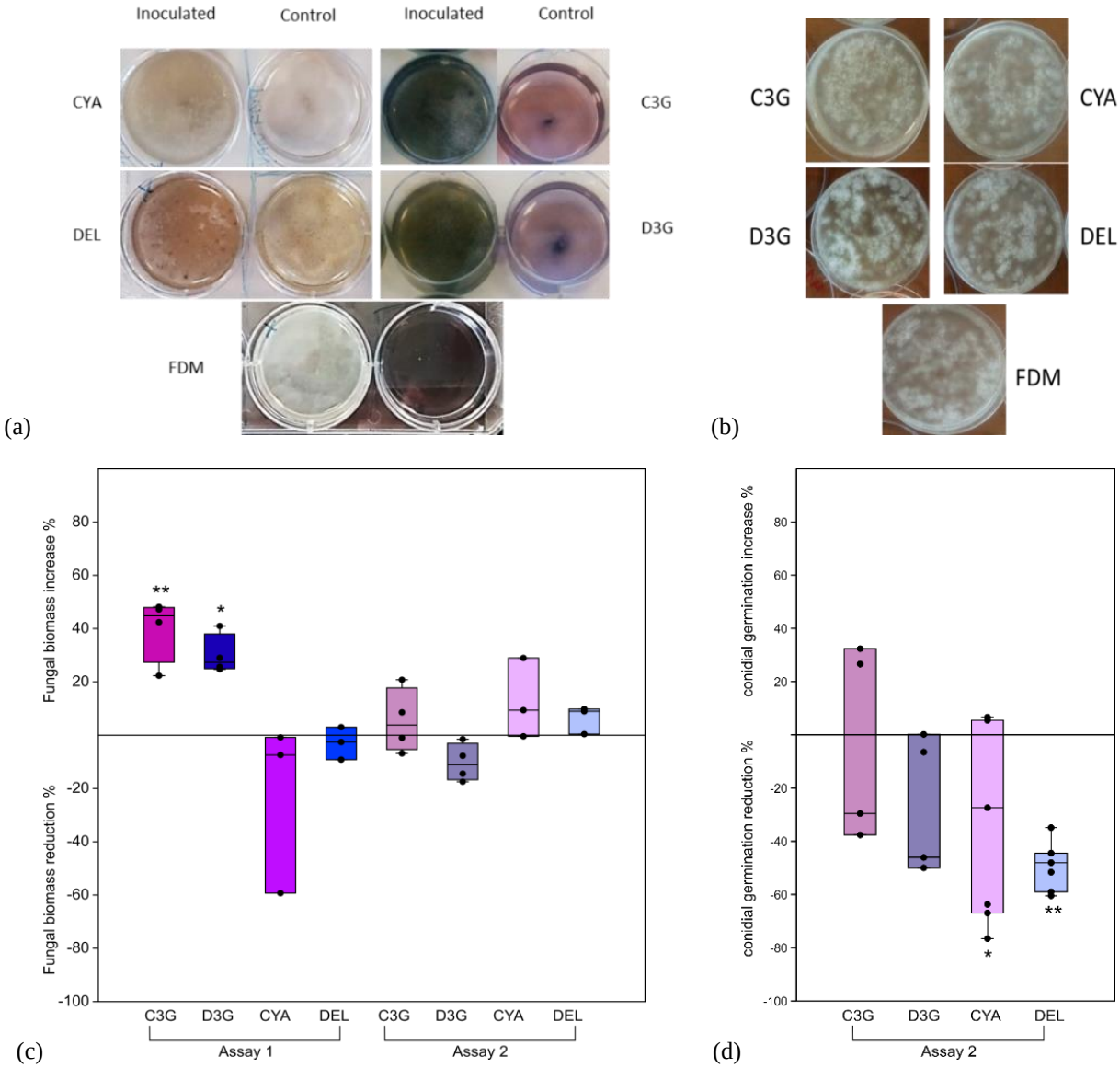

Fig. 2.2: (a) Wells appearance after 14 days of incubation in assay 1; (b) 8 mL petri dishes of assay 2 after 6 hours of incubation in supplemented media and 14 days in FDM anthocyanin-free media; (c) Increase or reduction of fungal biomass in comparison with the control condition in assay 1 and assay 2. (d) conidial germination reduction or increase due to anthocyanin treatments. "*" and

"**" indicate a statistical difference between the treatment and the control, with $p<0.05$ and $p<0.01$ respectively (ANOVA and Tukey test). C3G = cyanidin 3-*O*-glucoside; D3G = delphinidin 3-*O*-glucoside; CYA = cyanidin; DEL = delphinidin.

Fungal biomass in assay 1 ranged from 11.7 mg to 30.8 mg, while in assay 2, it ranged from 23.5 mg to 68.2 mg. As displayed in Fig. 2.2c, in the assay 1, C3G and D3G caused a significant increase in fungal biomass (compared to the mock treated control, inoculated FDM) of 45.72% and 25.37% (mean, respectively), while the same compounds in assay 2 presented no effect. No statistically relevant effect in fungal biomass growth was recorded for samples treated with cyanidin and delphinidin in both the assays. In assay 2, the conidial germination was checked after 6 hours. Percentage of germinated conidia ranged between 1.5% and 14.3%. Fig. 2.2d show that conidial germination in samples treated using C3G and D3G were statistically comparable to the control, while the anthocyanidins induced a significant reduction in conidial germination (median: -45.79% cyanidin, -49.79% delphinidin).

2.3.2. Delphinidin, C3G and D3G affected ENNs accumulation, but only delphinidin and D3G downregulated ENNs-related genes

In order to study the effect of the considered compounds on mycotoxins accumulation and on the expression of Enns–related and oxidative stress-related genes, a supplemented liquid culture was established in order to extract and quantify mycotoxins after 4 and 14 days of incubation, while RNA was extracted from mycelium at 4 days post inoculation. Enns-related genes and oxidative stress related genes were differentially affected by the treatments. As presented in Fig. 2.3a, delphinidin strongly downregulated *Esyn* (0.0102-fold ± 0.0076), *Kivr* (0.1122-fold ± 0.0692) and *MnSOD* (0.3497-fold ± 0.0619), while the upregulation of *CATP2* was not statistically significant. Similarly, D3G (Fig. 2.3b) downregulated *Esyn* (0.1405-fold±0.006), *Kivr* (0.2904-fold ± 0.0494), but it boosted *MnSOD* regulation (2.655-fold ± 0.2184), while *CATP2* had a basal expression. Cyanidin (Fig. 2.3c) had no effect on the regulation of the considered genes. Considering that C3G is the most abundant colored compound in pigmented genotypes, the effect of this flavonoid on *F. avenaceum* gene expression was studied more in detail, considering other genes related to oxidative stress (*CAT21*, *CAT1*, *CATP*, *CATP3*, *SOD*). As shown in Fig. 2.3d, the upregulation of *CAT21* (2.1020-fold ± 0.9251) and *CATP3* (1.7956-fold ± 0.8013) occurred, but no one of the considered genes was significantly expressed due to C3G treatment. Gene expression was confirmed by mycotoxins quantification. Total Enns accumulation after 4 days of incubation ranged from 1.7 µg/g to 757.30 µg/g, (EnnB range 0- 682.91 µg/g; EnnB1 range 1.50- 74.39 µg/g; EnnA < LOQ; EnnA1<LOQ), while after 14 days, total Enns accumulation was quantified in a range 81.68 µg/g to 4493.31 µg/g (EnnB: 44.15-3294.94 µg/g; EnnB1: 22.03-1031.99 µg/g; EnnA: 9.98-201.67 µg/g; EnnA1<LOQ). Fig. 2.3a-d show the % of increase or reduction of Enns accumulated in these two time points. In particular, delphinidin (Fig. 2.3a) reduced EnnB1 after 4 days of incubation (-90.8%), and after 14 days EnnA1 (-78.1%), EnnB (-97.0%) and EnnB1 (-82.9%) were negatively affected by the treatment. The treatment with D3G (Fig. 2.3b) reduced the accumulation of EnnA1 (-60.3%) after 14 dpi and EnnB1 after 4 days (-90.4%). The treatment with cyanidin (Fig. 2.3c) was ineffective for the reduction of all the considered Enns. Finally, C3G (Fig. 2.3d) at 4 dpi strongly reduced EnnB accumulation (-81.7%) as well as after 14 days of incubation EnnA1 (-91.7%), EnnB (-97.8%) and EnnB1 (-83.0%) were strongly reduced. As show in Table 2.2, a linear correlation occurred between Enns accumulation at 4 dpi and total Enns accumulation at 14 dpi. More in detail the accumulation of EnnB after 4 day of incubation is positively correlated with the accumulation of EnnB1 ($r = 0.57887$; $p<0.05$) and EnnA1 ($r = 0.53278$; $p<0.05$) after 14 days of incubation, as well as the accumulation of EnnB1 after 4 day of incubation is positively correlated with the accumulation of EnnB1 ($r = 0.58331$¸ $p<0.05$) and EnnA1 ($r = 0.52866$¸ $p<0.05$) after 14 days of incubation. Furthermore (Table 2.2), the accumulation of the considered Enns was strictly positively correlated each other in the same time point ($r > 0.9$; $p<0.01$).

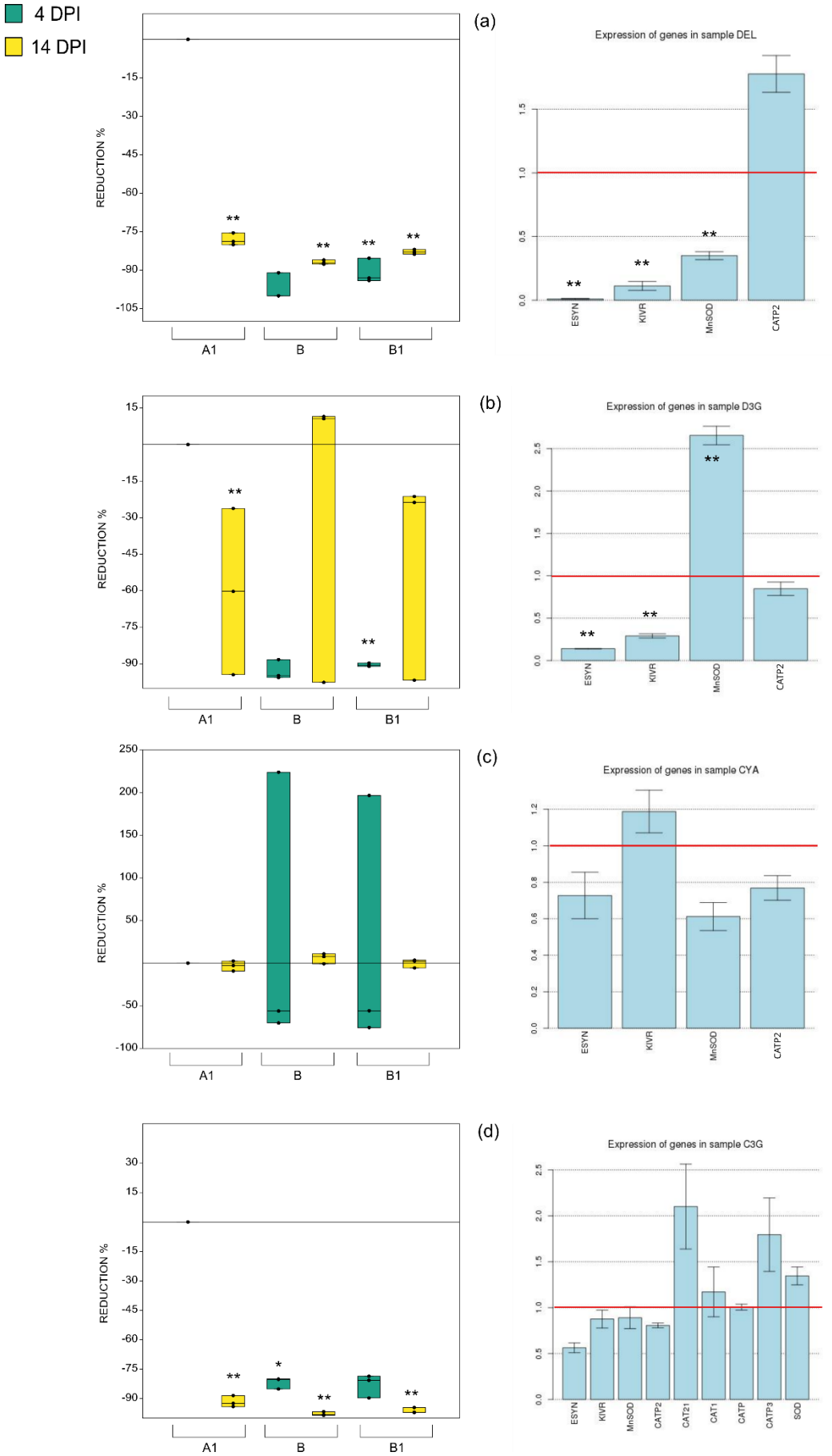

(caption in the next page)

Fig. 2.3: Box plots representing the Enns (A1, B, B1) reduction (left) in comparison with the control culture and bar chart showing the differential expression of the considered genes (right) in liquid culture supplemented with delphinidin DEL (a), D3G (b), cyanidin CYA (c) and C3G (d). Yellow boxes refer to 4 days of incubation, while green boxes are related to 14 days of incubation. Relative gene expression is expressed in mean fold-change ± SE and the red lines in the graphs highlight the basal expression (fold-change = 1). Data are rescaled on the untreated control. "*" and "**" indicate a statistical difference between the treatment and the control, with $p<0.05$ and $p<0.01$ respectively. ANOVA and Tukey test were used for mycotoxin reduction analysis while *t*-test was considered for relative gene expression.

Table 2.2: Correlation matrix among amount of enniatins in the 2 considered time points (n=18). Pearson's *r* coefficients below the main diagonal are displayed. "*" and "**" means that the *r* coefficient is statistically significant with $p<0.05$ and $p<0.01$ respectively.

	4 dpi Enn B	**4 dpi Enn B1**	**14 dpi Enn B**	**14 dpi Enn B1**	**14 dpi Enn A1**
4 dpi Enn B	1				
4 dpi Enn B1	0,99367**	1			
14 dpi Enn B	0,48091	0,46921	1		
14 dpi Enn B1	0,57887*	0,58331*	0,96208**	1	
14 dpi Enn A1	0,53278*	0,52866*	0,90988**	0,96114**	1

2.3.3. C3G had a dose dependent effect and the combination FA+C3G was similar to C3G alone

In order to study the antifungal and anti-mycotoxin effect of the main phenolic compounds naturally present in pigmented wheat grains, C3G (as the most abundant anthocyanin), ferulic acid (FA, as the most abundant phenolic acid) and their combination were considered at different concentrations. Fig. 2.4a shows the plates used in the assay after 14 days of incubation, while Fig. 2.4b shows the evolution in the well's absorbance (at 520 nm, suitable for anthocyanins detection) during the incubation period for the treatments with C3G. Data are reported as difference with the untreated control. The highest absorbance was recorded for the combination FA:C3G 0.5:0.2 mM, then it decreased during the considered period. Absorbance of samples treated using C3G 0.2 mM decreased from the starting point to 3 dpi and then remained stable. Lower concentrations of C3G and FA:C3G were stable during the considered period and closer to 0 than the higher concentrations, indicating similarity with the FDM untreated control.

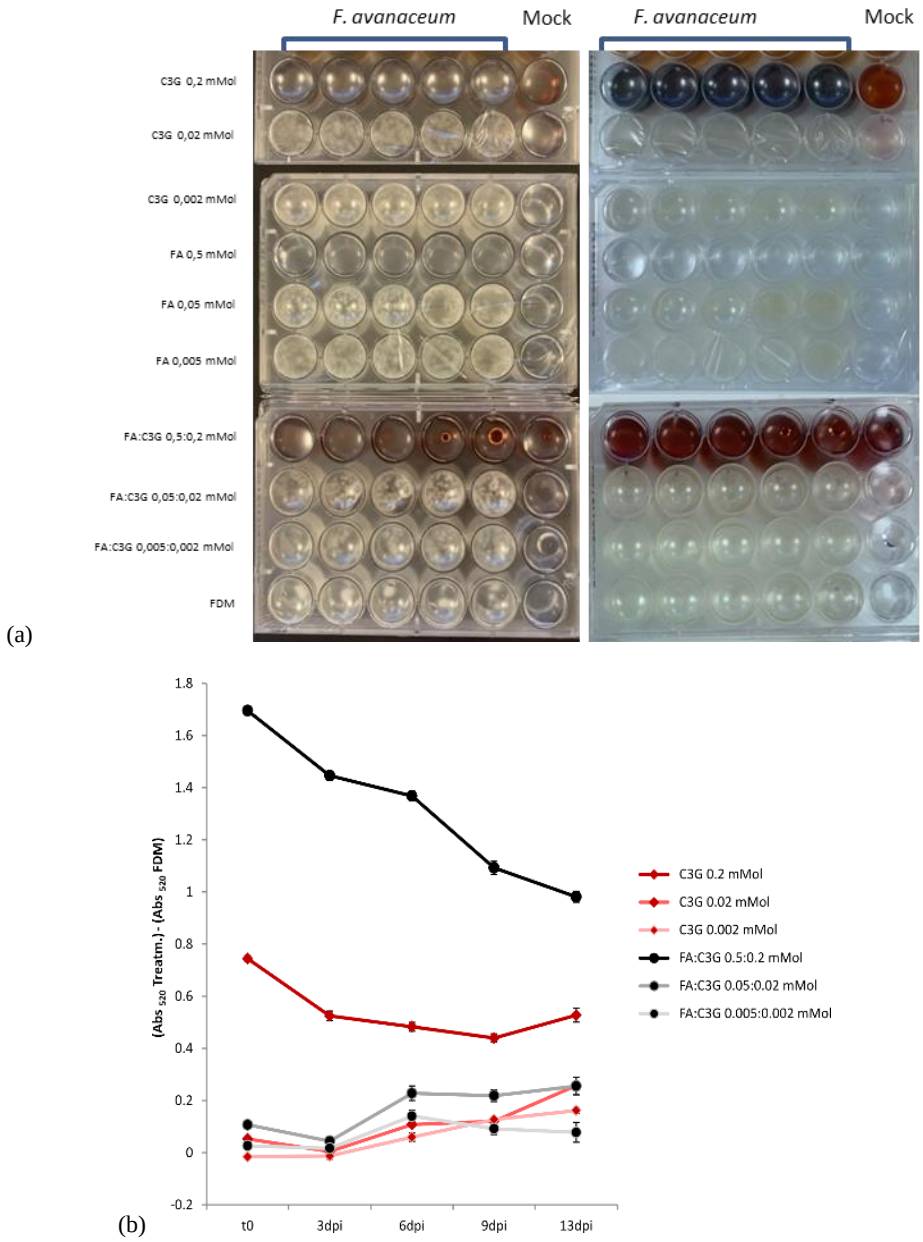

Fig. 2.4: (a) Multi-well plates containing supplemented FDM media after 14 days of incubation, black background (left) and white background (right); (b) Absorbance at 520 nm was measured on culture media during the incubation period (0-13 days post inoculation) in *F. avenaceum* inoculated wells treated using FA:C3G and C3G at different concentrations. Absorbance data are expressed as Abs = $(Abs^{520}{}_{Treatment})$–$(Abs^{520}{}_{FDM})$, in order to normalize the Abs signal from the contribute of the fungal biomass and highlight the evolution of the supplemented flavonoid. Points show mean value ± SE.

As presented in Fig. 2.5a, fungal biomass was significantly affected by some concentrations of C3G and ferulic acid, but not by the application of their combination. In particular, C3G at 0.2 mM caused a strong increase in fungal biomass (+117%) compared to the control, as well as ferulic acid at 0.005 mM (+72%) and ferulic acid at 0.05 mM (+75%), while the highest concentration of ferulic acid (0.5 mM) led to a strong reduction of fungal biomass (-70%). All the other treatments did not affect the fungal biomass. Considering Enns accumulation (B+B1+A1. Enn A was <LOQ), C3G at 0.002 mM and C3G at 0.02 mM were ineffective in Enns reduction, while the highest C3G concentration (0.2

mM) reduced Enns accumulation more than 90%, compared to the control (Fig. 2.5b). Ferulic acid were efficient in Enns reduction in all the considered concentrations (-66% FA 0.5 mM; -74% FA 0.05 mM; -46% FA 0.005 mM). The combination FA:C3G 0.002:0.005 mM was ineffective, while the other two considered combinations led to a reduction (-38% FA:C3G 0.05:0.02 mM) or a strong reduction (-89% Fa:C3G 0.5:0.2 mM) of the Enns accumulation compared to the control.

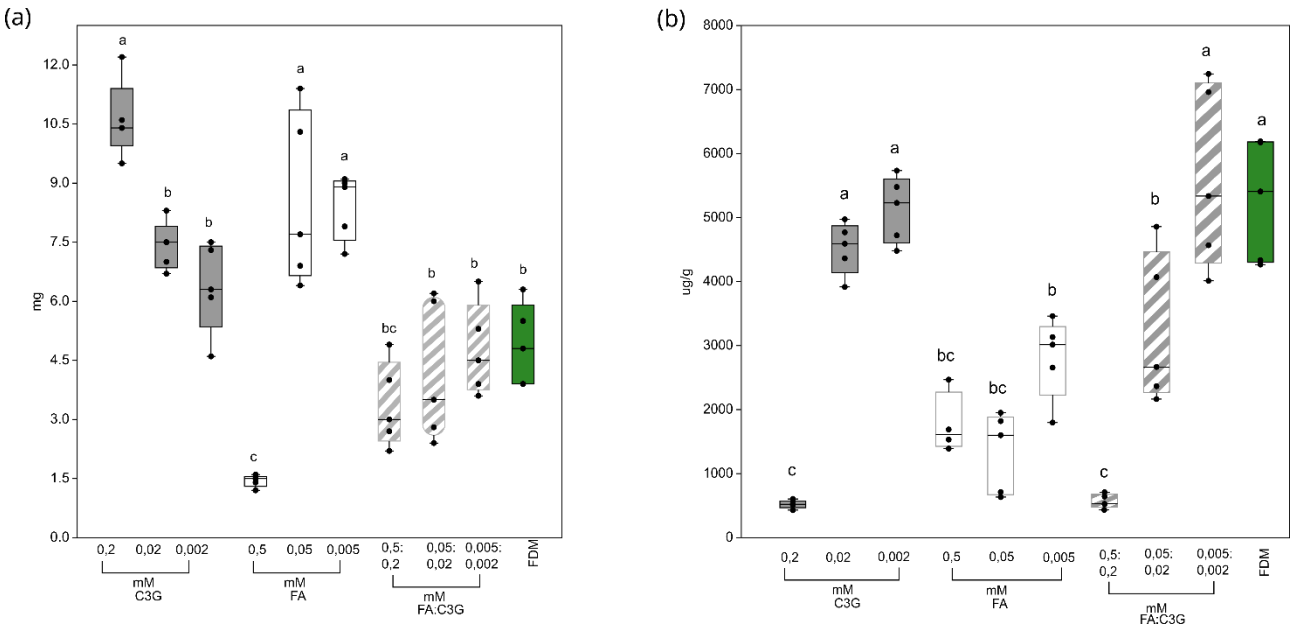

Fig. 2.5: Fungal biomass (left) and total (B+B1+A1) Enns accumulation (right) by *F. avenaceum* after 14 days post inoculation in FDM embedded cyanidin 3-*O*-glucoside (C3G, grey boxes), ferulic acid (FA, white boxes) or both (FA:C3G, stripes boxes) at different concentrations (expressed in mM) compared to the control (FDM, green boxes). Letters refer to statistical analysis (ANOVA and Tukey test; $p<0.01$).

A correlation matrix (Table 2.3) was computed among Enns, fungal biomass and C3G concentration, revealing a strong positive linear correlation between C3G concentration and fungal biomass (r = 0.88**) and a strong negative linear correlation between C3G concentration and Enns accumulation (r = -0.98**). Similarly, a correlation matrix (Table 2.4) was computed among Enns, fungal biomass and FA concentration. As shown, ferulic acid had a dose-dependent effect in biomass reduction (r = 0.93**), but not in Enns accumulation (r = 0.33 ns).

Table 2.3: Correlation matrix among fungal biomass, total amount of enniatins (Enns) and C3G concentration (n=15). Pearson's r coefficient below the main diagonal and p value below the diagonal are displayed. "**" means that the r coefficient is statistically significant ($p<0.01$).

	Enns	**C3G concentration**	**Biomass**
Enns	1		
C3G concentration	-0,98344**	1	
Biomass	-0,93483**	0,88235**	1

Table 2.4: Correlation matrix among fungal biomass, total amount of enniatins (Enns) and ferulic acid (FA) concentration (n=15). Pearson's *r* coefficient below the main diagonal and *p* value below the diagonal are displayed. "**" means that the *r* coefficient is statistically significant ($p<0.01$)

	Enns	**FA concentration**	**Biomass**
Enns	1		
FA concentration	0,32534	1	
Biomass	-0,35021	-0,93467**	1

2.4. Discussion

Different authors reported reduced mycotoxins accumulation in cereals grains rich in anthocyanins (Martin et al. 2017; Bernardi et al. 2018; Gozzi et al. 2023), especially in the purple pericarp grains, rich in cyanidin 3-*O*-glucoside. Plant-pathogen interaction is modulated by several mechanisms and different plant and pathogen metabolites may play a role. The *in vitro* assays aim to isolate the effect of a single component, trying to elucidate its contribution. In this chapter, the effect of anthocyanin treatments on Enns production and fungal growth of *F. avenaceum* was assessed using different in vitro assays. The different compounds showed a different influence on *F. avenaceum* growth and metabolism. Other authors proposed the antifungal effect of anthocyanins (Wen et al. 2016; Salhi et al. 2017; Salas-Gómez et al. 2023; Wang et al. 2023). This is in contrast with the results presented in this chapter, in which a stimulation of fungal growth is displayed due to C3G and D3G treatments. This discrepancy could be attributed to the material used in the assays: in this study, single pure anthocyanins were used, while in the other studies plant extract rich in anthocyanins were employed. The antifungal effect displayed by these plant extracts may be explained by the co-occurrence of a mixture of different anthocyanins and other phenylpropanoids (Wen et al. 2016; Salhi et al. 2017; Salas-Gómez et al. 2023; Wang et al. 2023). Our results suggest that, in our conditions, a single compound is unable to exert a strong antifungal activity on *F. avenaceum*. Further investigations are required to elucidate these evidences, considering more strains and *Fusarium* species. Other studies analyzed the effect of flavonoids on mycotoxin production in various fungal species. In particular, flavonoids like luteolin or naringenin inhibited trichothecene production in *F. graminearum* and *F. culmorum* at transcriptional level (Bilska et al. 2018), while ochratoxins production by *Aspergillus* spp. could be induced (Río et al. 2015) or reduced (Ricelli et al. 2019) by flavonoids. Few studies assessed the effect of phenolic acid on fungal growth and production of cyclodepsipeptides like beuvericin (Were et al. 2022) or Enns (Gautier et al. 2020). To the best of our knowledge, this is the first time that the anti-mycotoxigenic potential of anthocyanins is analyzed.

Further investigations are required to elucidate the mechanism of action of these compounds. However, some speculations are possible considering the available literature. Two aspects of anthocyanin chemistry may explain our findings: (1) the anthocyanins degradation dynamics due to pH changes; (2) the effect of glucosylation on anthocyanin molecules. pH is among the most important factors influencing anthocyanins transformation and degradation (Enaru et al. 2021). In this study, *F. avenaceum* induced a rapid increase of culture media pH, overcoming pH 5 in less than 48 hours and reaching pH 9 at the end point. This well documented behavior aims to create the best environment for fungal development and mycotoxins production. Considering the available literature (Loypimai et al. 2016; Weber and Larsen 2017; Rosales and Fabi 2022; Abedi-Firoozjah et al. 2022) an hypothetical dynamics of anthocyanin during *F. avenaceum* liquid culture is represented in Fig. 2.6. In particular, three forms of anthocyanidins can co-exist at a pH

range of 4–6: quinoidal blue species (which could be found abundantly at pH 2-4), carbinol pseudobase and a colorless chalcone (predominant at a pH between 5–6). Over pH 7 (reached after the 6th incubation day in this study), anthocyanins are degraded in colorless products, such as gallic acid (in the case of delphinidin and D3G) and protocatechuic acid (for cyanidin and C3G). Gallic acid is a hydroxybenzoic acid able to reduce the production of ochratoxin A in *Aspergillus carbonarius* (Romero et al. 2010) and trichothecenes in *F. graminearum* (Pagnussatt et al. 2014), while protocatechuic acid was hypothesized to be a fumonisin inhibitor (Wang et al. 2022) and it constrains ochratoxin A production by *Aspergillus* spp., without affecting fungal growth (Palumbo et al. 2007). Thus, a possible reason of the effect of anthocyanins on *F. avenaceum* highlighted in this study is the accumulation in the liquid culture of degradation products able to interfere with mycotoxins production, and these compounds could putatively be more active than the anthocyanins undamaged.

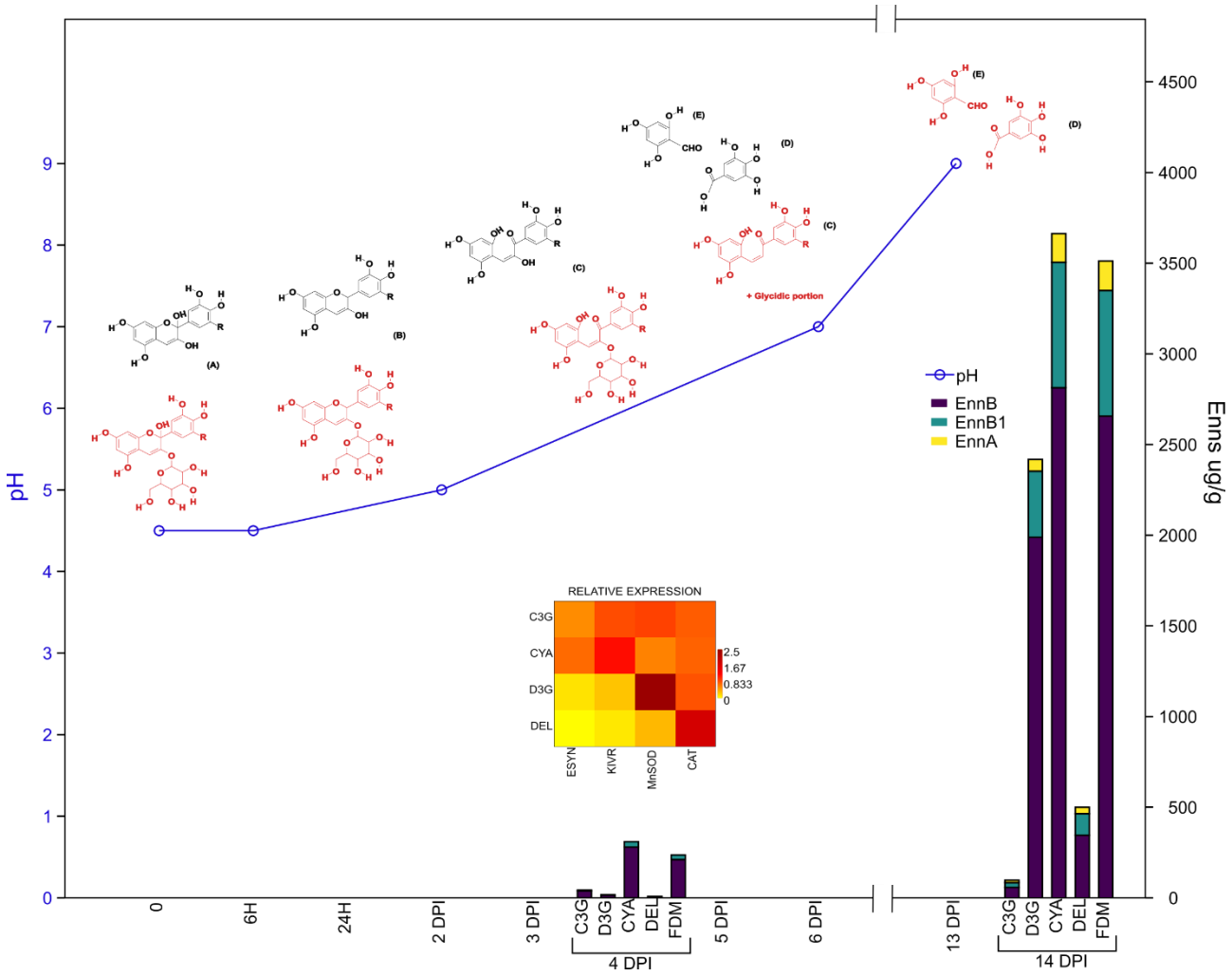

Fig. 2.6: Graphical representation of the results presented in Fig. 2.3 compared with the pH modifications recorded and the hypothetical degradation dynamics of considered anthocyanins. Blue line shows the pH. Black molecules are the anthocyanidins and the red molecules are the glycosylated forms. Radical -R in the molecule means –OH for delphinidin and D3G and –H for cyanidin and C3G. (A) quinoidal blue species; (B) carbinol pseudobase; (C) colorless chalcone; (D) gallic acid; (E) protocatechuic acid.

This hypothesis may explain the strong effect of delphinidin, while the less marked effect of D3G compared to delphinidin may be due to its glycosylation. Indeed, glycosylation reduces the free –OHs and the hydrogen-donating ability of the anthocyanidins, restricting their biological activity. On the other hand, the glycosylation increases polarity and stability of anthocyanidin in aqueous environment, slowing down the hydrolysis rate of the corresponding anthocyanin (Zhao et al. 2014). Thus, to produce its degradation products, D3G should lose the glucose moiety and it can occur by thermal degradation (Sinela et al. 2017), pH modification (Enaru et al. 2021) or active enzymatic degradation by *F. avenaceum* (Giménez et al. 2023; Rafiei, Vélëz, and Tzelepis 2021). This additional step in the degradation may decrease the activity of the glucoside. Furthermore, the release of the glycidic group may results in an additional source of glucose in the liquid culture, explaining the boost of fungal biomass due to glucosides treatments.

Futhermore, delphinidin and D3G differentially regulated *MnSOD*. Superoxide dismutases (SODs) are among the main scavengers of superoxide in the eukaryotic cells and they are essential to prevent cell damage due to reactive oxygen species (ROS) accumulation (Miller 2012). In previous studies, trichothecene biosynthetic enzymes and a key regulator of trichothecene production were greatly reduced in *MnSOD*-deletion mutants (Furukawa et al. 2017) and is known that SODs contribute to *Fusarium* spp. virulence (Szabó et al. 2020; Yao et al. 2016), while no literature is available about the relationship SODs-Enns regulation. Considering that in vitro stimulation of toxins biosynthesis in other *Fusarium* species has mostly been associated with oxidative stress due to H_2O_2 treatment or other oxidant compounds (Ponts et al. 2006; Schöneberg et al. 2018), liquid culture supplementation with antioxidant compounds, as the exogenous anthocyanins, may decrease oxidative stress and Enns accumulation (Hu et al. 2016; Apea-Bah and Beta 2021). This hypothesis is compatible with the downregulation of *MnSOD* by delphinidin and it is consistent with the findings of other authors (Savignac et al. 2023). Contrary, the upregulation of *MnSOD* was induced by D3G, suggesting the occurrence of an oxidative stress.

Even if delphinidin and D3G differ from cyanidin and C3G just for the presence of an additional –OH group, cyanidin and C3G behaved in a different way. The basal expression of *Esyn* and *Kivr* confirmed the inefficacy on mycotoxins reduction in sample treated with cyanidin, while in samples treated using C3G a strong reduction in Enns accumulation occurred, but without affecting the quantity of *Esyn* and *Kivr* transcripts accumulation (Fig. 2.5 and Fig. 2.6). Despite the presence of the glucose moiety, other studies showed that C3G could be more bioactive than cyanidin (Jing et al. 2020). The efficacy of C3G in Enns reduction may have multiple explanations, such as the occurrence of post-transcriptional regulation mechanism, as suggested for the mycotoxins regulation of other fungal species (Tumukunde et al. 2021; Adejor et al. 2024; Fanelli et al. 2013). In other studies, some microRNA-like RNAs (milRNAs) were found to regulate the production of trichothecenes (Guo et al. 2019) or other mycotoxins (Bai et al. 2015), while other authors showed as the ubiquitination plays an important role in *Fusarium* mycotoxins post-translational regulation process (Chen et al. 2024). In future studies, an assessment of these mechanisms is desirable.

Ferulic acid (FA) is the more representative hydroxycinnamic acid in cereals kernels, but it is also studied in food science for its ability to stabilize anthocyanins through copigmentation, by hydrogen bonds and π-π molecular interaction through the two molecules (Lv et al. 2022). The increasing absorbance of FA:C3G liquid media indicated the existence of a co-pigmentation process, as confirmed by other studies (Zhu et al. 2020). Our results suggest that *F. avenaceum* is able to metabolize C3G, using the glycidic portion to boost fungal growth, while ferulic acid confirm its strong antifungal activity at 0.5 mM (Gautier et al. 2020). The other FA concentrations could be considered as sub-lethal concentrations able to boost *Fusarium* growth, as shown by other studies (Schöneberg et al. 2018). Thus, C3G

showed a contrary influence on fungal biomass and Enns accumulation compared to ferulic acid, and the concurrent application of ferulic acid and C3G resulted in an intermediate effect in both the examined processes.

2.5. References

Abdel-Aal, E. S. M., Hucl, P., and Rabalski, I. (2018). Compositional and antioxidant properties of anthocyanin-rich products prepared from purple wheat. *Food Chemistry*, *254*(February), 13–19. https://doi.org/10.1016/j.foodchem.2018.01.170

Abedi-Firoozjah, R., Yousefi, S., Heydari, M., Seyedfatehi, F., Jafarzadeh, S., Mohammadi, R., Rouhi, M., and Garavand, F. (2022). Application of Red Cabbage Anthocyanins as pH-Sensitive Pigments in Smart Food Packaging and Sensors. *Polymers*, *14*(8). https://doi.org/10.3390/polym14081629

Adejor, J., Tumukunde, E., Li, G., Lin, H., Xie, R., and Wang, S. (2024). Impact of Lysine Succinylation on the Biology of Fungi. *Current Issues in Molecular Biology*, *46*(2), 1020–1046. https://doi.org/10.3390/cimb46020065

Apea-Bah, F., and Beta, T. (2021). Advances in understanding the nutritional value of antioxidants in wheat. In *Improving the nutritional and nutraceutical properties of wheat and other cereals* (pp. 29–72). https://doi.org/10.19103/AS.2021.0087.04

Aristimuño Ficoseco, M. E., Vattuone, M. A., Audenaert, K., Catalán, C. A. N., and Sampietro, D. A. (2014). Antifungal and antimycotoxigenic metabolites in *Anacardiaceae* species from northwest Argentina: isolation, identification and potential for control of Fusarium species. *Journal of Applied Microbiology*, *116*(5), 1262–1273. https://doi.org/10.1111/jam.12436

Atanasova-Penichon, V., Barreau, C., and Richard-Forget, F. (2016). Antioxidant secondary metabolites in cereals: Potential involvement in resistance to *Fusarium* and mycotoxin accumulation. *Frontiers in Microbiology*, *7*(APR), 1–16. https://doi.org/10.3389/fmicb.2016.00566

Bai, Y., Lan, F., Yang, W., Zhang, F., Yang, K., Li, Z., Gao, P., and Wang, S. (2015). SRNA profiling in Aspergillus flavus reveals differentially expressed miRNA-like RNAs response to water activity and temperature. *Fungal Genetics and Biology*, *81*, 113–119. https://doi.org/10.1016/j.fgb.2015.03.004

Beccari, G., Colasante, V., Tini, F., Senatore, M. T., Prodi, A., Sulyok, M., and Covarelli, L. (2018). Causal agents of Fusarium head blight of durum wheat (*Triticum durum* Desf.) in central Italy and their in vitro biosynthesis of secondary metabolites. *Food Microbiology*, *70*, 17–27. https://doi.org/10.1016/j.fm.2017.08.016

Bernardi, J., Stagnati, L., Lucini, L., Rocchetti, G., Lanubile, A., Cortellini, C., De Poli, G., Busconi, M., and Marocco, A. (2018). Phenolic profile and susceptibility to fusarium infection of pigmented maize cultivars. *Frontiers in Plant Science*, *9*(August), 1–13. https://doi.org/10.3389/fpls.2018.01189

Beta, T., Qiu, Y., Liu, Q., Borgen, A., and Apea-Bah, F. B. (2020). Purple Wheat (Triticum sp.) Seeds. In *Nuts and Seeds in Health and Disease Prevention* (pp. 103–125). Elsevier Inc. https://doi.org/10.1016/b978-0-12-818553-7.00010-3

Bilska, K., Stuper-Szablewska, K., Kulik, T., Buśko, M., Załuski, D., Jurczak, S., and Perkowski, J. (2018). Changes in phenylpropanoid and trichothecene production by *Fusarium culmorum* and *F. Graminearum sensu stricto* via exposure to flavonoids. *Toxins*, *10*(3). https://doi.org/10.3390/toxins10030110

Boutigny, A.-L., Barreau, C., Atanasova-Penichon, V., Verdal-Bonnin, M.-N., Pinson-Gadais, L., and Richard-Forget, F. (2009). Ferulic acid, an efficient inhibitor of type B trichothecene biosynthesis and Tri gene expression in *Fusarium* liquid cultures. *Mycological Research*, *113*(6), 746–753. https://doi.org/10.1016/j.mycres.2009.02.010

Boutigny, A., Barreau, C., and Richard-forget, F. (2010). Natural phenolic acids from wheat bran inhibit *Fusarium culmorum* trichothecene biosynthesis in vitro by repressing *Tri* gene expression. *European Journal of Plant Pathology* 275–286. https://doi.org/10.1007/s10658-010-9592-2

Castell, A., Arroyo-Manzanares, N., Palma-Manrique, R., Campillo, N., Torres, C., Fenoll, J., and Viñas, P. (2024). Evaluation of distribution of emerging mycotoxins in human tissues: applications of dispersive liquid–liquid microextraction and liquid chromatography-mass spectrometry. *Analytical and Bioanalytical Chemistry*, *416*(2), 449–459. https://doi.org/10.1007/s00216-023-05040-8

Chen, A., Han, X., Liu, C., Zhou, Y., Ren, Y., Shen, X., Shim, W. B., Chai, Y., Ma, Z., and Chen, Y. (2024). Profiling of deubiquitinases that control virulence in the pathogenic plant fungus *Fusarium graminearum*. *New Phytologist*. https://doi.org/10.1111/nph.19562

Coulet, F., Coton, M., Iperi, C., Belinger Podevin, M., Coton, E., and Hymery, N. (2024). Cytotoxic Effects of Major and Emerging Mycotoxins on HepaRG Cells and Transcriptomic Response after Exposure of Spheroids to Enniatins B and B1. *Toxins*, *16*(1). https://doi.org/10.3390/toxins16010054

Dambolena, J. S., Zygadlo, J. A., and Rubinstein, H. R. (2011). Antifumonisin activity of natural phenolic compounds: A structure–property–activity relationship study. *International Journal of Food Microbiology*, *145*(1), 140–146. https://doi.org/10.1016/j.ijfoodmicro.2010.12.001

Donaldson, G. C., Ball, L. A., Axelrood, P. E., and Glass, N. L. (1995). Primer sets developed to amplify conserved genes from filamentous ascomycetes are useful in differentiating *Fusarium* species associated with conifers. *Applied and Environmental Microbiology*, *61*(4), 1331–1340. https://doi.org/10.1128/aem.61.4.1331-1340.1995

Ederli, L., Beccari, G., Tini, F., Bergamini, I., Bellezza, I., Romani, R., and Covarelli, L. (2021). Enniatin b and deoxynivalenol activity on bread wheat and on *Fusarium* species development. *Toxins*, *13*(10), 1–17. https://doi.org/10.3390/toxins13100728

Enaru, B., Drețcanu, G., Pop, T. D., Stănilă, A., and Diaconeasa, Z. (2021). Anthocyanins: Factors Affecting Their Stability and Degradation. *Antioxidants (Basel, Switzerland)*, *10*(12). https://doi.org/10.3390/antiox10121967

Eranthodi, A., Schneiderman, D., Harris, L. J., Witte, T. E., Sproule, A., Hermans, A., Overy, D. P., Chatterton, S., Liu, J., Li, T., González-Peña Fundora, D., Zhao, W., and Foroud, N. A. (2020). Enniatin production influences *Fusarium avenaceum* virulence on potato tubers, but not on durum wheat or peas. *Pathogens*, *9*(2), 1–20. https://doi.org/10.3390/pathogens9020075

Fanelli, F., Ferracane, R., Ritieni, A., Logrieco, A. F., and Mulè, G. (2014). Transcriptional regulation of enniatins production by *Fusarium avenaceum*. *Journal of Applied Microbiology*, *116*(2), 390–399. https://doi.org/10.1111/jam.12371

Fanelli, Francesca, Iversen, A., Logrieco, A. F., and Mulè, G. (2013). Relationship between fumonisin production and FUM gene expression in *Fusarium verticillioides* under different environmental conditions. *Food Additives and Contaminants - Part A*, *30*(2), 365–371. https://doi.org/10.1080/19440049.2012.743039

Flachowsky, H., Szankowski, I., Fischer, T. C., Richter, K., Peil, A., Höfer, M., Dörschel, C., Schmoock, S., Gau, A. E., Halbwirth, H., and Hanke, M.-V. (2010). Transgenic apple plants overexpressing the *Lc* gene of maize show an altered growth habit and increased resistance to apple scab and fire blight. *Planta*, *231*(3), 623–635. https://doi.org/10.1007/s00425-009-1074-4

Furukawa, T., Yoshinari, T., and Sakuda, S. (2017). Intracellular superoxide level controlled by manganese superoxide dismutases affects trichothecene production in *Fusarium graminearum*. *FEMS Microbiology Letters* 6(October), 1–8. https://doi.org/10.1093/femsle/fnx213

Garmendia, G., Pattarino, L., Negrín, C., Martínez-Silveira, A., Pereyra, S., Ward, T. J., and Vero, S. (2018). Species composition, toxigenic potential and aggressiveness of *Fusarium* isolates causing Head Blight of barley in Uruguay. *Food Microbiology*, *76*(July), 426–433. https://doi.org/10.1016/j.fm.2018.07.005

Gauthier, L., Bonnin-Verdal, M.-N., Marchegay, G., Pinson-Gadais, L., Ducos, C., Richard-Forget, F., and Atanasova-Penichon, V. (2016). Fungal biotransformation of chlorogenic and caffeic acids by Fusarium graminearum: New insights in the contribution of phenolic acids to resistance to deoxynivalenol accumulation in cereals. *International Journal of Food Microbiology*, *221*, 61–68. https://doi.org/10.1016/j.ijfoodmicro.2016.01.005

Gautier, C., Pinson-Gadais, L., and Richard-Forget, F. (2020). Fusarium Mycotoxins Enniatins: An Updated Review of Their Occurrence, the Producing Fusarium Species, and the Abiotic Determinants of Their Accumulation in Crop Harvests. *Journal of Agricultural and Food Chemistry*, *68*(17), 4788–4798. https://doi.org/10.1021/acs.jafc.0c00411

Gautier, C., Pinson-Gadais, L., Verdal-Bonnin, M. N., Ducos, C., Tremblay, J., Chéreau, S., Atanasova, V., and Richard-Forget, F. (2020). Investigating the Efficiency of Hydroxycinnamic Acids to Inhibit the Production of Enniatins by *Fusarium avenaceum* and Modulate the Expression of Enniatins Biosynthetic Genes. *Toxins*, *12*(12), 1–17. https://doi.org/10.3390/toxins12120735

Giménez, P., Just-Borràs, A., Gombau, J., Canals, J. M., and Zamora, F. (2023). Effects of laccase from *Botrytis cinerea* on the oxidative degradation of anthocyanins. *Oeno One*, *57*(3), 243–253. https://doi.org/10.20870/oeno-one.2023.57.3.7567

Gozzi, M., Blandino, M., Dall'Asta, C., Martinek, P., Bruni, R., and Righetti, L. (2023). Anthocyanin Content and *Fusarium* Mycotoxins in Pigmented Wheat (*Triticum aestivum* L. spp. *aestivum*): An Open Field Evaluation. *Plants*, *12*(4). https://doi.org/10.3390/plants12040693

Guo, M. W., Yang, P., Zhang, J. B., Liu, G., Yuan, Q. S., He, W. J., Nian, J. N., Yi, S. Y., Huang, T., and Liao, Y. C. (2019). Expression of microRNA-like RNA-2 (Fgmil-2) and bioH1 from a single transcript in *Fusarium graminearum* are inversely correlated to regulate biotin synthesis during vegetative growth and host infection. *Molecular Plant Pathology*, *20*(11), 1574–1581. https://doi.org/10.1111/mpp.12859

Hammer, Ø., Harper, D. A. T., and Ryan, P. D. (2001). PAST: Paleontological Statistics Software Package for Education and Data Analysis. *Palaeontologia Electronica*, *4*(1), 9. http://palaeo-electronica.org/2001_1/past/issue1_01.htm

Hasuda, A. L., and Bracarense, A. P. F. R. L. (2024). Toxicity of the emerging mycotoxins beauvericin and enniatins: A mini-review. *Toxicon*, *239*(October 2023), 107534. https://doi.org/10.1016/j.toxicon.2023.107534

Hu, Y., Deng, L., Chen, J., Zhou, S., Liu, S., Fu, Y., Yang, C., Liao, Z., and Chen, M. (2016). An analytical pipeline to compare and characterise the anthocyanin antioxidant activities of purple sweet potato cultivars. *Food Chemistry*, *194*, 46–54. https://doi.org/10.1016/j.foodchem.2015.07.133

Jing, N., Song, J., Liu, Z., Wang, L., and Jiang, G. (2020). Glycosylation of anthocyanins enhances the apoptosis of colon cancer cells by handicapping energy metabolism. *BMC Complementary Medicine and Therapies*, *20*(1), 1–13. https://doi.org/10.1186/s12906-020-03096-y

Kumar, N., and Pruthi, V. (2014). Potential applications of ferulic acid from natural sources. *Biotechnology Reports*, *4*(1), 86–93. https://doi.org/10.1016/j.btre.2014.09.002

Lalak-Kańczugowska, J., Witaszak, N., Waśkiewicz, A., Bocianowski, J., and Stępień, Ł. (2023). Plant Metabolites Affect *Fusarium proliferatum* Metabolism and In Vitro Fumonisin Biosynthesis. In *International Journal of Molecular Sciences* (Vol. 24, Issue 3). https://doi.org/10.3390/ijms24033002

Lei, K. J., Zhang, L., Du, X. Y., An, Y., Chang, G. H., and An, G. Y. (2018). A chalcone synthase controls the verticillium disease resistance response in both Arabidopsis thaliana and cotton. *European Journal of Plant Pathology*, *152*(3), 769–781. https://doi.org/10.1007/s10658-018-1521-9

Li, Z., and Ahammed, G. J. (2023). Plant stress response and adaptation via anthocyanins: A review. *Plant Stress*, *10*, 100230. https://doi.org/10.1016/j.stress.2023.100230

Loypimai, P., Moongngarm, A., and Chottanom, P. (2016). Thermal and pH degradation kinetics of anthocyanins in natural food colorant prepared from black rice bran. *Journal of Food Science and Technology*, *53*(1), 461–470. https://doi.org/10.1007/s13197-015-2002-1

Lv, X., Li, L., Lu, X., Wang, W., Sun, J., Liu, Y., Mu, J., Ma, Q., and Wang, J. (2022). Effects of organic acids on color intensification, thermodynamics, and copigmentation interactions with anthocyanins. *Food Chemistry*, *396*(December 2021), 133691. https://doi.org/10.1016/j.foodchem.2022.133691

Lysøe, E., Harris, L. J., Walkowiak, S., Subramaniam, R., Divon, H. H., Riiser, E. S., Llorens, C., Gabaldón, T., Kistler, H. C., Jonkers, W., Kolseth, A. K., Nielsen, K. F., Thrane, U., and Frandsen, R. J. N. (2014). The genome of the generalist plant pathogen *Fusarium avenaceum* is enriched with genes involved in redox, signaling and secondary metabolism. *PLoS ONE*, *9*(11). https://doi.org/10.1371/journal.pone.0112703

Mandalà, G., Ceoloni, C., Busato, I., Favaron, F., and Tundo, S. (2021). Transgene pyramiding in wheat: Combination of deoxynivalenol detoxification with inhibition of cell wall degrading enzymes to contrast Fusarium Head Blight and Crown Rot. *Plant Science*, *313*, 111059. https://doi.org/10.1016/j.plantsci.2021.111059

Martin, C., Schöneberg, T., Vogelgsang, S., Bertossa, M., Mauch-mani, B., Mascher, F., Mauch-mani, B., Mascher, F., Martin, C., Schöneberg, T., Vogelgsang, S., Vincenti, J., and Bertossa, M. (2017). Factors of wheat grain resistance to Fusarium head blight. *Phytopathologia Mediterranea*. https://doi.org/10.14601/Phytopathol_Mediterr-20292

Martínez-Fraca, J., de la Torre-Hernández, M. E., and Meshoulam-Alamilla, M. (2022). In Search of Resistance Against Fusarium Ear Rot: Ferulic Acid Contents in Maize Pericarp Are Associated With Antifungal Activity and Inhibition of Fumonisin Production. *Frontiers in Plant Science*, *13*(April), 1–11.

https://doi.org/10.3389/fpls.2022.852257

Meca, G., Sospedra, I., Valero, M. A., Mañes, J., Font, G., and Ruiz, M. J. (2011). Antibacterial activity of the enniatin B, produced by *Fusarium tricinctum* in liquid culture, and cytotoxic effects on Caco-2 cells. *Toxicology Mechanisms and Methods*, *21*(7), 503–512. https://doi.org/10.3109/15376516.2011.556202

Mesny, F., Miyauchi, S., Thiergart, T., Pickel, B., Atanasova, L., Karlsson, M., Hüttel, B., Barry, K. W., Haridas, S., Chen, C., Bauer, D., Andreopoulos, W., Pangilinan, J., LaButti, K., Riley, R., Lipzen, A., Clum, A., Drula, E., Henrissat, B., … Hacquard, S. (2021). Genetic determinants of endophytism in the *Arabidopsis* root mycobiome. *Nature Communications*, *12*(1), 1–15. https://doi.org/10.1038/s41467-021-27479-y

Miller, A.-F. (2012). Superoxide dismutases: ancient enzymes and new insights. *FEBS Letters*, *586*(5), 585–595. https://doi.org/10.1016/j.febslet.2011.10.048

Nielsen, L. K., Cook, D. J., Edwards, S. G., and Ray, R. V. (2014). The prevalence and impact of Fusarium head blight pathogens and mycotoxins on malting barley quality in UK. *International Journal of Food Microbiology*, *179*, 38–49. https://doi.org/10.1016/j.ijfoodmicro.2014.03.023

Pagnussatt, F. A., Del Ponte, E. M., Garda-Buffon, J., and Badiale-Furlong, E. (2014). Inhibition of *Fusarium graminearum* growth and mycotoxin production by phenolic extract from Spirulina sp. *Pesticide Biochemistry and Physiology*, *108*, 21–26. https://doi.org/10.1016/j.pestbp.2013.11.002

Palumbo, J. D., O'Keeffe, T. L., and Mahoney, N. E. (2007). Inhibition of ochratoxin A production and growth of *Aspergillus* species by phenolic antioxidant compounds. *Mycopathologia*, *164*(5), 241–248. https://doi.org/10.1007/s11046-007-9057-0

Panel, E. C. (2014). Scientific Opinion on the risks to human and animal health related to the presence of beauvericin and enniatins in food and feed. *EFSA Journal*, *12*(8). https://doi.org/10.2903/j.efsa.2014.3802

Perochon, A., and Doohan, F. M. (2024). Trichothecenes and Fumonisins: Key Players in *Fusarium*–Cereal Ecosystem Interactions. In *Toxins* (Vol. 16, Issue 2). https://doi.org/10.3390/toxins16020090

Pinson-Gadais, L., Richard-Forget, F., Frasse, P., Barreau, C., Cahagnier, B., Richard-Molard, D., and Bakan, B. (2008). Magnesium represses trichothecene biosynthesis and modulates Tri5, Tri6, and Tri12 genes expression in *Fusarium graminearum*. *Mycopathologia*, *165*(1), 51–59. https://doi.org/10.1007/s11046-007-9076-x

Polano, C., Sanseverino, I., Ermolli, M., Porcel Rodriguez, E., Bisselink, B., Pozzoli, L., and Lettieri, T. (2024). *Mycotoxin fungal plant diseases and climate change: state of the art and beyond*. *KJ-NA-31-797-EN-N (online)*. https://doi.org/10.2760/690696

Ponts, N., Pinson-gadais, L., Verdal-Bonnin, M.-N., Barreau, C., and Richard-forget, F. (2006). Accumulation of deoxynivalenol and its15-acetylated form is significantly modulated by oxidative stress in liquid cultures of *Fusarium graminearum*. *FEMS Microbiology Letters* 258, 102–107. https://doi.org/10.1111/j.1574-6968.2006.00200.x

Rafiei, V., Vélëz, H., and Tzelepis, G. (2021). The role of glycoside hydrolases in phytopathogenic fungi and oomycetes virulence. *International Journal of Molecular Sciences*, *22*(17). https://doi.org/10.3390/ijms22179359

Rancurel, C., van Tran, T., Elie, C., and Hilliou, F. (2019). SATQPCR: Website for statistical analysis of real-time quantitative PCR data. *Molecular and Cellular Probes*, *46*, 101418. https://doi.org/10.1016/j.mcp.2019.07.001

Ricelli, A., De Angelis, M., Primitivo, L., Righi, G., Sappino, C., and Antonioletti, R. (2019). Role of some food-grade synthesized flavonoids on the control of ochratoxin a in *Aspergillus* carbonarius. *Molecules*, *24*(14). https://doi.org/10.3390/molecules24142553

Río, J. A. D., Díaz, L., Ortuño, A. M., García-Lidón, Á., and Porras, I. (2015). Metabolism of flavonoids and mycotoxins in citrus fruits infected by *Alternaria alternata*. *Acta Horticulturae*, *1065*, 1549–1554. https://doi.org/10.17660/ActaHortic.2015.1065.197

Romero, S. M., Alberto, M. R., and Vaamonde, G. (2010). Effect of gallic acid on *Aspergillus carbonarius* growth and ochratoxin A production. *World Mycotoxin Journal*, *3*(1), 45–48. https://doi.org/10.3920/WMJ2009.1181

Rosales, T. K. O., and Fabi, J. P. (2022). Nanoencapsulated anthocyanin as a functional ingredient: Technological

application and future perspectives. *Colloids and Surfaces B: Biointerfaces*, *218*(April). https://doi.org/10.1016/j.colsurfb.2022.112707

Rossetti, A., Mazzaglia, A., Muganu, M., Paolocci, M., Sguizzato, M., Esposito, E., Cortesi, R., and Balestra, G. M. (2017). Microparticles containing gallic and ellagic acids for the biological control of bacterial diseases of kiwifruit plants. *Journal of Plant Diseases and Protection*, *124*(6), 563–575. https://doi.org/10.1007/s41348-017-0096-6

Salas-Gómez, A. L., Espinoza Ahumada, C. A., Castillo Godina, R. G., Ascacio-Valdés, J. A., Rodríguez-Herrera, R., Segura Martínez, M. T. de J., Neri Ramírez, E., Estrada Drouaillet, B., and Osorio-Hernández, E. (2023). Antifungal In Vitro Activity of Phoradendron sp. Extracts on Fungal Isolates from Tomato Crop. *Plants*, *12*(3), 1–12. https://doi.org/10.3390/plants12030672

Salhi, N., Mohammed Saghir, S. A., Terzi, V., Brahmi, I., Ghedairi, N., and Bissati, S. (2017). Antifungal Activity of Aqueous Extracts of Some Dominant Algerian Medicinal Plants. *BioMed Research International*, *2017*. https://doi.org/10.1155/2017/7526291

Savignac, J.-M., Atanasova, V., Chereau, S., Ducos, C., Gallegos, N., Ortega, V., Ponts, N., and Richard-Forget, F. (2023). Carotenoids Occurring in Maize Affect the Redox Homeostasis of *Fusarium graminearum* and Its Production of Type B Trichothecene Mycotoxins: New Insights Supporting Their Role in Maize Resistance to Giberella Ear Rot. *Journal of Agricultural and Food Chemistry*, *71*(7), 3285–3296. https://doi.org/10.1021/acs.jafc.2c06877

Schöneberg, T., Kibler, K., Sulyok, M., Musa, T., Bucheli, T. D., Mascher, F., Bertossa, M., Voegele, R. T., and Vogelgsang, S. (2018). Can plant phenolic compounds reduce Fusarium growth and mycotoxin production in cereals? *Food Additives and Contaminants - Part A Chemistry, Analysis, Control, Exposure and Risk Assessment*, *35*(12), 2455–2470. https://doi.org/10.1080/19440049.2018.1538570

Senatore, M. T., Ward, T. J., Cappelletti, E., Beccari, G., McCormick, S. P., Busman, M., Laraba, I., O'Donnell, K., and Prodi, A. (2021). Species diversity and mycotoxin production by members of the *Fusarium tricinctum* species complex associated with Fusarium head blight of wheat and barley in Italy. *International Journal of Food Microbiology*, *358*(May), 109298. https://doi.org/10.1016/j.ijfoodmicro.2021.109298

Shirai, A., and Tanaka, A. (2024). Effects of ferulic acid combined with light irradiation on deoxynivalenol and its production in *Fusarium graminearum*. *Fungal Biology*, *128*(2), 1684–1690. https://doi.org/10.1016/j.funbio.2024.02.003

Sinela, A., Rawat, N., Mertz, C., Achir, N., Fulcrand, H., and Dornier, M. (2017). Anthocyanins degradation during storage of Hibiscus sabdariffa extract and evolution of its degradation products. *Food Chemistry*, *214*, 234–241. https://doi.org/10.1016/j.foodchem.2016.07.071

Sivankalyani, V., Feygenberg, O., Diskin, S., Wright, B., and Alkan, N. (2016). Increased anthocyanin and flavonoids in mango fruit peel are associated with cold and pathogen resistance. *Postharvest Biology and Technology*, *111*, 132–139. https://doi.org/10.1016/j.postharvbio.2015.08.001

Sohlberg, E., Virkajärvi, V., Parikka, P., Rämö, S., Laitila, A., and Sarlin, T. (2022). Taqman qPCR Quantification and *Fusarium* Community Analysis to Evaluate Toxigenic Fungi in Cereals. In *Toxins* (Vol. 14, Issue 1). https://doi.org/10.3390/toxins14010045

Sy-Cordero, A. A., Pearce, C. J., and Oberlies, N. H. (2012). Revisiting the enniatins: a review of their isolation, biosynthesis, structure determination and biological activities. *The Journal of Antibiotics*, *65*(11), 541–549. https://doi.org/10.1038/ja.2012.71

Szabó, B. K., Molnár, K. D., Vlaskality, S. D., and Körösi, K. (2023). Occurring *Fusarium* spp. in sorghum (*Sorghum bicolor* L. Moench) grains. *Acta Phytopathologica et Entomologica Hungarica*, *58*(2), 180–187. https://doi.org/10.1556/038.2023.00168

Szabó, Z., Pákozdi, K., Murvai, K., Csernoch, L., and Emri, T. (2020). FvmnSOD is involved in oxidative stress defence , mitochondrial stability and apoptosis prevention in *Fusarium verticillioides*. *Journal of Basic Microbiology November*, 994–1003. https://doi.org/10.1002/jobm.202000560

Treutter, D. (2006). Significance of flavonoids in plant resistance: A review. *Environmental Chemistry Letters*, *4*(3), 147–157. https://doi.org/10.1007/s10311-006-0068-8

Tumukunde, E., Xie, R., and Wang, S. (2021). Updates on the functions and molecular mechanisms of the genes involved in aspergillus flavus development and biosynthesis of aflatoxins. *Journal of Fungi*, *7*(8). https://doi.org/10.3390/jof7080666

Wagay, N. A., Lone, R., Rafiq, S., and Bashir, S. U. (2020). Phenolics: A Game Changer in the Life Cycle of Plants. In R. Lone, R. Shuab, and A. N. Kamili (Eds.), *Plant Phenolics in Sustainable Agriculture : Volume 1* (pp. 241–275). Springer Singapore. https://doi.org/10.1007/978-981-15-4890-1_11

Wang, F., Chen, Y., Hu, H., Liu, X., Wang, Y., Saleemi, M. K., He, C., and Haque, M. A. (2022). Protocatechuic acid: A novel detoxication agent of fumonisin B1 for poultry industry. *Frontiers in Veterinary Science*, *9*. https://doi.org/10.3389/fvets.2022.923238

Wang, Y., An, H., Guo, Y. N., Wang, Q., Shang, Y. Y., Chen, M. K., Liu, Y. X., Meng, J. X., Zhang, S. Y., Wei, J., and Li, H. H. (2023). Anthocyanins from *Malus* spp. inhibit the activity of *Gymnosporangium yamadae* by downregulating the expression of WSC, RLM1, and PMA1. *Frontiers in Microbiology*, *14*(May). https://doi.org/10.3389/fmicb.2023.1152050

Weber, F., and Larsen, L. R. (2017). Influence of fruit juice processing on anthocyanin stability. *Food Research International*, *100*(March), 354–365. https://doi.org/10.1016/j.foodres.2017.06.033

Wegener, C. B., and Jansen, G. (2007). Soft-rot Resistance of Coloured Potato Cultivars (Solanum tuberosum L.): The Role of Anthocyanins. *Potato Research*, *50*(1), 31–44. https://doi.org/10.1007/s11540-007-9027-4

Wegulo, S. N., Baenziger, P. S., Hernandez Nopsa, J., Bockus, W. W., and Hallen-Adams, H. (2015). Management of Fusarium head blight of wheat and barley. *Crop Protection*, *73*, 100–107. https://doi.org/10.1016/j.cropro.2015.02.025

Wen, H., Kang, J., Li, D., Wen, W., Yang, F., Hu, H., and Liu, C. (2016). Antifungal activities of anthocyanins from purple sweet potato in the presence of food preservatives. *Food Science and Biotechnology*, *25*(1), 165–171. https://doi.org/10.1007/s10068-016-0025-7

Were, E., Schöne, J., Viljoen, A., and Rasche, F. (2022). Phenolics mediate suppression of *Fusarium oxysporum* f. sp. *cubense* TR4 by legume root exudates. *Rhizosphere*, *21*. https://doi.org/10.1016/j.rhisph.2021.100459

Yao, S., Guo, Y., Wang, Y., Zhang, D., Xu, L., and Tang, W. (2016). A cytoplasmic Cu-Zn superoxide dismutase SOD1 contributes to hyphal growth and virulence of *Fusarium graminearum*. *Fungal Genetics and Biology*, *91*, 32–42. https://doi.org/10.1016/j.fgb.2016.03.006

Zhang, Y., Butelli, E., De Stefano, R., Schoonbeek, H., Magusin, A., Pagliarani, C., Wellner, N., Hill, L., Orzaez, D., Granell, A., Jones, J. D. G., and Martin, C. (2013). Anthocyanins Double the Shelf Life of Tomatoes by Delaying Overripening and Reducing Susceptibility to Gray Mold. *Current Biology*, *23*(12), 1094–1100. https://doi.org/10.1016/j.cub.2013.04.072

Zhao, C. L., Chen, Z. J., Bai, X. S., Ding, C., Long, T. J., Wei, F. G., and Miao, K. R. (2014). Structure-activity relationships of anthocyanidin glycosylation. *Molecular Diversity*, *18*(3), 687–700. https://doi.org/10.1007/s11030-014-9520-z

Zhu, Y., Chen, H., Lou, L., Chen, Y., Ye, X., and Chen, J. (2020). Copigmentation effect of three phenolic acids on color and thermal stability of Chinese bayberry anthocyanins. *Food Science and Nutrition*, *8*(7), 3234–3242. https://doi.org/10.1002/fsn3.1583

3. Physiological and morphological traits associated with Fusarium head blight response in a flavonoid-rich durum wheat genotype

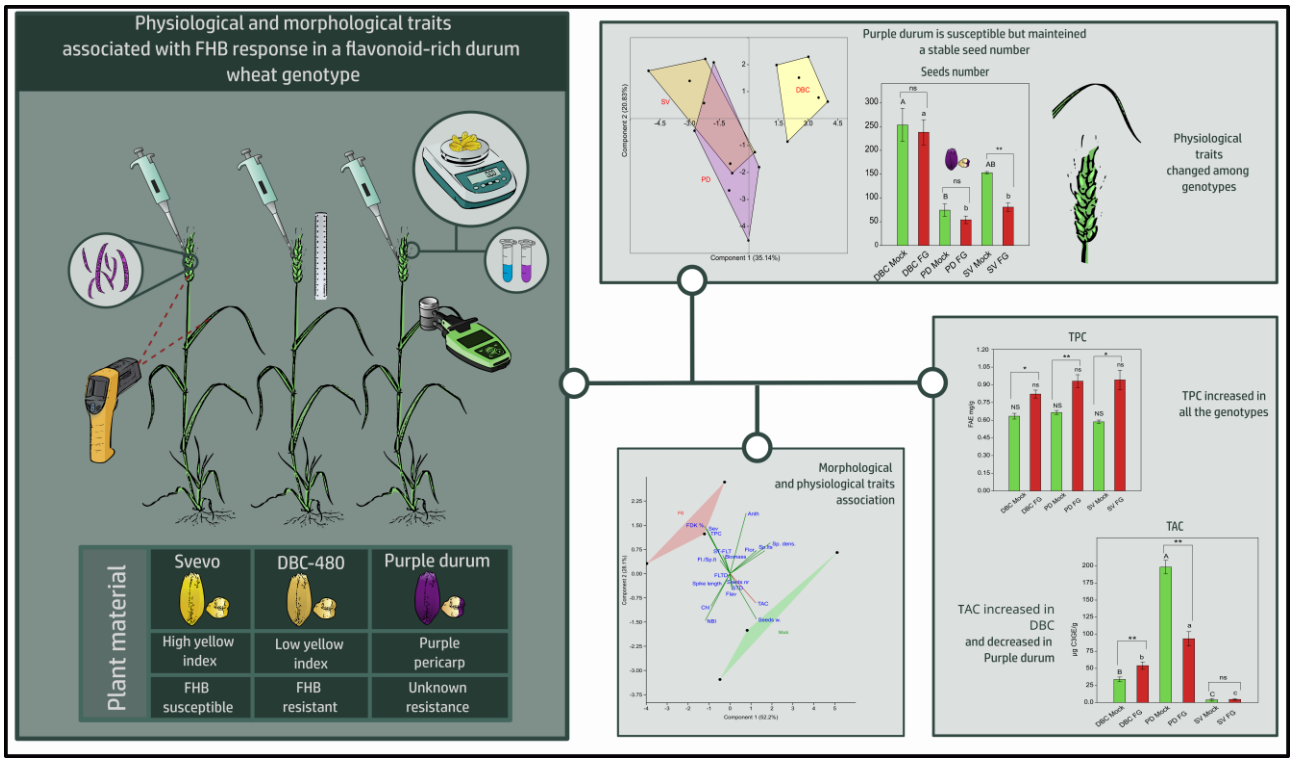

Abstract: Durum wheat is among the cereal crops with the highest susceptibility to Fusarium Head Blight (FHB), the most devastating wheat disease. Purple pericarp durum wheat genotypes, having anthocyanin-rich grains, are an unexplored group of accessions, which may provide valuable information about the role of flavonoids in wheat-*Fusarium* interaction. In this study, a purple pericarp durum wheat accession (Purple durum) was challenged with *Fusarium graminearum* infection, evaluating the different responses of physiological traits, in comparison with an FHB-resistant line (DBC-480) and a commercial FHB-susceptible cultivar (Svevo). Purple durum showed high susceptibility to FHB, but the infection did not affect the seed set, as for the resistant control. In Purple durum flag leaves, lower flavonoid content and higher temperature depression, compared to the resistant control, were detected. The infection affected the difference between the spike temperature and the flag leaf temperature in the resistant and the susceptible control in an opposite way, while the total phenolic content was always higher in the infected spikes. Instead, the total anthocyanin content (TAC) of the spikes was considerably lower in Purple durum subjected to the infection compared to the mock plants, while TAC increased in the infected resistant genotype, suggesting an involvement of flavonoids in the resistance mechanism of DBC-480. Association among morphological spike traits and physiological traits are discussed. Our results corroborate the importance of phenylpropanoids in FHB-wheat interaction and point attention on anthocyanin metabolism, suggesting to consider these metabolites, which are under-investigated for durum wheat resistance.

Publications:

Felici, L., Francesconi, S., Sestili, F., and Balestra G.M. Physiological and morphological traits associated with Fusarium head blight response in a flavonoid-rich durum wheat genotype. *J Plant Pathol* (2024). https://doi.org/10.1007/s42161-024-01663-7

3.1. Introduction

Durum wheat (*Triticum turgidum* L. subsp. *durum* (Desf.) Husn.) accounts for less than 7% of the total wheat produced worldwide, and it is concentrated in relatively small geographic regions where it is one of the main cereal crops, as in the Mediterranean basin (Martínez-Moreno et al. 2022). In these regions, durum wheat is used to produce semolina and several traditional foodstuffs (as pasta, bread, couscous, burghul and freekeh) (Paciulli et al. 2021; Conte et al. 2021; Boukid 2021), and could be considered as a relevant natural source of energy, vitamins, minerals, and other nutritional compounds, such as antioxidant bioactive molecules, including carotenoids, tocopherols and phenylpropanoids (Apea-Bah and Beta 2021). These bioactive molecules can give a different pigmentation to the grains. The typical yellow-amber color of semolina is due to the carotenoid pigment content in the whole kernel, and it is commercially identified as the yellow index (Ficco, et al. 2014a). In particular, modern durum wheat cultivars released in Europe and in Italy in the last decades show a considerably higher yellow index than the traditional ones (Digesù et al. 2009), most likely due to increasing breeding efforts focused on this commercial trait. Nevertheless, other colored durum wheat grains exist, such as anthocyanin-pigmented grains, even their use and diffusion are currently limited. Anthocyanin-pigmented grains have blue to blue-black, and red to purple grains. In these genotypes, anthocyanins in the grains are mainly present in the external layers, for instance purple genotypes express color in pericarp layer due to high concentration in compounds like cyanidin 3-*O*-glucoside (Böhmdorfer et al. 2018). Purple tetraploid wheat cultivars originated in Ethiopia (Tesemma et al. 1993; Kebebew et al. 2001), where they were naturally and artificially selected in the highlands for their adapted traits, like earlier maturity, shorter height, higher fertility, tillering capacity and harvest index (Belay et al. 1995). In the last decades interest on these genotypes is increasing for the production of biofortified staple food (Dwivedi et al. 2022; Kaur et al. 2023). Different studies investigated the environmental factors influencing the anthocyanins accumulation in pigmented wheat (Beleggia et al. 2021; Dwivedi et al. 2022), but several biotic stresses (plant diseases) can also influence the accumulation of secondary metabolites. Actually, wheat can produce numerous metabolites in response to stress (Sunic et al. 2023). Several research were focused on phenolic acids, flavonoids and other phenylpropanoid differentially accumulated in infected wheat cultivars with different susceptibility to diseases (Gunnaiah and Kushalappa 2014; Tu et al. 2023; Gauthier et al. 2016), while anthocyanins are usually under investigated, due to the low occurrence in wheat tissues. Different fungal pathogens can cause disease in durum wheat, such as mildew, brown rust, *Septoria* spp. and *Fusarium* spp. (Jbir et al. 2022). Among the main widespread cereal crops, tetraploid durum wheat has the major susceptibility to Fusarium head blight (FHB) (Gaikpa et al. 2020). FHB is the most devastating wheat disease due to the lack of resistant wheat varieties. Severe yield loss (10%–70%), reduced grain quality, and health problems caused by the accumulation of mycotoxins in food and feed are primary concerns in most of the wheat-growing areas in Asia, North America, South America and Europe due to FHB epidemics (McMullen et al. 2012; Zhu et al. 2019; Buerstmayr et al. 2020; Ma et al. 2020). *Fusarium graminearum* (teleomorph Gibberella zeae), one of the main causal agents of FHB, is a fungal hemi-biotrophic pathogen. Anthesis is the phenological stage with the highest susceptibility to the infection and, in a warm and humid environment, *Fusarium* spp. grows rapidly within 3-6 days after infection in wheat spikelets (McMullen et al. 2012). The fungus then colonizes tissues, causing necrosis. This results in water-filled tissues, causing the production of shriveled kernels and early bleaching, affecting photosynthesis. Wheat resistance to FHB is a complex trait, affected by the environment and controlled by several Quantitative Trait Loci (QTLs). Phenotyping for FHB resistance usually includes the measurement of one or more of the so-called FHB resistance components or types such as Type I resistance, defined as the plant ability to avoid initial penetration (studied by spray inoculation), or type II resistance describes the spread of head blight from the ovary to the other parts of the head, after artificial tip inoculation (Schroeder and Christensen 1963). No one of them is feasible

alone to draw a conclusion on FHB susceptibility/resistance, since they could not be correlated (Mesterhazy 2020). To date, very little is known about resistance of purple genotypes to FHB. Some research assessed the FHB tolerance of blue and purple bread wheat genotypes (Martin et al. 2017; Gozzi et al. 2023), while investigations on purple durum wheat genotypes are currently lacking.

In this study, three different durum wheat genotypes differing for their resistance to FHB and for grains pigmentation were artificially inoculated with *F. graminearum* spores, in order to evaluate the genotype × infection interaction on parameters describing production traits, metabolite-related traits, physiological-related traits and correlated them with disease-associated parameters and FHB resistance-associated plant morphological features. In particular, total phenolic content and total anthocyanin content modifications due to *F. graminearum* infection were investigated. Furthermore, screening for FHB resistance traits in these lines can potentially open new perspectives for breeding programs.

3.2. Materials and methods

3.2.1.Plant material and growth condition

Three durum wheat genotypes (*Triticum turgidum* subsp. *durum*) were used in the present study. Svevo is a commercial early maturing cultivar with high protein content and yellow index. Svevo was used as FHB susceptible control. Purple Durum is a pigmented durum wheat genotype (accession number NGB 6399), with purple grain pericarp, originally collected in Ethiopia and provided by Nordic Baltic Genebanks (GENBIS). The FHB-resistant durum wheat experimental line DBC-480, harboring the resistant quantitative trait locus *Fhb1*, was provided by IFA - Tulln (Prat et al. 2017). The experiments were carried out in a growth chamber equipped with white led light (Combo 600 W and Slim Natural Indoor bars, C-Led, Italy), controlled temperature and relative humidity. The kernels were germinated on paper soaked in sterile distilled water for 7 days at 20˚C with a 16 h photoperiod and then transferred to 9 x 9 cm pot filled with TYPical Brill soil. Plants were grown at 10°C with an 8 h photoperiod for 2 weeks to break the dormancy and then each plant was transferred in a 2 L pot (12.8 x 12.8 x 20 cm), filled using the same soil, and plants were grown at 20°C (±2°C), 16 h photoperiod and 60% relative humidity until the end of the experiment. The plants were fertilized using calcium nitrate (15.5-0-0+26.5 CaO, Haifa) at every transplanting event and at heading and using a micronutrient liquid fertilizer (NPK 4-7-7 +B+Cu+Fe+Mn+Zn, Flortis).

3.2.2. Fungal material and inoculum preparation

The highly virulent and DON-producing isolate of *F. graminearum* wild type 3824 was isolated for the first time by the University of Pisa (Tomassini et al. 2009). The inoculum was prepared using SNA culture media following literature references (Leslie and Summerell 2006; Francesconi et al. 2020). The conidial suspension was recovered, and the concentration adjusted to $1x10^6$ conidia mL^{-1} using a Thoma Chamber (0.100 mm depth and 0.0025 mm^2). The inoculum was prepared in sterile distilled water supplemented with 0.05% (v/v) of Tween-20.

3.2.3. Experimental design, infection technique and disease assessment

Plants were subjected to artificial inoculation at anthesis (Zadok stage 69) using a point inoculation technique (Zadoks et al. 1974). In brief, 10 μL of spore suspension were applied to the central spike floret of each plant (using a laboratory pipette), while 10 μL of sterile distilled water supplemented with 0.05% (v/v) of Tween-20 were applied for mock treated plants. For each genotype, three replicates consisting of 10 plants each, were considered for each treatment

(inoculated and mock treated) using a completely randomized experimental design. The FHB disease severity (%) was determined by counting the number of bleached spikelets (number of infected spikelets on the total number of spikelets per spike) for each inoculated spike from 3 to 21 days post infection (DPI) (Francesconi et al. 2019).

3.2.4. Temperature measurements

Temperature (°C) of spikes and flag leaves was assessed using an infrared thermometer (Fluke 561, Fluke Corporation, USA) on 3 randomly chosen plants for each replicate at 3 DPI and 7 DPI (Francesconi and Balestra 2020). The thermometer gun was focused at the upper side of the flag leaf for approximately 3 seconds at 10 cm of distance from the leaf, for flag leaf measurement, and then focused at the inoculated spikelet on the spike (marked with a red sign) in the same way, for spike temperature assessment. Real growth chamber temperature at measurement moment (air temperature) was recorded and then the following differences were calculated: air temperature-flag leaf temperature (Flag Leaf Temperature Depression, FLTD); air temperature–spike temperature (Spike Temperature Depression, STD); spike temperature – leaf temperature (ST-FLT). Temperature depressions (FLTD and STD) were considered instead of leaf and spike temperature because the different plants were measured in different days, due to the infection scalarity.

3.2.5. Dualex ® leaf-clip measurements

Chlorophyll (Chl), flavonols (Flv) and anthocyanins (Anth) content, and afterwards the nitrogen balance index of the flag leaves (NBI) was assessed by a non-destructive method (Cerovic et al. 2012), using a leafclip sensor (Dualex ® 4 Scientific, FORCE-A) considering the flag leaf on 3 randomly chosen plants for each replicate at 21 DPI.

3.2.6. Spike architecture traits

Spike architecture traits were evaluated at 21 DPI in all the plants (inoculated and mock) following literature references (Franco et al. 2021). Five different parameters were measured: (1) Spike length was measured as the distance in cm between the top and the bottom node of the rachis; (2) number of spikelets per spike (spikelets number) was the total number of spikelets per spike; (3) spike density was calculated dividing the number of spikelets in a spike and its length in cm; (4) number of florets (florets number) per spike was counted; (5) the average number of florets per spikelet (florets/spikelet) was estimated as the number of florets in the spike on the total number of spikelets in the spike.

3.2.7. Production parameters and Fusarium Damaged Kernels (FDK)

At maturity stage, spikes were harvested, and production parameters were assessed. For each replicate, the average kernel weight (seeds weight, as mean weight of the single seed) was assessed. Furthermore, the average of kernels produced for each spike (seeds number, total number of kernels on the number of spikes) was calculated. Kernels that were visually shriveled or chalky in appearance were designated as Fusarium Damaged Kernels (FDK). FDK parameter was expressed as percentage as follows:

$$FDK\ \% = \frac{Nr_{FDK} \times 100}{Nr_{tot}}$$

Where Nr_{FDK} is the number of FDK, and Nr_{tot} is the number of total produced kernels for each replicate. After these measurements, the kernels, the chaff and the rachis from each experimental sample (3 replicates consisting of 10 plants each) were homogenously milled into a fine flour using an electric coffee grinder, stored at 4°C and used for Total Phenolic Content (TPC), Total Anthocyanins Content (TAC) and fungal biomass assessment.

3.2.8. Total phenolic content (TPC)

A rapid, small-scale, high-throughput assay for approximating the total phenolic substrates on the basis of the improved Folin-Ciocalteu (F-C) method of Singleton and Rossi (Singleton and Rossi 1965), using ferulic acid as a standard, was used, following literature references with minor modification (Ainsworth and Gillespie 2007; Schiavi et al. 2022). In brief, free total phenols were extracted from 300 mg of flour using 1.5 ml of a solution of methanol/water (85:15) as solvent. The solid liquid extraction was performed in a 1.5 ml tube kept in agitation for 24 h in a rotary shaker (95 rpm) at room temperature. After 24 h, the flour and the solvent were separated by centrifugation (3 minutes, 13000x *g*, room temperature); 100 µL of the supernatant was used for the analysis. 750 µL of a 10-fold dilution of Folin-Ciocalteu reagent was added to the samples and incubated 10 minutes at room temperature. Then, 750 µL of a 2% sodium carbonate (Na_2CO_3) aqueous solution (w/v) was added and the mixture was incubated in the dark for 3 h. 200 µL of each sample were then transferred to a 96-well plate, considering 4 technical replicates for each experimental sample, and the absorbance was measured at 765 nm using a DR - 200B Microplate reader (Diatek instruments). Final results were expressed as ferulic acid equivalent (FAE), related to the initial real sample weight, and using a ferulic acid (CAS No: 537-98-4, Sigma-Aldrich) calibration curve (ranging from 25 to 350 mg L^{-1} with an $R^2 = 0.9908$).

3.2.9. Total Anthocyanin Content (TAC)

An estimation of the anthocyanin content in the mature spikes grinded samples was achieved using a pH differential method following the existing literature (Apea-Bah and Beta 2021) with some modifications. Briefly, for each sample 100 mg were used and two separated extractions (1 hour in a rotary shaker, 150 rpm at 25 °C) were performed, using two different solvents: acidified methanol (pH 1) and methanol adjusted to pH 4.5 (HCl and sodium acetate were used for pH correction). After the extraction, samples were centrifuged (13.300x *g* for 10 minutes), 200 µL of the supernatant were dispensed in 96-multiwell plates and the absorbance of both the extracts was measured at 520 nm and 700 nm using a DR-200B Microplate reader (Diatek instruments). Anthocyanin content was expressed as µg of cyanidin 3-*O*-glucoside equivalents (C3GE) on grams of samples and calculated as suggested by Apea-Bah and Beta (2021), considering the molecular weight of cyanidin 3-*O*-glucoside (449.2 g/mol), molar extinction coefficient of cyanidin 3-*O*-glucoside (26,900 $L.cm^{-1}.mol^{-1}$), and a path length of 0.5 cm. Three biological replicates and four technical replicates were considered.

3.2.10. Quantification of Fungal Biomass by Real-Time qPCR

100 mg of milled flour from each experimental sample was used for total genomic DNA extraction following the protocol of GRS Genomic DNA Kit – Plant (Grisp, Portugal). To obtain the *F. graminearum* calibration curve, 100 mg of fresh mycelium was scraped from a PDA plate cultured in the dark at 24 °C for 7 days in purity. DNA was quantified with a Qubit™ fluorometer 1.01 (Invitrogen) using the Qubit™ dsDNA BR Assay Kit (Thermo Fisher Scientific). Real-Time qPCR was performed following the instructions from Rotor Gene Q (Qiagen) and Xpert Fast SYBR (uni) Master Mix (Grisp). Wheat and fungal calibration curves were performed preparing four 1:10 serial dilutions (1:1, 1:10, 1:100, 1:1000) from fresh fungal mycelium and uninoculated wheat material DNAs (further details in the Supplementary material 3.1). Real-Time qPCR amplification conditions included: an initial denaturation step of 3 minutes at 95°C; 40 cycles of 5 seconds denaturation at 95°C, 30 seconds of annealing at 61°C and 20 seconds of elongation at 72°C. Real Time - qPCR was performed using the primer pair Tri6_10F/Tri6_4R for *F. graminearum* DNA quantification (Horevaj et al. 2011) and TaACT_F/TaACT_R for wheat DNA quantification (Mandalà et al. 2019). Data were

obtained from three technical replicates derived from three biological replicates. Results were expressed as ng of fungal DNA per ng of plant DNA.

3.2.11. Data analysis

Data normal distribution was checked using the Shapiro-Wilk normality test. For severity and fungal biomass data, due to their non-normal distribution, the statistical significance was assessed using the Kruskal–Wallis test (Kruskal and Wallis 1952) and a Dunn's test of multiple comparisons was performed. All the other data were analyzed using analysis of variance (ANOVA). Spike architecture traits were subjected to one-way ANOVA. All the remaining measurements (Chl, Flav, Anth, NBI, FLTD, STD, ST-FLT, FDK, TPC and TAC) were analyzed using both two - way ANOVA and one-way ANOVA. Two-way ANOVA was employed to study the genotype x infection interaction, and when this analysis was significant, one-way ANOVA were considered for each group (same genotype or same treatment), as shown in the Figures. Two levels of significance ($p < 0.05$, $p < 0.01$) were considered to assess the significance of the F values. When significant F values were calculated, pairwise analyses were carried out using the Tukey's test at 0.95 or 0.99 confidence levels. To evaluate parameters relationships, multivariate analysis (principal component analysis, PCA) were performed. For these analysis, due to the wide range of considered data, all data were transformed by a standardization using the Z-score method and the following equation (Mohamad and Usman 2013):

$$Z\,(x_{ij}) = \frac{x_{ij} - \mu_j}{\sigma_j}$$

Where, for each set of raw data, μ_j and σ_j are the sample mean and standard deviation of the j^{th} attribute respectively. Normality check, Kruskal–Wallis test, Dunn's test of multiple comparisons and PCAs, were performed in PAST ver. 4.05 (University of Oslo; Hammer and Harper 2005). One-way ANOVA, two-way ANOVA and Tukey's test were computed using the excel extension DSAASTAT ver. 1.022 (University of Perugia; Onofri and Pannacci 2014).

3.3. Results and Discussion

3.3.1.Purple durum is similar to the susceptible control, but the infection did not affect the seed set

In the present study, the resistant DBC-480, the susceptible Svevo and the purple pericarp durum wheat genotype Purple Durum have been challenged by *F. graminearum* infection. Following FHB severity (SEV) trend in the considered period (from 3 DPI to 21 DPI), our results showed that, starting from 6 DPI, symptoms recorded in Purple durum and Svevo displayed an overlapped trend (Fig. 3.1a). At the end of the considered period (21 DPI) 44% of the spikelets were bleached in DBC-480 spikes, while 80% of bleached spikelets were recorded in Svevo and Purple durum spikes. No symptoms were detected in mock treated plants.

Fungal biomass assessed in Purple Durum spikes (0.37±0.16 ng fungal DNA/ng plant DNA) was similar to the one assessed in Svevo spikes (1.21±0.58 ng fungal DNA/ng plant DNA), while in DBC-480 fungal biomass was significantly lower (0.002±0.001 ng fungal DNA/ng plant DNA) (Fig. 3.1b). In the mock treated control, fungal DNA (*Tri6*) was lower than 0.003 ng/µL, accounting for less than 0.08% of the total DNA. Considering the high sensitivity of Real Time qPCR and the completely randomized experimental design, traces of fungal DNA in the mock treated spikes are possible and do not invalidate the experiment.

The influence of the infection on yield was evaluated, considering the number and weight of produced seeds and the percentage of damaged kernels (FDK). According to our results, the genotype greatly affected the seed number (Fig. 3.1c, Table 1). In particular, the number of seeds per spike produced in DBC-480 (mean 24.6 ± 1.98) was higher than the one produced in Purple durum (mean 6.1 ± 0.71), and both of them were not influenced by the infection, while in the susceptible genotype Svevo *F. graminearum* infection led to a reduction (-54%) of produced seeds. This may suggest that the seed set (transition from ovule to seed upon fertilization) is not decreased by the infection in the resistant genotype DBC-480 and in Purple durum. Other authors studied the biochemical mechanisms (Ruan et al. 2012), the environmental factors (Ji et al. 2010) and the quantitative trait loci (QTL) associated with seed set and the grain number (Sakuma et al. 2019; Mizuno et al. 2021), also in association with FHB resistance (Hu et al. 2022). The preservation of seed set in DBC-480 is most likely related to the presence of the QTL *Fhb1* (Prat et al. 2017). It is possible that in Purple durum could be present some other compensation mechanisms which allow to maintain a stable seeds number, despite the infection. Further researches are needed to clarify this aspect. As expected, the infection reduced the kernel weight in all the considered genotypes (Fig. 3.1d). This trait is also influenced by the genotype. Indeed, seeds of DBC-480 showed higher weight than seeds of Svevo in both the conditions (with and without the infection), as well as Purple durum displayed an intermediate behavior between the resistant and the susceptible control. The reduction of seeds weight due to infection could be attributed to the occurrence of shriveled or chalky kernels. The mean of damaged kernels (FDK %, Fig. 3.1e) was lower in DBC-480 (40.7%) compared to Svevo (76.4%), while Purple Durum (70.6%) displayed once again and intermediate behavior. Some shriveled kernels were reported in the mock plants too (Fig. 3.1e). Unintentional contamination is a possible drawback of completely randomized design and the low level recorded in this study do not invalidate the experiment. Furthermore, considering that no symptoms were detected in mock treated plants the shriveled kernels in mock spikes is more likely the result of restricted biotic stress (such as water scarcity).

For an overall evaluation of the abovementioned disease related parameters, a multivariate analysis (PCA) was carried out. As shown in the scatterplot in Fig. 3.1f, the first two principal components were extracted and accounted for the 55.97% of the dataset variability. The convex hulls shown a partial overlapping of the data recorded from of Svevo and Purple durum, while DBC-480 clusters separately.

To the best of our knowledge, Purple durum (NGB 6399) has never been characterized for its putative resistance or susceptibility against FHB and similar investigations on other pigmented durum wheat genotypes are currently missing. According to the available literature, purple pericarp bread wheat genotypes are generally more resistant than blue aleurone and yellow bread wheat genotypes to FHB (Martin et al. 2017). Furthermore, purple pericarp bread wheat can accumulate less mycotoxins than the yellow ones (Gozzi et al. 2023). Research studies regarding black rice varieties are available, reporting to be resistant to biotic stresses (Lachagari et al. 2019) as well as pigmented maize (Bernardi et al. 2018). Considering the overall data that we obtained in the present study, Purple durum could be classified as a susceptible genotype, but considering the high nutritional value of purple durum wheat genotypes (Apea-Bah and Beta 2021), screening for resistance in pigmented durum wheat genotypes may be a fruitful area for further work.

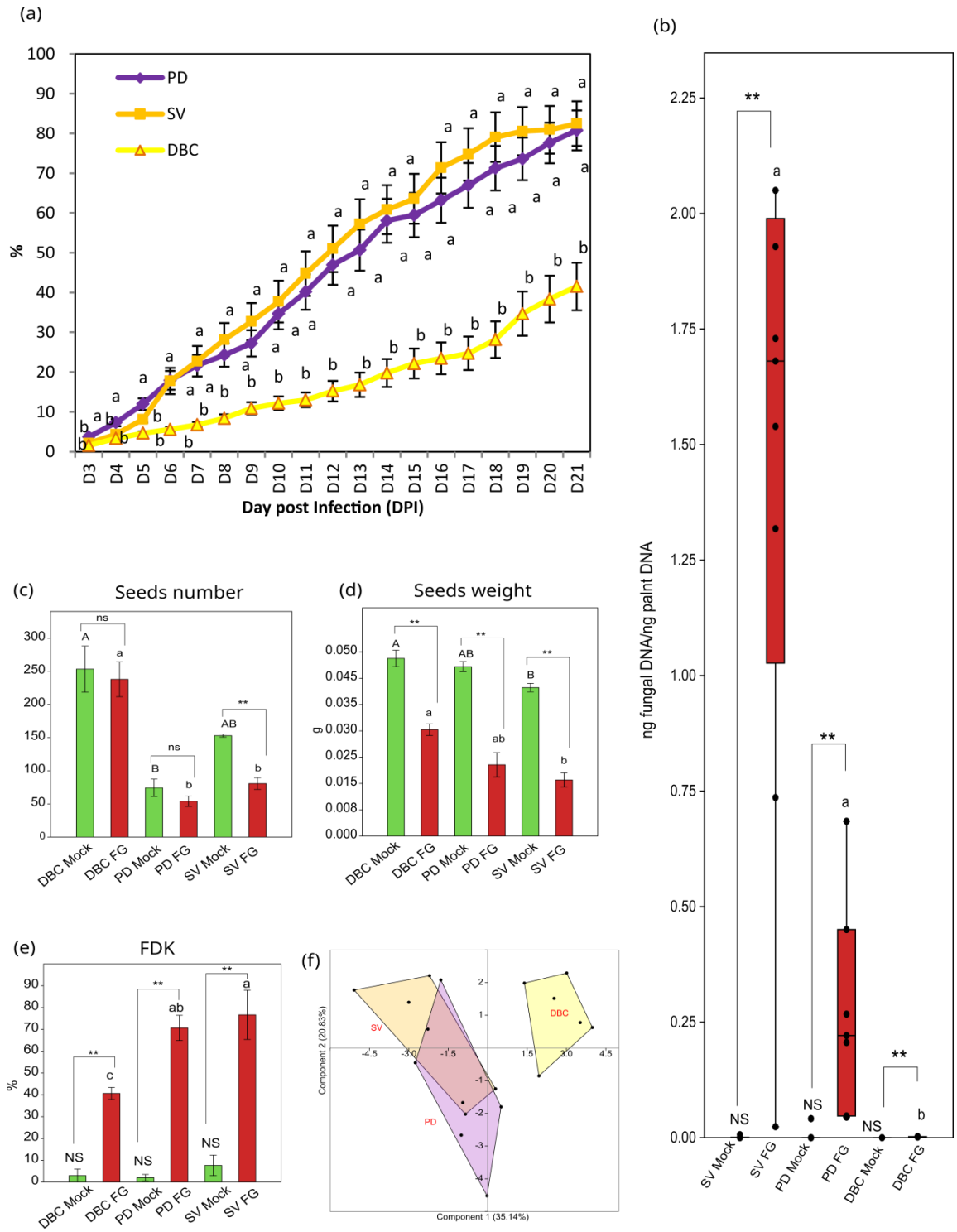

Fig. 3.1 Disease assessment in the three genotypes. (a) Mean FHB severity from 3 to 21 DPI in the considered genotypes. Error bars represent the standard error; (b) box plot of fungal biomass quantification; (c) mean seed number per spike; (d) mean single seed weight; (e) FDK %. For (b) letters refer to the statistical analysis performed using Kruskal–Wallis test and Dunn's test at a confidence level of 0.99 and P<0.01. For (c), (d) and (e) bar charts were plotted with Mean ± SE ANOVA analyzed data ($P < 0.05$) and letters refer to Tukey test. Upper case letters refer to mock thesis (green bars) while lower case letters refer to infected thesis (red bars). The symbols * and ** indicate significant differences at $p < 0.05$ and $p < 0.01$, respectively, while ns means not statistically significant. (f) PCA scatterplot among genotypes, considering the parameters in (a), (b), (c), (d) and (e).

3.3.2. Purple durum had a higher flag leaf temperature and spike temperature, but the infection only affected ST-FLT

Plant surface temperature can differ substantially from air temperature and it can change according to the physiological processes occurring in the plant (Still et al. 2019). In this study, flag leaf temperature depression (FLTD), spike temperature depression (STD) and differences between spike temperature and flag leaf temperature (ST-FLT) were measured at 3 and 7 DPI. At 3 DPI, values of flag leaf temperature were generally lower than values of air temperature, resulting in positive FLTD values. Purple durum showed higher FLTD than DBC-480 (Fig. 3.2a). Spike temperature was lower than air temperature in Svevo and Purple Durum but not in DBC-480, in which STD means were negative (Fig. 3.2b). Two-way ANOVA highlighted that FLTD and STD were influenced by the genotype and not by the infection (Table 3.1). On the other hand, ST-FLT (Fig, 3.2c) changed according to the genotype and there was an interaction between the genotype and the infection (Table 3.1). In particular, the ST-FLT (Fig. 3.2c) mean was positive in all the genotypes, indicating a higher temperature in the spike compared to the flag leaf. In DBC-480, spikes of infected plants were 1.2°C higher than the flag leaves, while in the healthy plants this difference was 0.69°C (Fig. 3.2c). The reverse occurred in the plants of the susceptible genotype, in which ST-FLT in the infected plants (0.15°C) was lower than in the healthy ones (0.99°C) (Fig. 3.2c), while in Purple durum the infection did not influences ST-FLT. The opposite reaction to infection of the resistant and the susceptible genotype in ST-FLT, may be potentially explained considering that the early reduction of stomatal conductance in the resistant genotypes implies a more efficient and faster response than the other genotypes (Kosaka et al. 2015; Francesconi and Balestra 2020). In this study, at 7 DPI the FLTD ranged from -1.10 °C to 3.10 °C, the STD ranged from -1.5 °C to 3.00°C, while the ST-FLT showed a range of -1.20°C to 2.40°C (Supplementary material 3.2), but none of the considered parameters at 7 DPI were influenced by the genotype or the infection (Table 3.1). This partially contrasts with the findings of other authors (Al Masri et al. 2016; Mahlein et al. 2019), who have found differences between healthy and infected plants at different infection stage (since 5 DPI) compared to the ones we analyzed (3 and 7 DPI). This discrepancy could be attributed to the more sensitive tools employed in the other studies (thermal imaging), while previous findings (Francesconi and Balestra 2020), obtained using infrared thermometer, are in agreement with this study. Furthermore, some authors (Tu et al. 2023; Fabre et al. 2019) suggested that the events driving the fate of the plat-pathogen interaction are shaped during the initial stages, supporting the fact that what happens at 2-3 DPI might be more informative than what might be measured later.

Table 3.1: *p* value from two-way ANOVA related to phenotypic parameters. Levels of significance $p < 0.05$ is marked as * and level $p < 0.01$ is marked as **.

	Genotype	Infection	Gen. x Infection
Seeds number	1.529×10^{-6}**	0.048*	0.248
Seeds weight	0.001**	1.037×10^{-8}**	0.195
FLTD 3 DPI	5.05×10^{-5}**	0.765	0.151
STD 3 DPI	8.05×10^{-5}**	0.837	0.434
ST-FLT 3 DPI	0.218	0.940	0.005**
FLTD 7 DPI	0.388	0.520	0.233
STD 7 DPI	0.965	0.570	0.166
ST-FLT 7 DPI	0.381	0.629	0.860
NBI index	0.008**	0.708	0.256
Chl index	0.002**	0.521	0.706
Flav index	1.99×10^{-11}**	0.192	0.214
Anth index	0.005**	0.900	0.522
TPC	0.325	8.59×10^{-6}**	0.214
TAC	0.0009291**	4.56×10^{-23}**	7.79×10^{-12}**

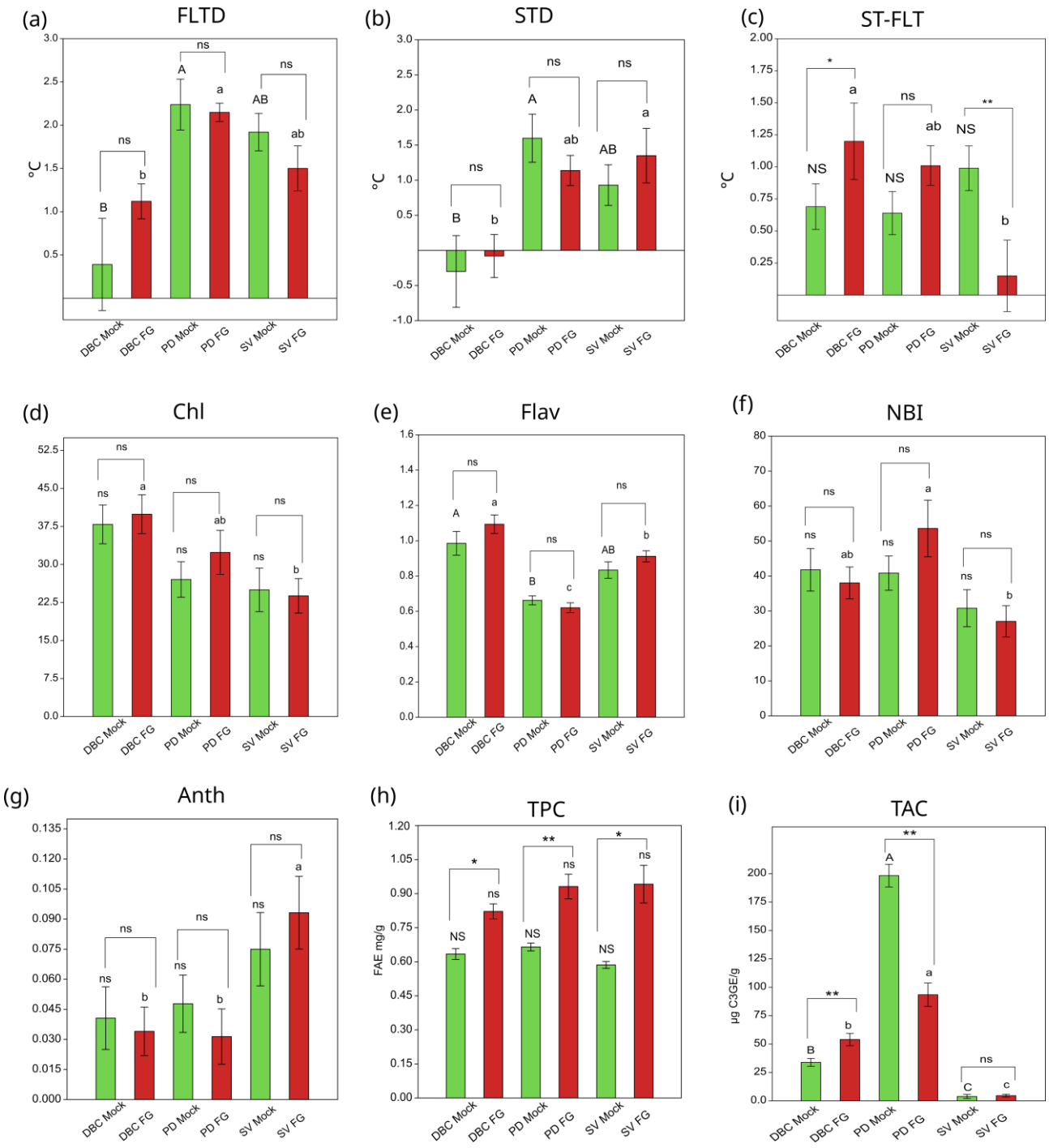

Fig. 3.2 Phenotypical parameters data representation of temperature parameters referred to 3 DPI (a-c), Dualex® indexes (d-g), total phenolic content (h) and total anthocyanin content (i). Bar charts were plotted with Mean ± SE. ANOVA analyzed data and letters refer to Tukey test. Upper case letters refer to mock treated plants (green bars) while lower case letters refer to infected treated plants (red bars). The symbols * and ** indicate significant differences at $p < 0.05$ and $p < 0.01$, respectively, while ns means not statistically significant. PD = Purple durum; SV = Svevo; DBC = DBC-480.

3.3.3. Infected Purple durum had a higher flag leaf NBI than DBC and SV

The Dualex® leaf clip is a portable, rapid, and easy-to-use instrument for assessing chlorophyll (Chl), and phenolic compounds as flavonols (Flav), and anthocyanin (Anth) content (Goulas et al. 2004; Cartelat et al. 2005; Cerovic et al. 2012). The Nitrogen Balance Index (NBI) is obtained as chlorophyll and flavonoid ratio and provides valuable

information about C/N allocation changes due to N deficiency and can also provide an indication of the activation of secondary metabolic pathways (Cartelat et al. 2005). In this study, we used Dualex® leaf clip on flag leaves and the measured Chl, Flav, Anth and NBI indices were unrelated with the infection, but they were influenced by the genotype (Table 3.1 and Fig. 3.2d-g). In particular, Purple durum had an intermediate Chl index (Fig. 3.2d) in infected plants compared to Svevo and DBC-480, and a lower Flav index (Fig. 3.2e), in both infected and healthy plants, compared to the other genotypes, resulting in a higher NBI in Purple durum infected spikes than in infected Svevo and DBC-480 (Fig. 3.2f). Finally, Anth index (Fig. 3.2g) (lower than 0.135 in the considered plants) was not influenced by the infection, but it was affected by the genotype in infected plants: it was higher in Svevo infected plants than in *Fusarium*-challenged Purple durum and DBC-480. Other authors (Bollina et al. 2011; Gunnaiah et al. 2012; Gunnaiah and Kushalappa 2014) suggested that resistant related metabolites could be induced by the infection or constitutively present in the resistant genotype and, thus, not affected by the infection. Our results may suggest that Dualex® indices did not detect induced resistance related metabolites in the leaves, but may indicate a reduced presence of constitutive secondary metabolites (flavonoids and anthocyanins) in Purple durum flag leaves, compared to the resistant and the susceptible genotypes. Indeed, even if Purple durum has pigmented seeds (due to the accumulation of flavonoids and anthocyanins), the genes driving the synthesis of these pigments are usually tissue and organ-specific (Jiang et al. 2018; Jiang et al. 2023), and thus what happens into the spikes may be independent of what happens into the leaves. Further research is needed to clarify the interaction between secondary metabolites in the leaves and FHB tolerance.

3.3.4. TPC and TAC suggested the involvement of secondary metabolism in DBC-480 resistance

Phenylpropanoids have a prominent role in plant-pathogen interaction. In particular, during plant-fungal interaction, they act as antimicrobials (Oufensou et al. 2020), anti-mycotoxins (Gautier et al. 2020), signaling molecules (Wagay et al. 2020) and precursor of lignin for cell wall strengthening (Siranidou et al. 2002; Lanoue et al. 2010; Brown et al. 2010). In this study, spikes harvested at maturity stage were used to quantify the Total Phenolic Content (TPC) and the Total Anthocyanin Content (TAC) and these estimations were compared among genotypes and treatments.

In wheat spikes, *p*-coumaric and ferulic acid are the two main phenolic compounds (McKeehen et al. 1999), thus, in the present study, TPC is expressed as ferulic acid equivalent (FAE). The TPC levels recorded in this research are in agreement with those obtained by Martini et al. (2015). The analysis revealed that this parameter was always higher in infected spikes, and it was strongly associated to the infection process and not to the genotype (Fig. 3.2h, Table 3.1). Indeed, the infection led to an increase of TPC of about 30% in DBC-480 spikes, 40% in Purple durum and 61% in Svevo. The observed increase in TPC could be attributed, from one side, to plants metabolism that actively strengthen cell wall through phenolic acids and lignin deposition in cell wall (Siranidou et al. 2002), and, on the other side, *F. graminearum* is able to synthetize, later in the infection process, feruloyl esterases and liberate ferulic acid from plant cell wall polymers (Balcerzak et al. 2012). However, this response is not specific: it occurred in this study in all the considered genotypes and, indeed, it is recognized as a general response to biotic stress (Wallis and Galarneau 2020).

Anthocyanins are a class of flavonoids that give a blue-purple color to various plant organs. They are accumulated particularly in pigmented tissues (where the blue-purple color is visible to the naked eye), but they could also be detected in tissues not having this characteristic color (Dinelli et al. 2009). In purple durum wheat accessions the main pigments are cyanidin 3-*O*-glucoside (ten times more abundant than the others), peonidin 3-*O*-galactoside, and malvidin 3-*O*-glucoside (Ficco et al. 2014). Not surprisingly, the purple genotype had the highest TAC value (198.29 ± 9.99 µg/g) among the genotypes analyzed in this study. This value also indicated that Purple durum is very rich in

anthocyanins compared to other purple pericarp durum wheat accessions investigated in other studies (Ficco et al. 2014b). Some anthocyanins were also detected in DBC-480 (33.8 ± 3.49 μg/g) and in Svevo (5.53± 0.92 μg/g) samples (Fig. 3.2i), and this was compatible with the findings of other authors (Dinelli et al. 2009). The infection strongly influenced the anthocyanins accumulation, with an interaction genotype x infection (Table 1), in particular TAC decreased in Purple durum (-53%) and, interestingly, increased in the resistant genotype (+59%) due to the infection, while it remained stable in the susceptible control ($p > 0.05$). Our results contrasted with the findings of Martin et al. (2017), who did not detect TAC variations in pigmented and resistant bread wheat genotypes during *F. graminearum* infection. Anthocyanins in Purple durum are mainly present in the kernels and the infection led to the presence of a high number of shriveled or less pigmented kernels, most likely causing the TAC reduction in Purple durum. DBC-480 is a resistant accession harboring *Fhb1* from Sumai 3. Other studies verified that flavonoids are important resistance related metabolites in Sumai 3, actively produced during *F. graminearum* infection (Gunnaiah and Kushalappa 2014; Zhao et al. 2022; Dong et al. 2023), but few research were specifically dedicated to the role of anthocyanins in disease resistance. It is important to specify that pH differential TAC assay, even if based on the specific anthocyanins changes due to pH (Enaru et al. 2021), could be biased by the presence of other colored compounds and flavonoids. Our results may suggest an implication of anthocyanins in DBC-480 resistance mechanism, more specific than the general phenolic acids biosynthesis, but further investigations are required to verify this aspect.

3.3.5. Spike architecture traits correlated with physiological traits

Spike architecture measurement (Fig. 3.3a-e) highlighted a different spike morphology among the considered genotypes. Spike length and the number of spikelets and florets were higher in the resistant genotype compared to Svevo and Purple Durum. On the contrary, spike density was higher in the susceptible genotype compared to DBC-480 and Purple Durum. Values of number of florets per spikelet stood around three for all the considered genotypes, except for Purple Durum, in which a higher number of sterile florets were recorded, in agreement with the low number of seed produced by Purple durum (Fig. 1).

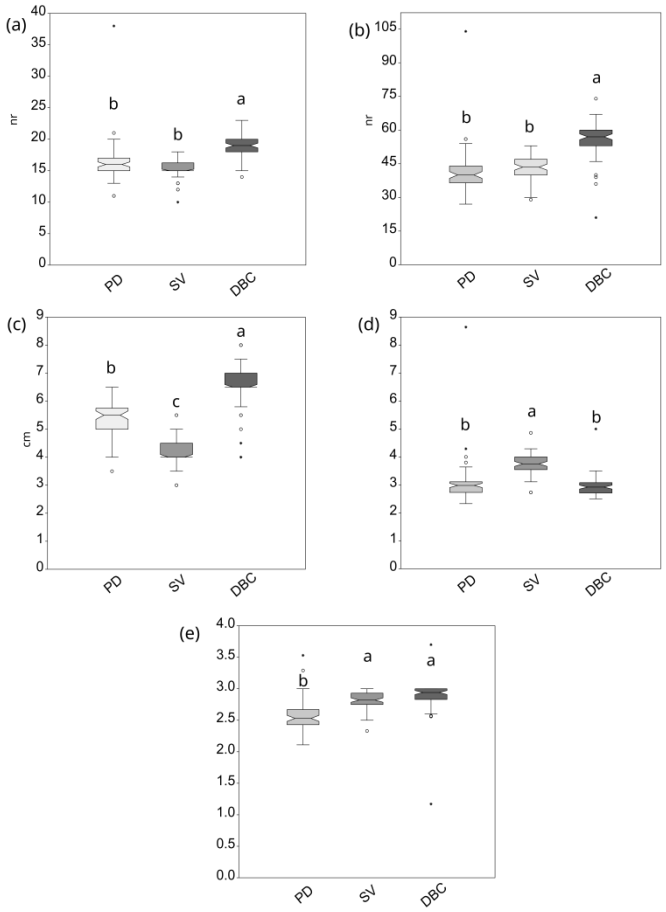

Fig. 3.3 Spike architecture traits. (a) Spikelets per spike; (b) Florets per spike.; (c) Spike length; (d) Spike density; (e) Florets per spikelet. Letters refer to the statistical analysis performed using one-way analysis of variance (ANOVA) with the Tukey test at a confidence level of 0.99 and $p < 0.01$. PD = Purple durum; SV = Svevo; DBC = DBC-480.

The associations between spike architecture traits with physiological traits and the disease were visualized using vector biplot of principal component analysis (PCA), one for each genotype. Biplot showed in Fig 4a-c represented the first two principal components (PC1 and PC2), accounting for 728% (DBC-480, Fig. 3.4a), 82.7% (Svevo Fig. 3.4b) and 80.3% (Purple durum Fig. 3.4c) of the total variance. Results highlighted that the considered parameters differentially clustered among the different genotypes. The more noteworthy associations are listed in the following paragraph. Temperature parameters referred to 7 DPI were not included in this analysis, because they were not influenced neither by the genotype neither by the infection.

In DBC-480, TPC, TAC, ST-FLT at 3 DPI and FLTD at 3 DPI grouped closely with disease parameters (severity at 21 DPI and FDK, while fungal biomass was not represented in PC1 and PC2), suggesting a direct correlation among these parameters, while number of spikelets, spike density and seeds weight were negatively associated with severity and FDK (Fig. 3.3a). Furthermore, florets number was associated with NBI, Chl index and spike length, and this group was negatively associated with Anth index, seeds number, Flav index and STD at 3 DPI (Fig. 3.4a).

In Svevo, STD at 3 DPI and TPC clustered with severity at 21 DPI and FDK, while TAC was not represented in PC1 and PC2 (Fig. 3.4b). Seeds number and seeds weight seemed negatively associated with disease parameters.

Furthermore, in Svevo the fungal biomass was associated with Anth index, Flav index and the spike architecture traits (spike length, florets number, spikelets number and florets/spikelets). The association fungal biomass – spike architecture traits may indicate a role of spike morphology in fungal diffusion in the spike, as also suggested by other authors (Jones et al. 2018), and discussed below. On the other side of the Svevo vector biplot, spike density clustered with FLTD at 3 DPI, Chl index and NBI.

In Purple durum (Fig. 3.4c) there was an association among TAC, seeds weight, STD at 3 DPI, Flav index and seeds number and this group is negatively associated with severity at 21 DPI, FDK, fungal biomass, TPC, ST-FLT 3 DPI and florets/spikelet (Fig. 3.4c). Spike density grouped closely in Purple durum with florets number and spikelets number and was negatively associated with spike length, Chl index, NBI and FLTD at 3 DPI.

In the Fig. 3.4a and 3.4c we also highlight that TAC is positively associated with SEV and FDK in DBC and negatively associated with the same variables in Purple durum, confirming what showed in Fig. 3.2i.

Literature related to morphological spike traits associated to FHB resistance is mainly focused on barley and bread wheat. Number of florets and number of spikelets per spike were poorly evaluated and results are contrasting (Franco et al. 2021; Jones et al. 2018; Tessmann and Van Sanford 2019). In this study, only in DBC-480 spikelets number was negatively associated with the severity, in accordance with Tessmann and Van Sanford (2019), while other authors found a lack of correlation (Jones et al. 2018; Franco et al. 2021). Spike density is one of the spike traits more studied in association with FHB, but results are contrasting. In this study, spike density was negatively associated with severity in DBC-480 and with fungal biomass in Svevo, in accordance with Tessmann and Van Sanford (2019). Other authors (Jones et al. 2018) found a positive association between spike density and AUDPC, (Huang et al. 2018) and revealed a positive correlation with severity, while other authors founds no correlation with the disease (Franco et al. 2021; Dahleen et al. 2012). Similarly, spike length in this study was positively associated with the fungal biomass in Svevo, while in DBC-480 and Purple durum it was only associated with physiological traits genotype-associated and independent from the disease. These findings partially contrast with the ones of Tessmann and Van Sanford (2019) and Huang et al. (2018), who have found a negative correlation between spike length and FHB resistance, while other authors founds no correlation (Franco et al. 2021; Jones et al. 2018). Finally, number of florets per spikelets is this study was the only morphological traits always associated to disease parameters (severity and FDK in DBC-480 and Purple durum, fungal biomass in Svevo), consistently with the findings of Franco et al. (2021). This trait is poorly investigated in relationship with FHB resistance and more research is desirable. FHB resistance QTLs are often responsible for agro-morphological traits (Sallam et al. 2024), but almost all the above mentioned authors highlighted as this relationship depends on the genotype, resulting in contrasting results. Considering that the influence of these traits on the disease resistance/susceptibility are mainly related to ecological aspects (such as dispersal mechanism of the pathogen, diffusion along the spike and on the interactions with the environment) (Jones et al. 2018), a more comprehensive study in the field using pigmented genotype is desirable, also because such investigation on durum wheat is lacking.

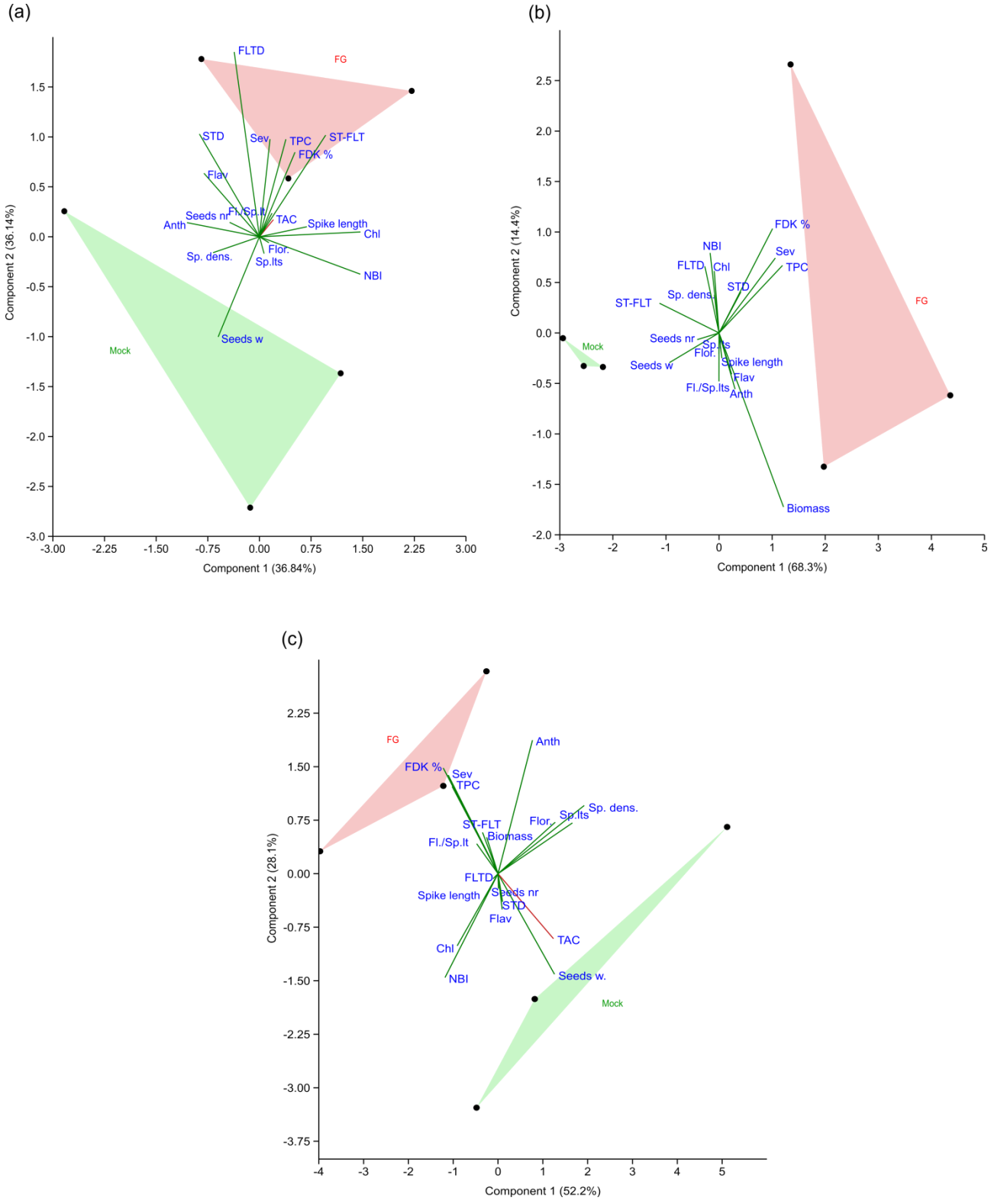

Fig. 3.4 PCAs' biplot of DBC-480 (a), Svevo (b) and Purple durum (c) samples. Green lines represent the vector biplot. Black points are the samples represented in the PCA bi-dimensional environment. Green triangle and red triangle represent the convex hulls of the mock group and infected group respectively. TAC (Total anthocyanin content) vector was highlighted in red. Sp.lts = number of spikelets per spike; Sp. dens. = Spike density; Fl./Sp.lt = Florets per spikelet; Seed nr = seed number; Seed w. = seed weight; Sev = severity 21 DPI. For the other abbreviations refer to the text.

3.4. Supplementary materials

3.4.1. Supplementary material 3.1: Additional information of real time qPCR for fungal biomass quantification

Table S3.1 Primers used in Real-Time qPCR.

Primer name	Primer sequence (5'-3')	Ref.
TaACT_77F	TCCTGTGTTGCTGACTGAGG	Mandalà et al. 2019
TaACT_312R	GGTCCAAACGAAGGATAGCA	Mandalà et al. 2019
Tri6_10F	TCTTTGTGAGCGGACGGGACTTTA	Horevaj, et al. 2011
TRI6_4R	ATCTCGCATGTTATCCACCCTGCT	Horevaj, et al. 2011

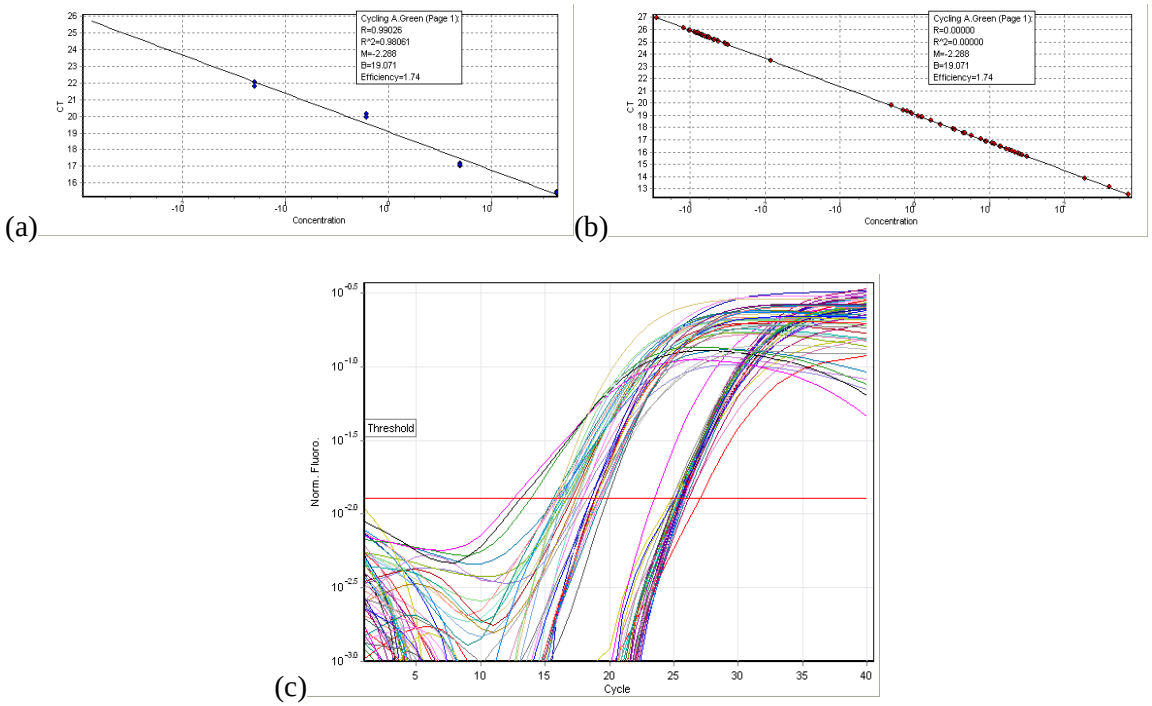

Fig. S3.1.1: qPCR analysis of *Tri6* in the considered genotypes. *Tri6* standard curve (a); interpolations with the standard curve (b) and amplification curves of the *Tri6* gene (c).

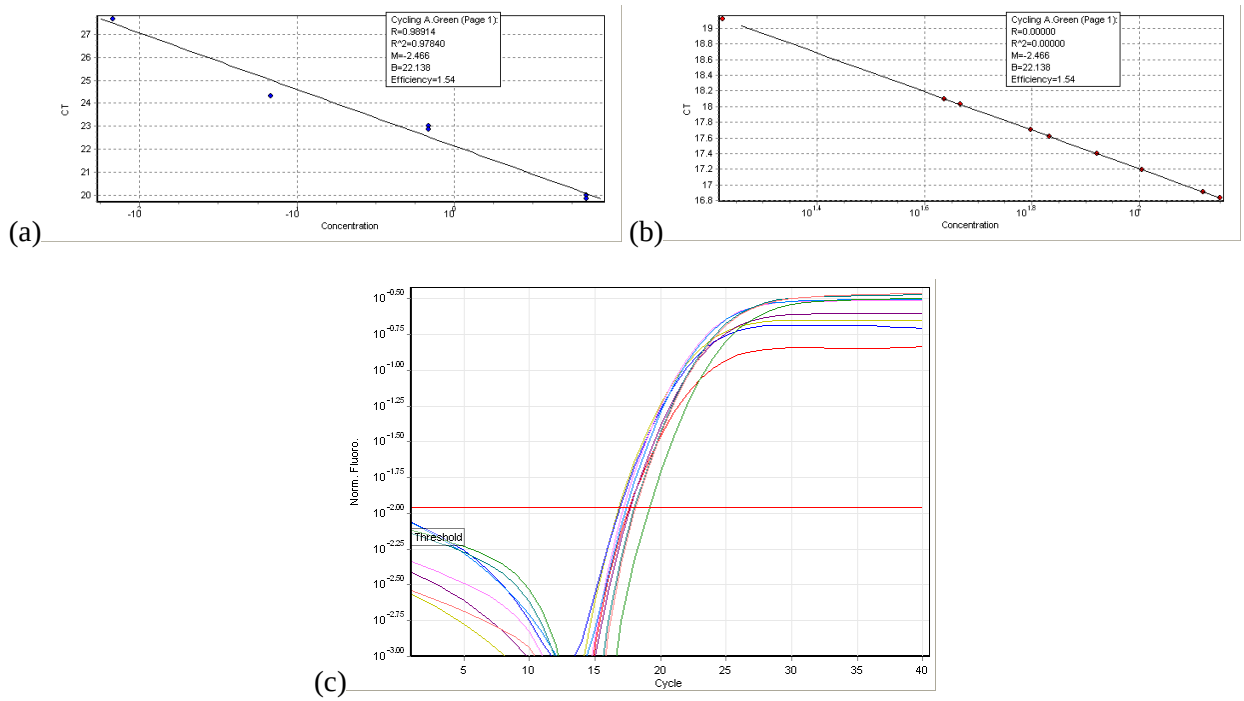

Fig. S3.1.2: qPCR analysis of *ACT* in the genotype "Svevo". *ACT* standard curve (a); interpolations with the standard curve (b) and amplification curves of the *ACT* gene (c).

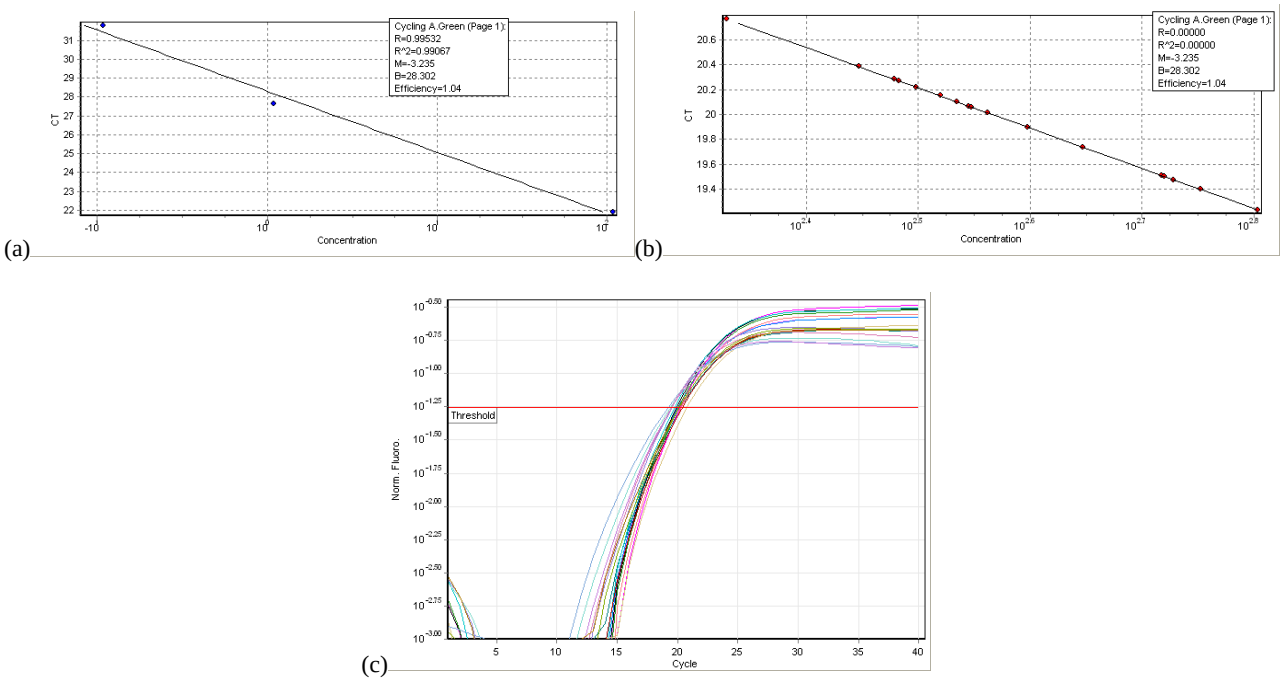

Fig. S3.1.3: qPCR analysis of *ACT* in the genotype "DBC-480". *ACT* standard curve (a); interpolations with the standard curve (b) and amplification curves of the *ACT* gene (c).

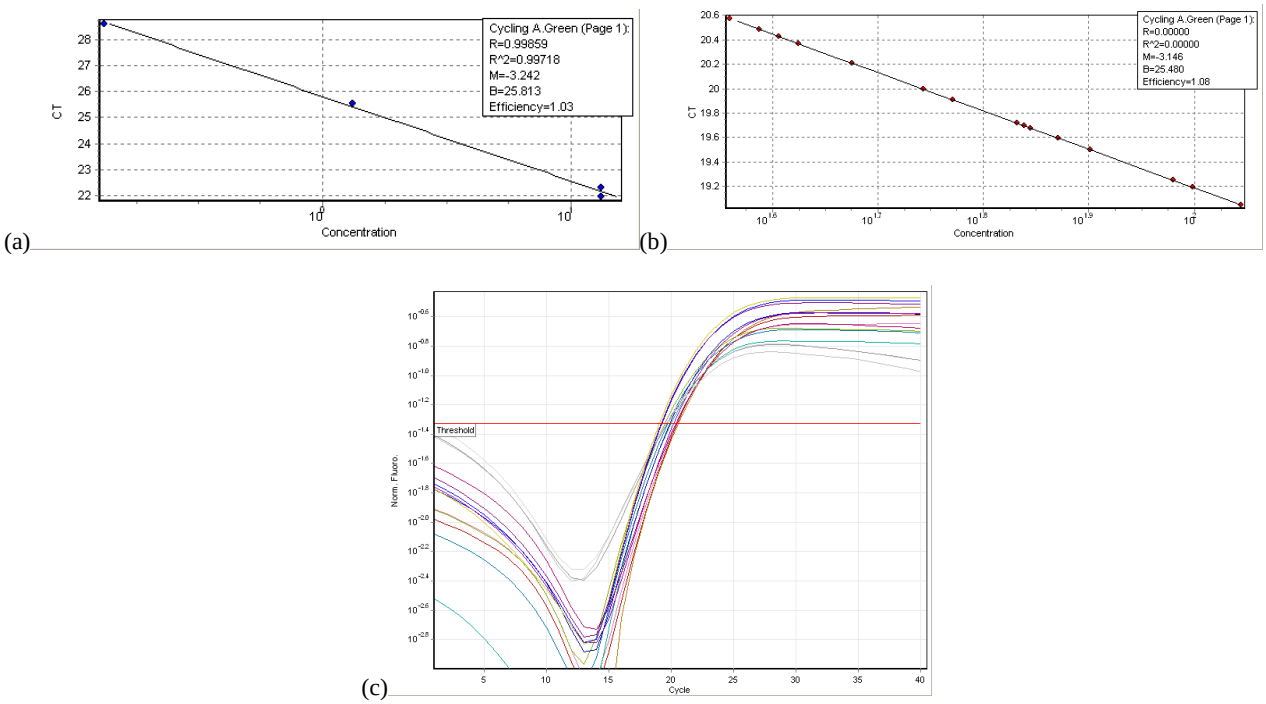

Fig. S3.1.4: qPCR analysis of *ACT* in the genotype "Purple durum". *ACT* standard curve (a); interpolations with the standard curve (b) and amplification curves of the *ACT* gene (c).

3.4.2. Supplementary material 3.2: FLTD, STD and ST-FLT referred to 7 DPI

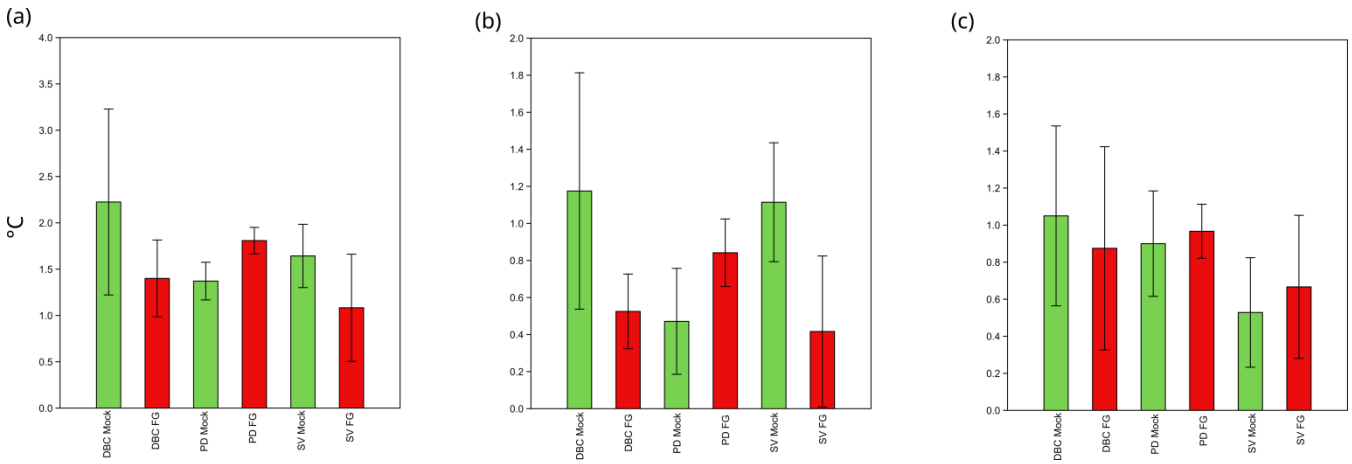

Fig. S3.2.1: Flag leaf temperature depression (a), spike temperature depression (b), spike temperature-leaf temperature difference (c) measured at 7 DPI. Data are plotted as mean +/- SE.

3.5. References

Ainsworth, E. A., and Gillespie, K. M. (2007). Estimation of total phenolic content and other oxidation substrates in plant tissues using Folin-Ciocalteu reagent. *Nature Protocols*, *2*(4), 875–877. https://doi.org/10.1038/nprot.2007.102

Al Masri, A., Hau, B., Dehne, H., and Mahlein, A. (2016). Impact of primary infection site of *Fusarium* species on head blight development in wheat ears evaluated by IR-thermography. *European Journal of Plant Pathology*, *147*(4), 855–868. https://doi.org/10.1007/s10658-016-1051-2

Apea-Bah, F., and Beta, T. (2021). Advances in understanding the nutritional value of antioxidants in wheat. In *Improving the nutritional and nutraceutical properties of wheat and other cereals* (pp. 29–72). https://doi.org/10.19103/AS.2021.0087.04

Balcerzak, M., Harris, L. J., Subramaniam, R., and Ouellet, T. (2012). The feruloyl esterase gene family of *Fusarium graminearum* is differentially regulated by aromatic compounds and hosts. *Fungal Biology*, *116*(4), 478–488. https://doi.org/10.1016/j.funbio.2012.01.007

Belay, G., Tesemma, T., Bechere, E., and Mitiku, D. (1995). Natural and human selection for purple-grain tetraploid wheats in the Ethiopian highlands. *Genetic Resources and Crop Evolution*, *42*(4), 387–391. https://doi.org/10.1007/BF02432143

Beleggia, R., Ficco, D. B. M., Pecorella, I., De Vita, P., Nigro, F. M., Giovanniello, V., and Colecchia, S. A. (2021). Effect of sowing date on bioactive compounds and grain morphology of three pigmented cereal species. *Agronomy*, *11*(3). https://doi.org/10.3390/agronomy11030591

Bernardi, J., Stagnati, L., Lucini, L., Rocchetti, G., Lanubile, A., Cortellini, C., De Poli, G., Busconi, M., and Marocco, A. (2018). Phenolic profile and susceptibility to *Fusarium* infection of pigmented maize cultivars. *Frontiers in Plant Science*, *9*(August), 1–13. https://doi.org/10.3389/fpls.2018.01189

Böhmdorfer, S., Oberlerchner, J. T., Fuchs, C., Rosenau, T., and Grausgruber, H. (2018). Profiling and quantification of grain anthocyanins in purple pericarp×blue aleurone wheat crosses by high-performance thin-layer chromatography and densitometry. *Plant Methods*, *14*(1), 1–16. https://doi.org/10.1186/s13007-018-0296-5

Bollina, V., Kushalappa, A. C., Choo, T. M., Dion, Y., and Rioux, S. (2011). Identification of metabolites related to mechanisms of resistance in barley against Fusarium graminearum, based on mass spectrometry. *Plant Molecular Biology*, *77*(4–5), 355–370. https://doi.org/10.1007/s11103-011-9815-8

Boukid, F. (2021). Cereal-Derived Foodstuffs from North African-Mediterranean: From Tradition to Innovation. In F. Boukid (Ed.), *Cereal-Based Foodstuffs: The Backbone of Mediterranean Cuisine* (pp. 117–150). Springer International Publishing. https://doi.org/10.1007/978-3-030-69228-5_5

Brown, N. A., Urban, M., van de Meene, A. M. L., and Hammond-Kosack, K. E. (2010). The infection biology of *Fusarium graminearum*: Defining the pathways of spikelet to spikelet colonisation in wheat ears. *Fungal Biology*, *114*(7), 555–571. https://doi.org/10.1016/j.funbio.2010.04.006

Buerstmayr, M., Steiner, B., and Buerstmayr, H. (2020). Breeding for Fusarium head blight resistance in wheat—Progress and challenges. *Plant Breeding*, *139*(3), 429–454. https://doi.org/10.1111/pbr.12797

Cartelat, A., Cerovic, Z. G., Goulas, Y., Meyer, S., Lelarge, C., Prioul, J. L., Barbottin, A., Jeuffroy, M. H., Gate, P., Agati, G., and Moya, I. (2005). Optically assessed contents of leaf polyphenolics and chlorophyll as indicators of nitrogen deficiency in wheat (*Triticum aestivum* L.). *Field Crops Research*, *91*(1), 35–49. https://doi.org/10.1016/j.fcr.2004.05.002

Cerovic, Z. G., Masdoumier, G., Ghozlen, N. Ben, and Latouche, G. (2012). A new optical leaf-clip meter for simultaneous non-destructive assessment of leaf chlorophyll and epidermal flavonoids. *Physiologia Plantarum*, *146*(3), 251–260. https://doi.org/10.1111/j.1399-3054.2012.01639.x

Conte, P., Piga, A., Del Caro, A., Urgeghe, P. P., and Fadda, C. (2021). Italian Dried Pasta: Conventional and Innovative Ingredients and Processing. In F. Boukid (Ed.), *Cereal-Based Foodstuffs: The Backbone of Mediterranean Cuisine* (pp. 89–116). Springer International Publishing. https://doi.org/10.1007/978-3-030-69228-5_4

Dahleen, L. S., Morgan, W., Mittal, S., Bregitzer, P., Brown, R. H., and Hill, N. S. (2012). Quantitative trait loci (QTL) for *Fusarium* ELISA compared to QTL for Fusarium head blight resistance and deoxynivalenol content in barley. *Plant Breeding*, *131*(2), 237–243. https://doi.org/10.1111/j.1439-0523.2012.01952.x

Digesù, A. M., Platani, C., Cattivelli, L., Mangini, G., and Blanco, A. (2009). Genetic variability in yellow pigment components in cultivated and wild tetraploid wheats. *Journal of Cereal Science*, *50*(2), 210–218. https://doi.org/10.1016/j.jcs.2009.05.002

Dinelli, G., Carretero, A. S., Di Silvestro, R., Marotti, I., Fu, S., Benedettelli, S., Ghiselli, L., and Gutiérrez, A. F. (2009). Determination of phenolic compounds in modern and old varieties of durum wheat using liquid chromatography coupled with time-of-flight mass spectrometry. *Journal of Chromatography A*, *1216*(43), 7229–7240. https://doi.org/10.1016/j.chroma.2009.08.041

Dong, Y., Xia, X., Ahmad, D., Wang, Y., Zhang, X., Wu, L., Jiang, P., Zhang, P., Yang, X., Li, G., and He, Y. (2023). Investigating the Resistance Mechanism of Wheat Varieties to Fusarium Head Blight Using Comparative Metabolomics. *International Journal of Molecular Sciences*, *24*(4). https://doi.org/10.3390/ijms24043214

Dwivedi, S. L., Mattoo, A. K., Garg, M., Dutt, S., Singh, B., and Ortiz, R. (2022). Developing Germplasm and Promoting Consumption of Anthocyanin-Rich Grains for Health Benefits. *Frontiers in Sustainable Food Systems*, *6*(April), 1–21. https://doi.org/10.3389/fsufs.2022.867897

Enaru, B., Drețcanu, G., Pop, T. D., Stănilă, A., and Diaconeasa, Z. (2021). Anthocyanins: Factors Affecting Their Stability and Degradation. *Antioxidants (Basel, Switzerland)*, *10*(12). https://doi.org/10.3390/antiox10121967

Fabre, F., Vignassa, M., Urbach, S., Langin, T., and Bonhomme, L. (2019). Time-resolved dissection of the molecular crosstalk driving Fusarium head blight in wheat provides new insights into host susceptibility determinism. *Plant, Cell and Environment*, *42*(7), 2291–2308. https://doi.org/10.1111/pce.13549

Ficco, D. B. M., Mastrangelo, A. M., Trono, D., Borrelli, G. M., De Vita, P., Fares, C., Beleggia, R., Platani, C., and Papa, R. (2014). The colours of durum wheat: A review. *Crop and Pasture Science*, *65*(1), 1–15. https://doi.org/10.1016/j.foodchem.2016.03.014

Ficco, D., De Simone, V., Colecchia, S. A., Pecorella, I., Platani, C., Nigro, F., Finocchiaro, F., Papa, R., and De Vita, P. (2014). Genetic variability in anthocyanin composition and nutritional properties of blue, purple, and red bread (*Triticum aestivum* L.) and durum (*Triticum turgidum* L. ssp. *turgidum* convar. *durum*) wheats. *Journal of Agricultural and Food Chemistry*, *62*(34), 8686–8695. https://doi.org/10.1021/jf5003683

Francesconi, S., and Balestra, G. M. (2020). The modulation of stomatal conductance and photosynthetic parameters is involved in Fusarium head blight resistance in wheat. *PLoS ONE*, *15*(6 june), 1–21. https://doi.org/10.1371/journal.pone.0235482

Francesconi, S., Mazzaglia, A., and Balestra, G. M. (2019). Different inoculation methods affect components of Fusarium head blight resistance in wheat. *Phytopathologia Mediterranea*, *58*(3), 679–691. https://doi.org/10.14601/Phyto-10942

Francesconi, S., Steiner, B., Buerstmayr, H., Lemmens, M., Sulyok, M., and Balestra, G. M. (2020). Chitosan Hydrochloride Decreases *Fusarium graminearum* Growth and Virulence and Boosts Growth, Development and Systemic Acquired Resistance in Two Durum Wheat Genotypes. *Molecules*, 1–29. https://doi.org/10.3390/molecules25204752

Franco, M. F., Lori, G. A., Cendoya, G., Alonso, M. P., Panelo, J. S., Malbrán, I., Mirabella, N. E., and Pontaroli, A. C. (2021). Spike architecture traits associated with type II resistance to fusarium head blight in bread wheat. *Euphytica*, *217*(209), 1–21. https://doi.org/doi.org/10.1007/s10681-021-02936-3

Gaikpa, D. S., Lieberherr, B., Maurer, H. P., Longin, C. F. H., & Miedaner, T. (2020). Comparison of rye, triticale, durum wheat and bread wheat genotypes for Fusarium head blight resistance and deoxynivalenol contamination. *Plant Breeding*, 139(2), 251–262. https://doi.org/https://doi.org/10.1111/pbr.12779

Gauthier, L., Bonnin-Verdal, M.-N., Marchegay, G., Pinson-Gadais, L., Ducos, C., Richard-Forget, F., and Atanasova-Penichon, V. (2016). Fungal biotransformation of chlorogenic and caffeic acids by *Fusarium graminearum*: New insights in the contribution of phenolic acids to resistance to deoxynivalenol accumulation in cereals. *International Journal of Food Microbiology*, *221*, 61–68. https://doi.org/10.1016/j.ijfoodmicro.2016.01.005

Gautier, C., Pinson-Gadais, L., Verdal-Bonnin, M. N., Ducos, C., Tremblay, J., Chéreau, S., Atanasova, V., and Richard-Forget, F. (2020). Investigating the Efficiency of Hydroxycinnamic Acids to Inhibit the Production of Enniatins by *Fusarium avenaceum* and Modulate the Expression of Enniatins Biosynthetic Genes. *Toxins*, *12*(12), 1–17. https://doi.org/10.3390/toxins12120735

Goulas, Y., Cerovic, Z. G., Cartelat, A., and Moya, I. (2004). Dualex: A new instrument for field measurements of epidermal ultraviolet absorbance by chlorophyll fluorescence. *Applied Optics*, *43*(23), 4488–4496. https://doi.org/10.1364/AO.43.004488

Gozzi, M., Blandino, M., Dall'Asta, C., Martinek, P., Bruni, R., and Righetti, L. (2023). Anthocyanin Content and Fusarium Mycotoxins in Pigmented Wheat (*Triticum aestivum* L. spp. *aestivum*): An Open Field Evaluation. *Plants*, *12*(4). https://doi.org/10.3390/plants12040693

Gunnaiah, R., and Kushalappa, A. C. (2014). Metabolomics deciphers the host resistance mechanisms in wheat cultivar Sumai-3, against trichothecene producing and non-producing isolates of *Fusarium graminearum*. *Plant Physiology and Biochemistry*, *83*, 40–50. https://doi.org/10.1016/j.plaphy.2014.07.002

Gunnaiah, R., Kushalappa, A. C., Duggavathi, R., Fox, S., and Somers, D. J. (2012). Integrated metabolo-proteomic approach to decipher the mechanisms by which wheat QTL (Fhb1) contributes to resistance against *Fusarium graminearum*. *PLoS ONE*, *7*(7). https://doi.org/10.1371/journal.pone.0040695

Hammer, Ø., and Harper, D. A. T. (2005). Basic Statistical Methods. In *Paleontological Data Analysis* (pp. 8–60). https://doi.org/10.1002/9780470750711.ch2

Horevaj, P., Milus, E. A., and Bluhm, B. H. (2011). A real-time qPCR assay to quantify *Fusarium graminearum* biomass in wheat kernels. *Journal of Applied Microbiology*, *111*(2), 396–406. https://doi.org/10.1111/j.1365-2672.2011.05049.x

Hu, W., Gao, D., Liao, S., Cheng, S., Jia, J., and Xu, W. (2022). Identification of a pleiotropic QTL cluster for Fusarium head blight resistance, spikelet compactness, grain number per spike and thousand-grain weight in common wheat. *Crop Journal*, *11*(2), 672–677. https://doi.org/10.1016/j.cj.2022.09.007

Huang, Y., Haas, M., Heinen, S., Steffenson, B. J., Smith, K. P., and Muehlbauer, G. J. (2018). Qtl mapping of fusarium head blight and correlated agromorphological traits in an elite barley cultivar rasmusson. *Frontiers in Plant Science*, *9*(August), 1–15. https://doi.org/10.3389/fpls.2018.01260

Jbir, T. G., Crutcher, F. K., Rickertsen, J., Fonseka, D., Friskop, A. J., and Kalil, A. K. (2022). Influence of Planting Date and Cultivar on Diseases of Spring Durum Wheat. *Plant Disease*, *106*(12), 3083–3090. https://doi.org/10.1094/PDIS-03-22-0548-RE

Ji, X., Shiran, B., Wan, J., Lewis, D. C., Jenkins, C. L. D., Condon, A. G., Richards, R. A., and Dolferus, R. (2010). Importance of pre-anthesis anther sink strength for maintenance of grain number during reproductive stage water stress in wheat. *Plant, Cell and Environment*, *33*(6), 926–942. https://doi.org/10.1111/j.1365-3040.2010.02130.x

Jiang, Q., Jiang, W., Hu, N., Tang, R., Dong, Y., Wu, H., Liu, T., Guan, L., Zhang, H., Hou, J., Chai, G., and Wang, Z. (2023). Light-Induced TaHY5-7A and TaBBX-3B Physically Interact to Promote PURPLE PERICARP-MYB 1 Expression in Purple-Grained Wheat. *Plants*, *12*(16). https://doi.org/10.3390/plants12162996

Jiang, W., Liu, T., Nan, W., Jeewani, D. C., Niu, Y., Li, C., Wang, Y., Shi, X., Wang, C., Wang, J., Li, Y., Gao, X., and Wang, Z. (2018). Two transcription factors TaPpm1 and TaPpb1 co-regulate anthocyanin biosynthesis in purple pericarps of wheat. *Journal of Experimental Botany*, *69*(10), 2555–2567. https://doi.org/10.1093/jxb/ery101

Jones, S., Farooqi, A., Foulkes, J., Sparkes, D. L., Linforth, R., and Ray, R. V. (2018). Canopy and Ear Traits Associated With Avoidance of Fusarium Head Blight in Wheat. *Frontiers in Plant Science 9*(July), 1–13. https://doi.org/10.3389/fpls.2018.01021

Kaur, M., Malik, P., Devi, U., Mukta, A., Kaur, A., Dhillon, G. S., Padhy, A. K., Sharma, H., Sharma, A., and Kaur, S. (2023). *Chapter 9 - Wheat biofortification: A molecular breeding outlook* (S. H. Wani, D. Wang, and G. B. T.-Q. T. L. M. in C. I. Pratap Singh (eds.); pp. 163–201). Academic Press. https://doi.org/10.1016/B978-0-323-85243-2.00014-3

Kebebew, F., Tsehaye, Y., and McNeilly, T. (2001). Diversity of durum wheat (Triticum durum Desf.) at in situ conservation sites in North Shewa and Bale, Ethiopia. *Journal of Agricultural Science*, *136*(4), 383–392.

https://doi.org/10.1017/S0021859601008887

Kosaka, A., Manickavelu, A., Kajihara, D., Nakagawa, H., and Ban, T. (2015). Altered gene expression profiles of wheat genotypes against Fusarium head blight. *Toxins*, *7*(2), 604–620. https://doi.org/10.3390/toxins7020604

Kruskal, W. H., and Wallis, W. A. (1952). Use of Ranks in One-Criterion Variance Analysis. *Journal of the American Statistical Association*, *47*(260), 583–621. https://doi.org/10.2307/2280779

Lachagari, V. B. R., Gupta, R., Lekkala, S. P., Mahadevan, L., Kuriakose, B., Chakravartty, N., Mohan Katta, A. V. S. K., Santhosh, S., Reddy, A. R., and Thomas, G. (2019). Whole Genome Sequencing and Comparative Genomic Analysis Reveal Allelic Variations Unique to a Purple Colored Rice Landrace (Oryza sativa ssp. indica cv. Purpleputtu). *Frontiers in Plant Science*, *10*. https://doi.org/10.3389/fpls.2019.00513

Lanoue, A., Burlat, V., Henkes, G. J., Koch, I., Schurr, U., and Röse, U. S. R. (2010). De novo biosynthesis of defense root exudates in response to *Fusarium* attack in barley. *New Phytologist*, *185*(2), 577–588. https://doi.org/10.1111/j.1469-8137.2009.03066.x

Leslie, J. F., and Summerell, B. A. (2006). *The Fusarium Laboratory Manual* (Vol. 66). Blackwell Publishing.

Ma, Z., Xie, Q., Li, G., Jia, H., Zhou, J., Kong, Z., Li, N., and Yuan, Y. (2020). Germplasms, genetics and genomics for better control of disastrous wheat Fusarium head blight. *Theoretical and Applied Genetics*, *133*(5), 1541–1568. https://doi.org/10.1007/s00122-019-03525-8

Mahlein, A., Alisaac, E., Masri, A. Al, Behmann, J., Dehne, H., and Oerke, E. (2019). Comparison and Combination of Thermal, Fluorescence, and Hyperspectral Imaging for Monitoring Fusarium Head Blight of Wheat on Spikelet Scale. *Sensors*. https://doi.org/doi.org/10.3390/s19102281

Mandalà, G., Tundo, S., Francesconi, S., Gevi, F., Zolla, L., Ceoloni, C., and D'Ovidio, R. (2019). Deoxynivalenol Detoxification in Transgenic Wheat Confers Resistance to Fusarium Head Blight and Crown Rot Diseases. *Molecular Plant-Microbe Interactions*, *32*(5), 583–592. https://doi.org/10.1094/MPMI-06-18-0155-R

Martin, C., Schöneberg, T., Vogelgsang, S., Bertossa, M., Mauch-mani, B., Mascher, F., Mauch-mani, B., Mascher, F., Martin, C., Schöneberg, T., Vogelgsang, S., Vincenti, J., and Bertossa, M. (2017). Factors of wheat grain resistance to Fusarium head blight. *Phytopathologia Mediterranea*. https://doi.org/10.14601/Phytopathol_Mediterr-20292

Martínez-Moreno, F., Ammar, K., and Solís, I. (2022). Global Changes in Cultivated Area and Breeding Activities of Durum Wheat from 1800 to Date: A Historical Review. In *Agronomy* (Vol. 12, Issue 5). https://doi.org/10.3390/agronomy12051135

Martini, D., Taddei, F., Ciccoritti, R., Pasquini, M., Nicoletti, I., Corradini, D., and D'Egidio, M. G. (2015). Variation of total antioxidant activity and of phenolic acid, total phenolics and yellow coloured pigments in durum wheat (*Triticum turgidum* L. var. *durum*) as a function of genotype, crop year and growing area. *Journal of Cereal Science*, *65*, 175–185. https://doi.org/10.1016/j.jcs.2015.06.012

McKeehen, J. D., Busch, R. H., and Fulcher, R. G. (1999). Evaluation of Wheat (Triticum aestivum L.) Phenolic Acids during Grain Development and Their Contribution to *Fusarium* Resistance. *Journal of Agricultural and Food Chemistry*, *47*(4), 1476–1482. https://doi.org/10.1021/jf980896f

McMullen, M., Bergstrom, G., De Wolf, E., Dill-Macky, R., Hershman, D., Shaner, G., and Van Sanford, D. (2012a). A Unified Effort to Fight an Enemy of Wheat and Barley: Fusarium Head Blight. *Plant Disease*, *96*(12), 1712–1728. https://doi.org/10.1094/PDIS-03-12-0291-FE

Mesterhazy, A. (2020). Updating the breeding philosophy of wheat to fusarium head blight (Fhb): Resistance components, qtl identification, and phenotyping—a review. In *Plants* (Vol. 9, Issue 12). https://doi.org/10.3390/plants9121702

Mizuno, N., Ishikawa, G., Kojima, H., Tougou, M., Kiribuchi-Otobe, C., Fujita, M., and Nakamura, K. (2021). Genetic mechanisms determining grain number distribution along the spike and their effect on yield components in wheat. *Molecular Breeding*, *41*(10). https://doi.org/10.1007/s11032-021-01255-8

Mohamad, I. Bin, and Usman, D. (2013). Standardization and its effects on K-means clustering algorithm. *Research Journal of Applied Sciences, Engineering and Technology*, *6*(17), 3299–3303.

https://doi.org/10.19026/rjaset.6.3638

Onofri, A., and Pannacci, E. (2014). Spreadsheet tools for biometry classes in crop science programmes. *Communications in Biometry and Crop Science*, *9*(2), 3–13.

Oufensou, S., Balmas, V., Azara, E., Fabbri, D., Dettori, M. A., Schu, C., Zehetbauer, F., Strauss, J., Delogu, G., and Migheli, Q. (2020). *Naturally Occurring Phenols Modulate Vegetative Growth and Deoxynivalenol Biosynthesis in Fusarium graminearum*. https://doi.org/10.1021/acsomega.0c04260

Paciulli, M., Littardi, P., Rinaldi, M., and Chiavaro, E. (2021). Wheat Bread in the Mediterranean Area: From Past to the Future. In F. Boukid (Ed.), *Cereal-Based Foodstuffs: The Backbone of Mediterranean Cuisine* (pp. 47–88). Springer International Publishing. https://doi.org/10.1007/978-3-030-69228-5_3

Prat, N., Guilbert, C., Prah, U., Wachter, E., Steiner, B., Langin, T., Robert, O., and Buerstmayr, H. (2017). QTL mapping of Fusarium head blight resistance in three related durum wheat populations. *Theoretical and Applied Genetics*, *130*(1), 13–27. https://doi.org/10.1007/s00122-016-2785-0

Ruan, Y. L., Patrick, J. W., Bouzayen, M., Osorio, S., and Fernie, A. R. (2012). Molecular regulation of seed and fruit set. *Trends in Plant Science*, *17*(11), 656–665. https://doi.org/10.1016/j.tplants.2012.06.005

Sakuma, S., Golan, G., Guo, Z., Ogawa, T., Tagiri, A., Sugimoto, K., Bernhardt, N., Brassac, J., Mascher, M., Hensel, G., Ohnishi, S., Jinno, H., Yamashita, Y., Ayalon, I., Peleg, Z., Schnurbusch, T., and Komatsuda, T. (2019). Unleashing floret fertility in wheat through the mutation of a homeobox gene. *Proceedings of the National Academy of Sciences of the United States of America*, *116*(11), 5182–5187. https://doi.org/10.1073/pnas.1815465116

Sallam, A. H., Haas, M., Huang, Y., Tandukar, Z., Muehlbauer, G., Smith, K. P., and Steffenson, B. J. (2024). Meta-analysis of the genetics of resistance to Fusarium head blight and deoxynivalenol accumulation in barley and considerations for breeding. *Plant Breeding*, *143*(1), 2–25. https://doi.org/10.1111/pbr.13121

Schiavi, D., Ronchetti, R., Di Lorenzo, V., Salustri, M., Petrucci, C., Vivani, R., Giovagnoli, S., Camaioni, E., and Balestra, G. M. (2022). Circular Hazelnut Protection by Lignocellulosic Waste Valorization for Nanopesticides Development. *Applied Sciences (Switzerland)*, *12*(5). https://doi.org/10.3390/app12052604

Schroeder, H. W., and Christensen, J. J. (1963). Factors affecting resistance of wheat to scab caused by Gibberella zeae. *Phytopathology*, *53*(7, 1), 831–838.

Singleton, V. L., and Rossi, J. A. (1965). Colorimetry of Total Phenolics with Phosphomolybdic-Phosphotungstic Acid Reagents. *American Journal of Enology and Viticulture*, *16*(3), 144 LP – 158. https://doi.org/10.5344/ajev.1965.16.3.144

Siranidou, E., Kang, Z., and Buchenauer, H. (2002). Studies on symptom development, phenolic compounds and morphological defence responses in wheat cultivars differing in resistance to Fusarium head blight. *Journal of Phytopathology*, *150*(4–5), 200–208. https://doi.org/10.1046/j.1439-0434.2002.00738.x

Still, C., Powell, R., Aubrecht, D., Kim, Y., Helliker, B., Roberts, D., Richardson, A. D., and Goulden, M. (2019). Thermal imaging in plant and ecosystem ecology: applications and challenges. *Ecosphere*, *10*(6). https://doi.org/10.1002/ecs2.2768

Sunic, K., D'Auria, J. C., Sarkanj, B., and Spanic, V. (2023). Metabolic Profiling Identifies Changes in the Winter Wheat Grains Following *Fusarium* Treatment at Two Locations in Croatia. *Plants*, *12*(4). https://doi.org/10.3390/plants12040911

Tesemma, T., Becker, H. C., Belay, G., Mitiku, D., Bechere, E., and Tsegaye, S. (1993). Performance of Ethiopian tetraploid wheat landraces at their collection sites. *Euphytica*, *71*(3), 221–230. https://doi.org/10.1007/BF00040411

Tessmann, E. W., and Van Sanford, D. A. (2019). Associations between morphological and FHB traits in a soft red winter wheat population. *Euphytica*, *215*(11), 1–16. https://doi.org/10.1007/s10681-019-2509-z

Tomassini, A., Sella, L., Raiola, A., D'Ovidio, R., and Favaron, F. (2009). Characterization and expression of *Fusarium graminearum* endo-polygalacturonases in vitro and during wheat infection. *Plant Pathology*, *58*(3), 556–564. https://doi.org/10.1111/j.1365-3059.2008.02019.x

Tu, Q., Wang, L., An, Q., Shuai, J., Xia, X., Dong, Y., Zhang, X., Li, G., and He, Y. (2023). Comparative transcriptomics identifies the key in planta-expressed genes of *Fusarium graminearum* during infection of wheat varieties. *Frontiers in Genetics*, *14*. https://doi.org/10.3389/fgene.2023.1166832

Wagay, N. A., Lone, R., Rafiq, S., and Bashir, S. U. (2020). Phenolics: A Game Changer in the Life Cycle of Plants. In R. Lone, R. Shuab, and A. N. Kamili (Eds.), *Plant Phenolics in Sustainable Agriculture : Volume 1* (pp. 241–275). Springer Singapore. https://doi.org/10.1007/978-981-15-4890-1_11

Wallis, C. M., and Galarneau, E. R. A. (2020). Phenolic Compound Induction in Plant-Microbe and Plant-Insect Interactions: A Meta-Analysis. *Frontiers in Plant Science*, *11*(December), 1–13. https://doi.org/10.3389/fpls.2020.580753

Zadoks, J. C., Chang, T. T., and Konzak, C. F. (1974). A decimal code for the growth of cereals. *Weed Research*, *14*, 415–421. https://doi.org/10.1111/j.1365-3180.1974.tb01084.x

Zhao, L., Su, P., Hou, B., Wu, H., Fan, Y., Li, W., Zhao, J., Ge, W., Xu, S., Wu, S., Ma, X., Li, A., Bai, G., Wang, H., and Kong, L. (2022). The Black Necrotic Lesion Enhanced *Fusarium graminearum* Resistance in Wheat. *Frontiers in Plant Science*, *13*(June), 1–15. https://doi.org/10.3389/fpls.2022.926621

Zhu, Z., Hao, Y., Mergoum, M., Bai, G., Humphreys, G., Cloutier, S., Xia, X., and He, Z. (2019). Breeding wheat for resistance to Fusarium head blight in the Global North: China, USA, and Canada. *The Crop Journal*, *7*(6), 730–738. https://doi.org/10.1016/j.cj.2019.06.003

4. Early and late responses to Fusarium Head Blight in durum wheat: focus on flavonoid and phenylpropanoid biosynthetic pathways

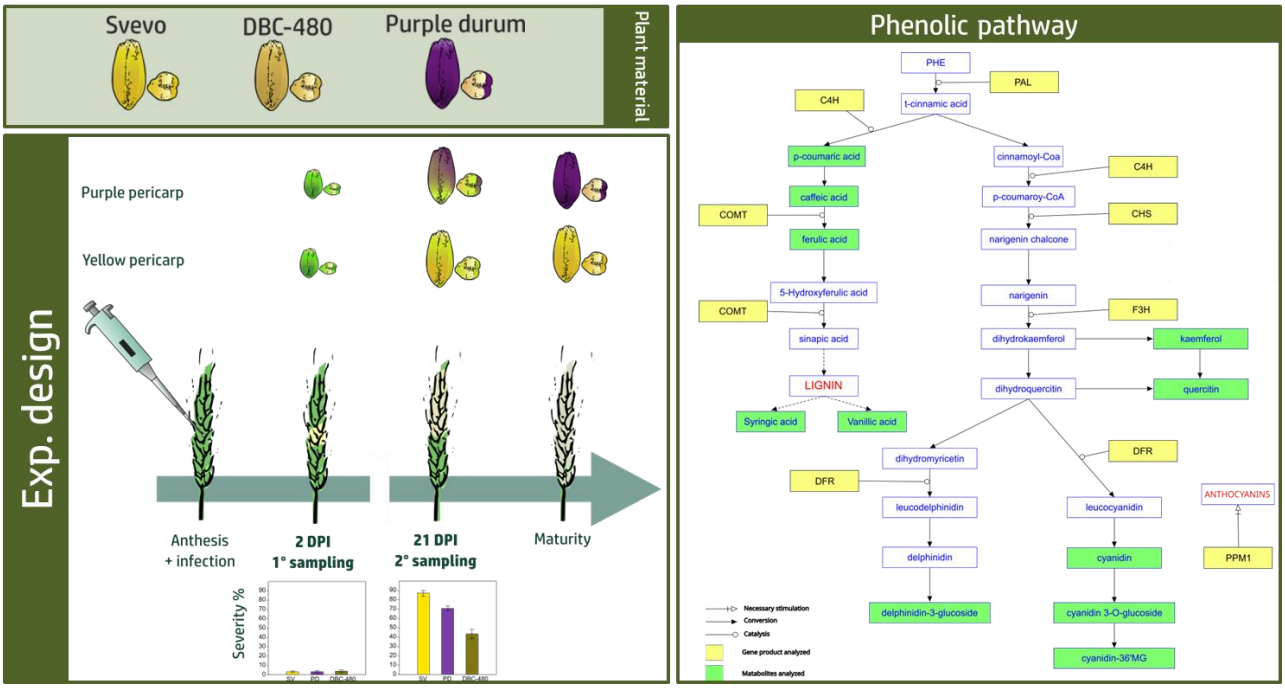

Abstract: Durum wheat is among the cereal crops most susceptible to Fusarium Head Blight (FHB), a fungal disease that can lead to significant yield losses. Despite this, only limited research efforts have been directed towards understanding FHB resistance in durum wheat. Wheat grains naturally contain phenolic compounds, and anthocyanins are particularly present in the so-called pigmented wheat genotypes, such as purple pericarp ones. In this study the effects of the biotic stress caused by *Fusarium graminearum* infection on phenylpropanoid biosynthetic pathway in durum wheat spikes were explored, considering three genotypes with different susceptibility (including a purple pericarp genotype), and two time points (an early stage time point: 2 days post infection, and a late stage time point: 21 days post infection). At early infection stage, the *F. graminearum* infection triggered upregulation of all the considered genes involved in the phenylpropanoid pathway in the resistant genotype, while, in the purple pericarp genotype, the infection caused an increase in quercetin accumulation in the soluble fraction of spike extract. At late infection stage, the infection caused (in all the genotypes) a degradation of secondary cell wall and the release of the hydroxycinnamic acids esterified with arabinoxylans (ferulic acid and *p*-coumaric acid) and lignin-derived monomers (vanillic acid). Furthermore, chalcone synthase gene (*CHS*) and the transcription factor *Ppm1* (Purple pericarp MYB 1) were boosted in the pigmented genotype due to infection at late infection stage. These findings contribute to the understanding of host-pathogen interactions for future breeding programs focused on improving FHB resistance in durum wheat varieties, with a particular focus on pigmented genotypes.

Publications:

L. Felici, F. Catellani, S. Francesconi, M. Vitali, F. Sestili, G. M. Balestra, 2024. "Early and late responses to Fusarium Head Blight in durum wheat: focus on phenylpropanoid biosynthetic pathway ". *Plant stress* [Manuscript under review]

4.1. Introduction

Phenylpropanoids (or phenolic compounds) are natural products abundantly produced by plants (Durazzo et al. 2019), which possess several biochemical properties, such as reducing capacity, binding properties (Belščak-Cvitanović et al. 2018), anti-inflammatory, antibacterial, antifungal, antigenotoxic (Daglia 2012) and antioxidant activity (Oufensou et al. 2020; Gautier et al. 2020; Brainina et al. 2019). Phenylpropanoid biosynthesis in plants has been studied in-depth. Briefly, the pathway begins with the deamination of L-phenylalanine by L-phenylalanine ammonia-lyase (PAL) and it can lead to several products. Indeed, the pathway branches out into different routes: one of them produce lignin monomers and then lignin (Goujon et al. 2003), while the production of naringenin chalcone from *p*-coumaroyl-CoA and malonyl-CoA molecules by CHS (chalcone synthase) starts the flavonoid branch of the pathway. Dihydroflavanols, colorless anthocyanin glycosides, are formed and subsequently catalyzed by anthocyanidin synthase (ANS) to produce colored anthocyanins (Sunil and Shetty 2022). Dihydroflavanols can be the substrate of other enzymes, such as the FLS (flavonol synthase) producing flavones like kaempferol or quercetin (Gebhardt et al. 2007). The genes involved in phenylpropanoid biosynthesis can be divided into structural genes (functional genes, which encode for the above-mentioned enzymes) and regulatory genes. The expression of structural genes during anthocyanin biosynthesis is directly regulated by the MYB-bHLH-WDR complex (Liu et al. 2021), which varies in the different plant species.

Wheat grains are surely an important source of carbohydrates, but they also naturally contain several antioxidant bioactive compounds, such as carotenoids, tocopherols and phenolic compounds (Abdel-Aal and Rabalski 2008). Anthocyanins are particularly accumulated in the so-called pigmented wheat genotypes. These cultivars have blue to blue-black, and red to purple grains which could be distinguished in purple pericarp (expressing purple color in pericarp layer), blue aleurone (rich in anthocyanins in the aleurone layer), and black (having both pigmented pericarp and aleurone layers) genotypes (Böhmdorfer et al. 2018). Although their distribution is currently limited, interest in these genotypes is increasing due to their nutritional value (Hu et al. 2007; Cory et al. 2018; Singh et al. 2020) and for the function of polyphenols in plant life. Indeed, pigments, anthocyanins and phenolic compounds are essential for plants, where they play a role in senescence regulation, protection from light damage, internal and external signaling, reproduction and reaction to several abiotic and biotic stresses (Wagay et al. 2020; Li and Ahammed 2023). Other studies showed that an increase in anthocyanin content or an alteration in phenylpropanoids biosynthetic pathway affects resistance response to bacterial (Wegener and Jansen 2007; Lei et al. 2018) and fungal pathogens (Zhang et al. 2013; Sivankalyani et al. 2016; Flachowsky et al. 2010). Furthermore, these pathways are interconnected with the synthesis of salicylic acid, the plant hormone responsible for activating systemic acquired resistance (SAR) (G. Hao et al. 2019).

Among the main biotic stresses of cereals, Fusarium Head Blight (FHB) stands out (McMullen et al. 2012). This disease is caused by several hemibiotrophic fungal pathogens belonging to *Fusarium* spp. genera, causing bleaching and necrosis on the spikes. Infection occurs during flowering through stomata or other openings and then the mycelium spreads along the rachis, leading to kernel disruption and mycotoxins contamination (Mielniczuk and Skwaryło-Bednarz 2020). Although no fully resistant cultivar is currently available, several Quantitative Trait Loci (QTLs) associated to the FHB resistance, such as *Fhb1*, have been identified, albeit with unclear functions, harbored by the bread wheat genotype Sumai-3 (Hao et al. 2020). Among the cereal crops, durum wheat (*Triticum turgidum* L. subsp. *durum* (Desf.) Husn.), used to produce semolina and several traditional food products in the Mediterranean basin (Conte et al. 2021; Boukid 2021), is particularly susceptible to FHB (Gaikpa et al. 2020).

This study aimed to explore the effect of the biotic stress caused by *Fusarium graminearum* infection on phenylpropanoid biosynthetic pathway in durum wheat spikes. Three genotypes with different susceptibility were artificially inoculated: Svevo (susceptible), DBC-480 (resistant) and Purple durum (susceptible). Two time points were considered: an early stage (2 days post-infection, DPI), chosen because SAR activation is more evident at this stage, and a late stage (21 DPI), selected as optimal for studying pigmentation-related traits. Changes in the pathway were detected by (I) differential gene expression (by RT-qPCR) of key structural and regulatory genes; (II) targeted metabolomics, using HPLC/MS-MS for the quantification of 14 different phenylpropanoids present in the spikes in soluble or cell wall bound fractions; (III) 2,2-Diphenyl-1-picrylhydrazyl (DPPH) scavenging assay to assess the antioxidant properties of the spike extracts.

4.2. Materials and methods

4.2.1.Plant material and growth condition

Three durum wheat genotypes (*Triticum turgidum* subsp. *durum*) were used in the present study. Svevo is a commercial early maturing cultivar with high protein content and yellow index, used as FHB susceptible control. Purple durum is a pigmented durum wheat genotype (accession number NGB 6399), with purple grain pericarp, provided by Nordic Baltic Genebanks (GENBIS). The FHB-resistant durum wheat experimental line DBC-480, harboring the introgression of the resistant quantitative trait locus *Fhb1* from Sumai-3, was provided by IFA - Tulln (Prat et al. 2017). The experiment was carried out in a growth chamber equipped with white led light (Combo 600 W and Slim Natural Indoor bars, C-Led, Italy), controlled temperature and relative humidity. The kernels were germinated on paper soaked in sterile distilled water for 7 days at 20˚C with a 16 h photoperiod and then transferred to 9 x 9 cm pot filled with TYPical Brill soil. Plants were grown at 10°C with an 8 h photoperiod for 2 weeks to break the dormancy and then each plant was transferred to a 2 L pot (12,8 x 12,8 x 20 cm), filled using the same soil, and plants were grown at 20°C (+/-2°C), 16 h photoperiod and 60% relative humidity until the end of the experiment. The plants were fertilized using calcium nitrate (15.5-0-0+26.5 CaO, Haifa) at every transplanting event and at heading and using a micronutrient liquid fertilizer (NPK 4-7-7 +B+Cu+Fe+Mn+Zn, Flortis).

4.2.2. Fungal material and inoculum preparation

Fungal material and inoculum preparation was the same already employed in chapter 3 and described in paragraph 3.2.2.

4.2.3. Experimental design, infection technique, disease evaluation and spike sampling

Plants were subjected to artificial inoculation at anthesis (Zadok stage 69) using a point inoculation technique. In brief, 10 μL of spore suspension were applied to the central spike floret of each plant (using a laboratory pipette), for the inoculated plants, while 10 μL of sterile distilled water supplemented with 0.05% (v/v) of Tween-20 were applied for mock plants. For each genotype, three replicates consisting of 10 plants each were considered for each treatment (inoculated and mock) using a completely randomized experimental design. The FHB disease severity (%) was determined by counting the number of bleached spikelets (number of infected spikelets on the total number of spikelets per spike) for each inoculated spike at 2 and 21 DPI (days post infection). At the same time points, three randomly chosen spikes were collected, suddenly frozen in liquid nitrogen and stored at -80°C until RNA/metabolites extraction. Three biological replicates were considered for each experimental group.

4.2.4. RNA extraction, quality check, quantification and cDNA synthesis

Spikes were grinded to a fine powder using mortar and pestle in liquid nitrogen. The RNAzol RT reagent (Sigma-Aldrich) was used to extract pure total RNA from 50 mg of fresh plant tissue (Chomczynski et al. 2010). Briefly, 1 mL of RNAzol RT reagent and 400 µL of RNAase-free water were added to the sample. Sample and solution were shacked at 500 RPM for 15 minutes and then centrifuged 15 minutes at 13000x *g*. The RNA-containing aqueous phase was precipitated with 1 mL isopropanol. The RNA pellet was washed with 75% ethanol and then resuspended in 50 µl of RNAase-free sterile deionized water. RNA purity was checked using a microvolume UV-Vis spectrophotometer (OPTIZEN NanoQ, KLAB, Republic of Korea) with A_{260}/A_{280} ratio of 1.7 to 2.1 and A_{260}/A_{230} of 1.6 to 2.3. RNA was quantified with a Qubit™ fluorometer 1.01 (Invitrogen) using the Qubit™ RNA BR Assay Kit (Thermo Fisher Scientific). The synthesis of cDNA was performed using 50 ng of RNA following the instructions provided by Xpert cDNA Synthesis Supermix with a gDNA eraser (GRiSP Research Solutions, Porto, Portugal) in a final volume of 20 µL. gDNA Contamination was checked through visualization on 1.5% agarose gel.

4.2.5. Primer design and relative gene expression

Starting from existing literature, mainly related to bread wheat (Ma et al. 2016; Jiang et al. 2018), the primer pairs for Real-Time qPCR were redesigned, adapted or verified on known sequences of durum wheat genome. Primer design was performed using the National Center for Biotechnology Information (NCBI) tool Primer-blast (https://blast.ncbi.nlm.nih.gov/Blast.cgi), using sequences obtained in Ensembl Plants (https://plants.ensembl.org/index.html) belonging to the INSDC Assembly GCA_900231445.1 (cv Svevo) (CNR). When annotation information was insufficient, sequences in NCBI (https://www.ncbi.nlm.nih.gov/) were considered. Primers were designed inside the exonic regions. The optimal annealing temperature was assessed by running a gradient PCR for each primer pair (range 59°C – 63 °C). Primers used in this study are listed in Supplementary material S4.1. The relative expression levels of the target genes were calculated on the basis of the Cq values of the three technical replicates derived from three independent biological replicates for each wheat genotype by applying the equation:

$$\text{Relative expression} = 2^{(-\Delta\Delta Cq)}$$

using *TaFNR*, *TaTUB* (Tenea et al. 2011), and *TaACT* (Tundo et al. 2016) as reference genes and the mock treatment to normalize the relative expression levels (Bustin et al. 2009). The RT-qPCR was performed following the instructions provided by Rotor-Gene Q (Qiagen, Hilden, Germany) and Xpert Fast SYBR (uni) MasterMix (GRiSP Research Solutions, Porto, Portugal), in a final volume of 10 µL. The amplification conditions consisted of (i) an initial denaturation step of 10 minutes at 95 °C; (ii) 40 cycles of 5 s denaturation at 95 °C; (iii) 30 s of annealing at the temperature indicated in Supplementary material S4.1, and (iv) 20 s of elongation at 72 °C. A final melt cycle (72–95 °C) was performed to confirm the unicity of the amplicons. NTC controls were included and the amplification was considered negative when a value of Cq ≥ 38 was detected.

4.2.6. Extraction of soluble metabolites and cell wall bound metabolites

Extraction procedure was adapted from existing literature (Doppler et al. 2022; Wang et al. 2013). Two hundred mg of grinded spikes, stored at -80°C, were freeze-dried and used for further extraction by adding 1 mL of a mixture of methanol and water (90:10) acidified with 5% formic acid. Samples were vortexed for 10 seconds, shaken for 10 minutes at 250 rpm, ultrasonicated for 5 minutes, and finally shaken for 5 minutes at 250 rpm. After centrifugation (5 minutes, 1300 rpm), the supernatant (extract I) was transferred to a new tube and the remaining pellet was used for a

second extraction. After the second extraction, the supernatant (extract II) was pooled with the extract I, filtered (Choice™ PTFE Syringe Filters 0.22 µm x 13 mm, Thermo Scientific, Waltham, MA, USA) and used for HPLC-MS/MS analysis. The remaining pellet was employed for cell wall hydrolysis, that was carried out using 1 mL of NaOH 3M under shaking conditions at room temperature for 2 hours at 250 rpm. After this step, 100 µL of 25% HCl were added to adjust the pH to 1-1.5 units and samples were extracted using 500 µL of ethyl acetate by shaking 10 minutes at 250 rpm. After centrifugation (10 minutes, 1300 rpm) the ethyl acetate phase was transferred in a new tube. Ethyl acetate extraction was repeated twice and the collected and combined extracts were dried using a nitrogen evaporator. The residue was reconstituted with a solution of methanol: formic acid 80:20, filtered (0.2µm) and used for the analysis. Soluble fraction (obtained by extraction using the mixture of methanol and water) and cell wall bound fraction (provided by hydrolysis) were analyzed separately.

4.2.7. Analytical determination of metabolites in durum wheat spike extracts

HPLC analyses were carried out using an HPLC 1260 Infinity II system (Agilent Technologies Italy S.p.A. Milan, Italy) coupled with QTRAP 5500 mass spectrometer (AB SCIEX S.r.l. Forster City, CA, USA) equipped with an ESI source, operating in MRM (multiple reaction monitoring) mode. The following phenolic acids and flavonoids were analyzed: caffeic acid, ferulic acid, gallic acid, *p*-coumaric acid, syringic acid, vanillic acid, 4-methoxyflavove, chlorogenic acid cyanidin 3-(6" malonylglucoside), cyanidin 3-glucoside, delphinin 3-glucoside, kaempferol, oenin chloride (Malvidin-3-*O*-glucoside), quercetin. All the analytical specifications are reported in Supplementary material S4.2.

4.2.8. Determination of Antioxidant Capacity (DPPH)

The free radical scavenging capacity of each extract was determined by the use of the 2,2-Diphenyl-1-picrylhydrazyl (DPPH) radical, according to the method of Dudonné et al. (2009) with few modifications. Briefly, a DPPH• solution in methanol (6×10^{-5} M) was prepared daily, and 1.5 mL of this solution was mixed with 50 µL of methanolic solutions of plant extracts. The samples were incubated for 20 minutes in the dark, and then dispensed in 96-well microplate (200 µL in each well, four technical replicates). The decrease in absorbance at 517 nm was measured (A_E) using a DR-200B Microplate reader (Diatek instruments). A blank sample containing 100 µL of methanol in the DPPH• solution was prepared daily, and its absorbance was measured (A_B) for each plate in 8 technical replicates. Radical scavenging activity was calculated using the following formula:

$$\% \text{ inhibition DPPH} = [(A_B - A_E)/A_B] \times 100$$

where A_B is the absorbance of the blank sample, and A_E stands for the absorbance of the plant extract.

4.2.9. Data analysis

Kruskal-Wallis test and Dunn's post-hoc test were employed to evaluate the effect of genotypes on severity and relative gene expression, the effect of the infection on metabolites quantification and DPPH radical scavenging activity. Two level of significance ($p<0.05$ and $p < 0.01$) was computed to assess the significance of the F values. Two-way PERMANOVA (with Bray–Curtis similarity index) was used to evaluate the combined effect of genotype and inoculation on metabolites composition of spike extracts. Linear correlation (Sperman's *rs* with Bonferroni correction) was employed to correlate metabolites quantification and DPPH scavenging activity. Two heatmaps (one for each time point) were generated to represent the relative expression levels of wheat genes after the inoculations and analyzed by hierarchical clustering, where both rows and columns are clustered using correlation distance and average linkage.

Summary statistics, normality test, Kruskal–Wallis test, Dunn's test of multiple comparisons, PERMANOVA and linear correlation were performed in PAST ver. 4.05 (University of Oslo) (Hammer et al. 2001). ClustVis (Tartu, Estonia) web tool (https://biit.cs.ut.ee/clustvis/) was used for heatmap generation and hierarchical clustering (Metsalu and Vilo 2015). A summary pathway with considered metabolites and genes were built using PathVisio (Maastricht University, NL) a free open-source pathway analysis and drawing software (Kutmon et al. 2015).

4.3. Results

4.3.1.Purple durum is a susceptible genotype

Plants were inoculated at anthesis and severity was evaluated at two different time points. As expected, the severity was very low at early stage, with no significant differences observed among genotypes (Purple durum, Svevo and DBC-480) (Fig. 4.1a). At late stage of infection, the median severity of the resistant genotype DBC-480 was notably low (26.07%), showing high resistance to the infection. In contrast, Purple durum exhibited a median severity (83.56%) compared to the susceptible genotype Svevo (100%), as displayed in Fig. 4.1b and in Supplementary material S4.3. Mock treated plants presented no visible symptoms.

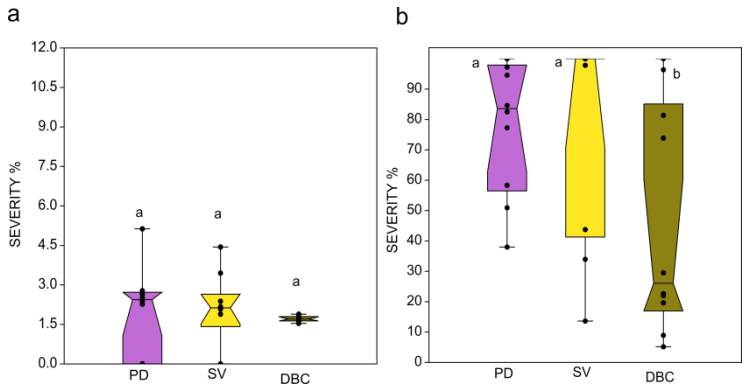

Fig. 4.1 Box plot of severity % at 2 DPI (a) and at 21 DPI (b). Different letters (a, b) into the subfigures refer to the statistical analysis performed using Kruskal-Wallis with the Dunn's test at a confidence level of 0.95 and $p < 0.05$. PD= Purple durum; SV= Svevo; DBC= DBC-480.

4.3.2. In the early infection stage, all the considered genes are upregulated in the resistant control DBC-480

The expression of key genes involved in the phenylpropanoid and flavonoid pathways in durum wheat spikes was evaluated under artificial inoculation. *In silico* analysis revealed that only a few of the primer pairs available in the literature (designed for bread wheat) were suitable for RT-qPCR amplification in durum wheat. For this reason, five out of the seven target genes were redesigned (Supplementary material S4.1). The specificity and differentiation of the products were verified through analysis of amplicon melting curves at the end of RT-qPCR (Supplementary material S4.1).

A graphical representation of the relative expression of the selected genes in the early infection stage (2 DPI) is shown in Fig. 4.2. *PAL* exhibited upregulation across all genotypes, with particularly notable increases in in DBC-480 (71.87-fold) and Purple durum (15.01-fold). Similarly, *Fusarium* infection increased the expression level of *C4H* in DBC-480

(5.68-fold) and Purple durum (3.13-fold) compared to Svevo. *CHS* was upregulated in DBC-480 (2.70-fold) and slightly upregulated in Purple durum (1.45-fold), while in Svevo it showed a basal expression. *DFR* was upregulated in the resistant genotype (6.30-fold), and slightly upregulated in the pigmented genotype (1.49-fold), compared to the susceptible control that showed basal expression level (1.11-fold). *COMT* and *F3H* were upregulated in DBC-480 (3.80-fold and 3.32-fold, respectively), whereas no significant differences were observed in the other genotypes.

4.3.3. In the late infection stage PAL and C4H are upregulated in Svevo while CHS and PPM1 are upregulated in Purple Durum

A clear change in the expression patterns among the different genotypes was evident in the late infection stage (21 DPI) compared to the early infection one, as shown in Fig. 4.2. *PAL* (38.40-fold) and *C4H* (57.47-fold) were strongly boosted in Svevo, compared to the 2 other genotypes. *CHS* was upregulated in Purple durum (4.14-fold) and Svevo (3.28-fold), whereas it was not differentially expressed in DBC-480 (0.92-fold). Interestingly, *PPM1* was boosted in Purple durum (6.19-fold) and Svevo (2.88-fold), compared to DBC-480 (1.04-fold), that showed a basal expression level. *COMT* and *F3H* were upregulated in Purple durum (4.79-fold and 1.49-fold, respectively), although these expression levels were not statistically different from those observed in the other two genotypes. *DFR* showed upregulation in DBC-480 (3.29-fold), in Svevo (2.68-fold), whereas no significant difference was observed in Purple durum (1.28-fold).

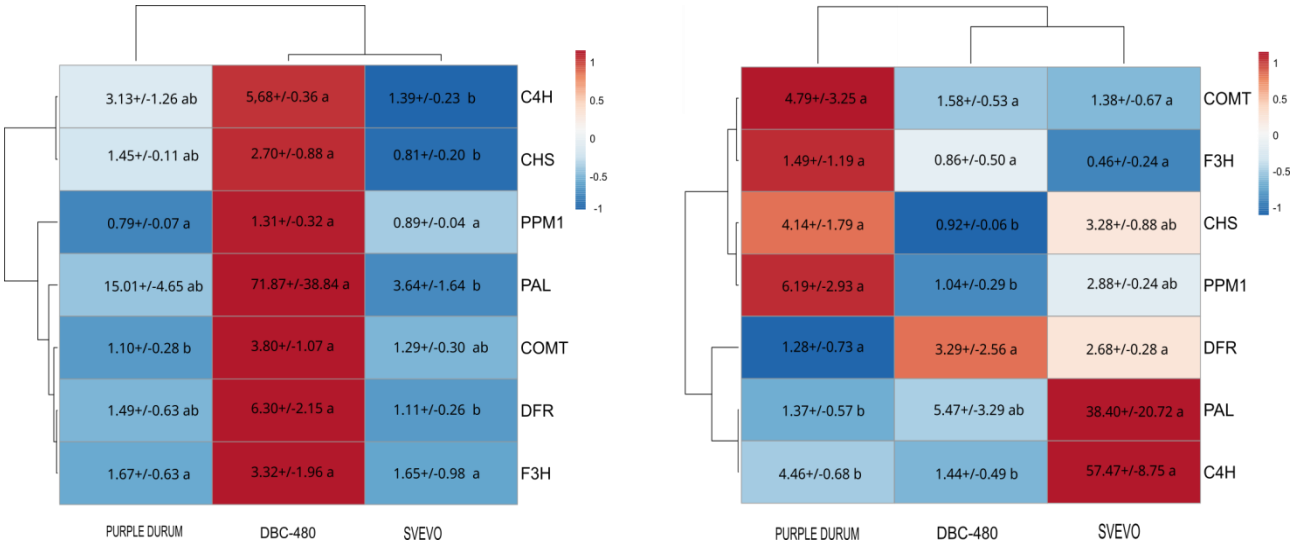

Fig. 4.2 Clustering analysis representing the relative expression of considered genes (rows) for each genotype (columns) due to *F. graminearum* infection, normalized on the un-infected (mock) control: (left) 2 DPI; (right) 21 DPI. Both rows and columns are clustered using correlation distance and average linkage. The heatmaps were constructed with the z-score (explained by the color legend at the right of the picture) by analyzing data with ClustVis software (Tartu, Estonia); numbers are the mean relative gene expression +/- SE; letters refer to statistical difference (Kruskal-Wallis; Dunn's post-hoc) among genotypes for each gene.

4.3.4. In the late infection stage soluble metabolites accumulation depends on both genotype and infection

Selected metabolites were extracted from spikes and quantified (using HPLC-MS/MS and reference standards), and expressed as ng/g of starting biomass, in terms of soluble and cell wall bound fraction. The results obtained from the

quantification of soluble metabolites are graphically displayed in Fig. 4.3a and 4.3b, while the data expressed in ng/g and the results of two-way PERMANOVA are shown in Supplementary file S4.4. At the early infection stage, the total amount of the considered metabolites stood below 900 ng/g. *p*-Coumaric acid was the most prevalent extracted compound. The two-way PERMANOVA analysis revealed that variability at the early infection stage depends exclusively on the genotype ($p < 0.01$). On the other hand, at 21 DPI, an increase in metabolite content was observed in infected Purple durum and Svevo compared to mock control plants (Fig. 4.3b). Indeed, in infected Purple durum and Svevo plants, the total amount of extracted metabolites was above 7000 ng/g, while in infected DBC-480, in mock DBC-480, Purple durum and Svevo plants this was below 2000 ng/g. Interestingly, a notable amount of cyanidin 3-(6" malonylglucoside) (1878.88 ng/g infected; 586.17 ng/g mock) and cyanidin 3-glucoside have been detected in Purple durum (670.92 ng/g infected; 138.31 ng/g mock), while vanillic acid was among the most abundant compounds detected in Purple durum and Svevo infected plants (829.53 ng/g Purple durum; 650.10 ng/g Svevo). The two-way PERMANOVA analysis revealed that variability at 21 DPI was dependent on the genotype and the infection ($p < 0.01$). Quantification of selected cell wall bound metabolites is shown in Fig. 4.3c and 4.3d and in Supplementary files S4.4. Notably, all the samples, at early and late infection stages, were mainly composed of ferulic acid, *p*-coumaric acid, vanillic acid and syringic acid and the total amount of selected metabolites was above 16000 ng/g. The two-way PERMANOVA analysis revealed that variability was independent from the genotype and the infection ($p > 0.05$).

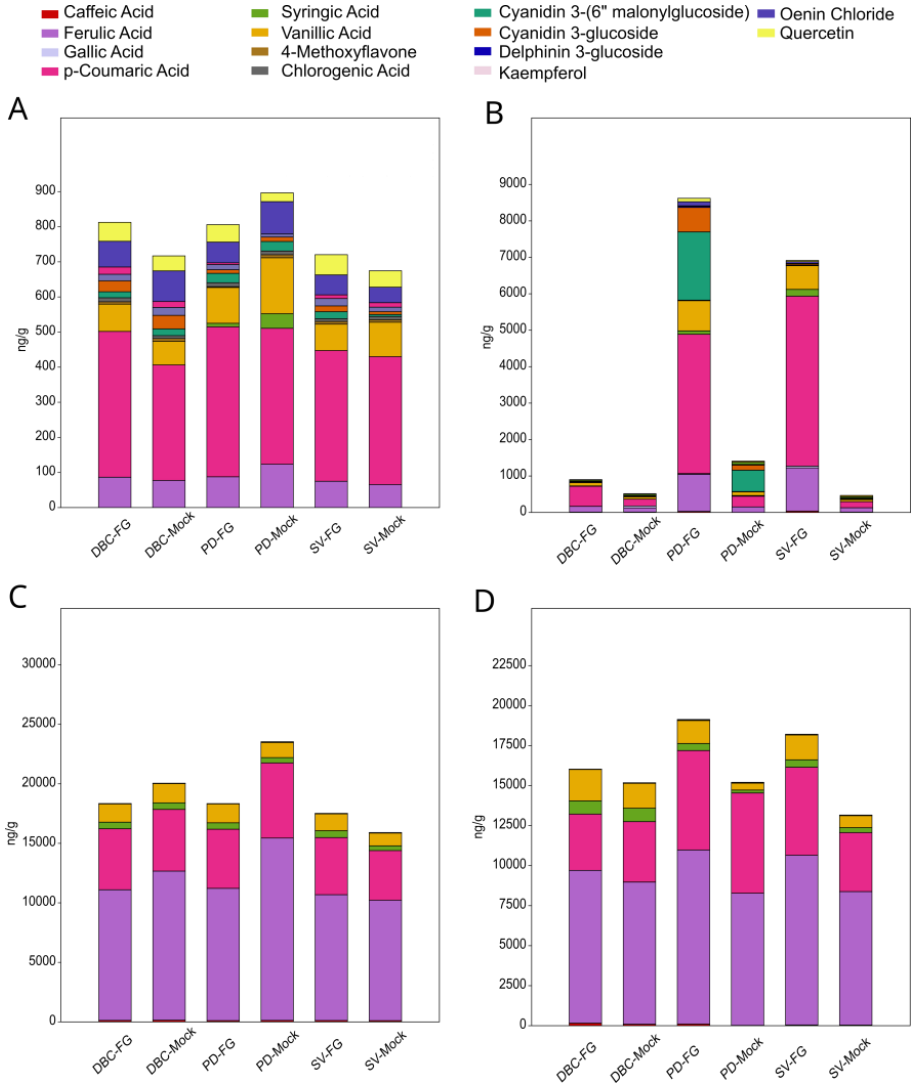

Fig. 4.3: Phenylpropanoids composition of DBC-480, Purple durum (PD) and Svevo (SV) *F. graminearum*-inoculated (FG) and Mock-treated spike extracts. (A) Soluble fraction at 2 DPI; (B) soluble fraction at 21 DPI; (C) cell wall bound fraction at 2 DPI; (D) cell wall bound fraction at 21 DPI.

4.3.5. Fusarium infection affects the accumulation of the selected metabolites

In order to focus on the infection effect, differences between the metabolite amounts in infected spikes (FG) and mock treated spikes were calculated for each considered metabolite (Table 4.1). Furthermore, statistical analysis was performed to compare FG-infected plants and mock treated plants (Kruskal-Wallis $p<0.05$, indicated as "*" and bold font in the Table 4.1). At the early time point (2 DPI), the detection of metabolites in the soluble fraction of Svevo infected spikes revealed an increase in the accumulation of ferulic acid (+14.50%), a decrease in vanillic acid (-23.31%) and a surprising increase of cyanidin 3-(6"-malonylglucoside) (+252.46%) compared to mock treated plants. Detection of metabolites in the cell wall bound fraction of Svevo infected spikes showed a consistent increase of *p*-coumaric acid (+15.50%) and syringic acid (+45.43%) due to the infection. In DBC-480 infected spikes there was an increase of *p*-coumaric acid in the soluble fraction (+26.24%), while Purple durum infected spikes presented an increase in soluble quercetin and a decrease in bound quercetin (+98.75% in soluble fraction; -35.99% in cell wall bound fraction). At the late infection stage (21 DPI) all the three genotypes showed a significant increase in the accumulation of phenolic acids in the soluble fraction in the infected spikes compared to the mock treated ones. In all genotypes, a notable increase in

p-coumaric acid (+189.64% DBC-480; +1202.41% Purple durum; +2706.82% Svevo) and vanillic acid (+44.51% DBC-480; +720.33% Purple durum; +1018.84% Svevo) was detected in soluble fraction, while an additional increase in ferulic acid was detected in Svevo and Purple durum soluble fraction (+569.64%; +880.29% respectively). An increase of soluble oenin (+83.76%) in infected spikes was statistically significant compared to the mock treated plants.

Table 4.1: Differences (expressed in %) between *F. graminearum* infected plants (FG) and Mock treated plants for each metabolite quantified by HPLC/MS-MS. The data presented in the table (%) were obtained as follow: % = [(ng.g^{-1}(FG)–ng.g^{-1}(Mock))/ng.g^{-1}(Mock)]x100. "*" indicates that the difference (%) is statistically significant (Kruskal-Wallis $p<0.05$).

		DBC 2 DPI		PD 2 DPI		SV 2 DPI		DBC 21 DPI		PD 21 DPI		SV 21 DPI	
Caffeic Acid	Soluble frac.	0.00		0.00		0.00		-1.17		0.00		307.31	
Caffeic Acid	Bound frac.	-12.55		-14.47		12.28		69.46		450.16		12.47	
Ferulic Acid	Soluble frac.	11.82		-29.04		**14.50**	*	35.87		**569.64**	*	**880.29**	*
Ferulic Acid	Bound frac.	-12.36		-27.46		4.47		7.46		31.64		27.17	
Gallic Acid	Soluble frac.	0.00		0.00		0.00		-100.00		0.00		0.00	
Gallic Acid	Bound frac.	0.00		0.00		0.00		0.00		0.00		0.00	
p-Coumaric Acid	Soluble frac.	**26.24**	*	10.34		2.18		**189.64**	*	**1202.41**	*	**2706.82**	*
p-Coumaric Acid	Bound frac.	-1.14		-21.27		**15.05**	*	-6.81		-0.76		49.29	
Syringic Acid	Soluble frac.	0.00		-75.68		0.00		0.00		404.15		0.00	
Syringic Acid	Bound frac.	0.14		19.69		**45.43**	*	-1.37		140.31		48.41	
Vanillic Acid	Soluble frac.	15.74		-36.01		**-23.31**	*	**44.91**	*	**720.33**	*	**1018.84**	*
Vanillic Acid	Bound frac.	-5.39		25.03		32.31		25.89		233.13		106.67	
4-Methoxyflavone	Soluble frac.	-17.37		-73.66		6.24		19.04		46.74		18.21	
4-Methoxyflavone	Bound frac.	-18.61		-38.41		5.09		-2.87		43.93		55.80	
Chlorogenic Acid	Soluble frac.	39.25		6.00		-14.42		-75.27		81.74		-21.05	
Chlorogenic Acid	Bound frac.	-12.10		-47.43		-12.22		-28.70		-21.89		36.00	
Cyanidin 3-(6" malonylglucoside)	Soluble frac.	-10.91		-1.53		**252.46**	*	-6.16		219.51		-15.38	
Cyanidin 3-(6" malonylglucoside)	Bound frac.	-17.86		-3.54		3.42		3.49		44.99		0.00	
Cyanidin 3-glucoside	Soluble frac.	-19.61		-17.87		101.39		207.48		385.09		392.66	
Cyanidin 3-glucoside	Bound frac.	-7.55		-100.00		-100.00		0.00		40.28		-100.00	
Delphinin 3-glucoside	Soluble frac.	-16.64		68.87		65.24		-11.34		123.67		11.30	
Delphinin 3-glucoside	Bound frac.	0.00		-69.66		-43.57		-100.00		109.12		-100.00	
Kaempferol	Soluble frac.	22.10		0.00		-17.66		0.00		147.27		-100.00	
Kaempferol	Bound frac.	0.00		-68.09		43.39		-39.43		-5.69		29.58	
Oenin Chloride	Soluble frac.	-15.94		-35.95		28.71		-15.47		**83.76**	*	24.78	
Oenin Chloride	Bound frac.	0.00		-100.00		4.27		0.00		0.93		0.00	
Quercetin	Soluble frac.	26.50		**98.75**	*	23.27		-67.36		228.26		5.10	
Quercetin	Bound frac.	-8.57		**-35.99**	*	-0.86		-68.37		52.44		50.41	

4.3.6. Antioxidant activity of spike extracts is affected by the infection

The antioxidant activity of the spikes' extracts (soluble fraction and cell wall bound fraction) was assessed by the DPPH assay. DPPH is based on the reactivity of 2,2-diphenyl-1-picrylhydrazyl, a free radical, which shows hydrogen acceptor ability towards antioxidants (Kurechi et al. 1980). At the early infection stage all the soluble extracts exhibited a DPPH radical scavenging activity ranging from 5% to 20% (Fig. 4.4 a-b-c-d), highlighting that the infection did not have any

significant effect on antioxidant activity (Fig. 4.4a). On the other hand, at 21 DPI, the DPPH radical scavenging activity of soluble fraction varied from 5% to 45% with the infection resulting in a notable increase in % DPPH inhibition across all genotypes (Fig. 4.4b). The infected spikes of pigmented genotype had the highest % inhibition of DPPH. Regarding the DPPH radical scavenging activities of the cell wall bound fraction, at 2 DPI, the infection led to an increase in the antioxidant activity in DBC-480 and Purple durum spikes' extracts (Fig. 4.4c). However, at 21 DPI, the antioxidant activity increased only in the infected resistant genotype (Fig. 4.4d).

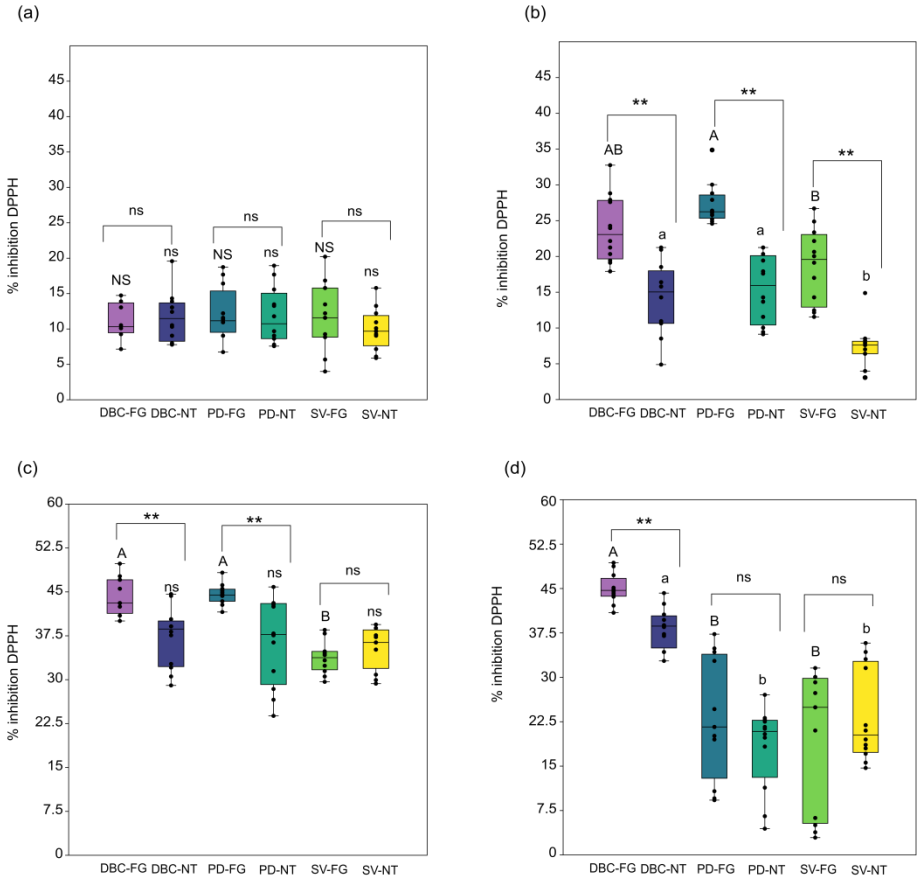

Fig. 4.4: DPPH scavenging activity of plant extracts, related to: (a) soluble fraction at 2 DPI; (b) soluble fraction at 21 DPI; (c) cell wall bound fraction at 2 DPI; (d) cell wall bound fraction at 21 DPI. Data were analyzed by Kruskal-Wallis test. Different letters indicate differences for $p < 0.05$ according to the Dunn's test. Upper case letters refer to statistical analysis of DPPH scavenging in infected plant while lower case letters refer statistical analysis of DPPH scavenging in mock treated plants. Statistical analysis between FG-infected spikes and mock treated ones (here indicated as "nt") were computed and the symbol "**" indicate significant differences at $p < 0.01$. "NS" or "ns" mean not significant difference.

4.3.7. Phenolic acids determine the antioxidant activity in soluble fraction but not in the cell wall bound fraction

A linear correlation (Sperman'*rs*) was computed in order to understand if antioxidant activity is more related to phenolic acids (PA), flavonoids (F) or to the total amount of the analyzed phenylpropanoids (PA+F). Data of %

inhibition DPPH, analyzed phenolic acid (PA, sum of the concentration of caffeic acid, ferulic acid, gallic acid, *p*-coumaric acid, syringic acid and vanillic acid), analyzed flavonoids (F, sum of the concentration of 4-methoxyflavone, chlorogenic acid, cyanidin 3-6" malonylglucoside, cyanidol 3-glucoside, delphinin 3-glucoside, kaempferol, oenin, quercetin) and the total amount of analyzed phenylpropanoids (PA+F) were used to run the linear correlation (Table 4.2 and Table 4.3). As displayed in Table 4.2, in the spikes' soluble fraction the DPPH scavenging activity correlates with phenolic acid content (*rs* = 0.5562) and total phenylpropanoids (*rs* = 0.6216). In the cell wall bound fraction (Table 4.3), total phenylpropanoids (PA+F) are strongly correlated with PA (*rs* = 0.9997), and there is no significant correlation between DPPH and phenylpropanoid composition.

Table 4.2: Sperman'*rs* coefficient related to soluble fraction. The symbol "**" indicate significant differences at $p < 0.01$.

SOLUBLE	Phenolic acids (PA)	Flavonoids (F)	Phenylpropanoids (PA+F)	% Inhibition DPPH
Phenolic acids (PA)	1			
Flavonoids (F)	0.16371	1		
Phenylpropanoids (PA+F)	0.78919**	0.5184**	1	
% Inhibition DPPH	0.5562**	0.11401	0.62161**	1

Table 4.3: Sperman'*rs* coefficient related to cell wall bound fraction. The symbol "**" indicate significant differences at $p < 0.01$.

BOUND	Phenolic acids (PA)	Flavonoids (F)	Phenylpropanoids (PA+F)	% Inhibition DPPH
Phenolic acids (PA)	1			
Flavonoids (F)	0.26847	1		
Phenylpropanoids (PA+F)	0.99974**	0.27284	1	
% Inhibition DPPH	0.30068	-0.4034	0.29811	1

4.4. Discussion

Phenylpropanoids have several biochemical properties, but probably the most relevant feature is their antioxidant activity, which means their ability to inhibit (reduce) all molecules having high Ox/Red potential (Brainina et al. 2019). Our results showed that the *F. graminearum* infection influenced DPPH scavenging activity of spikes and grains (Fig. 4.3 and Fig 4.4), and it could be influenced by phenolic acids or by flavonoids in the soluble fraction, while the considered metabolites did not explain the antioxidant activity in the cell wall bound fraction. In accordance with Wiwart et al. (2024), our results suggest that in durum wheat grains antioxidant activity is a complex trait which may depend on the concurrent accumulation of different groups of metabolites, rather than a single one or a single class. To understand the influence of *F. graminearum* infection on the phenylpropanoid pathway at early (2 DPI) and late (21 DPI) infection stage, in this study 14 key metabolites (hydroxybenzoic acids, hydroxycinnamic acids and flavonoids) were quantified by HPLC-MS/MS and, at the same time, the expression of structural genes encoding PAL, C4H, CHS, F3H, DFR, and COMT, and the transcription factor Ppm1 were analyzed in durum wheat spikes using qRT-PCR, considering three genotypes differing in FHB resistance and grains pigmentation. Results are summarized in Fig. 4.5.

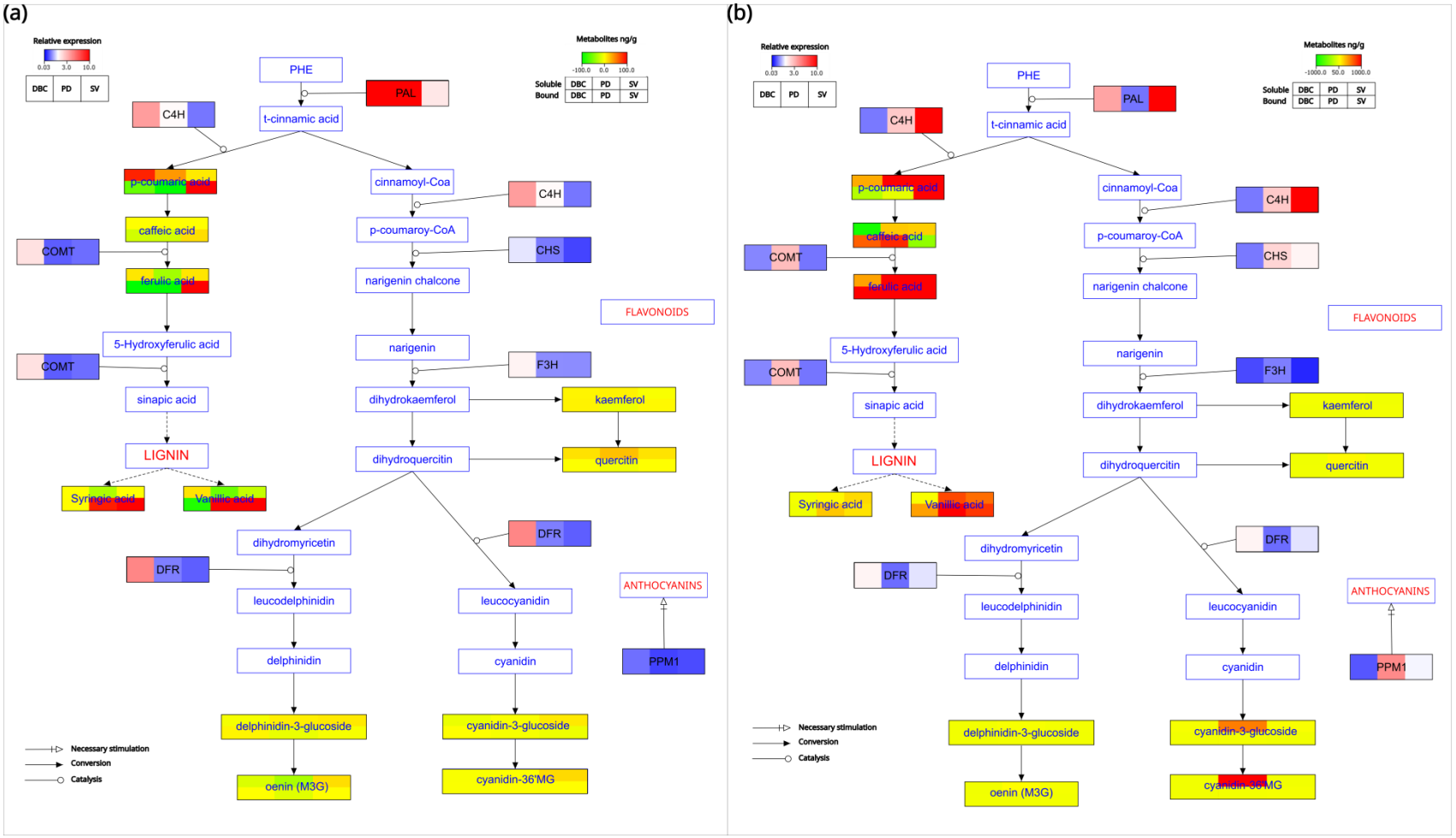

Fig. 4.5: Simplified phenylpropanoids pathway, indicating (by heatmaps) the metabolites increase or reduction due to infection and the relative expression of the coding genes or transcription factor analyzed in this study and presented in Fig. 4.2 and Table 4.1. Only the more interesting metabolites are displayed. Left pathway (a) refer to early infection stage, while right pathway (b) is related to late infection stage. PHE = phenylalanine; PAL = phenylalanine ammonia lyase; C4H = cinnamate 4-hydroxilase; COMT = Caffeic acid O-methyltransferase; CHS = chalcone synthase; F3H = flavone 3-hydroxylase; DFR = dihydroflavonol reductase; Ppm1 = Purple pericarp MYB1; M3G = malvidin 3-*O*-glucoside; DBC = DBC-480; PD = purple durum; SV = Svevo.

The starting point of the pathway is the conversion of phenylalanine into *t*-cinnamic acid through PAL enzyme (Fig. 4.5). According to our results, at the early infection stage, *PAL* is upregulated in all considered genotypes, with a notable boost in DBC-480, which harbors the QTL *Fhb1* from Sumai3, conferring Type II resistance (resistance to spread along the spike) (Prat et al. 2017). These findings are consistent with several other studies. Indeed, *PAL* up-regulation induced by *F. graminearum* has been previously reported in Type II resistant cv. Sumai3 (Golkari et al. 2007) and derived line CM82036 in association with the 3BS QTL (Steiner et al. 2009) or other QTLs (Kage et al. 2018; Dhokane et al. 2016). Moreover, different studies suggested that plants synthesize salicylic acid, from cinnamate produced by PAL (Huang et al. 2010), activating the systemic acquired resistance (SAR) (Zhong et al. 2021; Sorahinobar et al. 2016; Francesconi et al. 2020). Notably, the differential expression of *PAL* firstly occurs before 2 DPI (Wu et al. 2022). The strong activation of *PAL* and *C4H* genes in the late infection stage (21 DPI) in Svevo is interesting. Other authors (Li et al. 2020b) found that, in bread wheat subjected to abiotic stress (drought stress), the expression of *PAL*, *C4H*, and *4CL* genes reached a high level between 15 DAA (day post anthesis) and 25 DAA. The upregulation of *PAL* and *C4H* during fungal infection at 21 DPI may suggest a late activation of phenylpropanoid pathway in the susceptible genotypes, insufficient to counteract *F. graminearum* action. C4H (cinnamate-4-hydroxylase) is a class II monooxygenase, which hydroxylates cinnamic acid to produce *p*-coumaric acid (Zhang et al. 2020). *p*-Coumaric acid serves as a precursor of a myriad of organic compounds essential for plant metabolism, structure, development, and defense, including stilbenes, chalcones, flavonoids, hydroxycinnamates, and lignin (Zhang et al. 2020). Together with ferulic acid, *p*-coumaric acid is an essential component of commelinid monocots secondary cell wall, where these two hydroxycinnamic acids are esterified with arabinoxylans, forming a complex matrix of various polysaccharides, proteins and lignin (Saulnier et al. 2012). The plant cell wall is one of the constitutive barriers that pathogens need to overcome to colonize plant tissues (Miedes et al. 2014). Indeed, in this study, the cell wall bound phenylpropanoid fraction from wheat spikes was mainly represented by ferulic acid and *p*-coumaric acid (Fig. 4.2c-d), but their concentration remained invariable between infected and mock treated plants at both time points and in all considered genotypes. This is in agreement with other studies that identified ferulic acid and *p*-coumaric acid as constitutive resistant related compounds (Gunnaiah and Kushalappa 2014; Bollina et al. 2011). This means that they are related to resistance (due to their involvement in cell wall thickening), but are not induced by the infection. Nevertheless, according to our results obtained at the late time point (21 DPI), there is an increase in the soluble fraction of ferulic acid, *p*-coumaric acid and vanillic acid in all the considered genotypes. These findings may suggest that the increase of these phenolic compounds is the result of a catabolic process rather than a metabolic one. Indeed, during the infection, *Fusarium* spp. produced different cell wall degrading enzymes (CWDEs) to overcome the cell wall barrier, especially pectin degrading enzymes, such as xylanases (Kikot et al. 2009; Mandalà et al. 2021). Xylanases may degrade the link between arabinoxylans and phenolic acids, resulting in their release into the soluble fraction (Moreira and Filho 2016). Another important constituent of secondary cell wall is lignin. Lignin is a polymerized network of cinnamyl alcohols in plant cell walls that forms a network with the hemicelluloses, surrounding the cellulose microfibrils. Lignin biosynthesis occurs through the action of different enzymes (Goujon et al. 2003). Among them, *COMT* (Caffeic acid O-methyltransferase) resulted upregulated in the present study in the resistant genotype at the early infection stage. This is in agreement with other studies, where early *COMT* overexpression increased biotic and abiotic stress tolerance (Bhuiyan et al. 2007; Yang et al. 2019; Gunnaiah et al. 2012). On the other hand, the differential expression of *COMT* at the late infection stage was not statistically different among the genotypes, and vanillic acid, a lignin-derived monomer, increased into the soluble fraction in all the genotypes. These results may indicate a late microbial depolymerization of lignin (Wang et al. 2018).

A second branch of the phenylpropanoids pathway leads to the biosynthesis of flavonoids (Fig. 4.5). Among the key enzymes involved in the flavonoids biosynthetic pathway, there are chalcone synthase (CHS), flavone 3-hydroxylase (F3H) and dihydroflavonol reductase (DFR). According to our results, the genotype affects the differential expression of *CHS* at both considered time points. At the early time point, *CHS* was upregulated in DBC-480 compared to Svevo, while the opposite occurred at the late time point, when it was particularly upregulated in Purple durum too. These results corroborate the outcomes of different authors who found that chalcone synthase family genes regulate the early response (1-4 DPI) against fungal pathogens (Li et al. 2023c; Ahmad et al. 2023). Li et al. (2020b) found a late upregulation of *CHS* in wheat spikes (15-20 DPI) under drought stress, but few authors analyzed the role of *CHS* gene family in response to stress at late stage, so far. While *CHS* seams to play a crucial role in stress response, *F3H* appears less insightful. In this study, at the early time point, *F3H* is upregulated in DBC-480, similar to the other considered genes, while at the late infection stage, it is downregulated in Svevo and DBC-480 and upregulated in Purple durum, but the effect of the genotype was not significant in both time points. Consistently with these findings, other authors found that *F3H* is downregulated in bread wheat under abiotic stresses, both at early (3-6 DAA) and late (20-25 DAA) time points (Li et al. 2023a; Li et al. 2020b). The current investigation also found that there was a slight increase in quercetin accumulation in the soluble fraction of Purple durum spikes and a slight reduction of quercetin in cell wall bound fraction. Quercetin in wheat could be present in both the soluble fraction and bound to the cell wall, where its glycosylated forms are recognized as a constitutive resistance related metabolite against FHB (Gunnaiah and Kushalappa 2014). Quercetin is known for its antifungal activity (Lalak-Kańczugowska et al. 2023) and recently it was employed as a synthetic elicitor to stimulate tomato response against Fusarium wilt (Hassan et al. 2023). The fact that the increase of quercetin in the soluble fraction occurs only in the pigmented genotype may be related to a slight early activation of flavonoids biosynthetic pathway, most likely related to the regulation of other genes not included in this study (such as chalcone isomerase, *CHI*, or flavonol synthase, *FLS*). The flavonoid pathway eventually continues through the biosynthesis of anthocyanins (Li and Ahammed 2023). The synthesis of these water-soluble plant pigments starts with the reduction of dihydroflavanols to leucoanthocyanins by dihydroflavonol reductase (DFR). In this study, *DFR* was boosted in the resistant genotype at the early infection stage, while, in other studies, bread wheat under abiotic stresses showed a constitutive expression of this gene (Li et al. 2020b; Li et al. 2023a). The presence of anthocyanins in the yellow-pigmented genotype Svevo may appear surprising. Nevertheless, other authors have already identified cyanidin3-*O*-glucoside and anthocyanidin in soluble and bound extracts of durum wheat Svevo grains (Dinelli et al. 2009). The slight increase of cyanidin 3-(6" malonylglucoside) in Svevo after 2 days post infection can hardly be related to the regulation of *DFR* (which had basal expression in Svevo in this study) and it is most likely related to the regulation of other genes not included in this study. At the late infection stage, *DFR* is up-regulated in DBC-480 and Svevo and slightly upregulated in Purple durum, but the effect of the genotype was not meaningful. This finding is partially in contrast with Li et al. (2020a) who found that the structural and regulatory genes involved in anthocyanin biosynthesis in a purple bread wheat cultivar under drought stress (15 DAA and 24h post-stress induction) were downregulated, except for *TaDFR* that was upregulated (Li et al. 2020a). Interestingly, in this study, at the late infection stage, the transcription factor *Ppm1* was boosted in the pigmented genotype due to *F. graminearum* infection. The anthocyanin biosynthesis pathway is regulated by the MYB-bHLH-WD40 ternary complex (MBW) (Patra et al. 2013; Li and Ahammed 2023). Jiang et al. (2018) revealed that in bread wheat, the transcription factors MYB, located in the chromosome 7D (TaPpm1; 7D), and MYC, located in the chromosome 2A (TaPpb1; 2A), co-regulate anthocyanin production in the purple pericarp. Sharma et al. (2022) showed that pericarp-associated grain color is linked to abiotic stresses like temperature, drought, and UV irradiation. Li et al. (2020a) found that drought stress upregulates TaMYB-

4B1 at 15 DAA and 24h post-stress induction. To the best of our knowledge, this is the first report of a differential expression of *Ppm1* influenced by biotic stress in durum wheat. In the present study, we observed in Purple durum an increase in the soluble fraction at 21 DPI of cyanidin 3-(6" malonylglucoside), cyanidin 3-glucoside and oenin (malvidin 3-*O*-glucoside), but only differences related to the latter one were statistically significant. This discrepancy may be due to the infection which, at the late stage, can widely compromise the spikes leading to a high variability in their composition and a strong degradation of some compounds, as the anthocyanins (Enaru et al. 2021). Moreover, *Ppm1* is grain-specific (Jiang et al. 2018), but Purple durum can accumulate pigments in other parts of the spike, like the glumes (Supplementary material S4.3) and in the present study the whole spike was considered. Thus, *Ppm1* may not explain the whole variability in anthocyanins accumulation of the samples.

4.5. Supplementary materials:

4.5.1. **Supplementary file 4.1**: Primer pairs used in this study, qPCR melting curves and qPCR amplification curves

Table S4.1.1: Primer pairs used in this study. "*" means that accession number refer to NCBI database, while "**" indicate an Ensembl Plants accession number.

Gene and Accession number	Function	Primer Forward (5'-3')	Primer Revers (5'-3')	bp (DNA)	bp (cDNA)	Temp. Annealing °C	Reference
PAL X99705*	Phenylalanine ammonia lyase	CGATGCTCGTCCGAGTCAAT	CATGACCTCACAGAAGACGC	407	407	60	Francesconi and Balestra 2020
C4H TRITD3Av1G210690.3 **	Cinnamate-4-hydroxylase	CGCAACGTGGTGTTCGACAT	GGTGAAGAAGGGCACGGTCA	111	111	62	This study
COMT TRITD3Bv1G281330.3 **	Caffeic acid O-methyltransferase	ATGTCGGCGTTCGAGTACCA	GATGCCCTTGATGGTGGGGT	207	207	60	This study
CHS TRITD2Av1G006550.3 **	Chalcone synthase	GAGGACGCCTTCAAGCCATTG	GCGCATCCGTTCCTTGTTCA	126	126	60	This study
DFR AB276091.1*	Dihydroflavonol-4-reductase	CGTCGGGTTTCGTAGGGT	CCAGCAACGGCTTGTTCTTC	191	109	62	Ma et al. 2014 modified
F3H TRITD2Av1G269090.1 **	Flavanone 3-hydroxylase	CGAGCGACTCATGGGACTGT	CCAGCAACGGCTTGTTCTTC	103	103	59	This study
Ppm1 MG066451.1*	Trascription factor – Purple pericarp MYB 1	AGCTCATCGTCAGGCTCCAC	CCGAGCGTGCTGTTCCAGTA	122	122	59	This study
TaACT AB181991*	Actin	TCCTGTGTTGCTGACTGAGG	GGTCCAAACGAAGGATAGCA	350	236	61	Tundo et al. 2016
TaTUB TAU76745*	b-tubulin	CGAGGAGGGCGAGTACGA	AGCAAAGCACGACATGGACAT	79	79	61	Tenea et al. 2011
TaFNR AJ457980*	Ferredoxin-NADP(H)-oxidoreductase	CACCGGCCCAGTGATCTT	AAGGGCGTCTGCTCCAACT	259	69	61	Tenea et al. 2011

Melt curves and amplification curves of samples harvested at 21 DPI:

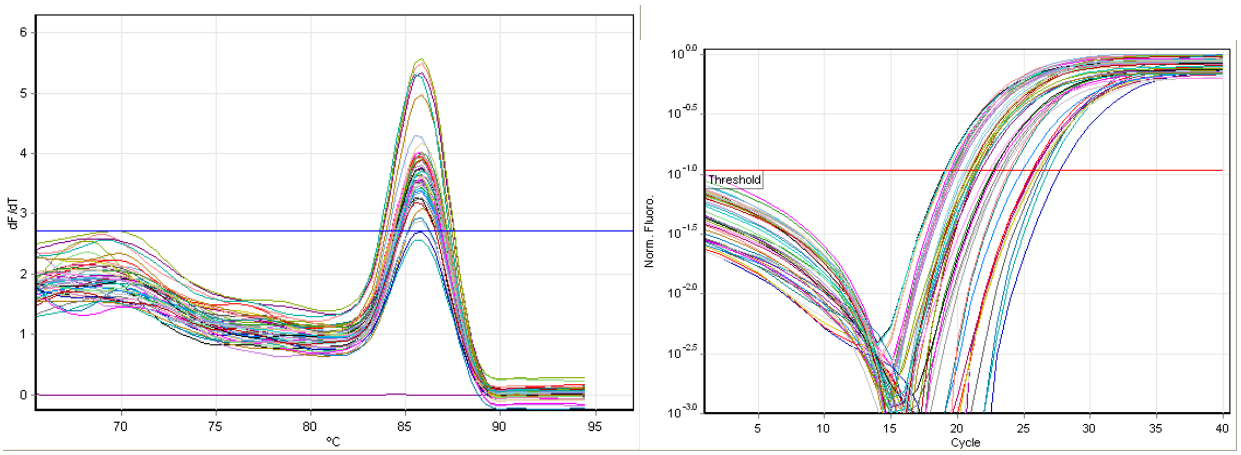

Fig. S4.1.1 (left) Melt curve *ACT*; (right) amplification curves *ACT*

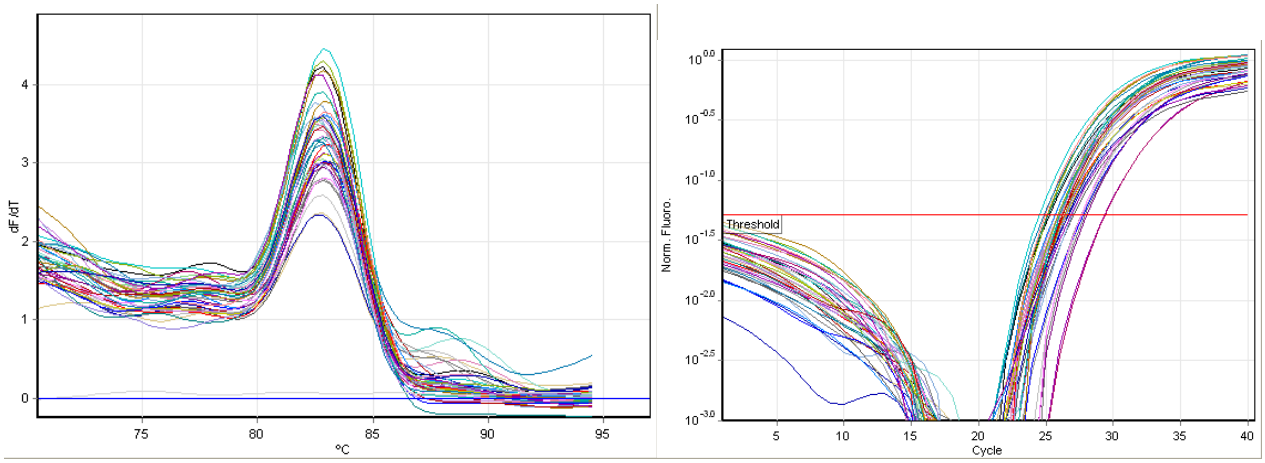

Fig. S4.1.2 (left) Melt curve *TUB*; (right) amplification curves *TUB*

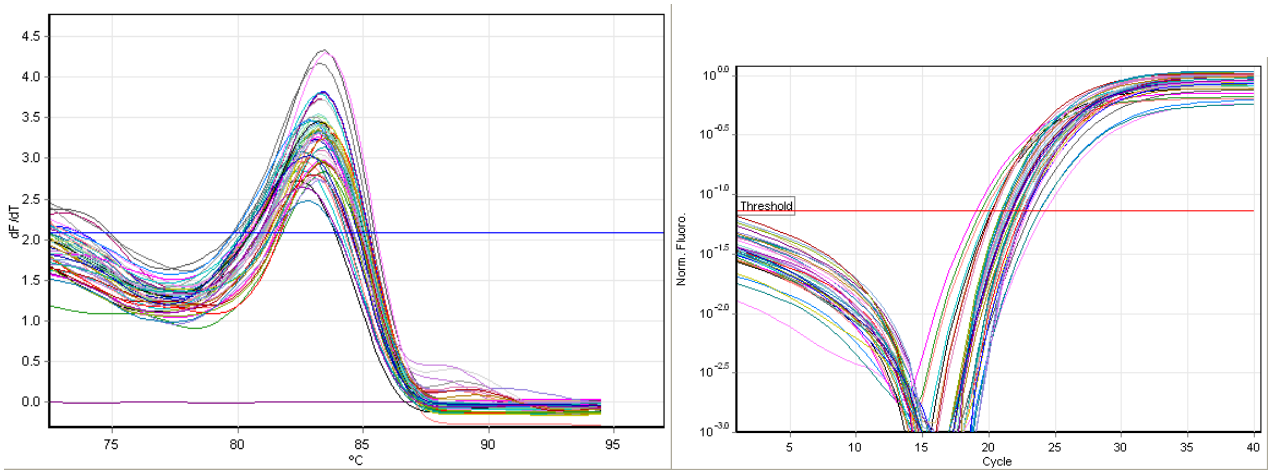

Fig. S4.1.3 (left) Melt curve *FNR*; (right) amplification curves *FNR*

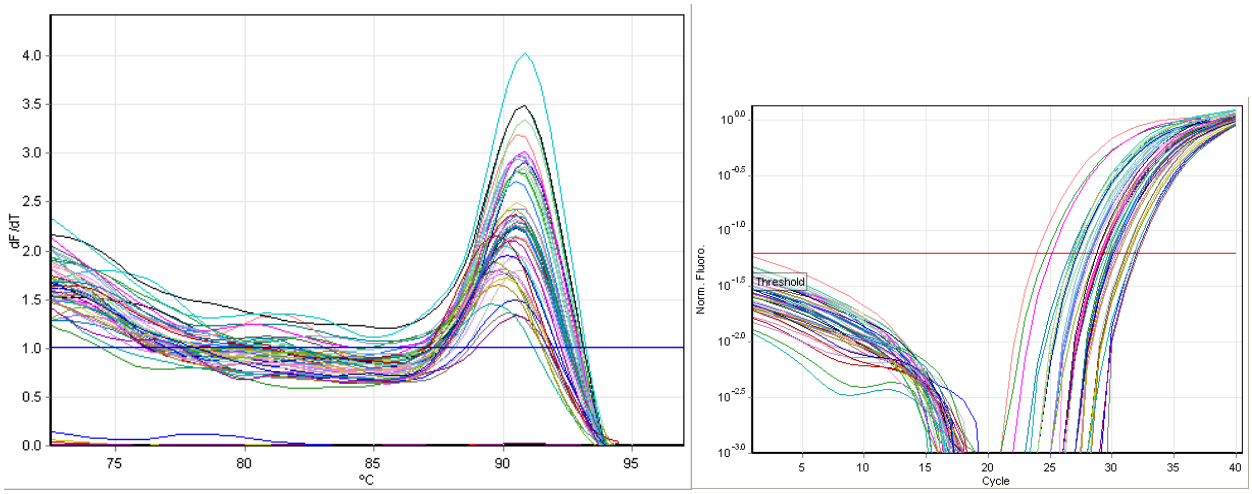

Fig. S4.1.4 (left) Melt curve *PAL*; (right) amplification curves *PAL*

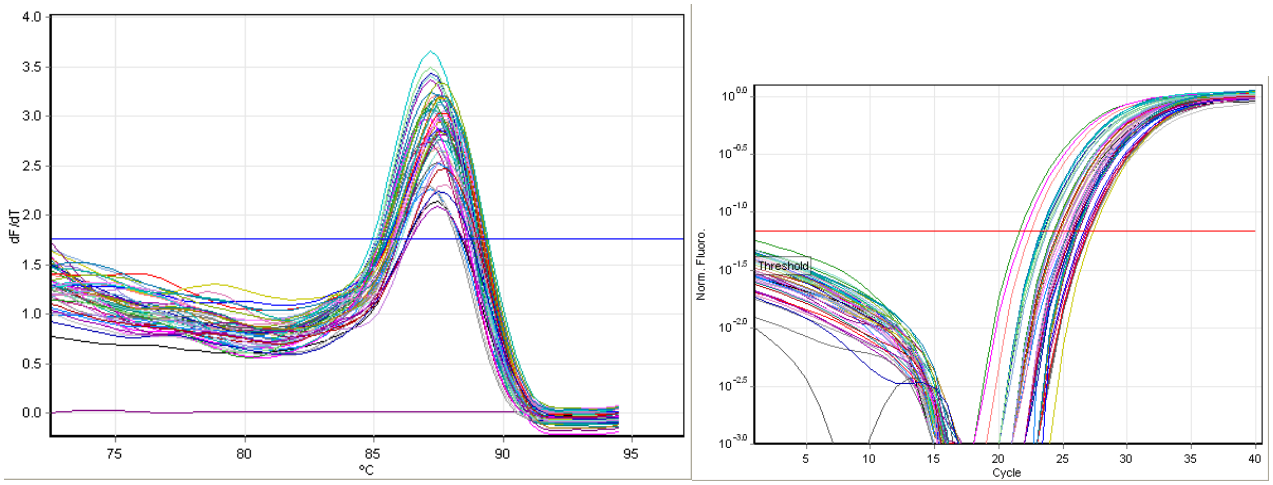

Fig. S4.1.5 (left) Melt curve *C4H*; (right) amplification curves *C4H*

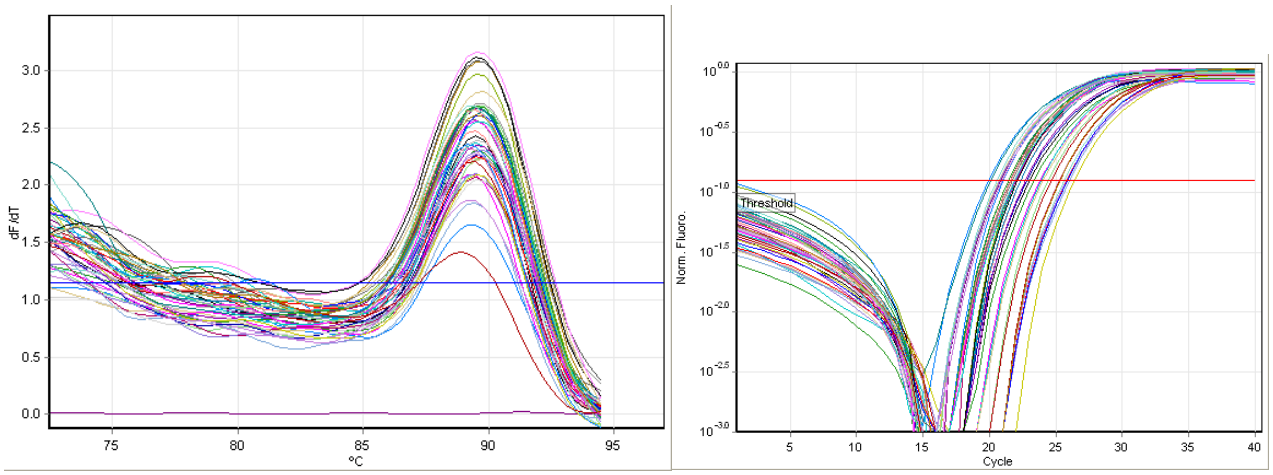

Fig. S4.1.6 (left) Melt curve *COMT*; (right) amplification curves *COMT*

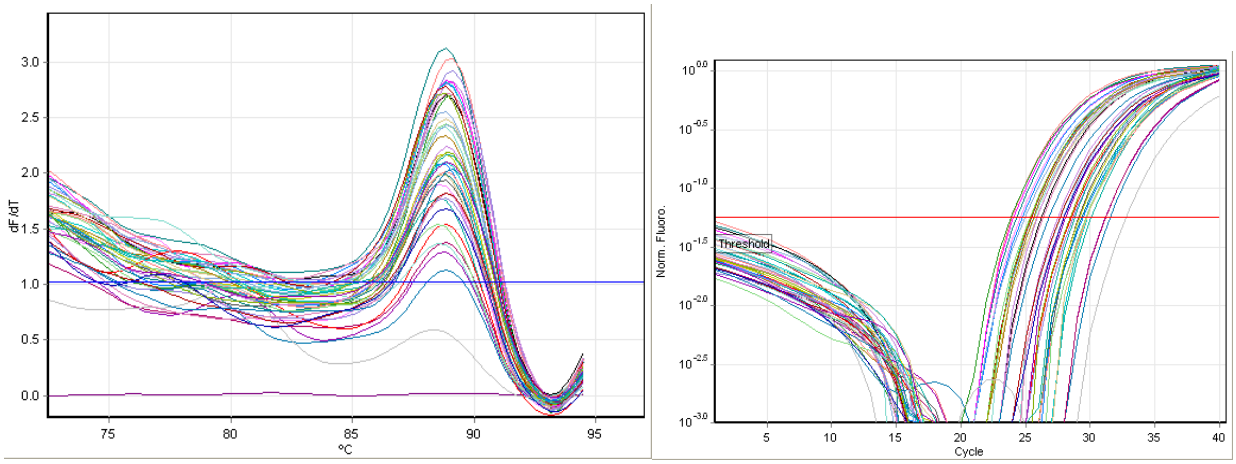

Fig. S4.1.7 (left) Melt curve *DFR*; (right) amplification curves *DFR*

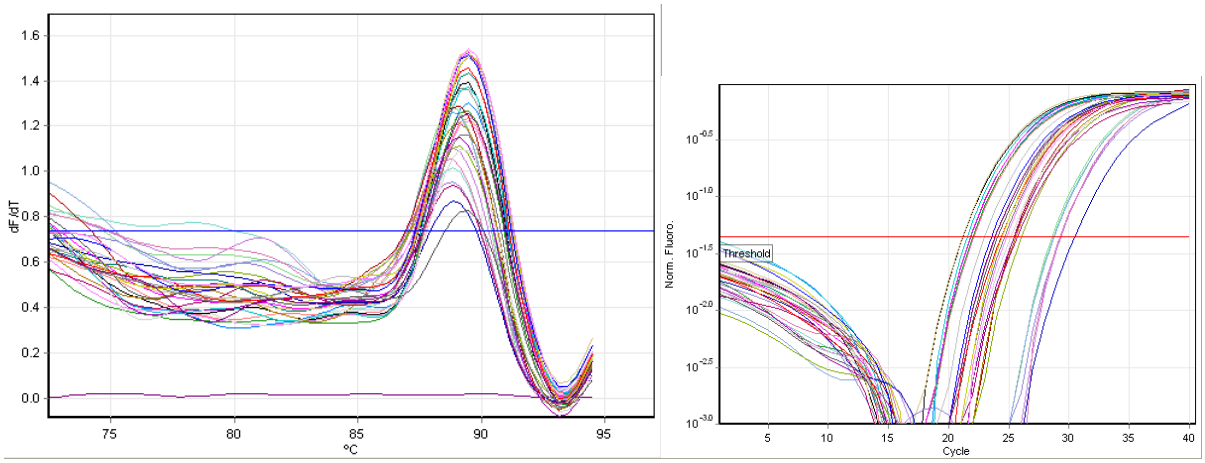

Fig. S4.1.8 (left) Melt curve *F3H*; (right) amplification curves *F3H*

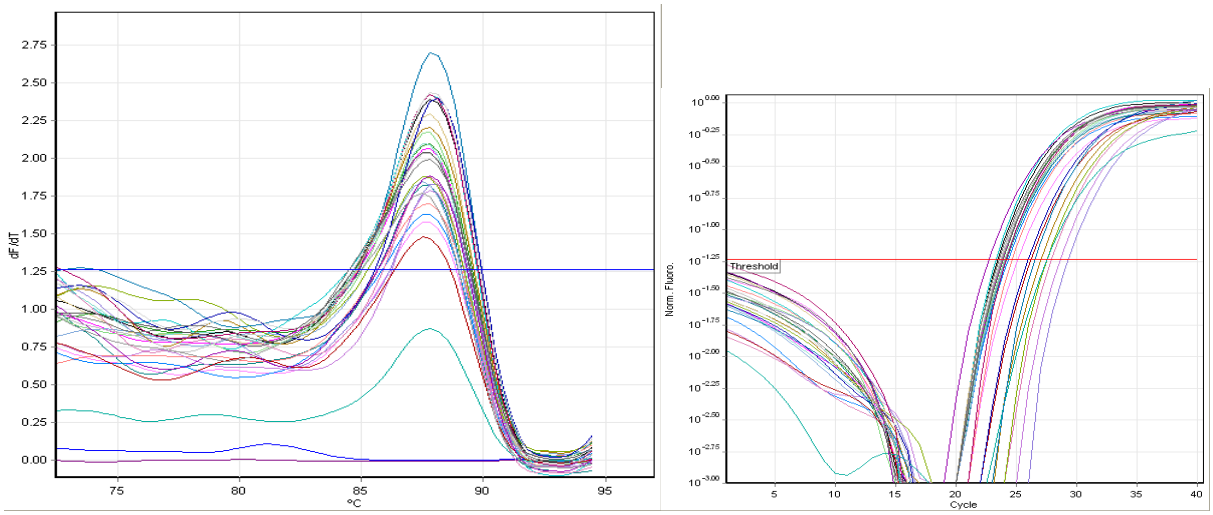

Fig. S4.1.9 (left) Melt curve *PPM1*; (right) amplification curves *PPM1*

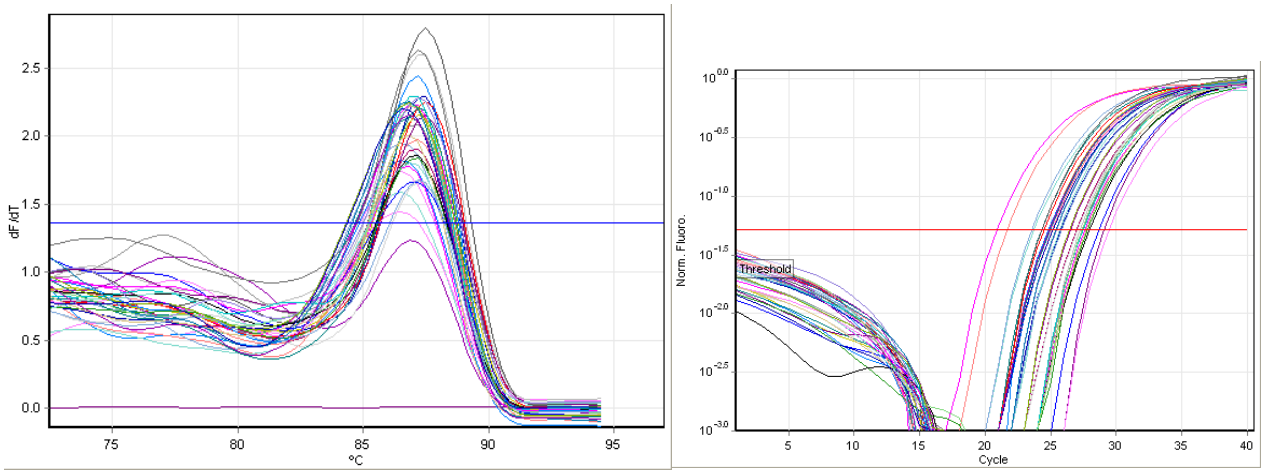

Fig. S4.1.10 (left) Melt curve *CHS*; (right) amplification curves *CHS*

4.5.2. **Supplementary file 4.2**: HPLC MS/MS methods

LC-MS/MS determination of phenolic acids

Chromatographic separation of phenolic acids was performed using an Acclaim Carbonyl C18 RSLC column (150 x 3 mm, 3 µm, Thermo Scientific, USA). Chromatography was performed using H_2O + 0.5% of acetic acid (A) and Acetonitrile (B) at a flow rate of 800 µL min^{-1}. Gradient elution started at 0% of B and was raised to 5% in 1 minute, to 13% in 1 minute, to 15% in 4 minutes, and to 21% in 1.50 minutes. After 1 minute in isocratic condition, mobile phase B was raised to 27% in 1 minute, to 50% in 1 minute and equilibrated for 1 minute. The initial conditions were then restored and the system was conditioned for 5 minutes. The column temperature was set at 35 °C, and the injection volume was 8 µL. The retention times (RTs) of the target analytes are reported in Table S4.2.1. Infusion of standard solutions of phenolic acids (10 µg L^{-1}) was performed to establish the best parameters for ionic transmission in mass spectrometry. Analyses were performed in negative MRM mode. Nebulizer, turbo, and curtain gases were respectively set at 30, 55, and 60 psi; the source temperature was set at 500 °C, the declustering and entrance potentials were set at -100 V and -10 V, respectively and the collision cell exit potential was set at -15 V. The optimized parameters for each analyte are reported in Table 4.2.1, together with precursor and product ions.

Table S4.2.1. Retention times (RTs) and optimized spectrometric conditions for each target analyte. The "*" indicates the ion chosen as quantifier.

	RTs (min)	Precursor Ion	Product Ions	Collision Energy (eV)	Collision Cell Exit Potential (V)
Caffeic Acid	8.73	179	135*	-25	-15
			107	-29	
Ferulic Acid	11.35	193	134*	-25	-15
			178	-17	
Gallic Acid	3.94	169	125*	-19	-15
			79	-28	
p-Coumaric Acid	11.54	163	119*	-28	-15
			117	-30	
Syringic Acid	7.77	197	121*	-25	-15
			138	-25	
Vanillic Acid	7.68	167	152*	-14	-15
			108	-26	

LC-MS/MS determination of flavonoids

Chromatographic separation of flavonoids was carried out using an Eclipse XDB-C18 column (2.1 x 150 mm, 3.5 µm, Agilent Technologies, USA). Chromatography was performed using H_2O (A) and methanol (B), both containing 0.5% of formic acid, at a flow rate of 550 µL min−1. Gradient elution started at 5% of B and, after 1 minute in isocratic condition, was raised to 100% in 2 minutes. The initial conditions were then restored, and the system was conditioned for 5 minutes. The column temperature was set at 45 °C, and the injection volume was 5 µL. The retention times (RTs) of the target analytes are reported in Table S4.2.2. Infusion of standard solutions of anthocyanins (10 µg L^{-1}) was performed to establish the best parameters for ionic transmission in mass spectrometry. Analysis was performed both in positive and negative MRM mode. Nebulizer, turbo, and curtain gases were respectively set at 30, 55, and 60 psi and

the source temperature was set at 500 °C. The optimized parameters for each analyte are reported in Table S4.2.2, together with precursor and product ions.

Table S4.2.2. Retention times (RTs) and optimized spectrometric conditions for each target analyte. The "*" indicates the ion that was chosen as quantifier.

	RTs (min)	Precursor Ion	Product Ions	Declustering Potential (V)	Entrance Potential (V)	Collision Energy (eV)	Collision Cell Exit Potential (V)
Chlorogenic Acid	2.79	353	191*	-50	-10	-24	-15
			161			-27	
Oenin Chloride	2.86	491	329*	-80	-10	-24	-15
			343			-29	
Kaempferol	3.32	285	93*	-80	-10	-39	-15
			117			-51	
Delphinin 3-glucoside	2.74	463	301*	-80	-10	-27	-15
			300			-32	
Cyanidol 3-glucoside	2.79	447	285*	-80	-10	-29	-15
			125			-25	
Quercetin	3.20	301	151*	-80	-10	-27	-15
			179			-25	
4-Methoxyflavone	3.68	253	210*	80	10	42	15
			238			33	
Cyanidin 3-(6"-malonylglucoside)	2.88	535	287*	80	10	30	15
			449			30	

4.5.3.**Supplementary file 4.3**: Spikes and grains morphology and appearance

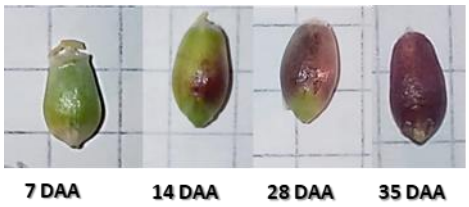

Fig. S4.3.1: Color development in Purple durum grains. Square dimension 0.5 cmx 0.5 cm.

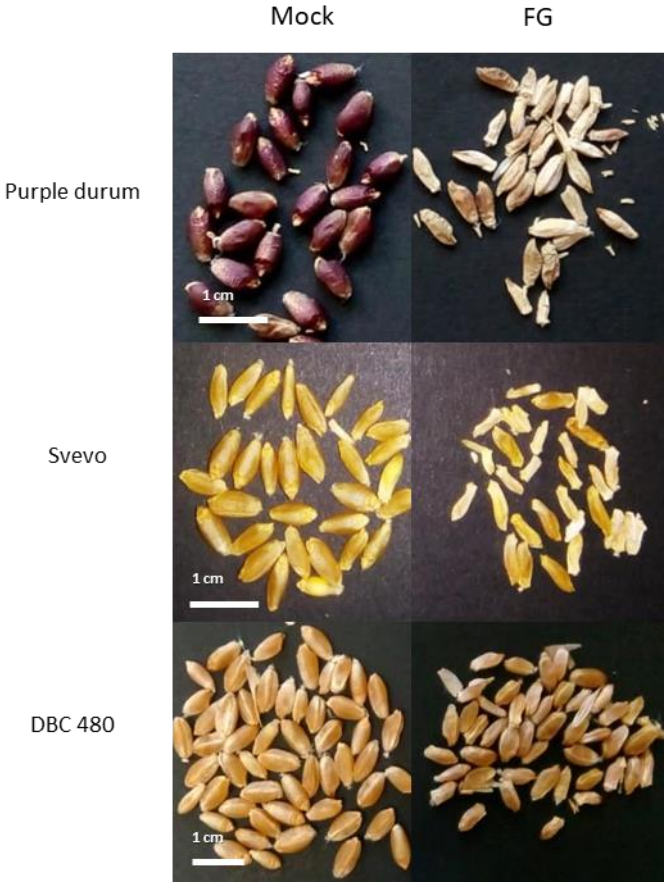

Fig. S4.3.2: Kernels morphology at maturity stage: grains from mock plant shown a normal shape, color and dimension, while kernels from infected plants (FG) were mostly damaged.

Fig. S4.3.3: Purple durum healthy spike at 30 DAA showing glumes pigmentation.

4.5.4. **Supplementary file 4.4**: Metabolites quantifications and PERMANOVA tables

Table S4.4.1: Quantification of selected metabolites. Data are expressed as ng g^{-1}. DBC=DBC-480; PD= Purple durum; SV=Svevo; nd= not detected; <LOQ = under limit of quantification.

		DBC-FG-2 DPI	DBC-NT-2 DPI	PD-FG-2 DPI	PD-NT-2 DPI	SV-FG-2 DPI	SV-NT-2 DPI	DBC-FG-21 DPI	DBC-NT-21 DPI	PD-FG-21 DPI	PD-NT-21 DPI	SV-FG-21 DPI	SV-NT-21 DPI
Caffeic Acid	**Soluble frac.**	< LOQ	< LOQ	< LOQ	< LOQ	< LOQ	< LOQ	8.95	9.06	29.02	0.00	35.60	8.74
	Bound frac.	125.61	143.64	106.45	124.47	115.82	103.15	161.34	95.21	104.37	18.97	47.41	42.15
Ferulic Acid	**Soluble frac.**	86.50	77.36	87.71	123.60	75.01	65.51	159.68	117.53	1018.69	152.13	1188.45	121.23
	Bound frac.	10976.09	12523.87	11112.99	15319.56	10570.25	10117.50	9544.25	8882.06	10874.86	8260.83	10605.00	8339.25
Gallic Acid	**Soluble frac.**	nd	nd	nd	nd	< LOQ	< LOQ	< LOQ	50.05	19.83	nd	46.40	nd
	Bound frac.	nd	nd	nd	nd	nd	nd	nd	nd	nd	nd	nd	nd
p-Coumaric Acid	**Soluble frac.**	415.34	329.02	427.16	387.12	372.37	364.42	550.55	190.08	3822.30	293.48	4663.49	166.15
	Bound frac.	5123.96	5183.19	4968.84	6311.00	4800.24	4172.45	3518.45	3775.62	6215.73	6263.27	5499.70	3683.96
Syringic Acid	**Soluble frac.**	<LOQ	<LOQ	10.11	41.59	<LOQ	<LOQ	8.58	<LOQ	92.25	18.30	186.86	<LOQ
	Bound frac.	555.21	554.45	539.49	450.73	578.08	397.51	826.71	838.18	439.06	182.70	462.88	311.90
Vanillic Acid	**Soluble frac.**	77.73	67.16	101.97	159.34	75.20	98.06	90.89	62.72	829.53	101.12	650.10	58.10
	Bound frac.	1529.25	1616.36	1585.83	1268.33	1417.38	1071.23	1963.54	1559.75	1435.57	430.94	1551.18	750.54
4-Methoxyflavone	**Soluble frac.**	6.62	8.01	2.25	8.54	7.64	7.19	2.36	1.98	11.77	8.02	8.13	6.87
	Bound frac.	3.35	4.12	3.73	6.05	3.92	3.73	3.06	3.15	6.08	4.23	5.45	3.50
Chlorogenic Acid	**Soluble frac.**	11.46	8.23	11.28	10.64	7.88	9.20	2.46	9.95	2.30	1.27	5.38	6.81
	Bound frac.	3.97	4.52	4.24	8.06	4.83	5.50	3.48	4.88	4.68	5.99	7.74	5.69
Cyanidin 3-(6" malonylglucoside)	**Soluble frac.**	17.11	19.20	26.75	27.17	19.96	5.66	9.04	9.63	1872.88	586.17	8.87	10.48
	Bound frac.	7.70	9.37	2.76	2.86	5.70	5.51	4.82	4.66	9.82	6.78	9.32	nd
Cyanidol 3-glucoside	**Soluble frac.**	31.06	38.63	10.29	12.53	16.38	8.13	19.59	6.37	670.92	138.31	33.65	6.83
	Bound frac.	3.68	3.98	nd	3.44	nd	6.82	nd	nd	11.39	8.12	nd	7.07
Delphinin 3-glucoside	**Soluble frac.**	18.78	22.53	14.86	8.80	21.03	12.73	5.32	6.00	33.97	15.19	6.58	5.91
	Bound frac.	3.53	nd	3.44	11.34	3.59	6.36	nd	2.76	5.91	2.83	nd	2.82
Kaempferol	**Soluble frac.**	20.65	16.92	4.86	nd	10.51	12.76	7.06	nd	9.73	3.94	nd	4.78
	Bound frac.	4.40	nd	2.77	8.67	7.52	5.24	4.06	6.70	9.32	9.88	9.55	7.37
Oenin Chloride	**Soluble frac.**	73.31	87.21	59.05	92.19	56.85	44.17	31.08	36.76	112.59	61.27	48.10	38.55
	Bound frac.	nd	nd	nd	11.87	3.68	3.53	nd	nd	5.50	5.45	3.07	nd
Quercetin	**Soluble frac.**	53.99	42.68	49.70	25.01	57.56	46.70	4.47	13.71	94.43	28.77	32.93	31.33
	Bound frac.	7.76	8.48	7.69	12.02	7.58	7.64	1.90	6.01	11.41	7.49	9.46	6.29

Table S4.4.2: Two-way PERMANOVA table (Permutation N: 9999) at 2 DPI, soluble fraction

Source	Sum of sqrs	df	Mean square	F	*p*
Genotype	0.077	2	0.038	30,255	0.004
Infection	0.014	1	0.014	11,164	0.374
Interaction	0.026	2	0.013	10,167	0.430
Residual	0.152	12	0.013		
Total	0.268	17			

Table S4.4.3: Two-way PERMANOVA table (Permutation N: 9999) at 21 DPI, soluble fraction

Source	Sum of sqrs	df	Mean square	F	*p*
Genotype	0.798	2	0.399	35.663	0.0073
Infection	0.837	1	0.837	74.783	0.0003
Interaction	0.312	2	0.156	13.926	0.2237
Residual	13.433	12	0.112		
Total	32.907	17			

Table S4.4.4: Two-way PERMANOVA table (Permutation N: 9999) at 2 DPI, cell wall bound fraction

Source	Sum of sqrs	df	Mean square	F	*p*
Genotype	0.030	2	0.015	19.009	0.1203
Infection	0.010	1	0.010	12.597	0.2968
Interaction	0.020	2	0.010	12.793	0.2961
Residual	0.094	12	0.008		
Total	0.154	17			

Table S4.4.5: Two-way PERMANOVA table (Permutation N: 9999) at 21 DPI, cell wall bound fraction

Source	Sum of sqrs	df	Mean square	F	*p*
Genotype	0.186	2	0.093	16.598	0.1593
Infection	0.046	1	0.046	0.819	0.4560
Interaction	0.056	2	0.028	0.503	0.7975
Residual	0.672	12	0.056		
Total	0.961	17			

4.6 References

Abdel-Aal, E.-S. M., and Rabalski, I. (2008). Bioactive Compounds and their Antioxidant Capacity in Selected Primitive and Modern Wheat Species. *The Open Agriculture Journal*, *2*(1), 7–14. https://doi.org/10.2174/1874331500802010007

Ahmad, S., Ali, S., Shah, A. Z., Khan, A., and Faria, S. (2023). Chalcone synthase (CHS) family genes regulate the growth and response of cucumber (Cucumis sativus L.) to Botrytis cinerea and abiotic stresses. *Plant Stress*, *8*(April), 100159. https://doi.org/10.1016/j.stress.2023.100159

Belščak-Cvitanović, A., Durgo, K., Huđek, A., Bačun-Družina, V., and Komes, D. (2018). Overview of polyphenols and their properties. In C. M. B. T.-P. P. Galanakis Recovery, and Applications (Ed.), *Polyphenols: Properties, Recovery, and Applications* (pp. 3–44). Woodhead Publishing. https://doi.org/10.1016/B978-0-12-813572-3.00001-4

Bhuiyan, N. H., Liu, W., Liu, G., Selvaraj, G., Wei, Y., and King, J. (2007). Transcriptional regulation of genes involved in the pathways of biosynthesis and supply of methyl units in response to powdery mildew attack and abiotic stresses in wheat. *Plant Molecular Biology*, *64*(3), 305–318. https://doi.org/10.1007/s11103-007-9155-x

Böhmdorfer, S., Oberlerchner, J. T., Fuchs, C., Rosenau, T., and Grausgruber, H. (2018). Profiling and quantification of grain anthocyanins in purple pericarp×blue aleurone wheat crosses by high-performance thin-layer chromatography and densitometry. *Plant Methods*, *14*(1), 1–16. https://doi.org/10.1186/s13007-018-0296-5

Bollina, V., Kushalappa, A. C., Choo, T. M., Dion, Y., and Rioux, S. (2011). Identification of metabolites related to mechanisms of resistance in barley against *Fusarium graminearum*, based on mass spectrometry. *Plant Molecular Biology*, *77*(4–5), 355–370. https://doi.org/10.1007/s11103-011-9815-8

Boukid, F. (2021). Cereal-Derived Foodstuffs from North African-Mediterranean: From Tradition to Innovation. In F. Boukid (Ed.), *Cereal-Based Foodstuffs: The Backbone of Mediterranean Cuisine* (pp. 117–150). Springer International Publishing. https://doi.org/10.1007/978-3-030-69228-5_5

Brainina, K., Stozhko, N., and Vidrevich, M. (2019). Antioxidants: Terminology, Methods, and Future Considerations. *Antioxidants (Basel, Switzerland)*, *8*(8). https://doi.org/10.3390/antiox8080297

Bustin, S. A., Benes, V., Garson, J. A., Hellemans, J., Huggett, J., Kubista, M., Mueller, R., Nolan, T., Pfaffl, M. W., Shipley, G. L., Vandesompele, J., and Wittwer, C. T. (2009). The MIQE guidelines: Minimum information for publication of quantitative real-time PCR experiments. *Clinical Chemistry*, *55*(4), 611–622. https://doi.org/10.1373/clinchem.2008.112797

Chomczynski, P., Wilfinger, W., Kennedy, A., Rymaszewski, M., and Mackey, K. (2010). RNAzol® RT: a new single-step method for isolation of RNA. *Nature Methods*, *7*(12), 4–5. https://doi.org/10.1038/nmeth.f.315

Conte, P., Piga, A., Del Caro, A., Urgeghe, P. P., and Fadda, C. (2021). Italian Dried Pasta: Conventional and Innovative Ingredients and Processing. In F. Boukid (Ed.), *Cereal-Based Foodstuffs: The Backbone of Mediterranean Cuisine* (pp. 89–116). Springer International Publishing. https://doi.org/10.1007/978-3-030-69228-5_4

Cory, H., Passarelli, S., Szeto, J., Tamez, M., and Mattei, J. (2018). The Role of Polyphenols in Human Health and Food Systems: A Mini-Review. *Frontiers in Nutrition*, *5*. https://doi.org/10.3389/fnut.2018.00087

Daglia, M. (2012). Polyphenols as antimicrobial agents. *Current Opinion in Biotechnology*, *23*(2), 174–181. https://doi.org/10.1016/j.copbio.2011.08.007

Dhokane, D., Karre, S., Kushalappa, A. C., and McCartney, C. (2016). Integrated metabolo-transcriptomics reveals Fusarium head blight candidate resistance genes in wheat QTL-Fhb2. *PLoS ONE*, *11*(5), 1–27. https://doi.org/10.1371/journal.pone.0155851

Dinelli, G., Carretero, A. S., Di Silvestro, R., Marotti, I., Fu, S., Benedettelli, S., Ghiselli, L., and Gutiérrez, A. F. (2009). Determination of phenolic compounds in modern and old varieties of durum wheat using liquid chromatography coupled with time-of-flight mass spectrometry. *Journal of Chromatography A*, *1216*(43), 7229–7240. https://doi.org/10.1016/j.chroma.2009.08.041

Doppler, M., Bueschl, C., Ertl, F., Woischitzschlaeger, J., Parich, A., and Schuhmacher, R. (2022). Towards a broader

view of the metabolome: untargeted profiling of soluble and bound polyphenols in plants. *Analytical and Bioanalytical Chemistry*, *414*(25), 7421–7433. https://doi.org/10.1007/s00216-022-04134-z

Dudonné, S., Vitrac, X., Coutière, P., Woillez, M., and Mérillon, J.-M. (2009). Comparative Study of Antioxidant Properties and Total Phenolic Content of 30 Plant Extracts of Industrial Interest Using DPPH, ABTS, FRAP, SOD, and ORAC Assays. *Journal of Agricultural and Food Chemistry*, *57*(5), 1768–1774. https://doi.org/10.1021/jf803011r

Durazzo, A., Lucarini, M., Souto, E. B., Cicala, C., Caiazzo, E., Izzo, A. A., Novellino, E., and Santini, A. (2019). Polyphenols: A concise overview on the chemistry, occurrence, and human health. *Phytotherapy Research*, *33*(9), 2221–2243. https://doi.org/10.1002/ptr.6419

Enaru, B., Drețcanu, G., Pop, T. D., Stănilă, A., and Diaconeasa, Z. (2021). Anthocyanins: Factors Affecting Their Stability and Degradation. *Antioxidants (Basel, Switzerland)*, *10*(12). https://doi.org/10.3390/antiox10121967

Flachowsky, H., Szankowski, I., Fischer, T. C., Richter, K., Peil, A., Höfer, M., Dörschel, C., Schmoock, S., Gau, A. E., Halbwirth, H., and Hanke, M.-V. (2010). Transgenic apple plants overexpressing the Lc gene of maize show an altered growth habit and increased resistance to apple scab and fire blight. *Planta*, *231*(3), 623–635. https://doi.org/10.1007/s00425-009-1074-4

Francesconi, S., and Balestra, G. M. (2020). The modulation of stomatal conductance and photosynthetic parameters is involved in Fusarium head blight resistance in wheat. *PLoS ONE*, *15*(6 june), 1–21. https://doi.org/10.1371/journal.pone.0235482

Francesconi, S., Steiner, B., Buerstmayr, H., Lemmens, M., Sulyok, M., and Balestra, G. M. (2020). Chitosan Hydrochloride Decreases *Fusarium graminearum* Growth and Virulence and Boosts Growth, Development and Systemic Acquired Resistance in Two Durum Wheat Genotypes. *Molecules*, 1–29. https://doi.org/10.3390/molecules25204752

Gaikpa, D. S., Lieberherr, B., Maurer, H. P., Longin, C. F. H., and Miedaner, T. (2020). Comparison of rye, triticale, durum wheat and bread wheat genotypes for Fusarium head blight resistance and deoxynivalenol contamination. *Plant Breeding*, *139*(2), 251–262. https://doi.org/10.1111/pbr.12779

Gautier, C., Pinson-Gadais, L., Verdal-Bonnin, M. N., Ducos, C., Tremblay, J., Chéreau, S., Atanasova, V., and Richard-Forget, F. (2020). Investigating the Efficiency of Hydroxycinnamic Acids to Inhibit the Production of Enniatins by Fusarium avenaceum and Modulate the Expression of Enniatins Biosynthetic Genes. *Toxins*, *12*(12), 1–17. https://doi.org/10.3390/toxins12120735

Gebhardt, Y. H., Witte, S., Steuber, H., Matern, U., and Martens, S. (2007). Evolution of flavone synthase I from parsley flavanone 3beta-hydroxylase by site-directed mutagenesis. *Plant Physiology*, *144*(3), 1442–1454. https://doi.org/10.1104/pp.107.098392

Golkari, S., Gilbert, J., Prashar, S., and Procunier, J. D. (2007). Microarray analysis of *Fusarium graminearum*-induced wheat genes: identification of organ-specific and differentially expressed genes. *Plant Biotechnology Journal*, *5*(1), 38–49. https://doi.org/10.1111/j.1467-7652.2006.00213.x

Goujon, T., Sibout, R., Eudes, A., MacKay, J., and Jouanin, L. (2003). Genes involved in the biosynthesis of lignin precursors in *Arabidopsis thaliana*. *Plant Physiology and Biochemistry*, *41*(8), 677–687. https://doi.org/10.1016/S0981-9428(03)00095-0

Gunnaiah, R., and Kushalappa, A. C. (2014). Metabolomics deciphers the host resistance mechanisms in wheat cultivar Sumai-3, against trichothecene producing and non-producing isolates of *Fusarium graminearum*. *Plant Physiology and Biochemistry*, *83*, 40–50. https://doi.org/10.1016/j.plaphy.2014.07.002

Gunnaiah, R., Kushalappa, A. C., Duggavathi, R., Fox, S., and Somers, D. J. (2012). Integrated metabolo-proteomic approach to decipher the mechanisms by which wheat QTL (Fhb1) contributes to resistance against *Fusarium graminearum*. *PLoS ONE*, *7*(7). https://doi.org/10.1371/journal.pone.0040695

Hammer, Ø., and Harper, D. A. T. (2005). Basic Statistical Methods. In *Paleontological Data Analysis* (pp. 8–60). https://doi.org/10.1002/9780470750711.ch2

Hao, G., Naumann, T. A., Vaughan, M. M., McCormick, S., Usgaard, T., Kelly, A., and Ward, T. J. (2019). Characterization of a *Fusarium graminearum* salicylate hydroxylase. *Frontiers in Microbiology*, *10*(JAN), 1–11.

https://doi.org/10.3389/fmicb.2018.03219

Hao, Y., Rasheed, A., Zhu, Z., Wulff, B. B. H., and He, Z. (2020). Harnessing Wheat Fhb1 for *Fusarium* Resistance. *Trends in Plant Science*, *25*(1), 1–3. https://doi.org/10.1016/j.tplants.2019.10.006

Hassan, A., Akram, W., Rizwana, H., Aftab, Z.-H., Hanif, S., Anjum, T., and Alwahibi, M. S. (2023). The Imperative Use of Bacillus Consortium and Quercetin Contributes to Suppress Fusarium Wilt Disease by Direct Antagonism and Induced Resistance. In *Microorganisms* (Vol. 11, Issue 10). https://doi.org/10.3390/microorganisms11102603

Hu, C., Cai, Y.-Z., Li, W., Corke, H., and Kitts, D. D. (2007). Anthocyanin characterization and bioactivity assessment of a dark blue grained wheat (*Triticum aestivum* L. cv. Hedong Wumai) extract. *Food Chemistry*, *104*(3), 955–961. https://doi.org/10.1016/j.foodchem.2006.12.064

Huang, J., Gu, M., Lai, Z., Fan, B., Shi, K., Zhou, Y.-H., Yu, J.-Q., and Chen, Z. (2010). Functional Analysis of the Arabidopsis PAL Gene Family in Plant Growth, Development, and Response to Environmental Stress. *Plant Physiology*, *153*(4), 1526–1538. https://doi.org/10.1104/pp.110.157370

Jiang, W., Liu, T., Nan, W., Jeewani, D. C., Niu, Y., Li, C., Wang, Y., Shi, X., Wang, C., Wang, J., Li, Y., Gao, X., and Wang, Z. (2018). Two transcription factors TaPpm1 and TaPpb1 co-regulate anthocyanin biosynthesis in purple pericarps of wheat. *Journal of Experimental Botany*, *69*(10), 2555–2567. https://doi.org/10.1093/jxb/ery101

Kage, U., Hukkeri, S., and Kushalappa, A. C. (2018). Liquid chromatography and high resolution mass spectrometry-based metabolomics to identify quantitative resistance-related metabolites and genes in wheat QTL-2DL against Fusarium head blight. *European Journal of Plant Pathology*, *151*(1), 125–139. https://doi.org/10.1007/s10658-017-1362-y

Kikot, G. E., Hours, R. A., and Alconada, T. M. (2009). Contribution of cell wall degrading enzymes to pathogenesis of *Fusarium graminearum*: A review. *Journal of Basic Microbiology*, *49*(3), 231–241. https://doi.org/10.1002/jobm.200800231

Kurechi, T., Kikugawa, K., and Kato, T. (1980). Studies on the Antioxidants. XIII. Hydrogen Donating Capability of Antioxidants to 2, 2-Diphenyl-1-picrylhydrazyl. *CHEMICAL and PHARMACEUTICAL BULLETIN*, *28*(7), 2089–2093. https://doi.org/10.1248/cpb.28.2089

Kutmon, M., van Iersel, M. P., Bohler, A., Kelder, T., Nunes, N., Pico, A. R., and Evelo, C. T. (2015). PathVisio 3: An Extendable Pathway Analysis Toolbox. *PLOS Computational Biology*, *11*(2), e1004085. https://doi.org/10.1371/journal.pcbi.1004085

Lalak-Kańczugowska, J., Witaszak, N., Waśkiewicz, A., Bocianowski, J., and Stępień, Ł. (2023). Plant Metabolites Affect *Fusarium proliferatum* Metabolism and In Vitro Fumonisin Biosynthesis. In *International Journal of Molecular Sciences* (Vol. 24, Issue 3). https://doi.org/10.3390/ijms24033002

Lei, K. J., Zhang, L., Du, X. Y., An, Y., Chang, G. H., and An, G. Y. (2018). A chalcone synthase controls the verticillium disease resistance response in both *Arabidopsis thaliana* and cotton. *European Journal of Plant Pathology*, *152*(3), 769–781. https://doi.org/10.1007/s10658-018-1521-9

Li, Jingchong, Geng, R., Kong, X., Li, L., Zhang, Z., and Liu, R. (2023a). Transcriptomic and physiological properties reveal the tolerance mechanism to difenoconazole toxicity in wheat (*Triticum aestivum* L.). *Ecotoxicology and Environmental Safety*, *255*(March). https://doi.org/10.1016/j.ecoenv.2023.114787

Li, Jingtao, Wang, C., Yang, L., Qiu, F., Li, Y., Zheng, Y., Liu, S., Song, L., and Liang, W. (2023b). Enhancing tomato resistance by exploring early defense events against Fusarium wilt disease. *Phytopathology Research*, *5*(1). https://doi.org/10.1186/s42483-023-00176-y

Li, Xiao lan, Lü, X., Wang, X. Hong, Peng, Q., Zhang, M. Sheng, And Ren, M. Jian. (2020a). Biotic and abiotic stress-responsive genes are stimulated to resist drought stress in purple wheat. *Journal of Integrative Agriculture*, *19*(1), 33–50. https://doi.org/10.1016/S2095-3119(19)62659-6

Li, Xiaorui, Zhang, X., Liu, G., Tang, Y., Zhou, C., Zhang, L., and Lv, J. (2020b). The spike plays important roles in the drought tolerance as compared to the flag leaf through the phenylpropanoid pathway in wheat. *Plant Physiology and Biochemistry*, *152*(April), 100–111. https://doi.org/10.1016/j.plaphy.2020.05.002

Li, Z., and Ahammed, G. J. (2023c). Plant stress response and adaptation via anthocyanins: A review. *Plant Stress*, *10*,

100230. https://doi.org/10.1016/j.stress.2023.100230

Liu, H., Liu, Z., Wu, Y., Zheng, L., and Zhang, G. (2021). Regulatory Mechanisms of Anthocyanin Biosynthesis in Apple and Pear. In *International Journal of Molecular Sciences* (Vol. 22, Issue 16). https://doi.org/10.3390/ijms22168441

Ma, D., Li, Y., Zhang, J., Wang, C., Qin, H., Ding, H., Xie, Y., and Guo, T. (2016). Accumulation of phenolic compounds and expression profiles of phenolic acid biosynthesis-related genes in developing grains of white, purple, and red wheat. *Frontiers in Plant Science*, *7*(APR2016), 1–11. https://doi.org/10.3389/fpls.2016.00528

Mandalà, G., Ceoloni, C., Busato, I., Favaron, F., and Tundo, S. (2021). Transgene pyramiding in wheat: Combination of deoxynivalenol detoxification with inhibition of cell wall degrading enzymes to contrast Fusarium Head Blight and Crown Rot. *Plant Science*, *313*, 111059. https://doi.org/10.1016/j.plantsci.2021.111059

McMullen, M., Bergstrom, G., De Wolf, E., Dill-Macky, R., Hershman, D., Shaner, G., and Van Sanford, D. (2012). A Unified Effort to Fight an Enemy of Wheat and Barley: Fusarium Head Blight. *Plant Disease*, *96*(12), 1712–1728. https://doi.org/10.1094/PDIS-03-12-0291-FE

Metsalu, T., and Vilo, J. (2015). ClustVis: a web tool for visualizing clustering of multivariate data using Principal Component Analysis and heatmap. *Nucleic Acids Research*, *43*(W1), W566–W570. https://doi.org/10.1093/nar/gkv468

Miedes, E., Vanholme, R., Boerjan, W., and Molina, A. (2014). The role of the secondary cell wall in plant resistance to pathogens. *Frontiers in Plant Science*, *5*(AUG), 1–13. https://doi.org/10.3389/fpls.2014.00358

Mielniczuk, E., and Skwaryło-Bednarz, B. (2020). Fusarium head blight, mycotoxins and strategies for their reduction. In *Agronomy* (Vol. 10, Issue 4). MDPI AG. https://doi.org/10.3390/agronomy10040509

Moreira, L. R. S., and Filho, E. X. F. (2016). Insights into the mechanism of enzymatic hydrolysis of xylan. *Applied Microbiology and Biotechnology*, *100*(12), 5205–5214. https://doi.org/10.1007/s00253-016-7555-z

Oufensou, S., Balmas, V., Azara, E., Fabbri, D., Dettori, M. A., Schu, C., Zehetbauer, F., Strauss, J., Delogu, G., and Migheli, Q. (2020). Naturally Occurring Phenols Modulate Vegetative Growth and Deoxynivalenol Biosynthesis in *Fusarium graminearum*. *ACS Omega* 5, 45, 29407–29415. https://doi.org/10.1021/acsomega.0c04260

Patra, B., Schluttenhofer, C., Wu, Y., Pattanaik, S., and Yuan, L. (2013). Transcriptional regulation of secondary metabolite biosynthesis in plants. *Biochimica et Biophysica Acta (BBA) - Gene Regulatory Mechanisms*, *1829*(11), 1236–1247. https://doi.org/10.1016/j.bbagrm.2013.09.006

Prat, N., Guilbert, C., Prah, U., Wachter, E., Steiner, B., Langin, T., Robert, O., and Buerstmayr, H. (2017). QTL mapping of Fusarium head blight resistance in three related durum wheat populations. *Theoretical and Applied Genetics*, *130*(1), 13–27. https://doi.org/10.1007/s00122-016-2785-0

Saulnier, L., Guillon, F., and Chateigner-Boutin, A. L. (2012). Cell wall deposition and metabolism in wheat grain. *Journal of Cereal Science*, *56*(1), 91–108. https://doi.org/10.1016/j.jcs.2012.02.010

Sharma, S., Kumar, A., Singh, D., Kumari, A., Kapoor, P., Kaur, S., Shreon, B., and Garg, M. (2022). Integrated transcriptional and metabolomics signature pattern of pigmented wheat to insight the seed pigmentation and other associated features. *Plant Physiology and Biochemistry*, *189*(August), 59–70. https://doi.org/10.1016/j.plaphy.2022.08.008

Singh, M., Thrimawithana, T., Shukla, R., and Adhikari, B. (2020). Managing obesity through natural polyphenols: A review. *Future Foods*, *1–2*, 100002. https://doi.org/10.1016/J.FUFO.2020.100002

Sivankalyani, V., Feygenberg, O., Diskin, S., Wright, B., and Alkan, N. (2016). Increased anthocyanin and flavonoids in mango fruit peel are associated with cold and pathogen resistance. *Postharvest Biology and Technology*, *111*, 132–139. https://doi.org/10.1016/j.postharvbio.2015.08.001

Sorahinobar, M., Niknam, V., Ebrahimzadeh, H., Soltanloo, H., Behmanesh, M., and Enferadi, S. T. (2016). Central Role of Salicylic Acid in Resistance of Wheat Against *Fusarium graminearum*. *Journal of Plant Growth Regulation*, *35*(2), 477–491. https://doi.org/10.1007/s00344-015-9554-1

Steiner, B., Kurz, H., Lemmens, M., and Buerstmayr, H. (2009). Differential gene expression of related wheat lines

with contrasting levels of head blight resistance after Fusarium graminearum inoculation. *Theoretical and Applied Genetics*, *118*(4), 753–764. https://doi.org/10.1007/s00122-008-0935-8

Sunil, L., and Shetty, N. P. (2022). Biosynthesis and regulation of anthocyanin pathway genes. *Applied Microbiology and Biotechnology*, *106*(5), 1783–1798. https://doi.org/10.1007/s00253-022-11835-z

Tenea, G. N., Peres Bota, A., Cordeiro Raposo, F., and Maquet, A. (2011). Reference genes for gene expression studies in wheat flag leaves grown under different farming conditions. *BMC Research Notes*, *4*(1), 373. https://doi.org/10.1186/1756-0500-4-373

Tomassini, A., Sella, L., Raiola, A., D'Ovidio, R., and Favaron, F. (2009). Characterization and expression of *Fusarium graminearum* endo-polygalacturonases in vitro and during wheat infection. *Plant Pathology*, *58*(3), 556–564. https://doi.org/10.1111/j.1365-3059.2008.02019.x

Tundo, S., Janni, M., Moscetti, I., Mandalà, G., Savatin, D., Blechl, A., Favaron, F., and D'Ovidio, R. (2016). PvPGIP2 Accumulation in Specific Floral Tissues But Not in the Endosperm Limits *Fusarium graminearum* Infection in Wheat. *Molecular Plant-Microbe Interactions : MPMI*, *29*(10), 815–821. https://doi.org/10.1094/MPMI-07-16-0148-R

Wagay, N. A., Lone, R., Rafiq, S., and Bashir, S. U. (2020). Phenolics: A Game Changer in the Life Cycle of Plants. In R. Lone, R. Shuab, and A. N. Kamili (Eds.), *Plant Phenolics in Sustainable Agriculture : Volume 1* (pp. 241–275). Springer Singapore. https://doi.org/10.1007/978-981-15-4890-1_11

Wang, J., Liang, J., and Gao, S. (2018). Biodegradation of Lignin Monomers Vanillic, p-Coumaric, and Syringic Acid by the Bacterial Strain, Sphingobacterium sp. HY-H. *Current Microbiology*, *75*(9), 1156–1164. https://doi.org/10.1007/s00284-018-1504-2

Wang, L., Yao, Y., He, Z., Wang, D., Liu, A., and Zhang, Y. (2013). Determination of phenolic acid concentrations in wheat flours produced at different extraction rates. *Journal of Cereal Science*, *57*(1), 67–72. https://doi.org/10.1016/j.jcs.2012.09.013

Wegener, C. B., and Jansen, G. (2007). Soft-rot Resistance of Coloured Potato Cultivars (*Solanum tuberosum* L.): The Role of Anthocyanins. *Potato Research*, *50*(1), 31–44. https://doi.org/10.1007/s11540-007-9027-4

Wiwart, M., Suchowilska, E., Stuper-Szablewska, K., Przybylska, A., Wachowska, U., and Gontarz, D. (2024). Variation in the concentrations of phenolic compounds and carotenoids in the grain of a large collection of *Triticum durum* Desf. accessions. *Journal of Cereal Science*, *116*(November 2023). https://doi.org/10.1016/j.jcs.2023.103842

Wu, F., Zhou, Y., Shen, Y., Sun, Z., Li, L., and Li, T. (2022). Linking Multi-Omics to Wheat Resistance Types to Fusarium Head Blight to Reveal the Underlying Mechanisms. *International Journal of Molecular Sciences*, *23*(4). https://doi.org/10.3390/ijms23042280

Yang, W.-J., Du, Y.-T., Zhou, Y.-B., Chen, J., Xu, Z.-S., Ma, Y.-Z., Chen, M., and Min, D.-H. (2019). Overexpression of TaCOMT Improves Melatonin Production and Enhances Drought Tolerance in Transgenic *Arabidopsis*. In *International Journal of Molecular Sciences* (Vol. 20, Issue 3). https://doi.org/10.3390/ijms20030652

Zhang, B., Lewis, K. M., Abril, A., Davydov, D. R., Vermerris, W., Sattler, S. E., and Kang, C. (2020). Structure and function of the cytochrome p450 monooxygenase cinnamate 4-hydroxylase from *Sorghum bicolor*. *Plant Physiology*, *183*(3), 957–973. https://doi.org/10.1104/pp.20.00406

Zhang, Y., Butelli, E., De Stefano, R., Schoonbeek, H., Magusin, A., Pagliarani, C., Wellner, N., Hill, L., Orzaez, D., Granell, A., Jones, J. D. G., and Martin, C. (2013). Anthocyanins Double the Shelf Life of Tomatoes by Delaying Overripening and Reducing Susceptibility to Gray Mold. *Current Biology*, *23*(12), 1094–1100. https://doi.org/10.1016/j.cub.2013.04.072

Zhong, Q., Hu, H., Fan, B., Zhu, C., and Chen, Z. (2021). Biosynthesis and Roles of Salicylic Acid in Balancing Stress Response and Growth in Plants. In *International Journal of Molecular Sciences* (Vol. 22, Issue 21). https://doi.org/10.3390/ijms222111672

5. Comparative transcriptomics in pigmented genotypes having different susceptibility to FHB

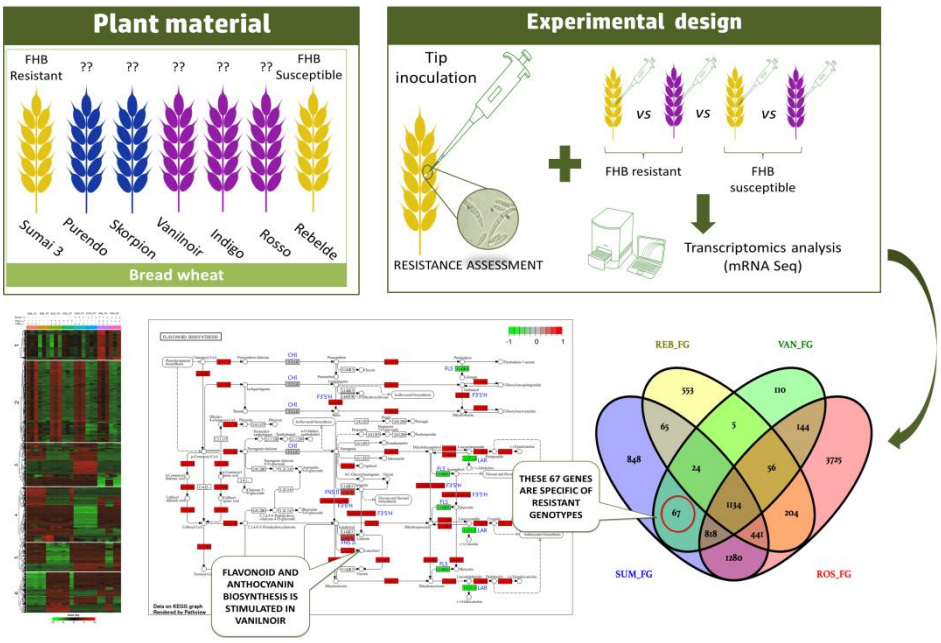

Abstract: Fusarium head blight (FHB) resistance in bread wheat is still challenging and no clear evidences regarding the role of pigmented wheat varieties (rich in anthocyanins in the grains) has been addressed so far. In this study, a resistant pigmented genotype and a susceptible pigmented genotype were selected among five lines (two having blue aleurone and three having purple pericarp) and used for a comparative transcriptomics analysis against a resistant control (Sumai3) and a susceptible cultivar (Rebelde), looking for differentially expressed genes due to *Fusarium graminearum* infection. Vanilnoir was selected as resistant line and Rosso as susceptible one, both having purple pericarp. Vanilnoir showed type II resistance, most likely thanks to the reinforcement of cell wall, supported by the upregulation of pathways and function related to the accumulation of lignin and hydroxycinnamic acid amides. The susceptible genotypes showed a growth–defence trade-off unbalanced towards growth, stimulated by the upregulation of cytokinins biosynthetic pathway. Noteworthy, flavonoids biosynthesis was boosted in the resistant genotypes compared to the susceptible ones, but in the purple pigmented genotypes it was more stimulated by the infection than in the yellow pigmented lines. More in detail, while in Sumai3 and Rosso the production of flavan-3-ols was favored to the detriment of anthocyanins, in infected Vanilnoir spikes the simultaneous production of anthocyanins and flavones was stimulated, both potentially involved in its resistance mechanism. Furthermore, ten LRR receptor-like protein kinases (LRR-RLKs) were exclusively up-regulated in the FHB-resistant genotypes together with two genes from the MAPK signaling. Further investigation on these genes can provide valuable information about the specific cross-talk between wheat and *F. graminearum*.

Publications:

Selected oral presentation: **Felici L.**, C. Miccoli, S. Turco, F. Castellani, L. Narduzzi, S. Francesconi, A. M. Garcia-Campaña, S. Palombieri, F. Sestili, M. Vitali, G.M. Balestra, "High polyphenolic wheat genotypes: a study on Fusarium Head Blight (FHB) resistance", Abstracts of presentations at the XXVIII Congress of the Italian Phytopathological Society (SIPaV). *J Plant Pathol* 105, 1237–1323 (2023). https://doi.org/10.1007/s42161-023-01500-3

Manuscript in preparation

5.1. Introduction

Fusarium head blight (FHB) is a major concern for wheat production, as it is counted as fourth in the top-10 most devastating fungal plant diseases (Dean et al. 2012). Resistance to FHB in wheat is quantitative and polygenic, indeed, different types of resistances are described in literature (Schroeder and Christensen, 1963; Gorash et al. 2020). *Fhb1* is the major Quantitative Trait Locus (QTL) contributing to type II resistance (which means resistance to the spread into the spikes) and has been localized in the distal segment of the chromosome 3BS in the genome of the bread wheat Sumai3 (Cuthbert et al. 2006). Despite *Fhb1* is the most extensively studied, best validated and the most widely deployed FHB resistance QTL in wheat breeding programs worldwide, its function is still unknown, since several independent research teams reported contradictory results (McMullen et al. 2012; Rawat et al. 2016; Su et al. 2019; Li et al. 2019). Despite type I (resistance to initial infection) and type II are the most exploited resistance type, also type III, IV and V have been proposed: type III FHB resistance is referred to the variations of DON accumulation in resistance and susceptible cultivars (Miller and Arnison, 1986), type IV FHB resistance is related to lower kernel infection, while type V FHB resistance indicates prevention of grain yield under infection conditions (Mesterhazy 1995).

The presence of anthocyanins in grains give rise to the pigmented wheat varieties, which are grouped into purple, blue and black genotypes, depending on anthocyanins type and accumulated amount, and whose cultivation is nowadays not widespread. Particularly, in blue and purple wheat varieties, anthocyanins accumulate in the aleurone and in the pericarp, respectively (Knievel et al. 2009; Beta et al. 2020). These molecules are biosynthesized during the multi-branched flavonoid pathway, that comprises both structural (phenylalanine ammonia-lyase (*PAL*), 4-coumarate-CoA ligase (*4CL*), chalcone synthase (*CHS*), chalcone isomerase (*CHI*), flavanone 3-hydroxylase (*F3H*), flavonoid 3'-hydroxylase (*F3'H*), flavonoid 3'5'-hydroxylase (*F3'5'H*), dihydroflavonol 4-reductase (*DFR*), anthocyanidin synthase (*ANS*), glucosyltransferase (*GT*), methyltransferase (MT), and acyltransferase (*AT*)), and regulatory genes (*MYB*, *bHLH*, and *WD40* encoding for transcription factors) (Li et al. 2020; Ficco et al. 2014). Despite many researchers investigated pigmented rice (Ryu et al. 1998; Abdel-Aal et al. 2006; Sompong et al. 2011) and maize (Moreno et al. 2005; Del Pozo-Insfran et al. 2006), comprehensive works regarding disease resistance in pigmented wheat genotypes are still lacking. Indeed, Bernardi et al (2018) investigated the ability of pigmented maize cultivars to control *Fusarium* spp. diseases, finding out that the cultivar "Rostrato Rosso", with grains rich in anthocyanin content, was resistant to *F. verticillioides.* Also, Pilu et al (2011) investigated the role of purple pericarp and blue aleurone maize cultivars for the management of fumonisin contamination, by developing six maize populations differing in their constitution of regulatory genes responsible for the accumulation of anthocyanins in the aleurone layer or in the pericarp, but these genotypes were not able to counteract fumonisin accumulation into the grains. These evidences have been also confirmed by Venturini et al (2015 and 2016), stating that pigmentation in the maize pericarp did not affect *F. verticillioide*s symptoms as much as fumonisin contamination compared to the non-pigmented genotype. Indeed, the authors state that the disease reduction was highly correlating with field location instead of maize genotype and, only when an anti-insect protection was applied, the authors recorded a disease control in the pigmented genotype compared to the non-pigmented one.

In this scenario, selection of FHB resistant traits is still challenging and no clear evidences regarding the role of pigmented wheat varieties has been already described. Thus, the aim of the present work was to investigate the role of pigmented wheat genotypes in response to FHB by exploiting the power of transcriptomics. We employed phenotypic-

based evaluations to look for FHB-resistance associated traits in pigmented wheat varieties (FHB susceptibility assay). After that, we compared the transcriptome of FHB resistant and susceptible pigmented bread wheat varieties with already well characterized FHB resistant and susceptible non-pigmented bread wheat varieties in order to elucidate the role of purple pericarp and blue aleurone traits in response to FHB.

5.2. Materials and Methods

5.2.1.Fungal material and inoculum preparation

Fungal material and inoculum preparation was the same used in chapter 3 and described in paragraph 3.2.2.

5.2.2.Plant material

In this study, five pigmented bread wheat (*Triticum aestivum*) lines with a high content of polyphenols were characterized: Purendo (developed by the Crop Development Center, Saskatoon, Canada) and Skorpion (Agrotest Fyto, Ltd., Kroměříž, Czech Republic) (Martinek et al. 2013), with blue aleurone; Vanilnoir (bred by Agroscope /DSP, pedigree: Runal/W'ST479-77//KONINI), Rosso (Saatzucht Donau GesmbH. and CoKG, Austria) and Indigo (developed by KWS Ltd, UK), with a purple pericarp, a bread wheat commercial cultivar, Rebelde, and the resistant line Sumai3, were included as controls.

5.2.3.FHB susceptibility assay

5.2.3.1. Plant grow condition and disease assessment

For *Fusarium* susceptibility assays (which included the analysis of severity, DON quantification, fungal biomass quantification, FDK, Folin-Ciocalteau assay), plants were grown in a greenhouse located in Viterbo (Italy, 42°25'38.44"N; 12° 4'49.69"E) under controlled conditions. The kernels were germinated in seedling trays filled with TYPical Brill soil for 7 days at 20˚C with a 16 h photoperiod. Subsequently, plants underwent a 2-week period at 5°C with an 8-hour photoperiod to break dormancy before being transplanted into 5L pots filled with the same soil, with 10 plants per pot. Throughout the experiment, plants were kept at 20°C (+/-5°C) with natural light supplemented by LED lighting to ensure a 16-hour photoperiod. Artificial infections were performed at anthesis (Zadok stage 69) *via* point inoculation. For inoculated plants, 10 µL of spore suspension were applied to the central spike floret of each plant using a laboratory pipette, while mock plants received 10 µL of sterile distilled water supplemented with 0.05% v/v Tween-20. Spikes were covered with clear plastic bags for 48 hours after the inoculum with the aim to maintain high humidity levels (>80%). A completely randomized experimental design was employed, with 10 plants of each genotype considered for each treatment (inoculated and mock). The experiment was replicated three times, with inoculation taking place between December 2021 and November 2022.

The FHB disease severity (%) was determined by counting the number of bleached spikelets (number of infected spikelets divided by the total number of spikelets per spike) for each inoculated spike from 3 to 21 DPI (day post infection) (Francesconi et al. 2019). The Area Under the Disease Progress Curve (AUDPC) was calculated for each spike using the following equation (Sparks et al. 2008):

$$\mathrm{AUDPC} = \sum_{i=1}^{N_{i-1}} \frac{(y_i + y_{i+1})}{2}(t_{i+1} - t_i)$$

Where y_i = disease severity at the i^{th} observation, t_i = days at the i^{th} observation, and N = total number of observations.

5.2.3.2. Fusarium Damaged Kernels (FDK)

At maturity stage, ten spikes and plantlets from each independent replicate from each experimental group (wheat genotype x treatment) were harvested and considered as three biological replicates to be used for FDK calculation, TPC assessment, fungal biomass and DON quantification. Kernels that were visually shriveled or chalky in appearance were designated as *Fusarium* Damaged Kernels (FDK). FDK parameter was expressed as percentage [%FDK = 100 × (number of FDK)/(number of total produced kernels)]. After these measurements, the kernels, the chaff and the rachis from each experimental sample (3 replicate consisting of 10 plants each) were homogenously milled into a fine flour using an electric coffee grinder (Moulinex, France), stored at 4°C and used for Total Phenolic Content (TPC) and fungal biomass assessment.

5.2.3.3. Total phenolic content (TPC)

A rapid, small-scale, high-throughput assay for approximating the total phenolics and other antioxidant substrates on the basis of the improved Folin-Ciocalteu (F-C) method of Singleton and Rossi (Singleton and Rossi 1965), using ferulic acid as a standard, was used, following literature references with minor modification (Ainsworth and Gillespie 2007; Schiavi et al. 2022). Procedure was already described in paragraph 3.2.8. Final results were expressed as ferulic acid equivalent (FAE) using a ferulic acid calibration curve (range from 25 to 350 mg L^{-1} concentration and $R^2 = 0.9908$).

5.2.3.4. Quantification of Fungal Biomass by Real-Time qPCR

For the quantification of fungal biomass, 100 mg of *F. graminearum* fresh mycelium, scraped from a PDA plate cultured in the dark at 24 °C for 7 days in purity, and 100 mg of plant material were subjected to total DNA genomic extraction following the protocol of the GRS Genomic DNA Kit – Plants (GRiSP Research Solutions, Porto, Portugal). DNA was quantified with a Qubit™ fluorometer 1.01 (Invitrogen, Waltham, United States) using the Qubit™ dsDNA BR Assay Kit (Thermo Fisher Scientific, Waltham, United States). DNA from inoculated samples was diluted to 10 ng/ul, while wheat calibration curves were performed using four serial dilutions 1:10 (1:1, 1:10, 1:100, 1:1000) from uninoculated wheat material DNAs. A specific calibration curve was obtained for each wheat genotype and for *F. graminearum* quantification. Real- Time qPCR was performed following the instructions from Rotor Gene Q (Qiagen, Hilden, Germany) and Xpert Fast SYBR (uni) Master Mix (GRiSP Research Solutions, Porto, Portugal). Real-Time qPCR amplification conditions included an initial denaturation step of 3 minutes at 95°C, 40 cycles of 5 seconds denaturation at 95°C, 30 seconds of annealing at 60°C and 20 seconds of elongation at 72°C. gDNA quantification of *F. graminearum* was determined through the amplification of TRI6 gene while plant gDNA was obtained through the amplification of actin (see table S5.1 for primers). Data were obtained from three technical replicates derived from three biological replicates. Results were expressed as ng of fungal DNA per ng of plant DNA.

5.2.3.5. Mycotoxins quantification

300 mg of homogenized samples belonging to three biological replicates for each experimental group (inoculated and mock) were considered in this analysis. Subsequently, 1 mL of a cold water solution containing methanol, acetonitrile and formic acid (37.5:37.5:0.1 v/v/v) was added, followed by vortexing all samples for 10 seconds. Afterwards, the samples are subjected to ultrasonication for 15 minutes in an ultrasonic bath. Following sonication, the samples were centrifuged for 10 minutes at 14000 rpm, and 600 µl of the supernatant was transferred into a new Eppendorf tube,

paying attention to not disturb the pellet, with 300 µl of a water solution containing 0.1% v/v of formic acid. After a brief vortex (10 sec), samples were filtered and stored at 4°C until analysis. LC-MS/MS determination of DON was carried out using a Synergi Fusion RP (4µm, 2 x 50 mm, Phenomenex, USA). Chromatography was performed using H_2O + 2 mM acetate buffer (A) and methanol (B) at a flow rate of 800 µL min^{-1}. Gradient elution started at 5% of B and was raised to 100% in 0.5 minutes and equilibrated for 0.5 minutes. The initial conditions were then restored and the system was conditioned for 4 minutes. The column temperature was set at 25 °C, and the injection volume was 5 µL. The retention time (RT) of the target analyte was 1.55 min. Infusion of standard solution of DON (10 µg L^{-1}) was performed to establish the best parameters for ionic transmission in mass spectrometry. Analysis was performed in positive MRM mode. The ion source and curtain gasses were respectively set at 55, 60 and 30 psi; the source temperature was set at 500 °C, the declustering and entrance potentials were set at 80 V and 10 V, respectively and the collision cell exit potential was set at 15 V. Quantification of DON was performed based on 297 → 249 transition (quantifier, collision energy (CE) = 15 eV) and 297 → 203 transition (qualifier, CE = 25 eV). Limits of detection and quantification, calculated as the minimum concentration of the analyte that produces a signal-to-noise ratio greater than 3 and 10, were 0.15 and 0.50 µg L^{-1}, respectively.

5.2.4. Comparative transcriptomics

5.2.4.1. Plant grow condition and sampling procedure

Plants were grown in a climatic growth chamber under strong controlled conditions with the aim to minimize the environmental variability which is unavoidable within a greenhouse. Seeds were sterilized, germinated and the dormancy was broken as already reported for the susceptibility assay. After an artificial vernalization, plants were grown at 20°C (+/-2°C) with a 16 h photoperiod and a 60% relative humidity until the end of the experiment. The growth chamber was equipped by white LED light (Combo 600 W and Slim Natural Indoor bars, C-Led, Italy), controlled temperature and relative humidity. All plants were fertilized using calcium nitrate (15.5-0-0+26.5 CaO, Haifa) at each transplanting event while, at heading, a micronutrient liquid fertilizer (NPK 4-7-7 +B+Cu+Fe+Mn+Zn, Flortis) was preferred. Artificial inoculations were performed via point inoculation, as already reported. At 2 dpi, three spikes from all the genotypes were collected, rapidly frozen using liquid nitrogen, and stored at -80°C. collected spikes were used for mRNA sequencing (RNAseq) and for RT- qPCR. Only four wheat varieties were considered for mRNA sequencing for a direct comparison between resistant/susceptible and pigmented/non-pigmented genotypes: the most resistant among all pigmented genotypes; the corresponding most susceptible pigmented genotype, and Sumai3 (FHB resistant), Rebelde (FHB sensitive) as controls.

5.2.4.2. Transcriptomics analysis

For the resistant control (Sumai3), the susceptible control (Rebelde), the more resistant pigmented genotype and the more susceptible pigmented genotype, three spikes were collected at 2 DPI and used as biological replicates for transcriptomic experiment. Frozen spikes were grinded in liquid nitrogen with mortar and pestle, and 100 mg were used for the total RNA extraction following the protocol of RNeasy Plant Mini Kit (Qiagen, Hilden, Germany). RNA was eluted in 30 µl of RNAse free water and the concentration was assessed through a Qubit™ fluorometer 1.01 (Thermo Fisher Scientific, Waltham, MA, United States) using the Qubit™ RNA BR Assay Kit (Thermo Fisher Scientific, Waltham, MA, USA). Purity was checked using a µDrop™ Plate (Thermo Fisher Scientific, Waltham, MA, United States). Samples with a suitable concentration (>20 ng/µl) and with good ratios (A_{260}/A_{280}>1.8 and A_{260}/A_{230} between 2.0 and 2.2) were then sent to Novogene Company (Cambridge, United Kingdom) for sequencing. Library preparation

was followed by sequencing using Illumina platform in paired-end mode with a read length of 150 bp. Raw reads quality was evaluated using FastQC (Andrews 2010). Clean reads were mapped to the *Triticum aestivum* genome (Chinese Spring IWGSC RefSeq v.1.0 reference) using HISAT2 v2.1 (Kim et al. 2019). Count matrices were generated from the alignment outputs with featureCounts v2.0.5 (Liao et al. 2014). Read counts data was uploaded to iDEP v1.0 (Ge et al. 2018) for evaluating reproducibility and reliability of the data by Principal Component Analysis (PCA), Pearson's correlation among replicates and K-mean clustering (hierarchical distance and linkage average). After normalization and log2 transformation, the differentially expressed genes were identified through DESeq2 using an adjusted p-value cut-off of $p \leq 0.05$ (Love et al. 2014). To identify major function involved in FHB response, gene ontology (GO) enrichment and pathway enrichment (considering Kyoto Encyclopedia of Genes and Genomes, KEGG, pathway maps) were performed. Enrichment *p*-value were calculated based on one-sided hypergeometric test, which was then adjusted for multiple testing using the Benjamini-Hochberg procedure and converted to FDR (false discovery rate). After the analysis, pathways were filtered based on an FDR cutoff (0.05), then the significant pathways were sorted by FDR.

5.2.4.3. Relative expression of selected genes and RNAseq validation

The relative expression of genes listed in Table S5.1 was evaluated as involved in disease response and polyphenolic metabolism for a double purpose: evaluate the relative expression of these genes in the genotypes excluded from RNAseq and validate the transcriptomics analysis. For the genotypes excluded from transcriptomics analysis, total purified RNA was extracted from 100 mg of treated and mock spikelets, following the instructions provided by GRS Total RNA Kit-Plant (GRiSP Research Solutions, Portugal). The RNA was resuspended in 30ul of RNAse free sterile distilled water. The RNA was then resuspended in 50ul of RNAse free sterile distilled water. All the RNA extracted was quantified using Qubit™ RNA BR Assay Kit (Thermo Fisher Scientific, Waltham, United States). 50 ng of the total purified RNA was converted in cDNA following the instructions provided by Xpert cDNA Synthesis Supermix with a gDNA eraser (GRiSP Research Solutions, Porto, Portugal) in a final volume of 20 µL. Real-Time qPCR was performed following the instructions from Rotor Gene Q (Qiagen, Hilden, Germany) and Xpert Fast SYBR (uni) Master Mix (GRiSP Research Solutions, Portugal) in a final volume of 10 µL. For the primer pairs developed in this study, sequence similarity searches were conducted using known sequences sourced from Ensembl Plants (https://plants.ensembl.org/index.html). These sequences underwent BLASTn analysis (https://blast.ncbi.nlm.nih.gov/) to extract the respective cDNA. Real-Time qPCR primers were then strategically designed within the exonic regions using Primer-BLAST (https://blast.ncbi.nlm.nih.gov/tools/primer-blast/). To determine the optimal annealing temperature, a gradient PCR was conducted for each primer pair. Real-Time qPCR amplification conditions included an initial denaturation step of 3 minutes at 95°C; 40 cycles of 5 seconds denaturation at 95°C, 30 seconds of annealing at the temperature indicated in Table S5.1 and 20 seconds of elongation at 72°C. A final melt cycle (60 – 99 °C) was performed to confirm the unicity of the amplicons. No template controls (NTC) were included in the analysis and the amplification was considered as negative when a value of Cq ≥ 38 was detected. RT-qPCR was performed using the primer pairs listed in Table S5.1. The relative expression levels of the target genes were determined by calculating the average Cq values of three technical replicates obtained from three independent biological replicates for each wheat genotype. The following equation was employed:

$$Relative\ expression = 2^{-\Delta\Delta Cq}$$

Between all the genotypes and treatments, *TaFNR* and *TaACT* showed the most stable expression levels among the reference genes, thus these genes were used for internal normalization. Furthermore, mock treatments were used to normalize the relative expression levels.

5.2.5.Data analysis

For susceptibility assay (severity, AUDPC, DON, TPC, fungal biomass, FDK), differences among genotypes in the same group (FG or NT) and between groups in the same genotypes (FG *vs* NT) were analyzed using one-way ANOVA and Tukey test (confidence level of 0.95 and $p < 0.05$), calculated using Past 4.0 (Hammer and Harper 2005). Past 4.0 was used also for PCA analysis (related to phytopathological assay), the matrix showing RT-qPCR results and for the ordinary least square (OLS) regression used to compare RT-qPCR and RNAseq data. For RNAseq analysis, the following software and tools were used: R environment v.4.2.3, iDEP 1.13 (Ge, Son, and Yao 2018), Shiny GO (Ge, Jung, and Yao 2020), Venny (Oliveros 2007).

5.3. Results

5.3.1. Pigmented genotypes exhibited distinct responses to F. graminearum infection

Five pigmented genotypes were artificially inoculated and their reactions to *F. graminearum* infection were studied considering different parameters. In terms of severity, Skorpion (blue) and Rosso (purple) displayed heightened sensitivity, with 81% and 69% of spikelets affected at 21 dpi, respectively, compared to the FHB-susceptible control Rebelde, which exhibited a severity of 63% (Fig. 5.1a). Conversely, Vanilnoir showed a severity of only 17%, mirroring the trend observed in the FHB-resistant genotype Sumai3, which showed a severity of 12% at 21 dpi. Regarding the other tested pigmented genotypes, both Purendo (blue) and Indigo (purple) demonstrate severity levels of 41% and 28%, respectively. The severity trend was analyzed calculating the AUDPC (Fig. 5.1b) and performing one-way ANOVA (Fig. 5.1b). According to this analysis, Indigo (4.17±1.19), Purendo (3.38±0.80), Rosso (6.17±1.54) and Skorpion (9.85±0.96) were similar to the susceptible control Rebelde (6.29±0.95), while the Vanilnoir (2.69±0.53) was the only line similar to the resistant control (1.07±0.16). No symptoms were detected in mock treated plants.

Fungal biomass quantification was achieved using Real-Time qPCR (Fig. S5.1). The quantification of fungal biomass reveals notable differences across different genotypes (Fig. 5.1c). A different pattern was observed for the fungal biomass quantification in the wheat spikes of Purendo, Indigo and Rosso where these genotypes were less effective in controlling fungal spread (mean: 6.88, 5.96 and 6.13 ng of fungal DNA/ng of plant DNA respectively), a result that is totally comparable to that of the susceptible control Rebelde (4.55 ng of fungal DNA/ng of plant DNA). The Vanilnoir genotype displayed limited fungal biomass accumulation, with a measured ratio of 1.74 ng of fungal DNA per ng of plant DNA, confirming severity and AUDPC data. Interestingly, in Skorpion genotype there is the most reduced pathogen spread with 0.79 ng of fungal DNA/ng of plant DNA, comparable to the FHB resistant Sumai3 (1.04 ng of fungal DNA/ng of plant DNA) and statistically similar to all the non-inoculated controls, which ranged from 0.00 to 0.47 ng/ng. Traces of fungal DNA in the mock treated spikes were detected in mock treated plants, most likely due to the completely randomized experimental design.

DON is the most abundant trichothecene produced by *F. graminearum* wt 3824. Traces of DON were detected in mock plant, in quantity lower that the European Union maximum limits (of 750 $\mu g\ kg^{-1}$), while the artificial infection led to a

consistent accumulation of DON, abundantly above the limits (Fig. 5.1d). In particular in Skorpion (208.38±81.48 mg/kg, mean ± SE) and Purendo (93.90±5.81 mg/kg) DON was considerably higher than in Sumai3 (15.89±1.32 mg/kg), while in Rebelde (67.72±24.69 mg/kg), Indigo (48.48±11.58 mg/kg), Rosso (50.96±8.53 mg/kg), and Vanilnoir (95.04±56.05 mg/kg) DON level was intermediate between Skorpion and Sumai3.

Total phenolic content (TPC) of mature spikes is another parameter typically linked to the infection process (Fig. 5.1e). Without the infection, Vanilnoir and Indigo were the lines with the highest TPC (42.33 ± 1.35 mg FAE/g and 34.09 ± 1.54 mg FAE/g respectively, mean ± SE). In the resistant genotype 26.66 ± 2.86 mg FAE/g accumulated in the mock spikes. A level of TPC comparable to Sumai3 was detected in mock spikes of Indigo (34.09±1.54 mg FAE/g), Rebelde (22.66±1.52 mg FAE/g), Rosso (16.30±2.37 mg FAE/g) and Skorpion (19.52±1.08 mg FAE/g). Purendo accumulated the lowest level of total phenolic acids (13.29±0.87 mg FAE/g). The infection modified the TPC of all the considered genotypes. In particular, compared to mock plants TPC increased in infected Rebelde (+95%), Sumai (+34%), Purendo (+57%) and Vanilnoir (+26%) and strongly increased in Rosso (+275%) and Skorpion (+124%). Interestingly in Indigo infected spikes a reduction (-23%), in comparison with the mock plants, was recorded.

Following the evaluation of disease progression, the Fusarium Damaged Kernel (FDK) % was taken into account as an indication of yield reduction due to infection. In infected thesis FDK ranged from 3.19% to 100% (Fig. 5.1f). Infected Skorpion had the highest FDK (73.61±19.08 %, mean ± SE), which was statistically different from FDK recorded for infected Sumai3 (9.35±2.39 %). The other infected genotypes, Rebelde (31.54±3.31 %), Indigo (24.64±9.03 %), Purendo (25.74±6.31 %), Rosso (37.52±14.14 %) and Vanilnoir (32.27±18.51 %) were statistically similar to both Sumai3 and Skorpion. This trait was visually evaluated and some shriveled kernels (less than 10%), potentially caused by unintentional *Fusarium* infection or by abiotic stress (like drought stress), were detected in mock thesis. Notably, for Sumai3 and Vanilnoir the difference among mock and infected thesis was not statistically significant.

For an overall evaluation of the different disease parameters, multivariate analysis (PCA) was computed. In the scatter plot, showed in Fig. 5.1g, the first two principal components are displayed and accounted for 78.9% of the overall variance. The three replicates of the different genotypes clearly cluster together, with few overlapping. Sumai3 infected samples are represented close to the mock treated samples, in the bi-dimensional PCA environment, while Rebelde infected samples clustered at the opposite side. Indigo, Purendo and Vanilnoir clusters were located between Rebelde and Sumai3, while Rosso and Skorpion were the genotypes positioned furthest from Sumai3.

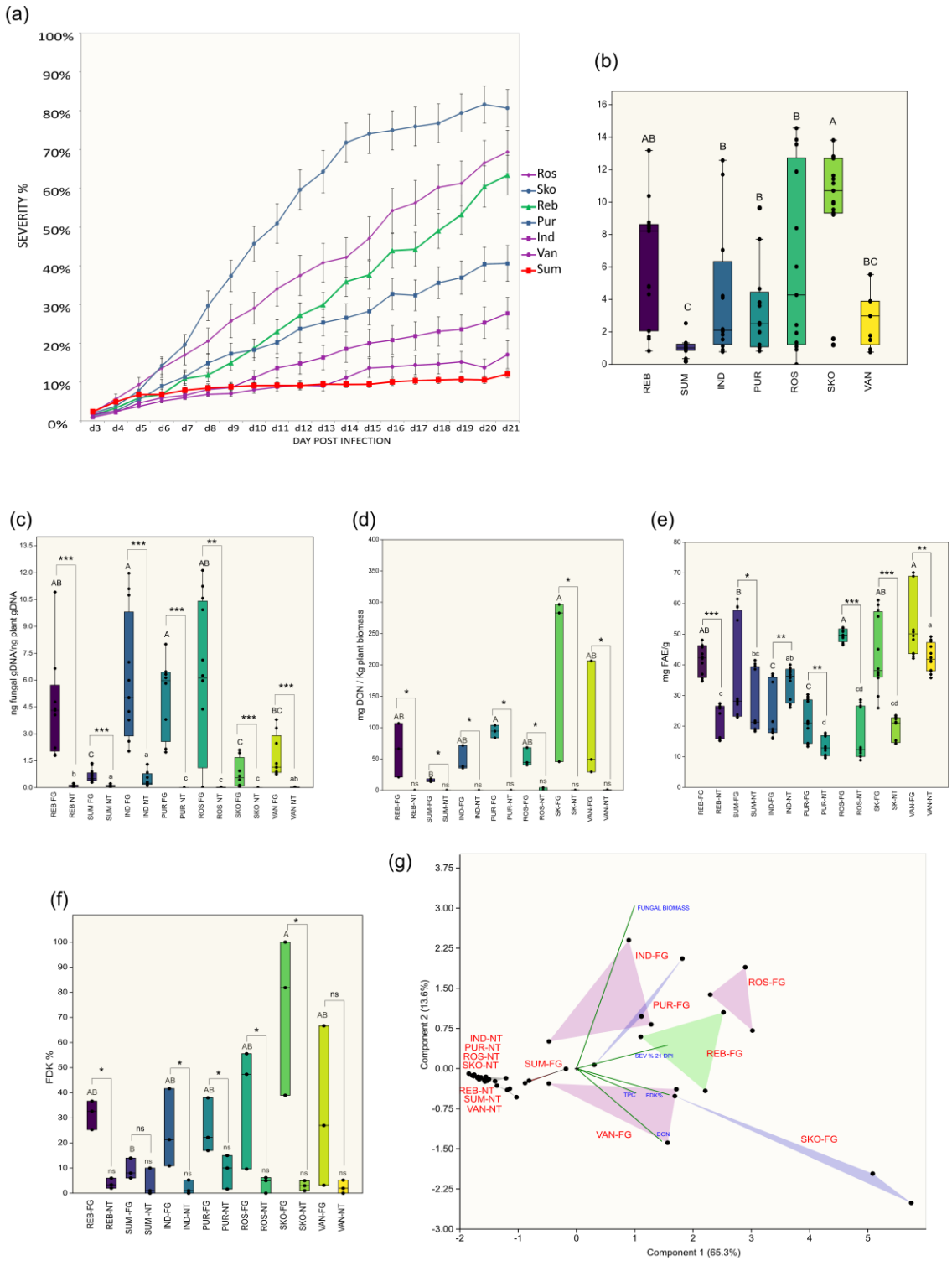

Fig. 5.1: Disease parameters, showing (a) severity trend during the considered period (mean and SE plotted), and box plots displaying (b) AUDPC, (c) fungal biomass, (d) DON accumulation, (e) TPC, (f) FDK and (g) principal component analysis scatterplot, showing the convex hulls of each thesis (convex hull color: purple = purple pericarp genotype; blue = blue aleurone genotype; red = resistant control; green = susceptible control) and the vector bi-plot for the first two principal components. In the box plots, differences among genotypes in the same group (FG or NT) were analyzed using one-way ANOVA and Tukey test (confidence level of 0.95 and $p < 0.05$); same letter (a, b, c, d) means no statistically different; upper case letters refer to FG group, while lowercase letters refer to NT group; differences between the two treatments (FG *vs* NT) in the same genotype were analyzed using one-way ANOVA and three confidence level: 0.95 (*$p < 0.05$), 0.99 (**$p < 0.01$) and 0.999 (***$p < 0.001$). ns = not significant, NT = Mock treated, FG = *F. graminearum infected*, REB = Rebelde, SUM = Sumai3, IND = Indigo, PUR = Purendo, ROS = Rosso, SKO = Skorpion, VAN = Vanilnoir.

5.3.2. Comparative transcriptomics among Sumai3, Rebelde, Vanilnoir and Rosso

Considering the results of the FHB susceptibility assay (Fig 5.1 a-g), Vanilnoir was chosen as the most resistant pigmented genotype and Rosso as the most susceptible pigmented genotype. Transcriptome obtained from their spikes were sequenced and compared to the ones of Sumai3 and Rebelde. After the removal of low-quality and short reads, from 82 million to 145 million total number of reads for each sample remained for analysis (Fig. S5.2). Reads were mapped against the Chinese Spring IWGSC RefSeq v.1.0 reference, with a mean library alignment rates (uniquely mapped reads) of 71.5% (the unmapped reads in mean were: 7.3% of unmapped reads, 10.3% of multi-mapping, 10.1% of no features and 0.8% of ambiguity) (Fig. S5.2). Read counts data was uploaded to iDEP v1.13 and filtered, obtaining 74607 genes. Pearson's coefficient of correlation matrix indicated a high level of reproducibility between replicate libraries (Fig. S5.3-6). *r* Values ranged from 0.9 to 0.97, the exception being Rebelde mock (where $r = 0.84$ between mock replicate 1 and replicate 3) and Rebelde infected (where $r = 0.87$ between replicate 1 and replicate 3 and $r = 0.86$ between replicate 2 and replicate 3). Principal component analysis (PCA, Fig. 5.2) indicated that genotypes and FG *vs* mock-inoculated replicates clustered separately, with few overlapping. Overall, the transcriptome results reported herein indicated quality RNA transcriptome data suitable for differential expression analysis.

Fig. 5.2: PCA of RNAseq analyzed samples, considering log-transformed read counts.

Before the identification of differentially expressed genes (DEGs) all reads were clustered by K-mean clustering and represented in the heatmap in Fig. 5.3, providing a macroscopic view of the dataset. Six clusters were identified, and Gene Ontology (GO) enrichment was computed to highlight the significantly represented GO terms for each cluster. Notably, in all the clusters, the most enriched terms were related to stress response and fungal infection, suggesting a general reprogramming due to the infection across the genotypes. In cluster 1 (Fig. 5.3) the most enriched terms were related to cell wall organization and biogenesis. The cluster 2 grouped gene strictly related to reaction to the infection (shared among all the considered genotypes, regardless the resistance), and the main enriched terms were “Glutathione metabolic process”, “Phenylpropanoid catabolic process”, “Lignin metabolic process” and “Detoxification”. Cluster 3 were particularly enriched in terms like “Chromatin remodeling”, “Nucleosome organization”, and “Protein-DNA complex assembly”, suggesting the involvement of gene expression activation. Genes grouped in cluster 4 were enriched in terms related to chitin demolition and protein synthesis. In cluster 5 and 6 the only enriched GO terms for the biological function were “Defense response”.

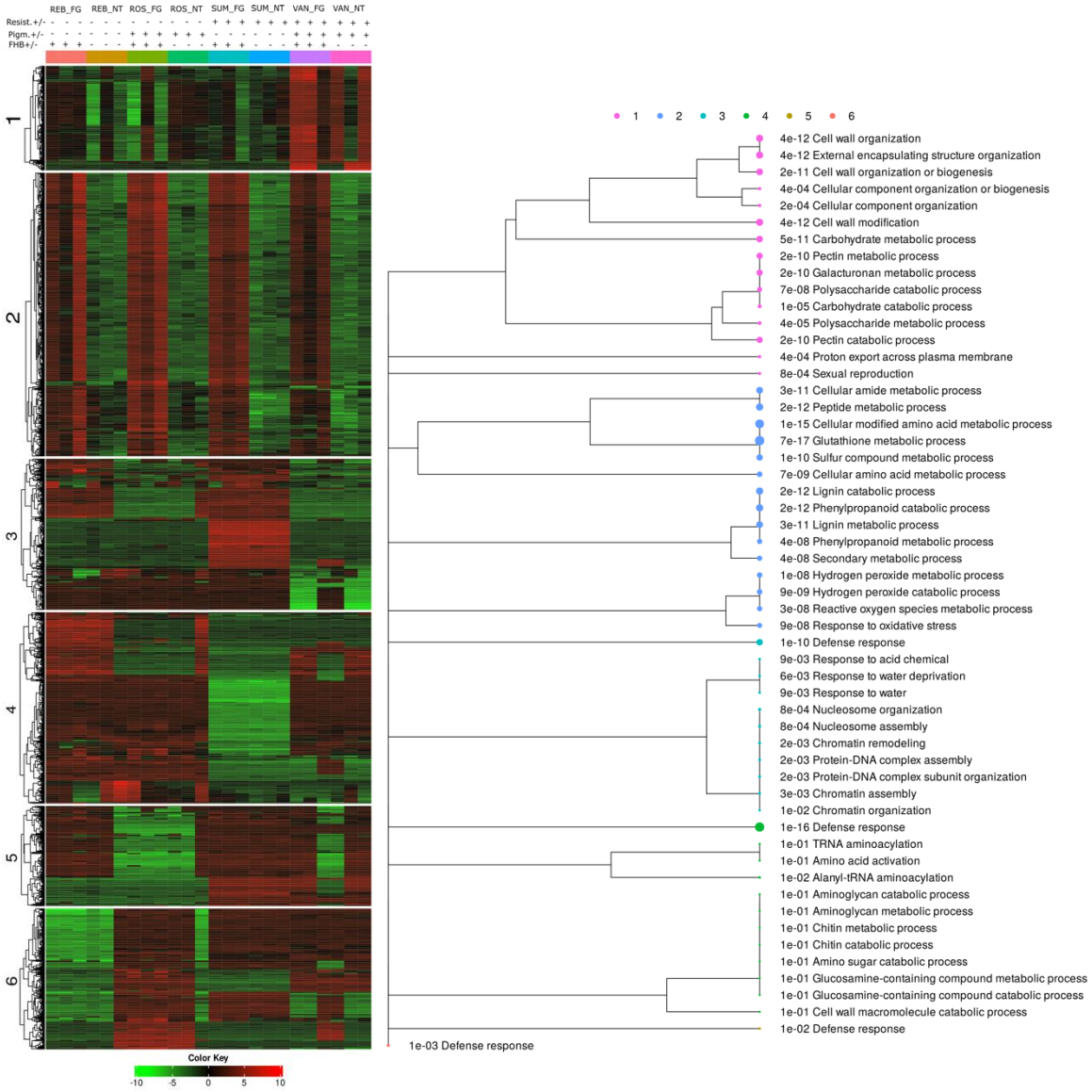

Fig. 5.3: Heatmap and k-mean clustering (left) showing log-transformed read counts in the 24 samples. Red color in the heatmap means high number of reads, while green means low number of reads. Six clusters were assigned. Tree on the right show for each cluster the top ten enriched biological process. Circle color indicate the cluster number while circle dimension is correlated with FDR (indicated in the tree before the terms).

5.3.2.1. Gene ontology and pathway enrichment of differentially expressed genes

Differential gene expression analysis, using DeSeq2 and the IWGSC Chinese Spring RefSeq cDNA reference, identified 9474 wheat genes differentially expressed in response to inoculation (FG *vs* Mock) in the different genotypes. More wheat genes were upregulated than downregulated (Fig 5.4), especially in the resistant genotypes Sumai3 and Vanilnoir (Fig. 5.4a; Sumai3, 4491 upregulated and 186 downregulated; Fig. 5.4b Vanilnoir, 2340 upregulated and 18 downregulated), while in Rebelde and Rosso an higher number of downregulated DEGs were reported in comparison with Sumai3 and Vanilnoir (Fig. 5.4c, Rebelde: 2110 upregulated and 372 downregulated, Fig 5.4d Rosso: 6135 upregulated and 1667 downregulated).

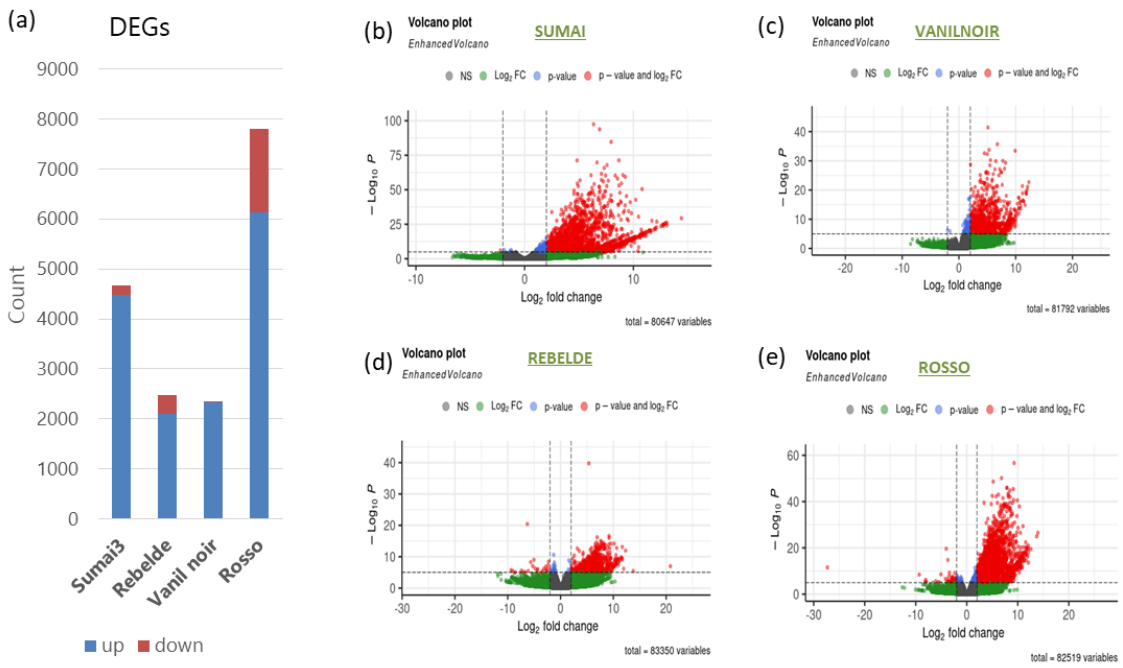

Fig. 5.4: General information on DEGs obtained by RNAseq. (a) number of DEGs; (b-e) volcano plots showing a significance measure on the Y-axis (-log10(p-value)) and an effect size on the X-axis (the logarithmized fold-change).

In addition, GO and KEGG enrichment analyses were performed to analyze the functions of the DEGs. GO enrichment analysis assigned the DEGs to a huge number of biological processes, molecular functions and cellular components, reported for each genotype and divided in up and downregulated in Table 5.1. The top ten enriched GO terms (sorted by increasing FDR) are shown in Fig. 5.5-5.8.

Table 5.1. Number of GO enriched terms (up or downregulated) assigned to the DEGs. BP = Biological process; CC = cellular components; MF = molecular function.

	BP		CC		MF	
	UP	**DOWN**	**UP**	**DOWN**	**UP**	**DOWN**
Rebelde	100	93	22	20	100	37
Rosso	100	100	17	51	100	100
Sumai3	100	18	14	16	100	13
Vanilnoir	100	0	11	21	78	0

In Rebelde GO enrichment analysis assigned the upregulated DEGs to 100 biological processes, 100 molecular functions and 22 cellular components, while the downregulated DEGs were assigned to 93 biological processes, 37 molecular functions, and 20 cellular components. The top ten most enriched biological process categories for downregulated DEGs were related to cellulose metabolic process and cellular polysaccharide biosynthetic process (Fig. 5.5). Cellulose synthase activity was the top downregulated molecular function term and Golgi membrane the most enriched downregulated cellular component, suggesting a general downregulation of cell wall biosynthesis (Fig. 5.5a and c). The top three most enriched upregulated biological processes were related to glutathione metabolic process and aromatic amino acid family metabolic process (L-phenylalanine) (Fig 5.5b and c). The top enriched upregulated cellular component was the extracellular region, and the top upregulated molecular function was the glutathione transferase

activity. Furthermore (data not shown in the figure) 3 genes encoding for proteins related to jasmonic acid biosynthetic process were significantly downregulated (12.83 fold enrichment; FDR=0.0329).

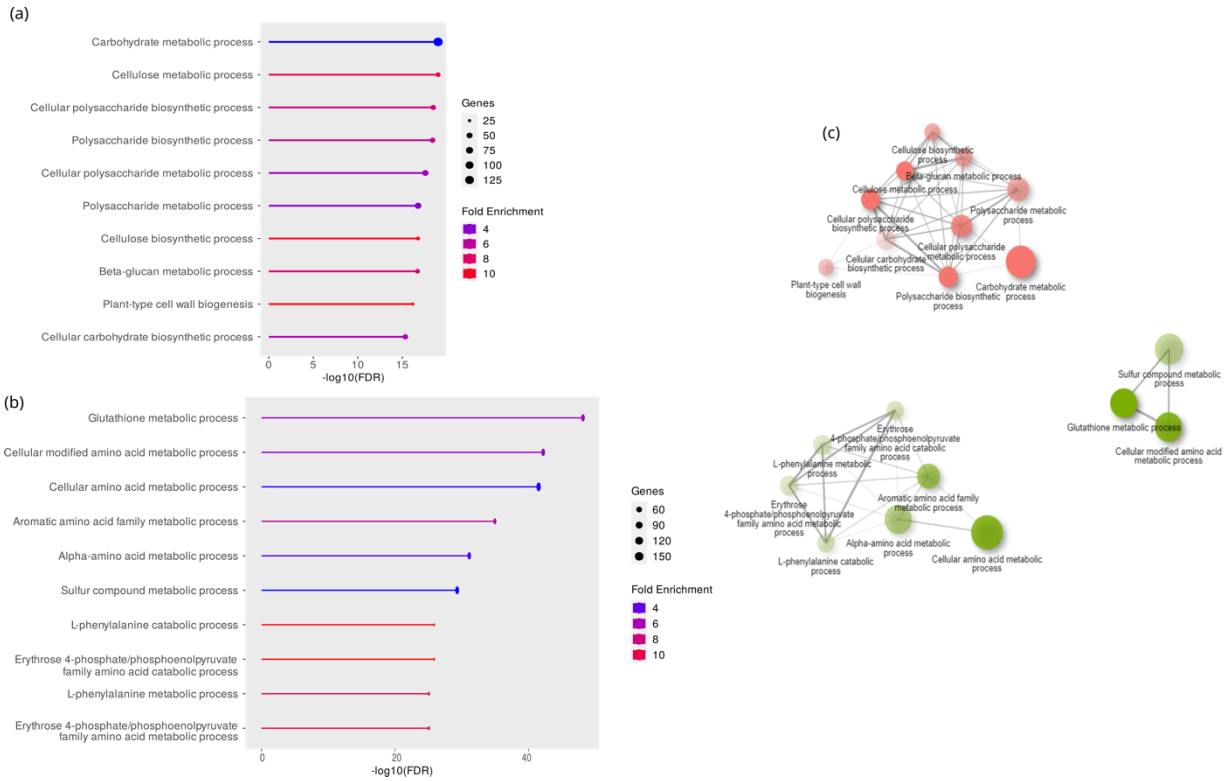

Fig. 5.5: Gene ontology (biological process) enrichment of Rebelde top ten DEGs. (a) most enriched terms related to downregulated DEGs; (b) most enriched terms related to upregulated DEGs; (c) network showing connection among the cited terms (red = downregulated; green = upregulated).

In Rosso (Fig. 5.6) the main enriched biological processes terms for downregulated DEGs were associated to cytoskeleton organization, photosynthesis and plant defense while the most enriched biological processes for upregulated DEGs were linked to peptide, cellular amide and glutathione metabolic processes. Consistently, the top enriched cellular components for upregulated DEGs was the cytosolic ribosome, while the top term for downregulated DEGs was the chloroplast. The top upregulated enriched molecular function was the glutathione transferase activity, while cytoskeletal protein binding function was significantly downregulated.

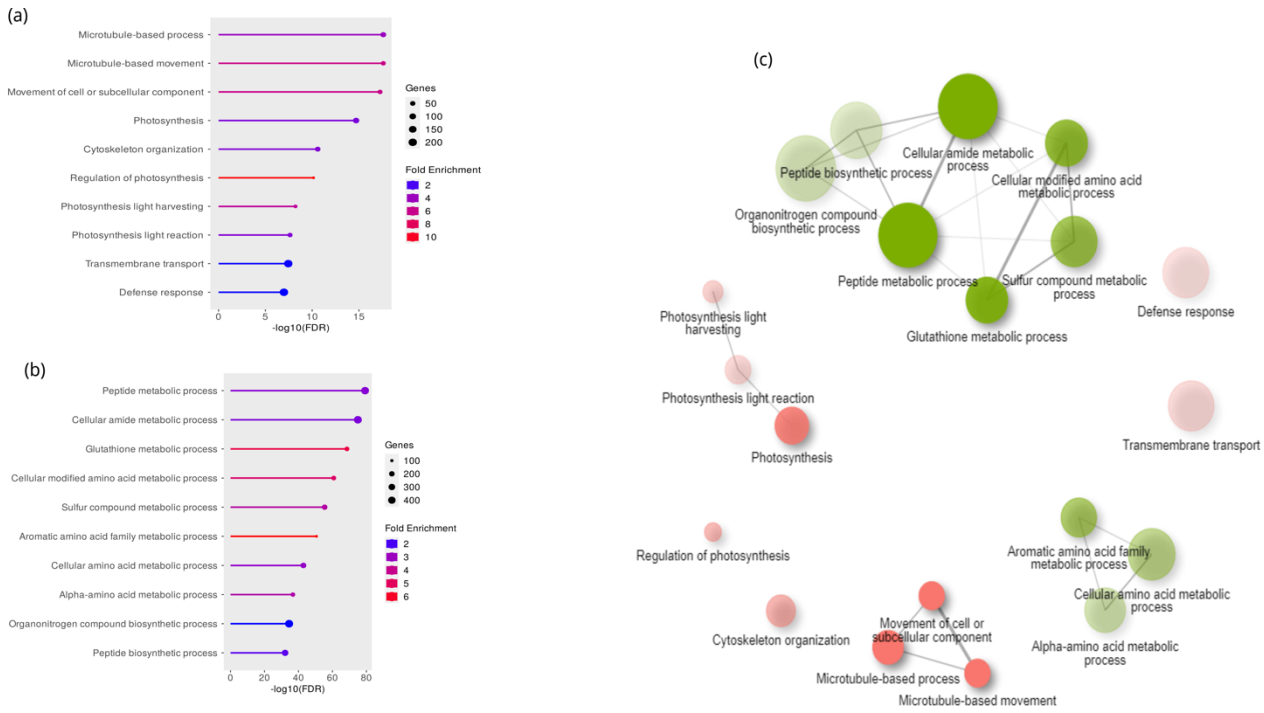

Fig. 5.6: Gene ontology (biological process) enrichment of Rosso top ten DEGs. (a) most enriched terms related to downregulated DEGs; (b) most enriched terms related to upregulated DEGs; (c) network showing connection among the cited terms (red = downregulated; green = upregulated).

Glutathione metabolic process was also among the top enriched upregulated biological process in Sumai3 (Fig. 5.7), together with GO terms related to synthesis of phenylpropanoids (suggested by terms like “cinnamic acid metabolic process” and “L-phenylalanin metabolic process”). Indeed, the most enriched molecular function for upregulated DEGs was the ammonia-lyase activity and the top cellular component was the extracellular region. In the resistant genotype the main downregulated biological processes were associated to the cytokinin-activated signaling pathway and the glycerolipidic biosynthetic pathway. Among the cellular components the chloroplast was the main associated to downregulated DEGs and the zinc ion binding was the most suppressed molecular function.

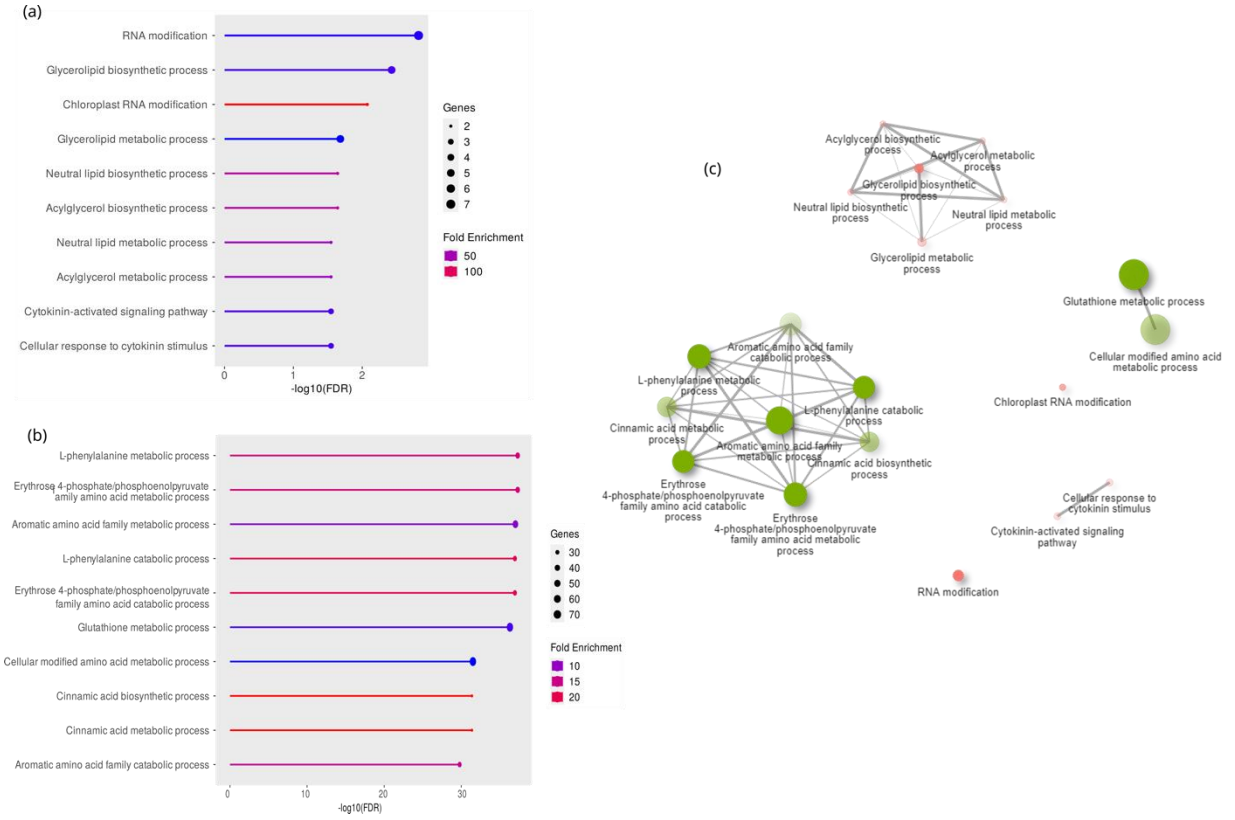

Fig. 5.7: Gene ontology (biological process) enrichment of Sumai3 top ten DEGs. (a) most enriched terms related to downregulated DEGs; (b) most enriched terms related to upregulated DEGs; (c) network showing connection among the cited terms (red = downregulated; green = upregulated).

Finally, for Vanilnoir (Fig. 5.8) only upregulated DEGs were significantly assigned to 100 biological processes and 78 molecular function, with “glutathione metabolic process” and “aromatic amino acid family metabolic process” as main enriched biological process terms and “glutathione transferase activity” and “ammonia-lyase activity” as main molecular function terms. Considering cellular components, upregulated DEGs were mainly assigned to extracellular region and apoplast cellular components, while downregulated DEGs were related to the histone methyltransferase complex.

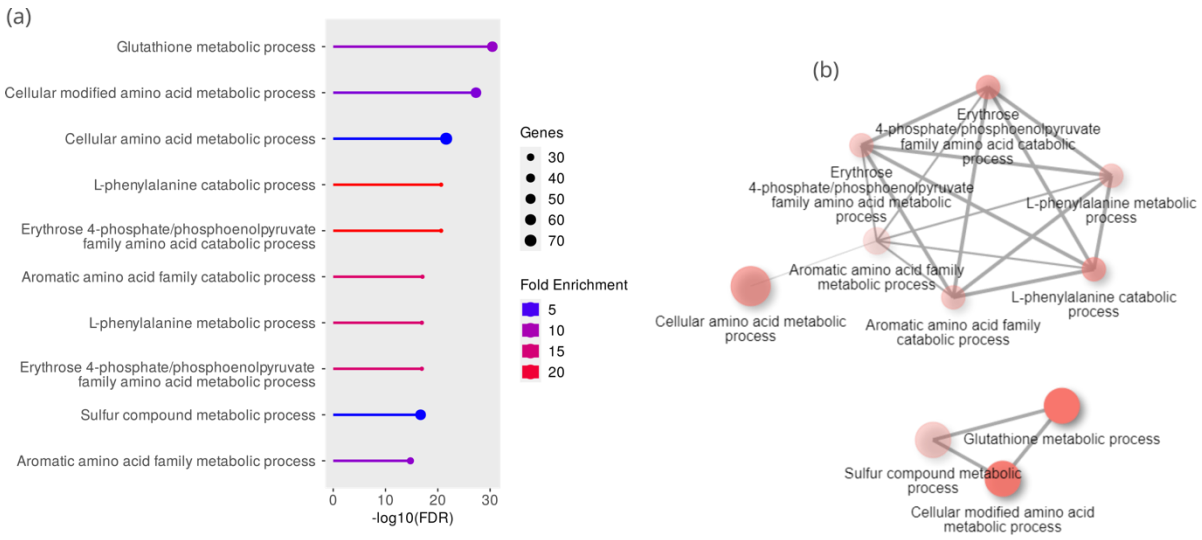

Fig. 5.8: Gene ontology (biological process) enrichment of Vanilnoir top ten DEGs. (a) most enriched terms related to upregulated DEGs; (b) network showing connection among the cited terms.

According to GO enrichment analysis, the four genotypes shared similar upregulated biological processes. To deepen this finding and highlight the differences among genotypes, a Venn's diagram was created considering all the enriched upregulated terms resulted from the enrichment analysis (Fig. 5.9a).

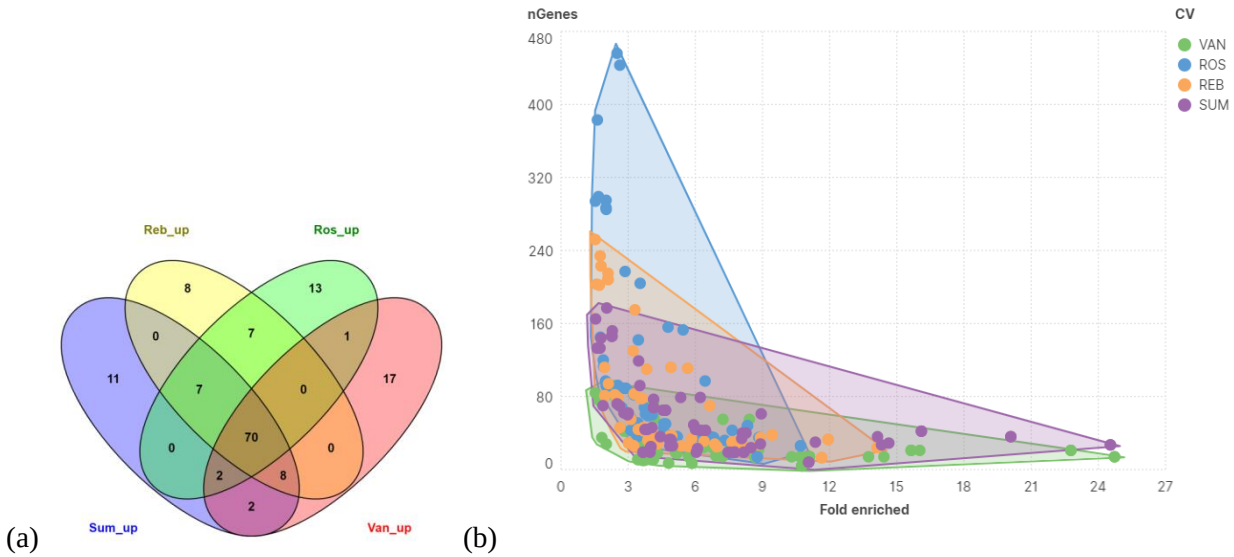

Fig. 5.9: (a) Venn's diagram showing the significantly upregulated enriched terms (biological process) shared among the genotypes. (b) Graphical representation of the 70 biological process terms significantly enriched in the four genotypes. Each dot represents a GO term, having a different number of genes differentially expressed (nGenes) and different fold enrichment in the four genotypes. Convex hulls show the distribution of the terms. Different color refers to different genotype. Image created using SCImago Graphica.

Among the 145 enriched biological processes assigned to upregulated DEGs, 70 were commonly upregulated in all the genotypes. In this group there were several of the abovementioned functions, such as "L-phenylalanine metabolic process", "Erythrose 4-phosphate/phosphoenolpyruvate family amino acid metabolic process", and "Glutathione

metabolic process". Other noteworthy functions enriched in all the genotypes were: "Ethylene-activated signaling pathway", "Response to ethylene" and "Cellular response to ethylene stimulus", as well as "Response to biotic stimulus" (which comprehend genes encoding for pathogenesis-related protein PR1, putative fatty acid binding proteins involved in systemic acquired resistance and chitinases), and the terms "Cellular detoxification" and "Detoxification". As expected, all these functions were recognized to be strongly related to wheat response to FHB (as argued in the Discussion paragraph). While no differences were noted in the biological processes activated in response to infection across various genotypes, significant variations emerged between resistant and susceptible lines when examining the expression levels of individual processes. Notably, when considering the number of genes associated to each term and their relative fold enrichment (as reported in Fig. 5.9b), it becomes evident that Vanilnoir and Sumai3 exhibited comparatively lower gene counts for certain biological functions while displaying a high fold enrichment. In particular cinnamic acid metabolic process was the highest fold enriched terms (24.54 fold enriched in Sumai, with 27 genes, and 24.73 fold enriched in Vanilnoir, with 14 DEGs), followed by L-phenylalanine catabolic process (20.09 fold enriched in Sumai, with 36 genes, and 22.77 fold enriched in Vanilnoir, with 21 genes), and Erythrose 4-phosphate/phosphoenolpyruvate family amino acid metabolic process (36 genes 20.09 fold enriched in Sumai and 21 genes 22.77 fold enriched in Vanilnoir). On the other hand, Rebelde and Rosso reported a higher number of DEGs assigned to the 70 common terms but having lower fold enrichment (*i.e.* "Cellular amide metabolic process" was assigned to 456 genes in Rosso but was only 2.50 fold enriched, or "Small molecule metabolic process" was assigned to 383 genes in Rebelde, but having 1.62 fold enrichment).

Furthermore, 11 biological processes were exclusively upregulated in Sumai3, including signal transduction, regulation of gibberellic acid mediated signaling pathway and response to chitin. Other 8 terms were exclusively assigned to Rebelde (such as positive regulation of developmental growth, regulation of organ growth, response to heat, cellular response to organic substance) and 13 only to Rosso (such as defense response to fungus, chorismate metabolic process, positive regulation of growth). Finally, Vanilnoir was significantly enriched in terms related to the regulation of gene expression (like regulation of transcription DNA-templated or regulation of nucleic acid-templated transcription), and the DEGs which received these biological processes mainly had transcription factor function related to the ethylene-activated signaling pathway.

Moreover, DEGs were assigned to 56 KEGG pathways. The KEGG enrichment analysis (Fig. 5.10) showed that the upregulated DEGs (for all the considered genotypes) were significantly associated with: glutathione metabolism, phenylalanine tyrosine and tryptophan biosynthesis, MAPK signaling pathway, phenylalanine metabolism, phenylpropanoid biosynthesis, plant-pathogen interaction, betalain biosynthesis, tyrosine metabolism, isoquinoline alkaloid biosynthesis and biosynthesis of secondary metabolites. Some pathways were exclusively enriched in one or more genotypes. Flavone and flavonol biosynthesis, cysteine and methionine metabolism and C5-branched dibasic acid metabolism were only assigned to Rebelde upregulated DEGs. Ribosome and sphingolipid metabolism were enriched solely in Rosso. Flavonoid biosynthesis, monoterpenoid biosynthesis, thiamine metabolism and steroid biosynthesis were assigned only to Sumai3 upregulated DEGs, while five pathways were commonly assigned to Vanilnoir and Sumai3 upregulated DEGs (diterpenoid biosynthesis, tryptophan metabolism, metabolic pathways, nitrogen metabolism and amino sugar and nucleotide sugar metabolism). Notably, flavonoid biosynthesis were upregulated in Sumai3 and downregulated in Rebelde.

Downregulated DEGs were assigned to 28 pathways. 17 of them were only associated to DEGs of Rosso, and included different pathway of primary metabolism (such as photosynthesis, photosynthesis-antenna proteins, carbon metabolism, carbon fixation, aminoacyl-tRNA biosynthesis) and secondary metabolism (such as biosynthesis of various plant secondary metabolites and carotenoid biosynthesis). In addition to flavonoid biosynthesis, biosynthesis of nucleotide sugars, amino sugar and nucleotide sugar metabolism, biosynthesis of secondary metabolites, ubiquinone and other terpenoid-quinone biosynthesis, plant hormone signal transduction and phenylpropanoid biosynthesis were exclusively downregulated in Rebelde. Finally, brassinosteroid biosynthesis, nucleocytoplasmic transport and endocytosis were significantly downregulated in Vanilnoir.

Fig. 5.10: KEGG pathway enrichment visualized using SCImago Graphica. Shape, color and dimension of the marks were related to up/down- regulation, FDR and Fold enrichment, as explained in the legend on the right.

5.3.2.2. Phenylpropanoids biosynthetic pathway

Considering that the accumulation of phenolic compounds is the distinctive feature of pigmented genotype and that phenylpropanoids and flavonoids biosynthetic pathways were significantly enriched in RNAseq analysis, these two pathways were studied more in detail.

As shown in the KEGG pathway representation showed in fig. 5.11, all genes involved in phenylpropanoids biosynthetic pathway (KEGG map00940) were mostly upregulated in Sumai3 and Vanilnoir, while some of them were downregulated in Rebelde and Rosso (Fig. 5.12). These downregulated genes in Rebelde e Rosso encoded for: the 4-coumarate-CoA ligase (4CL; EC:6.2.1.12), ligases involved in forming carbon-sulfur bonds as acid-thiol ligases; the shikimate O-hydroxycinnamoyltransferase (HCT; EC:2.3.1.133) or putrescine hydroxycinnamoyltransferase 1-like; the 5-*O*-(4-coumaroyl)-D-quinate 3'-monooxygenase (C3'H, EC:1.14.14.96), upregulated in Rosso and downregulated in Rebelde; the caffeoyl-CoA O-methyltransferase (CCoAOMT; EC:2.1.1.104), upregulated in Rosso and downregulated in Rebelde; the coniferyl-aldehyde dehydrogenase (COMT; EC:1.2.1.68) involved in the synthesis of ferulic acid and sinapic acid.

5.3.2.3. Flavonoids and anthocyanin biosynthetic pathways

Flavonoids biosynthetic pathway (KEGG map00941) was mainly activated in Sumai3 and Vanilnoir, with some downregulated function. DEGs encoding flavonoid 3'-monooxygenase (F3'5'H; EC:1.14.14.82), flavone synthase II (FNS II, EC:1.14.19.76) were downregulated in Sumai3, DEGs encoding for flavonol synthase (FLS, EC:1.14.20.6) and the leucoanthocyanidin reductase (LAR, EC:1.17.1.3) were downregulated in both Suami3 and Vanilnoir, while genes encoding for chalcone isomerase (CHI, EC:5.5.1.6) were downregulated in Sumai3 and having basal expression in Vanilnoir (Fig 5.13).

In Rebelde and Rosso this pathway was mainly suppressed. For Rebelde the only upregulated genes encoded for trans-cinnamate 4-monooxygenase (C4H, EC:1.14.14.91). For Rosso, in addition to C4H, also genes encoding for anthocyanidin reductase (ANR, EC:1.3.1.77), 5-*O*-(4-coumaroyl)-D-quinate 3'-monooxygenase (C3'H, EC:1.14.14.96), caffeoyl-CoA O-methyltransferase (CCoAOMT, EC:2.1.1.104) and bifunctional dihydroflavonol 4-reductase/flavanone 4-reductase (DFR, EC:1.1.1.219- 1.1.1.234) were upregulated, while naringenin 3-dioxygenase (F3H, EC:1.14.11.9) function was basally expressed (Fig. 5.14).

In the anthocyanin biosynthetic pathway (KEGG map00942) the only gene differentially expressed due to the infection was the one encoding for anthocyanidin 3-*O*-glucosyltransferase (BZ1, EC:2.4.1.115), which can glucosylate the anthocyanidins delphinidin, peonidin, pelargonidin and malvidin, forming their glucosilated forms. This function was suppressed in Rebelde, Rosso and Sumai, while it was upregulated in Vanilnoir.

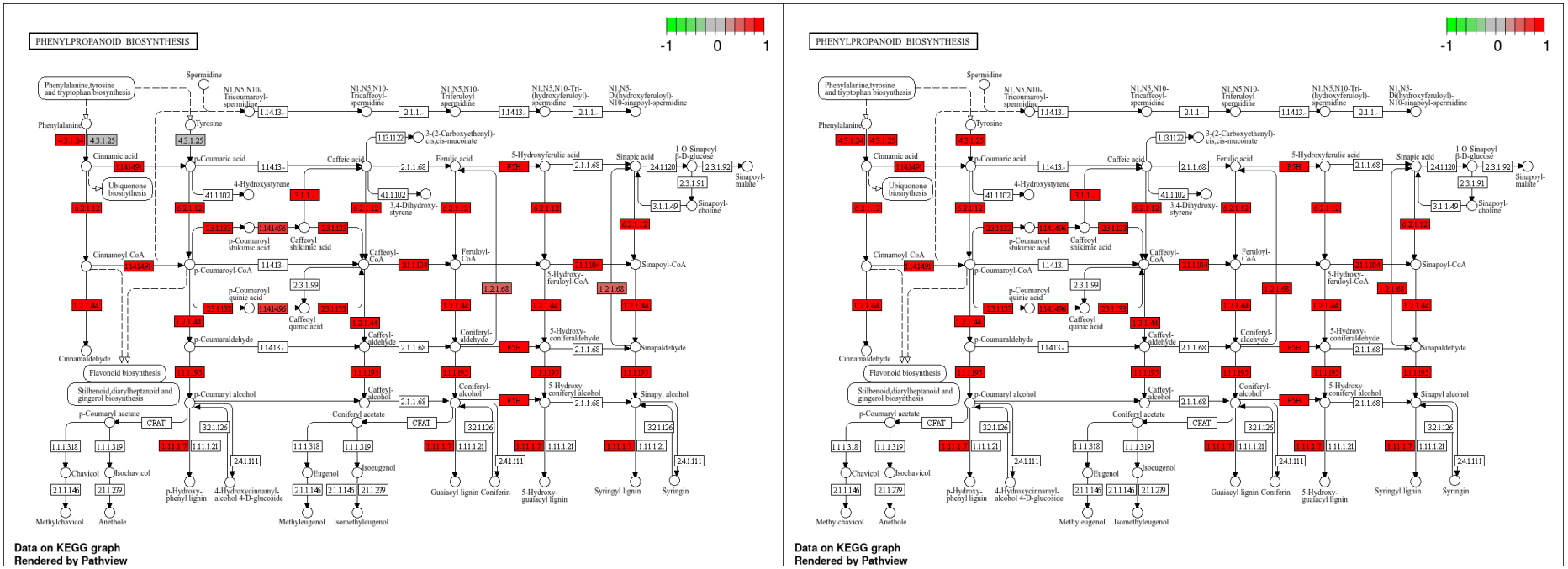

Fig. 5.11: Phenylpropanoid biosynthesis pathway of Sumai (left) and Vanilnoir (right) reconstructed based on unigenes of *Triticum aestivum* associated with flavonoid biosynthesis. The map was drawn using Kyoto Encyclopedia of Genes and different color represent differential expression of corresponding genes (obtained using iDEP 1.13).

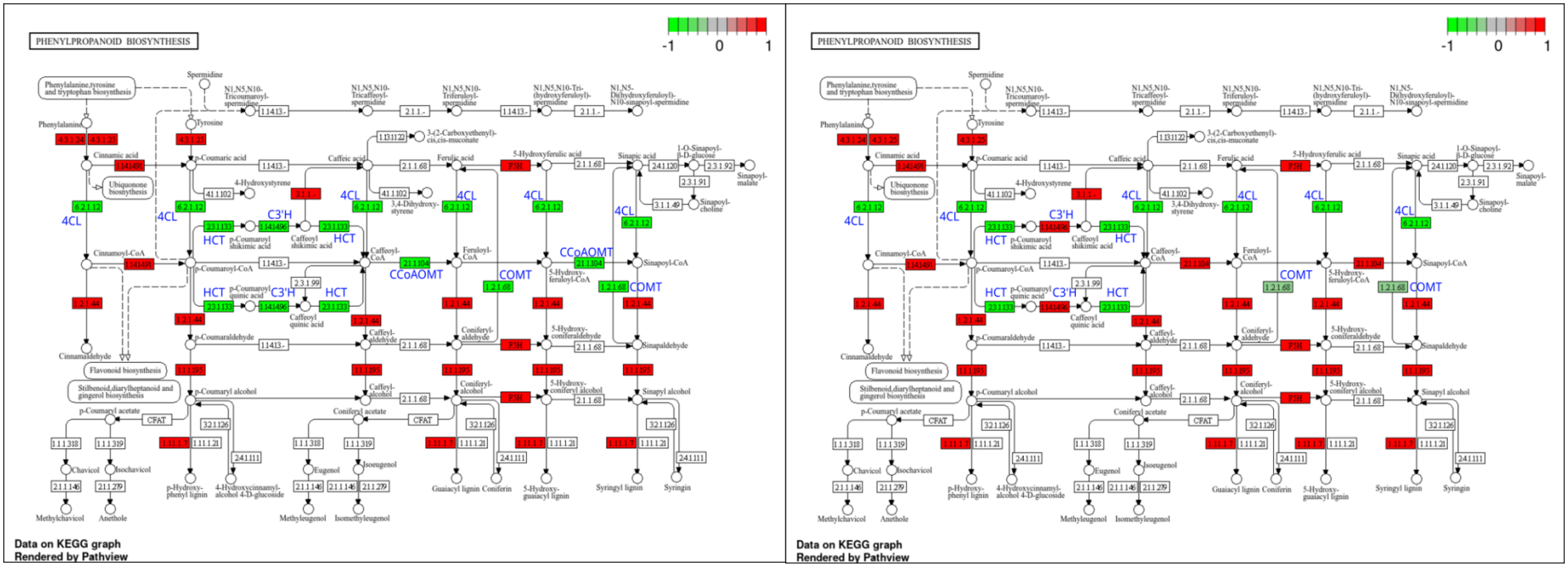

Fig. 5.12: Phenylpropanoid biosynthesis pathway of Rebelde (left) and Rosso (right) reconstructed based on unigenes of *Triticum aestivum* associated with flavonoid biosynthesis. The map was drawn using Kyoto Encyclopedia of Genes and different color represent differential expression of corresponding genes (obtained using iDEP 1.13). Enzymes names highlighted in blue are explained in the text.

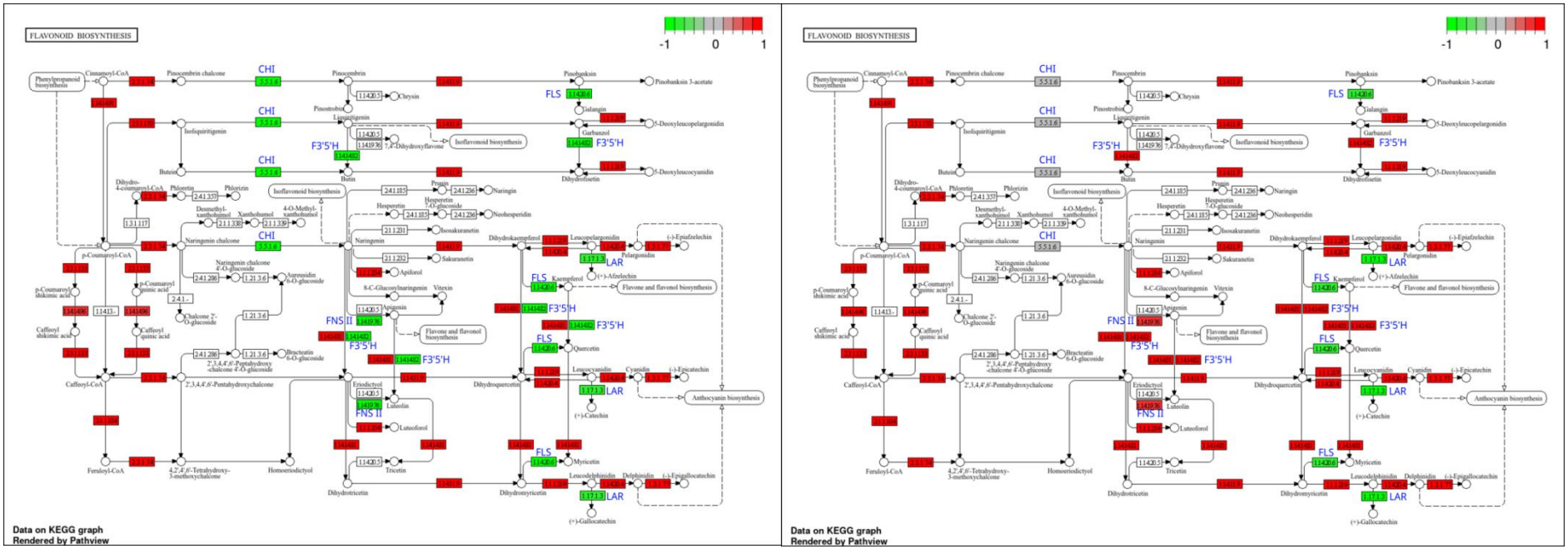

Fig. 5.13: Flavonoid biosynthesis pathway of Sumai (left) and Vanilnoir (right) reconstructed based on unigenes of *Triticum aestivum* associated with flavonoid biosynthesis. The map was drawn using Kyoto Encyclopedia of Genes and different color represent differential expression of corresponding genes (obtained using iDEP 1.13). Enzymes names highlighted in blue are explained in the text.

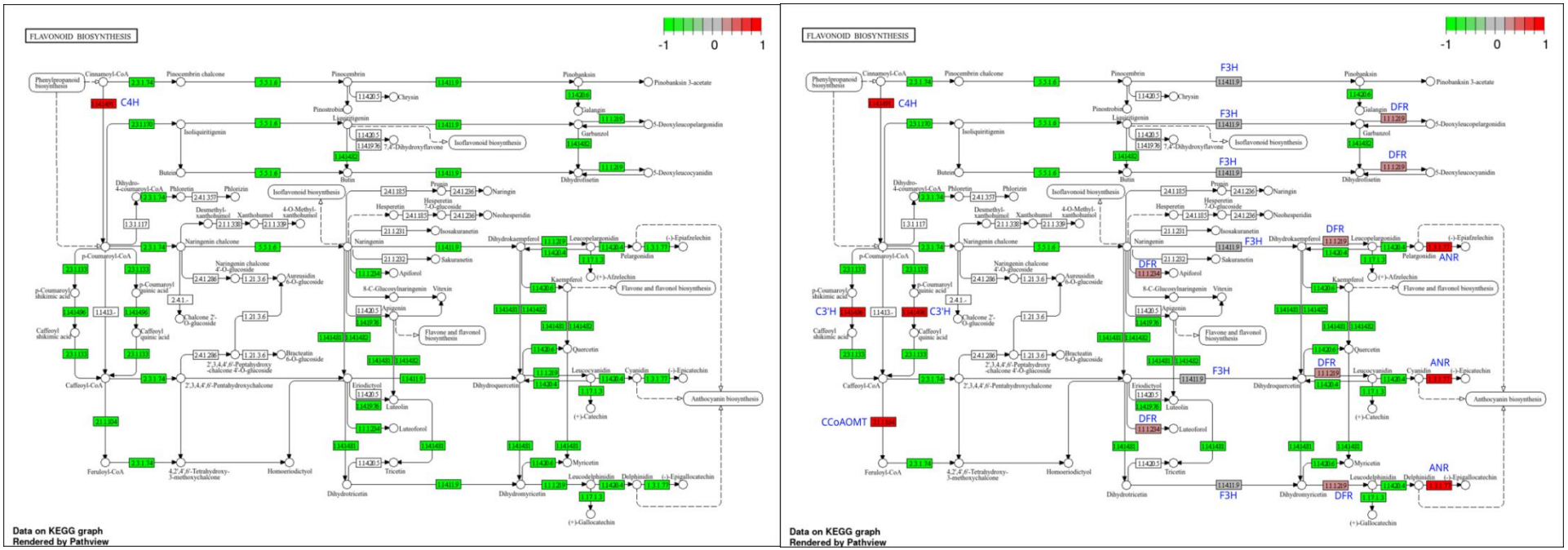

Fig. 5.14: Flavonoid biosynthesis pathway of Rebelde (left) and Rosso (right) reconstructed based on unigenes of *Triticum aestivum* associated with flavonoid biosynthesis. The map was drawn using Kyoto Encyclopedia of Genes and different color represent differential expression of corresponding genes (obtained using iDEP 1.13). Enzymes names highlighted in blue are explained in the text.

5.3.2.4. Common differentially regulated genes in Vanilnoir and Sumai3

In order to focus the attention on the similarities between Sumai3 and Vanilnoir and rise hypothesis on Vanilnoir resistance mechanism, Venn's diagrams reporting common statistically significant upregulated DEGs (Fig. 5.15a) and common statistically significant downregulated DEGs (Fig. 5.15b) were created. Only 67 genes were specifically upregulated in Vanilnoir and Sumai3, while no common downregulated gene was recorded. Considering that both Sumai3 and Vanilnoir showed Type II resistance, this group of upregulated genes was analyzed more in detail, looking for the best annotation for each single gene.

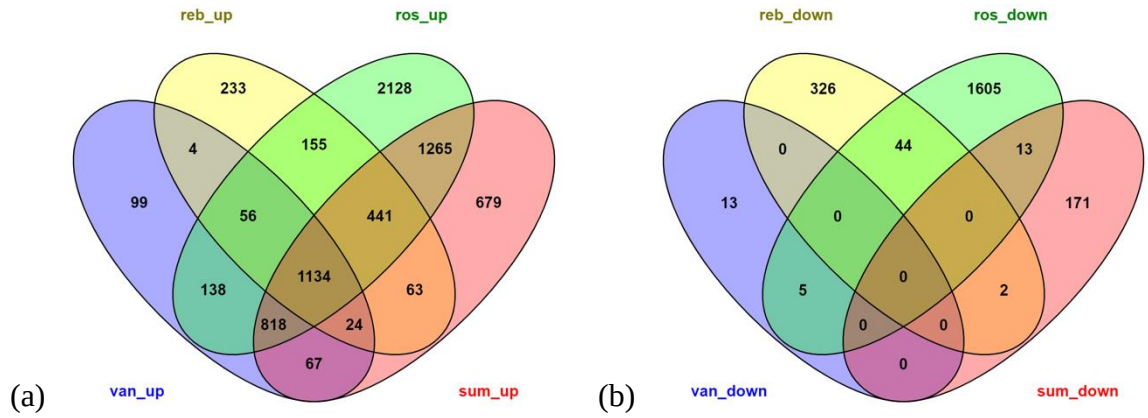

Fig. 5.15: Venn's diagrams showing number of upregulated DEGs (a) and downregulated DEGs (b) in common among the different groups.

The genes having relative expression < 1 Log2FoldChange were excluded, reducing from 67 to 57 genes. On these 57 genes, 9 encoded receptors belonging to the family of leucine-rich repeat receptor-like kinases (LRR-RLKs) (Table 5.2), while 4 encoded for disease resistance proteins and for pathogen related protein (Table 5.3). Other function were significantly upregulated in both Sumai and Vanilnoir (Table 5.4), all of them having some connection with reaction to disease, such as: TRAESCS3A02G448400 and TRAESCS5D02G276300 encoding for key enzymes for lignin biosynthesis; TRAESCS3B02G526600, TRAESCS3D02G249500, and TRAESCS1B02G454200 encoding for chitinases; TRAESCS5D02G522300 and TRAESCS2A02G539000 encoded for an enzyme and a protein (respectively) related to ions chelation and detoxification. Four genes encoded for transcription factors: CBFIIIa-6.2 (related to cold stress), WRKY19-like, AP2/ERF and B3 domain-containing protein and dof-zinc finger protein DOF3.1-like. Notably 2 genes encoded for flavonoids biosynthesis related genes, in particular a scopoletin glucosyltransferase-like (TRAESCS7D02G170700) and the anthocyanidin reductase ((2S)-flavan-3-ol-forming) (ANR, TRAESCS2D02G481600). Some genes were not annotated on IWGCS assembly, resulting as "unknown function" or as "uncharacterized locus". The amino acid sequences related to these genes were aligned using tbalstn (NCBI) in order to find the orthologues (the best matching entries are listed in Table 5.5). The alignment results suggested that TRAESCS3D02G265500 may encode for an additional LRR-RLKs, TRAESCS3A02G501400 for ADP-ribosylation factor-like protein 6-interacting protein 4 (which showed antifungal function and DON affinity), TRAESCS7A02G333400 may encode for an anthocyanin 5-aromatic acyltransferase-like (ACT), TRAESCS7A02G420300 for an iron-phytosiderophore transporter, TRAESCS5B02G520800 may encode for a small

defense-associated protein, while TRAESCS3D02G518600 is a non-translating CDS. For two genes (TRAESCS3D02G368600 and TRAESCS2B02G223100) no function was assigned for either *T. aestivum* genes or for their orthologues.

Table 5.2: Common DEGs in Vanilnoir and Sumai encoding for membrane receptors

Ensembl Gene ID	Locus in IWGSC (NCBI)	Type	Chr	Position (Mbp)	Description	VAN Log2 foldchange	SUM Log2 foldchange
TRAESCS5D02G193700	123124720	protein_coding	5D	297.957977	probable LRR receptor-like protein kinase At1g51890	7.45	7.20
TRAESCS2D02G574000	123047593	protein_coding	2D	638.804298	PREDICTED: Triticum aestivum probable LRR receptor-like serine/threonine-protein kinase At3g47570 (LOC123047593), mRNA	7.20	4.59
TRAESCS2B02G132500	123040676	protein_coding	2B	98.81723	G-type lectin S-receptor-like serine/threonine-protein kinase At2g19130	6.78	4.58
TRAESCS4B02G216000	123094977	protein_coding	4B	455.754699	G-type lectin S-receptor-like serine/threonine-protein kinase At2g19130	5.25	6.40
TRAESCSU02G092400	123150067	protein_coding	Un	81.993945	wall-associated receptor kinase 3-like	4.89	3.55
TRAESCS2B02G008300	123039952	protein_coding	2B	4.751819	Serine/threonine-protein kinase	4.79	5.95
TRAESCS5D02G095300	123124440	protein_coding	5D	104.595635	putative leucine-rich repeat receptor-like protein kinase At2g19210	4.56	4.18
TRAESCS5D02G398800	123122835	protein_coding	5D	464.697435	probable LRR receptor-like serine/threonine-protein kinase At3g47570	2.38	3.10
TRAESCS7A02G476700	123149196	protein_coding	7A	670.821522	probable LRR receptor-like serine/threonine-protein kinase At3g47570	1.18	1.89

Table 5.3: Common DEGs in Vanilnoir and Sumai encoding for disease related proteins

Ensembl Gene ID	Locus in IWGSC (NCBI)	Type	Chr	Position (Mbp)	Description	VAN Log2 foldchange	SUM Log2 foldchange
TRAESCS1A02G056700	123085180	protein_coding	1A	36.794163	PREDICTED: Triticum aestivum disease resistance protein Pik-1-like (LOC123085180)	4.04	4.25
TRAESCS2D02G330100	123049485	protein_coding	2D	423.208979	disease resistance protein RGA5-like	4.02	2.46
TRAESCS6A02G403200	123131399	protein_coding	6A	610.642323	barwin-like (PR4)	2.77	3.94
TRAESCS1A02G025500	123186100	protein_coding	1A	12.207569	disease resistance protein RPM1-like	2.24	2.83

Table 5.4: Common DEGs Vanilnoir and Sumai encoding for other functions (continue in the next page)

Ensembl Gene ID	Locus in IWGSC (NCBI)	Type	Chr	Position (Mbp)	Description	Function	VAN Log2 foldchange	SUM Log2 foldchange
TRAESCS5D02G522300	123126125	protein_coding	5D	542.990667	probable aldo-keto reductase 2	detoxificatoin	7.86	6.10
TRAESCS5D02G488400	123125977	protein_coding	5D	523.313281	acetylserotonin O-methyltransferase 1-like	Melatonin bios.	7.19	5.34
TRAESCS3B02G306900	123065605	protein_coding	3B	492.757903	early nodulin-like protein 1	Transport - early nodulin	6.88	7.81
TRAESCS7D02G076900	123170740	protein_coding	7D	45.279189	protein NRT1/ PTR FAMILY 2.13-like	Transporter - nitrate	6.45	6.79
TRAESCS2B02G132700	123040678	protein_coding	2B	99.247357	UDP-glucosyltransferase 29-like	terpens - triterpene saponins	6.42	4.92
TRAESCS2B02G445400	123039362	protein_coding	2B	638.519552	ent-kaurene oxidase-like protein 1	Hormones - gibberellins	5.43	8.52
TRAESCS7D02G131600	123168278	protein_coding	7D	83.455283	probable glutathione S-transferase GSTU6	GTS	5.37	3.96
TRAESCS3A02G448400	123059112	protein_coding	3A	688.578347	probable cinnamyl alcohol dehydrogenase 1	CAD – Lignin bios.	4.68	3.36
TRAESCS3D02G429600	123075288	protein_coding	3D	544.276834	probable glutathione S-transferase GSTU6	GST	3.87	5.30
TRAESCS3B02G471900	123066248	protein_coding	3B	720.263004	probable glutathione S-transferase GSTU6	GST	3.72	5.41
TRAESCS5A02G004600	123101938	protein_coding	5A	3.175334	obtusifoliol 14-alpha demethylase-like	Lipids – biosynthesis	3.66	4.13
TRAESCS5D02G183700	101290585	protein_coding	5D	285.453966	alpha-dioxygenase 1	Lipids - fatty acid bios.	3.09	3.10
TRAESCS7D02G170700	123167517	protein_coding	7D	123.15669	scopoletin glucosyltransferase-like	Flavonoids – coumarins bios.	3.06	3.04
TRAESCS5A02G383900	123107811	protein_coding	5A	581.572707	Glycosyltransferase	extracellular polysaccharides bios.	3.00	3.29
TRAESCS5D02G433200	123125681	protein_coding	5D	489.01296	dehydrin Rab15-like	stress tolerance	2.90	2.56
TRAESCS2D02G481600	123054723	protein_coding	2D	584.533176	anthocyanidin reductase ((2S)-flavan-3-ol-forming)-like	Flavonoids – flavan-3-ol bios.	2.85	2.35
TRAESCS5A02G312000	780570	protein_coding	5A	523.615616	CBFIIIa-6.2	TF - cold stress	2.57	2.41

TRAESCS1B02G440600	123147346	protein_coding	1B	662.016062	transcription factor WRKY19-like	TF – WRKY	2.57	2.89
TRAESCS3B02G526600	123072409	protein_coding	3B	768.740001	glucan endo-1,3-beta-glucosidase GIII-like	Chitinase	2.57	2.89
TRAESCS3D02G249500	123078821	protein_coding	3D	349.641324	glucan endo-1,3-beta-glucosidase 14-like	Chitinase	2.56	3.11
TRAESCS3B02G574600	123066863	protein_coding	3B	805.003162	(S)-8-oxocitronellyl enol synthase ISY1-like	Monoterpene bios.	2.32	1.57
TRAESCS2B02G279200	123045097	protein_coding	2B	385.560644	cytochrome P450 81Q32-like	Oxidoreductase	2.04	2.47
TRAESCS5A02G382800	123104984	protein_coding	5A	580.799815	calmodulin-like protein 4	Calcium sensors-MAPK	2.03	1.99
TRAESCS1A02G283100	123058813	protein_coding	1A	480.80872	glycerol-3-phosphate acyltransferase 5-like	Lipids - lysophosphatidic acid bios.	1.89	1.78
TRAESCS3B02G125100	123064986	protein_coding	3B	99.170508	dof zinc finger protein DOF3.1-like	TF - Zinc finger	1.84	1.85
TRAESCS7D02G122600	123167867	protein_coding	7D	76.731499	glutamyl-tRNA reductase 3, chloroplastic-like	Chlorophyll	1.81	2.64
TRAESCS2A02G539000	123186474	protein_coding	2A	751.546349	heavy metal-associated isoprenylated plant protein 39-like	Detoxificatoin	1.79	1.63
TRAESCS1B02G454200	123148549	protein_coding	1B	670.142374	PREDICTED: Triticum aestivum glucan endo-1,3-beta-glucosidase 13-like (LOC123148549), mRNA	Chitinase	1.78	2.30
TRAESCS3D02G368600	123075025	protein_coding	3D	481.878036	uncharacterized LOC123075025	Unknown	1.73	2.94
TRAESCS5D02G276300	123121951	protein_coding	5D	378.956602	cinnamoyl-CoA reductase 1-like	Lignin bios.	1.73	1.65
TRAESCS1A02G125400	123041840	protein_coding	1A	149.352287	IQ domain-containing protein IQM1-like	stomatal mouvement	1.70	1.97
TRAESCS2B02G223100	123044467	protein_coding	2B	212.930775	uncharacterized LOC123044467	Unknown	1.64	2.77
TRAESCS1A02G372300	123066132	protein_coding	1A	548.789228	AP2/ERF and B3 domain-containing protein Os05g0549800-like	TF - AP2	1.49	1.73
TRAESCS7D02G047000	123164097	protein_coding	7D	24.326011	bisdemethoxycurcumin synthase-like	Polyketide bios.	1.47	2.20
TRAESCS5A02G433600	123107990	protein_coding	5A	617.183146	mitogen-activated protein kinase mpkC-like	MAPK	1.28	2.23
TRAESCS3D02G373600	123079894	protein_coding	3D	487.222616	magnesium transporter MRS2-E-like	Transporter – Magnesium	1.20	2.81
TRAESCS6D02G230500	123145030	protein_coding	6D	323.712099	probable trehalose-phosphate phosphatase 1	Trehalose bios.	1.16	1.75
TRAESCS2B02G444500	123046467	protein_coding	2B	637.444754	36.4 kDa proline-rich protein-like	Proline	1.14	1.70

Table 5.5: Common DEGs in Vanilnoir and Sumai with unknown function on *T. aestivum*, but having putative annotation in other species. This table show the results of the alignment obtained using tblastn (NCBI).

VAN Log2 fold change	SUM Log2 fold change	Ensembl Gene ID	Locus in IWGSC (NCBI)	Description of best mach (tbalstn)	Scientific Name	Max Score	Total Score	Query Cover	E value	Per. ident	Acc. Len	Accession	biological process	molecular function	cellular component
7.023	4.074	TRAESCS3D02G265500	Not assigned	PREDICTED: *Aegilops tauschii* subsp. *strangulata* F-box/FBD/LRR-repeat protein At5g22700-like (LOC109754131), mRNA	*Aegilops tauschii* subsp. *strangulata*	808	808	100%	0	99.74%	1179	XM_020313086.1	-	protein binding	-
6.833	5.671	TRAESCS3A02G501400	uncharacterized LOC123059478	PREDICTED: *Triticum dicoccoides* ADP-ribosylation factor-like protein 6-interacting protein 4 (LOC119282543), mRNA	*Triticum dicoccoides*	73.9	73.9	100%	2.00E-14	49.38%	599	XM_037562738.1	-	-	-
6.598	3.781	TRAESCS7A02G333400	Not assigned	PREDICTED: *Hordeum vulgare* subsp. *vulgare* anthocyanin 5-aromatic acyltransferase-like (LOC123413340), mRNA	*Hordeum vulgare* subsp. *vulgare*	602	602	100%	0	70.89%	1480	XM_045106282.1	-	-	-
6.391	6.023	TRAESCS7A02G420300	Not assigned	PREDICTED: *Hordeum vulgare* subsp. *vulgare* iron-phytosiderophore transporter YSL15-like (LOC123412249), transcript variant X2, mRNA	*Hordeum vulgare* subsp. *vulgare*	966	966	100%	0	93.35%	2082	XM_045105196.1	transmembrane transport	oligopeptide transmembrane transporter activity	integral component of membrane
3.850	6.950	TRAESCS5B02G520800	Not assigned	PREDICTED: *Aegilops tauschii* subsp. *strangulata* protein SDA1 homolog (LOC109756272), mRNA	*Aegilops tauschii* subsp. *strangulata*	277	277	78%	1.00E-90	69.11%	765	XM_020315127.1	-	-	-

5.3.2.5. RNAseq validation and relative expression in the other pigmented lines

Five key genes for flavonoids biosynthesis and defense response were validated by RT-qPCR, across the 4 considered genotypes, obtaining 20 comparison RNAseq *vs* RT-qPCR. These considered genes encoded for: phenylalanine ammonia-lyase (PAL, TRAESCS2A02G380800), cinnamate 4-hydroxylase (C4H, TRAESCS3B02G167400), β-1,3-glucanase (PR2, TRAESCS1D02G237500), dihydroflavonol 4-reductase (DFR, TRAESCS3A02G226600), and chalcone synthase (CHS, TRAESCS2A02G025700). Changes in the expression levels of the five genes were consistent with the transcriptomic data (r^2= 0.65, p = 0.0001; Fig. S5.7), which verified the reliability of the transcriptome data.

The relative expression of these genes was analyzed also in the pigmented genotypes excluded from the RNAseq analysis (Purendo, Skorpion and Indigo).

A graphical representation of the relative expression of the selected genes in the seven genotypes is shown in Fig. 5.16. *PR2* was boosted in Rebelde (4.95 Log_2 fold-change) and upregulated in Indigo (1.30 Log_2 fold-change), while in Vanilnoir, Skorpion and Sumai3 it showed a basal expression (-0.37, -0.25, and 0.45 Log_2 fold-change respectively) and it was downregulated in Rosso (-2.76 Log_2 fold-change), and Purendo (-2.65 Log_2 fold-change). *PAL* exhibited upregulation across all genotypes, with particularly notable increases in Rosso (3.78 Log_2 fold-change), Sumai (3.75 Log_2 fold-change), Rebelde (3.81 Log_2 fold-change) and Purendo (2.49 Log_2 fold-change). Similarly, *Fusarium* infection increased the expression level of *C4H* in all the genotypes, but in particular in Rebelde (2.23 Log_2 fold-change) and Purendo (2.08 Log_2 fold-change). *DFR* was downregulated in Rebelde (-1.24 Log_2 fold-change), Purendo (-1.90 Log_2 fold-change) and Indigo (-1.72 Log_2 fold-change), showed basal expression level in Rosso (0.06 Log_2 fold-change), Sumai (-0.20 Log_2 fold-change) and Skorpion (-0.19 Log_2 fold-change) and upregulated in Vanilnoir (1.86 Log_2 fold-change). *CHS* was downregulated in Rosso (-1.61 Log_2 fold-change), Sumai3 (-0.59 Log_2 fold-change), Rebelde (-1.99 Log_2 fold-change) and Skorpion (-0.57 Log_2 fold-change), upregulated in Vanilnoir (0.72 Log_2 fold-change) and Indigo (1.16 Log_2 fold-change) and is showed a basal expression in Purendo (-0.07 Log_2 fold-change).

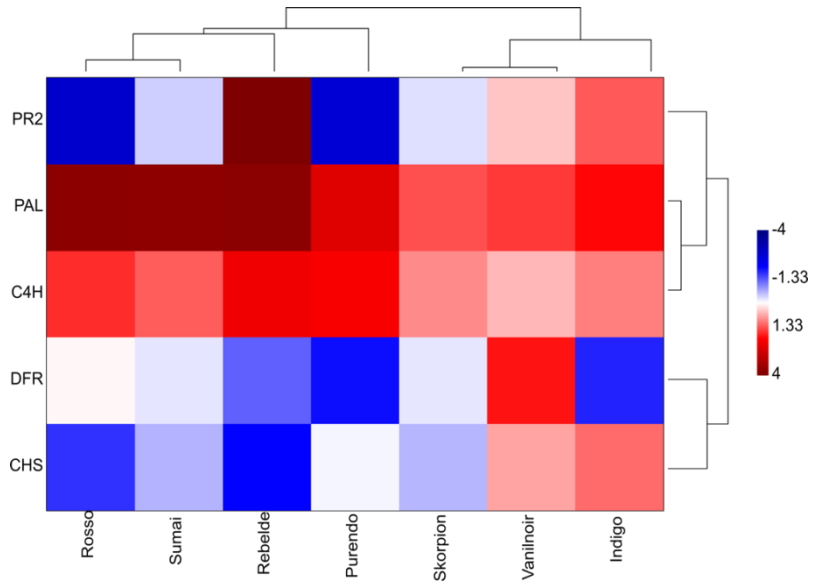

Fig. 5.16: Clustering analysis representing the relative expression of considered genes (rows) for each genotype (columns) due to *F. graminearum* infection, normalized on the un-infected (mock) control. Both rows and columns are clustered using correlation distance and average linkage. The heatmaps were constructed with Log_2 Fold Change.

5.4. Discussion

5.4.1. FHB susceptibility/resistance in pigmented genotypes

Interest on pigmented bread wheat genotypes is increasing in the last years, due to their high nutritional value (Liu et al. 2010). Despite this, very few research efforts were focused on the evaluation of an important agronomic feature like their FHB tolerance. In this study a wide variation in susceptibility among the different genotypes was reported. Other authors suggested that purple pericarp bread wheat genotypes could be more resistant than blue aleurone ones (Martin et al. 2017; Gozzi et al. 2023). Our results partially corroborate this finding.

Vanilnoir (purple pericarp) resulted as the most resistant genotype, confirming the results obtained by Martin et al. (2017). In particular, the reduced severity (21 DPI), AUDPC and fungal biomass accumulation after point inoculation on florets suggested the presence of a type II resistance mechanism, similar to the one of Sumai3 (Zhang et al. 2018). Furthermore, Vanilnoir resulted a genotype having high TPC in the spike, with and without the infection, which may indicate the presence of constitutive metabolites (phenylpropanoids and phenolic acids) having a role in FHB tolerance (Zhou et al. 2007; Stuper-Szablewska et al. 2016). In contrast with Martin et al. (2017), Vanilnoir accumulated a considerable amount of DON.

Indigo (purple pericarp) showed an intermediate behavior between Rebelde and Sumai3, considering severity at 21 DPI and AUDPC, in accordance with Martin et al. (2017), and confirmed by the notable amount of fungal biomass accumulated.

Similarly to Indigo, Purendo (blue aleurone) showed an intermediate severity trend, AUDPC, fungal biomass, DON contamination and FDK between the resistant and the susceptible controls. Purendo is known to accumulate a remarkable amount of anthocyanins in the aleurone layer (Abdel-Aal et al. 2008). Martin et al. (2017) reported its high susceptibility to yellow rust, but its response to FHB have never been evaluated before.

Rosso is a purple pericarp genotype, but it could be considered as very susceptible to FHB, considering the high severity at 21 DPI and high AUDPC, confirmed by a marked accumulation of fungal biomass. Rosso was previously evaluated by Gozzi et al. (2023), who found a reduced DON accumulation compared to blue aleurone genotypes, like Skorpion. This finding contrast with our results, in which DON contamination in Rosso and Skorpion was not statistically different.

In this study Skorpion showed the highest severity, AUDPC, DON contamination and FDK among the considered genotypes, thus it can be considered as very susceptible, as previously reported by Martinek et al. (2013). Despite this, Skorpion showed the lowest accumulation of fungal biomass in the spike. Fungal biomass quantification is commonly employed for specific assessing of pathogen presence and diffusion in plant tissue (Knight and Sutherland 2015). However, when evaluating the susceptibility of a variety, it should be considered that symptom severity must not have to reflect the extent of fungal growth in the infected tissue (Weihmann et al. 2016). This may happen because during pathogen infection and FHB development, plant vessels become blocked, preventing water and nutrient supplies as a defense mechanism, and causing sudden spike wilting (Kang and Buchenauer 2000; Kheiri et al. 2019; Brown et al. 2010). This may result in wilted tips, with heads showing bleaching and wilting symptoms above the point of inoculation. Head bleaching due to natural absence of water and nutrients could be easily confounded with direct FHB symptoms (caused by fungal spread along the spike) (Zwart et al. 2008). A putative explanation for the limited fungal biomass could be that Skorpion overreacted to the infection, leading to the complete wilting of spike tips. This may

reduce fungal biomass accumulation but resulted in a strong yield reduction as well. An alternative supposition could be that Skorpion may lacks efficient detoxification mechanisms (Luo et al. 2023), able to counteract DON phytotoxicity (Ederli et al. 2021; Perochon and Doohan 2024), resulting in a rapid necrotization in the infection site and, thus, the wilting of the overlying spike tip. These speculations on Skorpion infection mechanism should be verified in further research.

The increase of total phenolic content in *Fusarium* infected wheat spikes may derive from two different situations: an increased biosynthesis of phenolic acids (Ma et al. 2016) or a degradation of plant cell wall (rich in ferulic acid and p-coumaric acid) by fungal enzymes (Kikot et al. 2009; Mandalà et al. 2021), resulting in the released in the soluble fraction of the cell wall bound phenolic acids (Goujon et al. 2003). Considering that TPC was evaluated at maturity stage, the increased in infected spikes is most likely due to the degradation of plant cell walls occurred during the infection process. Notably, the susceptible genotypes (Rebelde, Rosso and Skorpion) showed a stronger increase (>95%, $p<0.0001$) of TPC than the resistant (Sumai3 and Vanilnoir) and the tolerant genotypes (Indigo, Purendo). This observation may suggest that the susceptible genotypes undergo a relevant and extensive cell wall degradation, due to a more aggressive fungal infection than in the resistant or tolerant genotypes.

Considering the pigmented genotypes excluded from transcriptomics analysis, the two blue aleurone lines showed a downregulation or a basal expression of genes related to flavonoids biosynthesis (CHS and DFR), while Indigo upregulated CHS and PR2 and downregulated DFR due to the infection. This suggest that the FHB-tolerance of Indigo may be related to the activity of the β-1,3-glucanase encoded by PR2, thought to provide basal resistance against fungal pathogens (Mackintosh et al. 2007), but also flavonoids could be involved, through the production of chalcones or flavones (Ahmad et al. 2023), but not through the production of leucoanthocyanidins. On the other hand, the blue aleurone lines, known for the active anthocyanins accumulation in the grains (Abdel-Aal and Hucl 2003), appeared incapable of exploiting flavonoids biosynthesis for defense.

However, according to our results, resistance to FHB occurred independently from the grains pigmentation, since purple pericarp genotypes or blue aleurone genotypes could be very susceptible, tolerant or very resistant. This is in accordance with other study on pigmented maize, which indicates that flavonoids alone may not be completely effective in the resistance (Venturini et al. 2016). However, a more extensive evaluation in the field, considering FHB severity in a higher number of pigmented genotypes, is desirable.

5.4.2. Pathways and function commonly upregulated due to disease in the considered genotypes

Transcriptomics analysis was carried out to compare four different bread wheat genotypes (Sumai3, Vanilnoir, Rebelde and Rosso) with different FHB resistance and different grain pigmentation. Despite their diverse genetic backgrounds and differences extending beyond FHB resistance and grain pigmentation, this comparative analysis allowed to highlight key biosynthetic and metabolic reprogramming due to *F. graminearum* infection, emphasizing variation related to resistance. Indeed, RNAseq revealed that several pathways and functions were commonly activated in all the considered genotypes, independently of the resistance and the pigmentation, while other pathways or function were specifically activated.

Among the pathways activated in all the genotypes, tyrosine and phenylalanine metabolism play a pivotal role to understand the other upregulated functions. Tyrosine is an aromatic amino acid synthesized de novo via the shikimate pathway. It serves as a precursor of numerous specialized metabolites that have diverse physiological roles as electron

carriers, antioxidants, attractants, and defense compounds (Schenck and Maeda 2018). With the action of tyrosine decarboxylase, tyrosine is further converted into tyramine, precursor for the biosynthesis of tyramine-derived hydroxycinnamic acid amides (HCAAs) (Liu et al. 2022). Tyrosine decarboxylase is shared with other pathways, such as isoquinoline alkaloid biosynthesis pathway (KEGG map taes00950) and betalain biosynthesis pathway (KEGG map taes00965). This may explain the enrichment of this two pathways in all the genotypes (confirmed by other studies like Li et al. 2022), even though alkaloids and betalain have never been reported in wheat (Timoneda et al. 2019). Hydroxycinnamic acids, like *p*-coumaric acid, ferulic acid and cinnamic acid, are phenylpropanoids synthetized by following shikimate pathway, where phenylalanine is the starter precursor molecule (Macoy et al. 2015). HCAAs pathway is an important accessory branch pathway of the phenylpropanoids (Kim et al. 2021). HCAAs are formed by the condensation of hydroxycinnamoyl-CoA thioesters with phenylethylamines such as tyramine, or polyamines such as putrescine (Liu et al. 2022). In wheat, untargeted metabolomic and proteomic analyses indicated that HCAAs were the major factor influencing *F. graminearum* resistance (Gunnaiah et al. 2012). However, other Authors reported as HCAAs, synthesized as a result of *F. graminearum* infection, were observed regardless of susceptibility and occurring at different times after infection (Whitney et al. 2022).

Glutathione S-transferase (GST) activity was among the most recurring molecular function term assigned to the upregulated DEGs in the four genotypes. Glutathione (GSH) has been widely reported to play an important role in plant responses against biotic stress (Dubreuil-Maurizi and Poinssot 2012). Plant glutathione S-transferases (GSTs) are ubiquitous and multifunctional enzymes encoded by large gene families (Gullner et al. 2018). GSTs may act as an amide carrier protein for HCAAs translocation to the plasma membrane (Macoy et al. 2015). Furthermore, in wheat-*Fusarium* interaction, the protective role of GCTs was mainly attributed to two functions: DON detoxification by the formation of DON-glutathione conjugates (Gardiner et al. 2010; Schweiger et al. 2013) and antioxidant activity against reactive oxygen species (ROS) (Foroud et al. 2012). Although specific GST family members has been observed in wheat and barley in association with FHB resistance (Foroud et al. 2012; Dhokane et al. 2016; Huang et al. 2016), up-regulation of GSTs has been observed in FHB-resistant as well as FHB-susceptible wheat material following *F. graminearum* infection (Pan et al. 2018), in accordance with our results.

Thus, two of the functions recognized to be highly related to FHB resistance (biosynthesis of HCAAs and GST activity) were upregulated in all the considered genotypes, regardless the resistance and the pigmentation. A deeper analysis revealed that, while the glutathione metabolic process did not show a different fold enrichment among the genotypes, cinnamic acid metabolic process was the process with the highest fold enrichment in the two resistant genotypes. Fold enrichment is defined as the percentage of genes in a list belonging to a pathway, divided by the corresponding percentage in the background. As a measure of effect size, fold enrichment indicates how drastically genes of a certain pathway is overrepresented (Ge et al. 2018). Therefore, even if tyrosine and phenylalanine metabolism leading to the production of HCAAs was commonly upregulated in all the genotypes, these pathways may be a discriminant function of the two resistant genotypes evaluated in this study, Sumai3 and Vanilnoir.

5.4.3. In the susceptible genotypes, FHB caused the down-regulation of the primary and energy metabolism

In the two susceptible genotypes, GO terms like “Cellular polysaccharide metabolic process”, “Cellulose biosynthetic process”, and “Plant-type cell wall biogenesis” were commonly downregulated. Together with the downregulation of the phenylpropanoid biosynthesis pathway, these terms suggested a general suppression of cell wall biosynthesis. Thus

the weakening of plant cell wall may play a key role in the susceptibility of Rosso and Rebelde, considering that FHB-resistant genotypes typically are able to strength cell wall and maintain cell wall integrity (Chen et al. 2023).

Similarly, microtubule-based process and the cytoskeleton organization were exclusively downregulated function in Rosso and Rebelde. Vesicle trafficking and cytoskeleton rearrangements are required to implement the cellular re-organization during a stress (Dörmann et al. 2014) and several studies showed the functions of the actin cytoskeleton in defense signaling, regulating the crosstalk between the nucleus, the Golgi apparatus, the endoplasmic reticulum (ER), and the plasma membrane (Kobayashi and Kobayashi 2008; Porter and Day 2016). Furthermore, virulence factors of different pathogens (effectors or toxins) specifically target the cytoskeleton components or actin binding proteins (Porter and Day 2016). The susceptible genotypes considered in this study may lack the ability to rearrange the cytoskeleton, complicating signal transduction, or the ability to counteract pathogen effectors targeted to cytoskeletal functions. Xue et al. (2015) showed that Fusarium wilt affected cytoskeleton organization in susceptible common bean genotypes, but reports about suppression of microtubule-based process in wheat infected by *F. graminearum* are currently lacking.

Finally, function related to the photosynthesis were generally suppressed in Rosso. Chloroplast is an organelle responsible for photosynthesis, but it is also crucial for plant defense, since it is the place for synthesizing defense phytohormone salicylic and jasmonic acid (Kangasjärvi et al. 2012; Medina-Puche et al. 2020). Generally, the maintenance of normal photosynthesis is crucial for plant defense (Huot et al. 2014). Thus Rosso may be unable to counteract pathogen effectors targeting chloroplast defense (Xu et al. 2019; de Torres Zabala et al. 2015) or, simply, may lack the ability to maintain an efficient photosynthesis during the infection process (Xin-long Gao et al. 2023).

5.4.4. Different response to hormonal stimuli

The role of the well-known defense phytohormones - salicylic acid (SA), jasmonic acid (JA), and ethylene (ET) - in the wheat defense response to Fg-challenge has been extensively described with a consensus model of early biotrophic SA followed by later necrotrophic stage JA/ET responses (Kazan and Gardiner 2018; Pan et al. 2018; Wang et al. 2018).

Salicylic acid (SA) is a key defense hormone contributing to defense against biotrophic and hemibiotrophic pathogens (Glazebrook 2005), inducing systemic acquired resistance (SAR), the inducible form of plant defense that confers broad-spectrum immunity to secondary infections, beyond the initial infection site (Tripathi et al. 2019). In this study, none of the genes in the SA-mediated defense pathway, either for biosynthesis or signaling, was found to be differentially expressed in the considered genotype, as similarly reported by Xiao et al. (2013). However, even if the enrichment of GO terms like “cellular response to SA stimulus” and “SA-mediated signaling pathway” was lacking, the activation of SAR may occur as well, indicated by the activation of PAL and the biosynthesis of PR1 in all the genotypes. Indeed, PR1 is a key marker of SAR (Wang et al. 2018).

Noteworthy, *F. graminearum* has a short biotrophic growth phase, rapidly switching to necrotrophy (Brown et al. 2010) thus even JA and ethylene ET may play a key role (Li and Yen 2008). As for SA, GO terms related to “JA biosynthesis” and “JA metabolism” were not enriched among up-regulated DEGs, but “JA metabolism” appeared in down-regulated DEGs of Rebelde. “Ethylene-activated signaling pathway” was, instead, a biological process activated in all the genotypes, and in particular Vanilnoir was significantly enriched in genes having transcription factor function related to the ethylene-activated signaling pathway. In wheat –Fg interaction, the role of ET remains uncertain, with conflicting reports highlighting mediation of both resistance (Foroud et al. 2018) and susceptibility (X. Chen et al. 2009) in early

and late responses (Wang et al. 2018). In this study ET appeared as a key hormone for disease signaling and transduction, but without enhancing susceptibility or resistance or changing due to grain pigmentation.

Furthermore, some growth promoting hormones were involved in reaction to the infection.

Cytokinin biosynthesis was stimulated in Sumai3, Rebelde and Rosso, through zeatin biosynthetic pathway, but in Sumai3 "Cellular response to cytokinin stimulus" was significantly downregulated. Cytokinins play a key role in the growth–defense trade-off and they can even help plant defend through cytokinin-induced immunity (Albrecht and Argueso 2017). In this study, results suggest that in Rosso and Rebelde the trade-off may be mainly directed to the growth instead of the defense, hypothesis supported by the enrichment in biological processes related to positive regulation of developmental growth exclusively in the susceptible genotypes.

In Sumai3 and Vanilnoir diterpenoid biosynthesis, leading to gibberellins productions, was stimulated, but also a negative regulation of gibberellic acid mediated signaling pathway was reported. Gibberellins (GA) are involved in the regulation of a wide range of plant physiological processes, including seed germination, root, leaf, stem and fruit growth, but also GA involvement in plant defense was demonstrated (Yimer et al. 2018; De Bruyne et al. 2014). Exogenous GA application on wheat was found to modulate primary and secondary metabolism, producing a general metabolic shift underlying its reduction in FHB severity (Buhrow et al. 2021). In this study GA biosynthesis stimulation occurred only in resistant genotypes, but the signaling pathway was negatively regulated. Thus, their role in disease resistance could not be excluded, but their mode of action remains unclear and require further investigations.

5.4.5. Focus on phenylpropanoids, flavonoids and anthocyanin biosynthetic pathway

Phenylpropanoids is a class of plant secondary metabolites frequently reported as involved in plant defense to biotic or abiotic stresses (Ramaroson et al. 2022; Treutter 2006). Some of them could be constitutively found in plants, representing constitutive defense against abiotic (Singh et al. 2023) or biotic stress (Gunnaiah et al. 2012), while several authors reveals the importance of phenylpropanoid biosynthesis for the induced resistance to biotic stresses (Hölscher et al. 2016; Li et al. 2023; Yang et al. 2023; Xing et al. 2024). Different authors showed as phenylpropanoids and flavonoids accumulation is stimulated in FHB resistant wheat genotypes (such as Sumai3) due to the infection (Gunnaiah and Kushalappa 2014; Karre et al. 2017; Kumar et al. 2020). Purple pigmented genotypes, rich in flavonoids, having different FHB are interesting models to study these pathways, but investigation including these genotypes are currently lacking.

Most of the metabolites produced in the phenylpropanoid pathway (KEGG map00940) are related to FHB resistance and play an essential role in Type II resistance by thickening the secondary cell wall (thanks to the accumulation of lignin and HCAAs) or inhibiting the activity of the plant cell wall degrading enzymes (Wu et al. 2022). In this study, structural genes in phenylpropanoid pathway were mainly upregulated in all the considered genotypes, but some key genes (*4CL*, *HCT*, *CCoAOMT*, *C3'H*, *COMT*) were differentially regulated among resistant and susceptible, purple and yellow pigmented genotypes. In particular, *4CL*, *HCT* and *COMT* were upregulated in the resistant genotypes and downregulated in susceptible ones, suggesting a direct involvement in the resistance. *4CL*, hub gene in the phenylpropanoid pathway, was considered by Dhokane et al. (2016) to be a potential candidate R gene conferring high rachis resistance to FHB and identified as putative resistance genes localized within the QTL-*Fhb2* region. Similarly, *HCT* and *COMT*, most likely regulated by *WRKY* transcription factors (Karre et al. 2019), were found to be upregulated in FHB resistant genotypes (Dhokane et al. 2016; Karre et al. 2017; Xinlong Gao et al. 2024), confirming our results.

Furthermore, the purple genotype Rosso differ from Rebelde for the upregulation of *CCoAOMT* and *C3'H*. Caffeoyl-CoA-*O*-methyltransferase (CCoAOMT) is the main regulator determining the efficiency of lignin synthesis and composition (Wu et al. 2022). The expression of *CCoAOMT* is induced in resistant wheat genotypes at an early stage of infection which improves the efficiency of lignin synthesis and obtains Type II resistance (Ding et al. 2011). The coumaroyl shikimate 3-hydroxylase enzyme (C3'H) is one of three membrane-bound cytochrome P450 monolignol enzymes and central for the formation of lignin (Funnell-Harris et al. 2019). *C3'H* have been implicated in defense responses to pathogens in *Arabidopsis* (Franke et al. 2002), but few is known about his effect on FHB resistance. Presumably, overexpression of both *C3'H* and *CCoAOMT* may be implicated in biosynthesis of lignin precursors and, thus, enhancement of cell wall reinforcement. The role of *C3'H* in FHB defense should be verified in further research.

Flavonoids biosynthetic pathway (KEGG map00941) produce different metabolites related to disease response and resistance (Ramaroson et al. 2022; Treutter 2006). The altered regulation of structural genes due to the infection, suggest a different orientation of flavonoid pathway in the genotypes evaluated in this study, potentially allowing the production of some compounds rather others. In Rebelde, genes downstream of *C4H* were strongly downregulated, suggesting a suppression of the whole flavonoids' biosynthetic pathway. Differently, Rosso basally expressed *F3H*, indicating a constitutive conversion of flavones (like naringenin or eriodictyol) to dihydroflavones (such as dihydrokaempferol or dihydromyricetin), subsequently catalyzed by *DFR* (basally expressed) to produce leucoanthocyanidins (Saigo et al. 2020), while anthocyanin synthase (*ANS*), which form anthocyanidin, was downregulated, and anthocyanidin reductase (*ANR*) was upregulated. This pattern suggests that, in Rosso, anthocyanidin are not actively synthetized but rather they are used as a substrate to produce flavan-3-ols, precursors of tannins, by ANR. In Sumai3, the entire pathway was stimulated, included the *ANS* downregulated in Rosso. This is in agreement with other studies which highlighted the role of flavonoid biosynthetic pathway in FHB resistance (Gunnaiah et al. 2012; Gunnaiah and Kushalappa 2014; Karre et al. 2017; Kumar et al. 2020). However, some functions were suppressed, potentially hindering the production of some compounds, such as kaempferol or quercetin (produce by flavonol synthase, FLS), catechin (obtained by the reduction of leucoanthocyanidins through *LAR*) and glycosylated anthocyanins (such as cyanidin 3-*O*-glucoside, produced by glycosylation of anthocyanidins through *BZ1*). Finally, Vanilnoir showed the more FHB-activated flavonoids pathway among the considered genotypes. *FLS* and *LAR* were the only genes downregulated, while anthocyanidins (stimulated by the upregulation of *ANS*) were catalyzed by both *ANR* and *BZ1*, presumably allowing the production of flavan-3-ols and anthocyanins. Flavan-3-ols are known for their protective action against fungal disease in plants, usually produced by the infection-induced overexpression of *ANR* and *LAR* (Galindo-González and Deyholos 2016; Su et al. 2022; Ullah et al. 2017). Different studies found anthocyanins (such as pelargonidin 3-*O*-glucoside and malvidin 3-*O*-glucoside) biosynthesis stimulated by FHB infection in resistant yellow pigmented wheat genotypes (Karre et al. 2017; Gunnaiah and Kushalappa 2014; Kumar et al. 2020). Other authors showed that the loss of anthocyanins and accumulation of condensed tannins could be due to the utilization of anthocyanidins for flavan-3-ols production rather than for anthocyanins formation, suggesting that the production of these compounds could be competitive (Mahajan and Yadav 2014). While Sumai3 and Rosso favored the production of flavan-3-ols to the detriment of anthocyanins, infected Vanilnoir seems to stimulate the simultaneous production of anthocyanins and flavones, both potentially involved in its resistance mechanism. However, these hypotheses should be verified through further metabolomics studies.

5.4.6. Similarity with Sumai3 may suggest the putative resistance mechanism of Vanilnoir

Vanilnoir and Sumai3 showed strong and rapid reaction to *F. graminearum* infection. In addition to the activation of the aforementioned pathways and synthesis of metabolites, which likely contribute to Type II resistance, it's probable that specific receptors play a crucial role in recognizing pathogen-associated molecular patterns.

In this study 10 LRR receptor-like protein kinases (LRR-RLKs) were exclusively up-regulated in the FHB-resistant genotypes. One or more kinases identified in this work and referred to as pattern recognition receptors (PRRs), could contribute to the perception of *F. graminearum* in the FHB-resistant genotypes. Upon recognition of specific pathogen-associated molecular patterns (PAMPs) by PRRs, the PAMP-triggered immunity response is activated, leading to activation of MAP kinases, ROS production and transcriptional reprogramming (Soltabayeva et al. 2022). A large number of predicted PRRs are present in wheat. Shumayla et al. (2016) identified 531 TaLRRK genes in *Triticum aestivum*, which were distributed throughout the A, B, and D sub-genomes and chromosomes. However, very few have been characterized. Pan et al. (2018) identified 5 receptor protein kinases strongly upregulated in FHB-resistant wheat genotypes challenged with *F. graminearum*. Karre et al. (2017) demonstrated that the silencing of barley HvCERK1 (able to recognize the fungal elicitor chitin) compromised resistance to FHB disease and elucidated its impact on downstream resistance-related metabolite accumulation. Thapa et al. (2018) identified and characterized a wheat LRR gene (*TaLRRK-6D*) and deduced that it is a signaling molecule involved in the wheat response to DON. Thus, our results concur with previous studies, confirming that LRR genes are induced as part of the early cereal response to FHB disease also for the genotypes considered in our work. However, the annotation of genes identified in this study should be verified (since they are “probable” or “predicted” proteins) and more information about their ligand and their cellular location are required. Further investigations focused on these genes could be promising to reveal specific cross-talk between wheat and *F. graminearum*.

Moreover, MAPK signaling pathway was significantly stimulated in all the genotypes. Mitogen-activated protein kinase (MAPK) cascades are highly conserved signaling modules downstream of receptors/sensors that transduce extracellular stimuli into intracellular responses in eukaryotes. MAPK pathways form a key network in plant defense responses (Meng and Zhang 2013), also following the recognition of pathogen-associated molecular patterns, which can trigger non-host-mediated defenses (Ligterink et al. 1997; Asai et al. 2002; Rudd et al. 2008). The MAPK cascades in cereals-pathogen interaction were described in detail in rice affected by bacterial blight (Yang et al. 2015) and in wheat challenged by *Septoria* leaf blotch disease (Rudd et al. 2008), while few mitogen-activated protein kinase where specifically described in wheat challenged by FHB (Gao et al. 2011; Karre et al. 2017). Other authors obtained the upregulation of MAPK signaling pathway through *F. graminearum* infection: 29 genes from the MAPK signaling pathway were found to be differentially expressed by Kumar et al. (2020), while Li et al. (2022) found that the expression of genes related to MAPK was lower in susceptible wheat grains than in resistant wheat grains. In this study 118 genes from the MAPK signaling pathway were upregulated in the four genotypes due to *F. graminearum* infection and only TRAESCS5A02G382800 (encoding for a calmodulin-like protein) and TRAESCS5A02G433600 were commonly upregulated in Sumai3 and Vanilnoir, but not in the susceptible genotypes. Further investigation on these genes can provide valuable information about the specific cross-talk between wheat and *F. graminearum*.

5.5. Supplementary Tables and Figures

Table S5.1: List of primers for qRT-PCR

Gene	Species	Accession number	Function	Primer pairs (5'-3')	bp (cDNA)	Ann temp (°C)	Reference
FgTRI6	*Fusarium graminearum*	AB017495.1	Trichothecene Transcriptional Regulator	F:TCTTTGTGAGCGGACGGGACTTTA	245	60	Horevaj et al. 2011
				R:ATCTCGCATGTTATCCACCCTGCT			
TaACT	*Triticum aestivum*	AB181991	Actin	F:TCCTGTGTTGCTGACTGAGG	236	61	Tundo et al. 2016
				R:GGTCCAAACGAAGGATAGCA			
TaTUB	*Triticum aestivum*	TAU76745	Beta-Tubulin	F:CGAGGAGGGCGAGTACGA	79	61	Tenea et al. 2011
				R:AGCAAAGCACGACATGGACAT			
TaFNR	*Triticum aestivum*	AJ457980	Ferredoxin- NADP(H)-Oxidoreductase	F:CACCGGCCCAGTGATCTT	69	61	Tenea et al. 2011
				R:AAGGGCGTCTGCTCCAACT			
TaGAPDH	*Triticum aestivum*	EF592180	Glyceraldehyde-3-Phosphate Dehydrogenase	F:AACGACCCCTTCATCACCAC	150	60	Wei et al. 2015
				R:GTTCCTGCAGCCAAACACAG			
TaPAL	*Triticum aestivum*	X99705	Phenylalanine Ammonia Lyase	F:CGATGCTCGTCCGAGTCAAT	407	60	Francesconi et al. 2020b
				R:CATGACCTCACAGAAGACGC			
TaC4H	*Triticum aestivum*	XM_044485958.1	Cinnamate-4-Hydroxylase	F:CGCAACGTGGTGTTCGACAT	111	62	This study
				R:GGTGAAGAAGGGCACGGTCA			
TaDFR	*Triticum aestivum*	AB162139.1	DihydroFlavonol 4-Reductase	F:CGTCGGGTTTCGTAGGGT	109	60	Ma et al. 2014
				R:CCAGCAACGGCTTGTTCTTC			
TaCHS	*Triticum aestivum*	AY286095.1	Chalcone Synthase	F:GAGGACGCCTTCAAGCCATTG	126	60	This study
				R:GCGCATCCGTTCCTTGTTCA			
TaPR2	*Triticum aestivum*	Y18212	B -1,3 - Endoglucanase	F:AACGTGCGCCCCTACTACC	398	60	Francesconi et al. 2020a
				R:GCGTCGAACAGGCTCGTGTA			

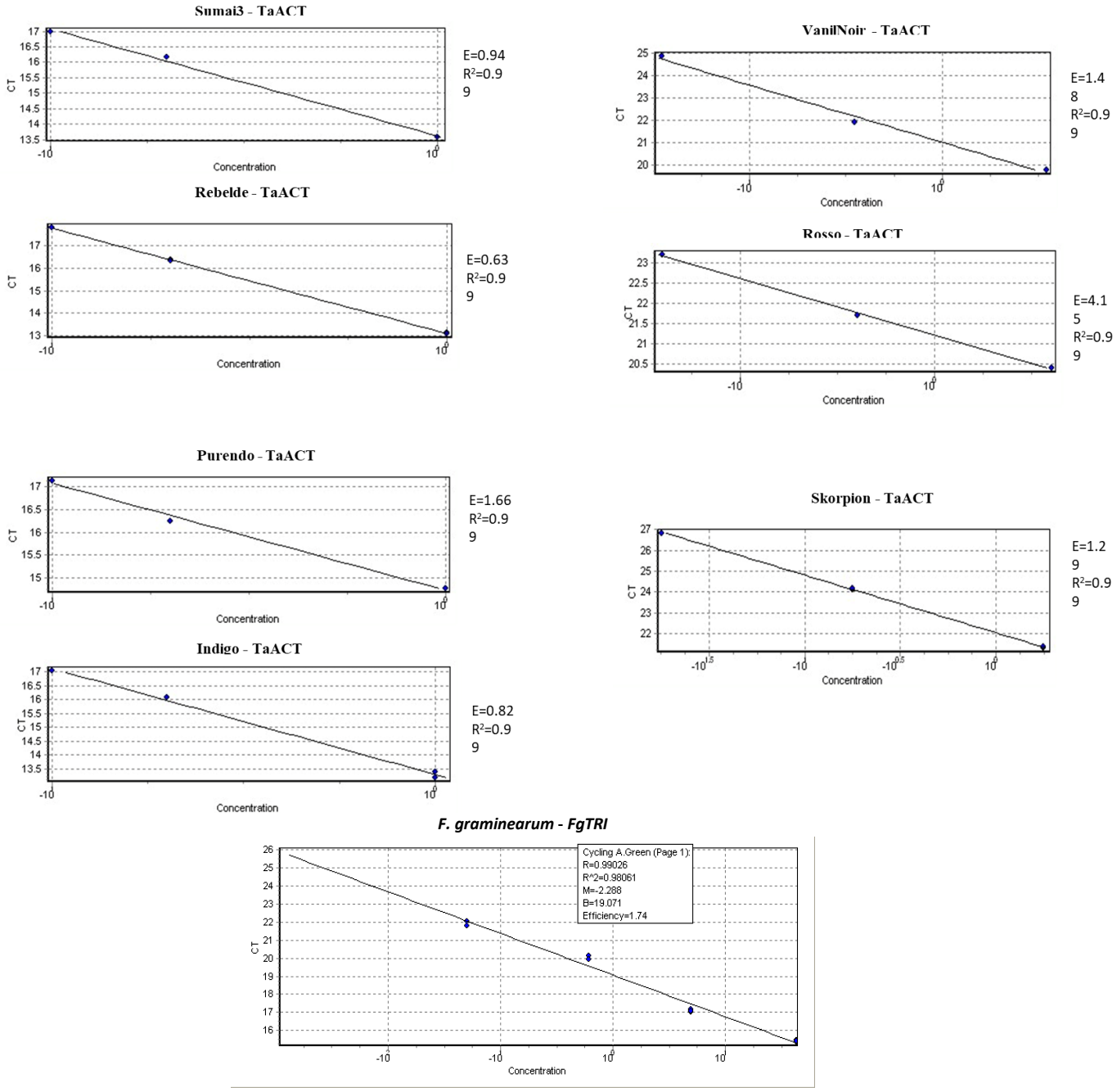

Fig S5.1: Standard curves generated for the *TaACT* gene in Sumai 3, Rebelde, Purendo, Indigo, Vanilnoir, Rosso, and Skorpion and for the *FgTRI* for *F. graminearum*, for the Real-Time qPCR quantification of fungal biomass.

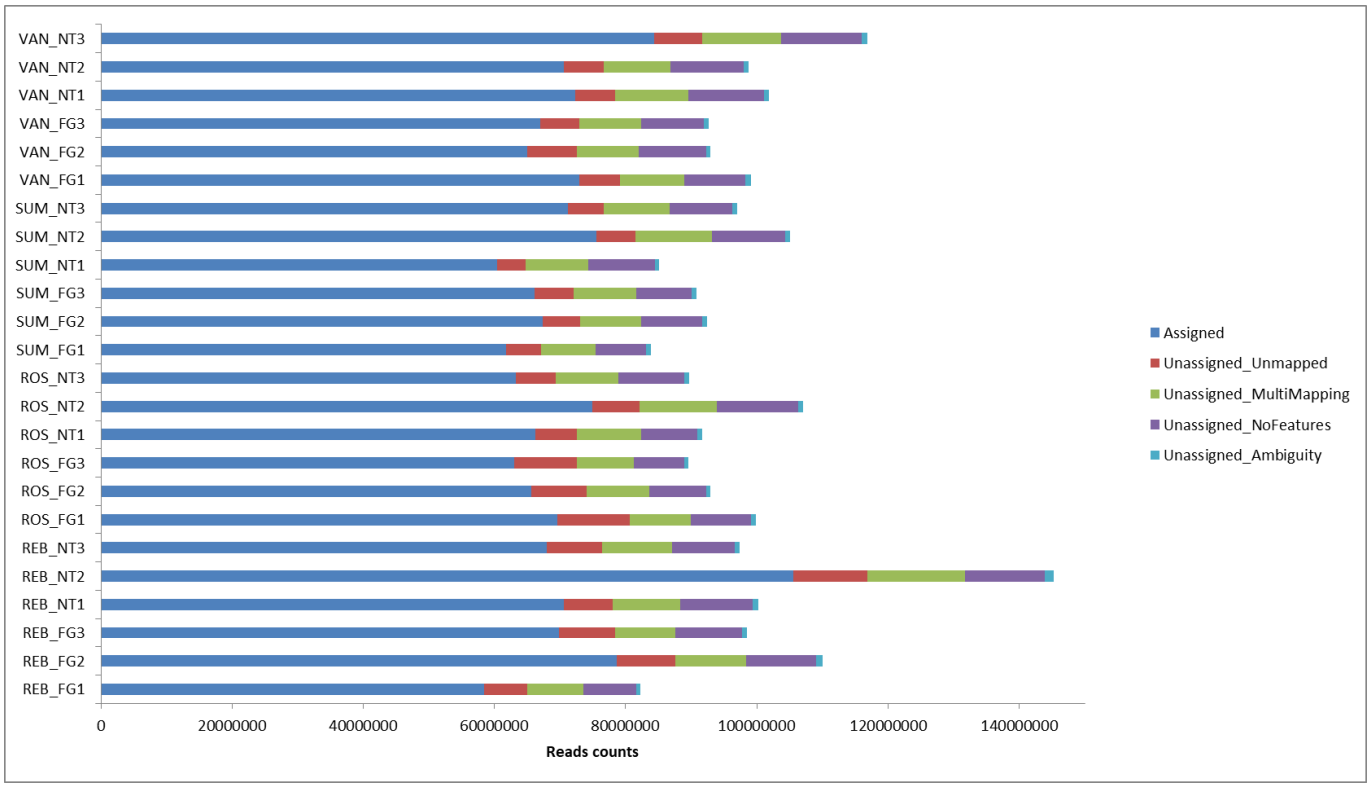

Fig. S5.2: Number of mapped reads for each sample analyzed by RNAseq. REB = Rebelde; SUM = Sumai3; ROS = Rosso; Van = Vanilnoir; FG = infected samples; NT = mock treated samples.

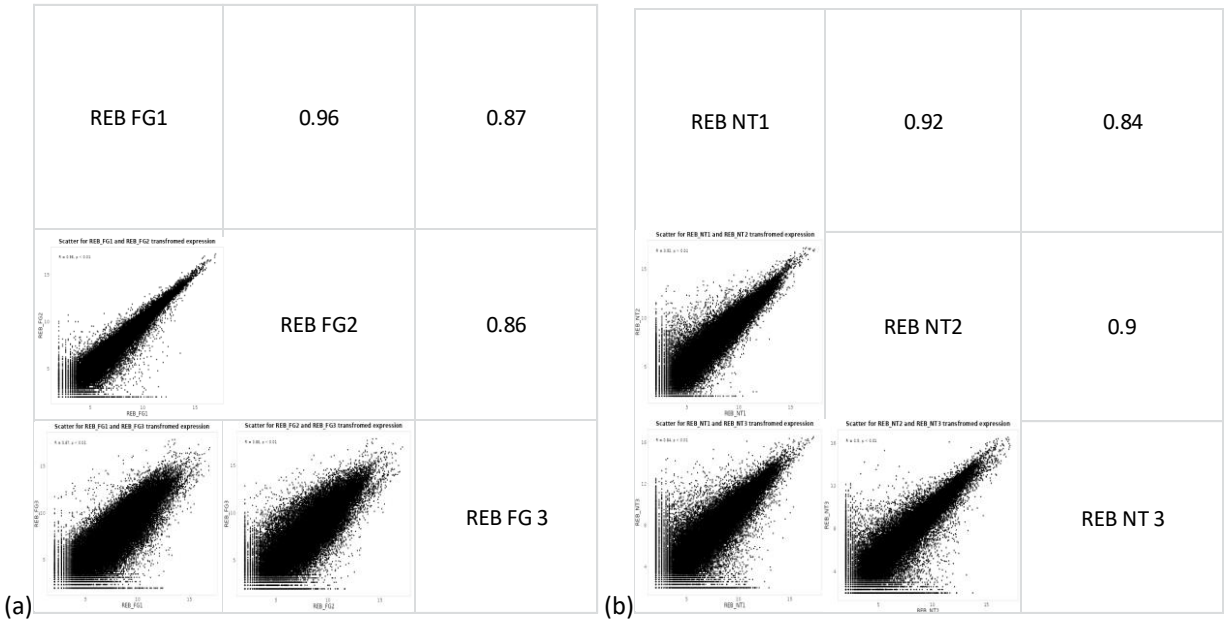

Fig. S5.3: Pearson's coefficient of correlation matrix and scatter plots showing relationships between replicate libraries, using log-transformed read counts of (a) Rebelde infected (FG) and (b) Mock treated (NT). Numbers in the upper, right-hand panels indicate Pearson's coefficient of correlation.

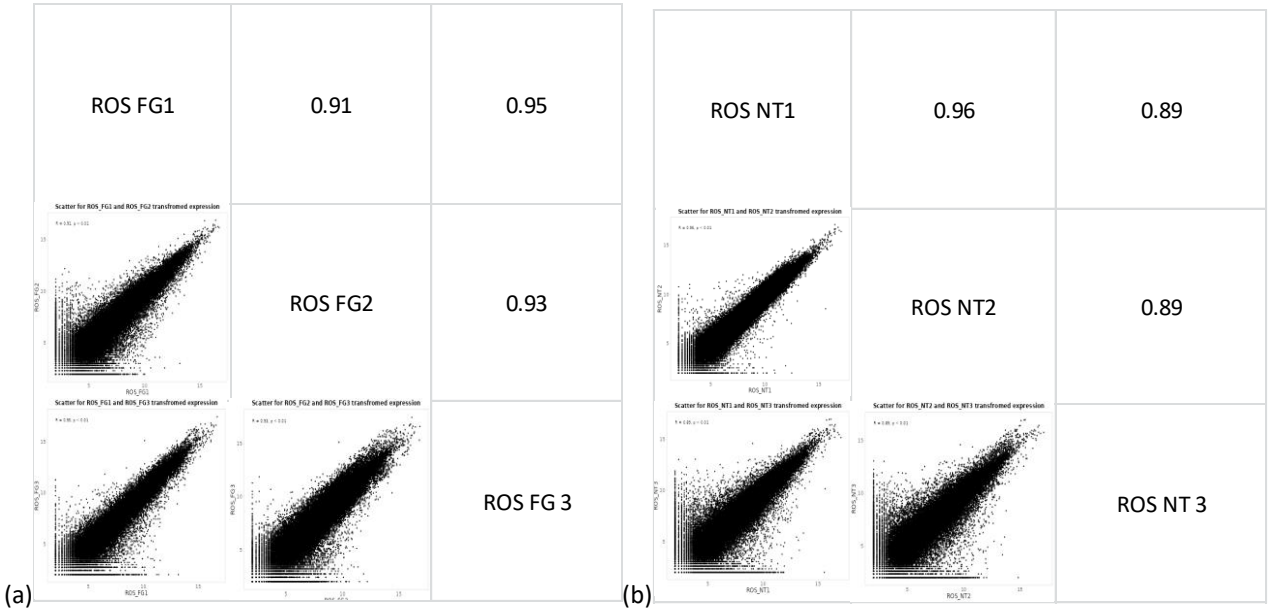

Fig. S5.4: Pearson's coefficient of correlation matrix and scatter plots showing relationships between replicate libraries, using log-transformed read counts of (a) Rosso infected (FG) and (b) Mock treated (NT). Numbers in the upper, right-hand panels indicate Pearson's coefficient of correlation.

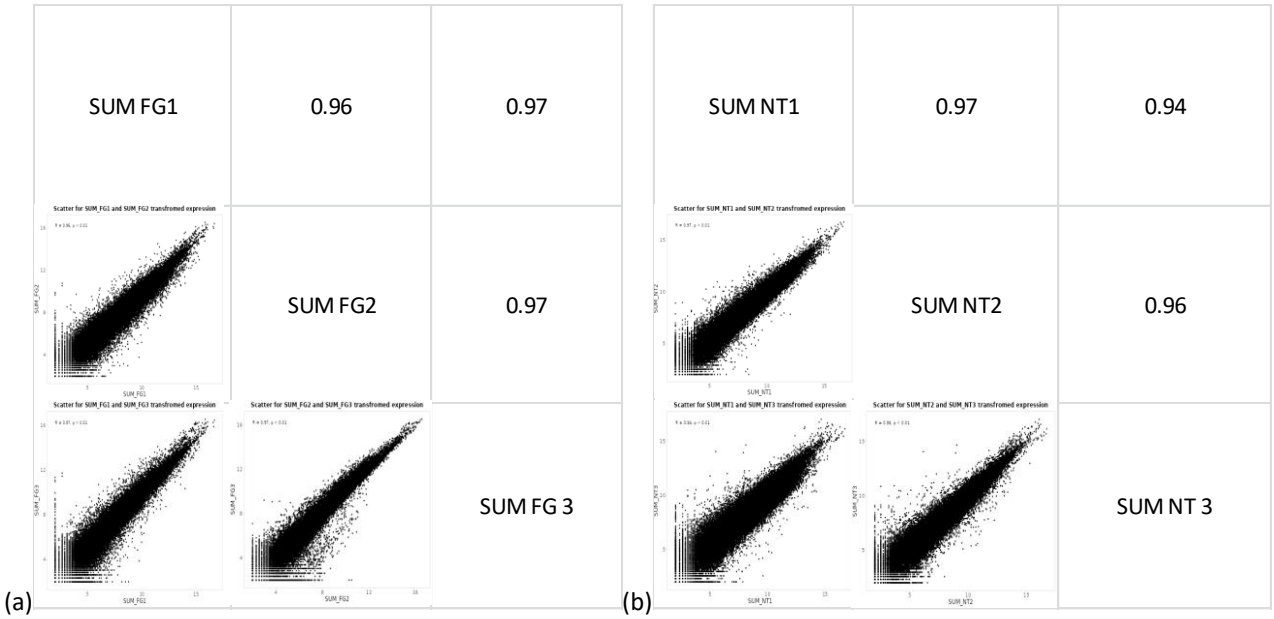

Fig. S5.5: Pearson's coefficient of correlation matrix and scatter plots showing relationships between replicate libraries, using log-transformed read counts of (a) Sumai3 infected (FG) and (b) Mock treated (NT). Numbers in the upper, right-hand panels indicate Pearson's coefficient of correlation.

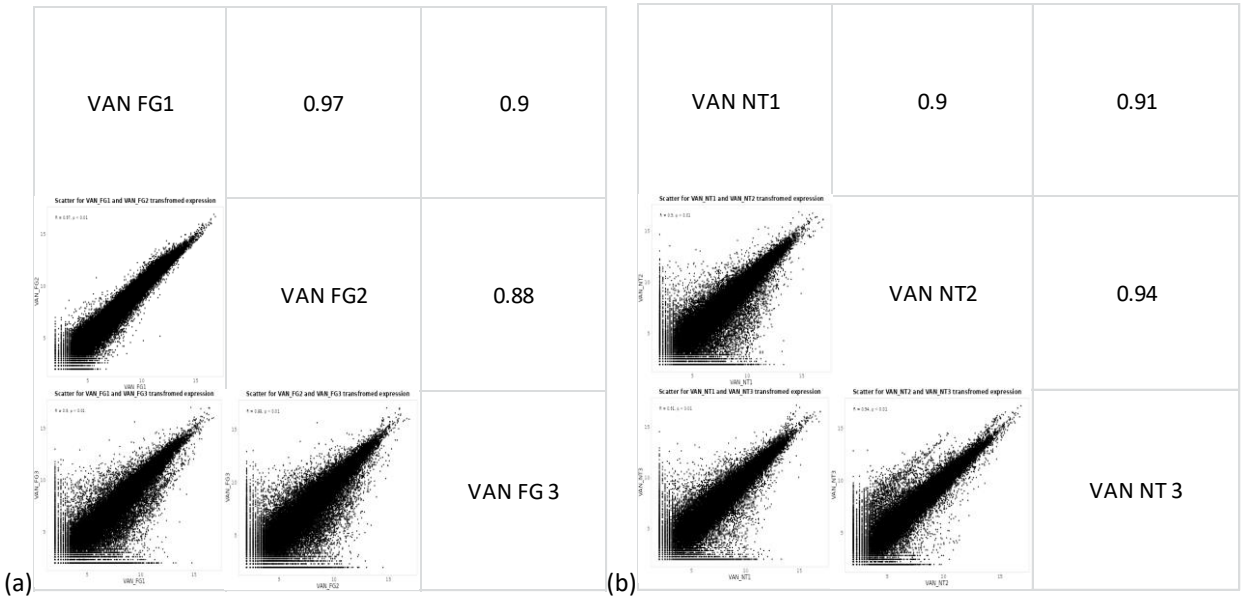

Fig. S5.6: Pearson's coefficient of correlation matrix and scatter plots showing relationships between replicate libraries, using log-transformed read counts of (a) Vanilnoir infected (FG) and (b) Mock treated (NT). Numbers in the upper, right-hand panels indicate Pearson's coefficient of correlation.

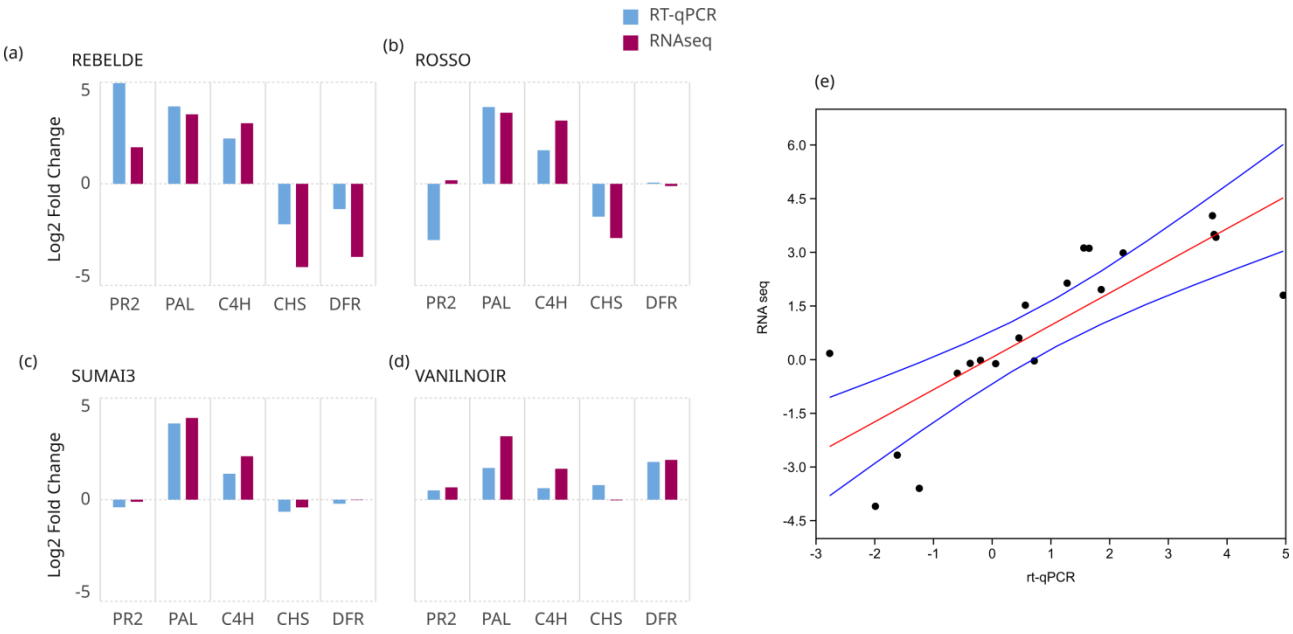

Fig. S5.7: Verification of transcriptomic results. (a), (b), (c) and (d) show the expression (Log2 Fold Change) of the target genes in Rebelde, Rosso, Sumai3 and Vanilnoir respectively, comparing RT-qPCR vs RNAseq results (image created using SCImago Graphica); (e) ordinary least square (OLS) regression between RNAseq and RT-qPCR data, showing a positive correlation (r^2= 0.6495; permutation p = 0.0001).

5.6. References

Abdel-Aal, E. S. M., Abou-Arab, A. A., Gamel, T. H., Hucl, P., Young, J. C., and Rabalski, I. (2008). Fractionation of blue wheat anthocyanin compounds and their contribution to antioxidant properties. *Journal of Agricultural and Food Chemistry*, *56*(23), 11171–11177. https://doi.org/10.1021/jf802168c

Abdel-Aal, E. S. M., and Hucl, P. (2003). Composition and stability of anthocyanins in blue-grained wheat. *Journal of Agricultural and Food Chemistry*, *51*(8), 2174–2180. https://doi.org/10.1021/jf021043x

Abdel-Aal, E. S. M., Young, J. C., and Rabalski, I. (2006). Anthocyanin composition in black, blue, pink, purple, and red cereal grains. *Journal of Agricultural and Food Chemistry*, *54*(13), 4696–4704. https://doi.org/10.1021/jf0606609

Ahmad, S., Ali, S., Shah, A. Z., Khan, A., and Faria, S. (2023). Chalcone synthase (CHS) family genes regulate the growth and response of cucumber (*Cucumis sativus* L.) to *Botrytis cinerea* and abiotic stresses. *Plant Stress*, *8*(April), 100159. https://doi.org/10.1016/j.stress.2023.100159

Ainsworth, E. A., and Gillespie, K. M. (2007). Estimation of total phenolic content and other oxidation substrates in plant tissues using Folin-Ciocalteu reagent. *Nature Protocols*, *2*(4), 875–877. https://doi.org/10.1038/nprot.2007.102

Albrecht, T., and Argueso, C. T. (2017). Should I fight or should I grow now? The role of cytokinins in plant growth and immunity and in the growth–defence trade-off. *Annals of Botany*, *119*(5), 725–735. https://doi.org/10.1093/aob/mcw211

Andrews, S. (2010). *A quality control tool for high throughput sequence data - Babraham Bioinformatics*. http://www.bioinformatics.babraham.ac.uk/projects/fastqc/

Asai, T., Tena, G., Plotnikova, J., Willmann, M. R., Chiu, W.-L., Gomez-Gomez, L., Boller, T., Ausubel, F. M., and Sheen, J. (2002). MAP kinase signalling cascade in *Arabidopsis* innate immunity. *Nature*, *415*(6875), 977–983. https://doi.org/10.1038/415977a

Bernardi, J., Stagnati, L., Lucini, L., Rocchetti, G., Lanubile, A., Cortellini, C., De Poli, G., Busconi, M., and Marocco, A. (2018). Phenolic profile and susceptibility to *Fusarium* infection of pigmented maize cultivars. *Frontiers in Plant Science*, *9*(August), 1–13. https://doi.org/10.3389/fpls.2018.01189

Beta, T., Qiu, Y., Liu, Q., Borgen, A., and Apea-Bah, F. B. (2020). Purple Wheat (Triticum sp.) Seeds. In *Nuts and Seeds in Health and Disease Prevention*. Elsevier Inc. https://doi.org/10.1016/b978-0-12-818553-7.00010-3

Brown, N. A., Urban, M., van de Meene, A. M. L., and Hammond-Kosack, K. E. (2010). The infection biology of *Fusarium graminearum*: Defining the pathways of spikelet to spikelet colonisation in wheat ears. *Fungal Biology*, *114*(7), 555–571. https://doi.org/10.1016/j.funbio.2010.04.006

Buhrow, L. M., Liu, Z., Cram, D., Sharma, T., Foroud, N. A., Pan, Y., and Loewen, M. C. (2021). Wheat transcriptome profiling reveals abscisic and gibberellic acid treatments regulate early-stage phytohormone defense signaling, cell wall fortification, and metabolic switches following *Fusarium graminearum*-challenge. *BMC Genomics*, *22*(1), 1–21. https://doi.org/10.1186/s12864-021-08069-0

Chen, C., Guo, Q., He, Q., Tian, Z., Hao, W., Shan, X., Lu, J., Barkla, B. J., Ma, C., and Si, H. (2023). Comparative transcriptomic analysis of wheat cultivars differing in their resistance to Fusarium head blight infection during grain-filling stages reveals unique defense mechanisms at play. *BMC Plant Biology*, *23*(1), 433. https://doi.org/10.1186/s12870-023-04451-0

Chen, X., Steed, A., Travella, S., Keller, B., and Nicholson, P. (2009). *Fusarium graminearum* exploits ethylene signalling to colonize dicotyledonous and monocotyledonous plants. *New Phytologist*, *182*(4), 975–983. https://doi.org/10.1111/j.1469-8137.2009.02821.x

Cuthbert, P. A., Somers, D. J., and Brulé-Babel, A. (2007). Mapping of Fhb2 on chromosome 6BS: a gene controlling Fusarium head blight field resistance in bread wheat (*Triticum aestivum* L.). *Theoretical and Applied Genetics*, *114*(3), 429–437. https://doi.org/10.1007/s00122-006-0439-3

David Miller, J., and Arnison, P. G. (1986). Degradation of deoxynivalenol by suspension cultures of the fusarium head blight resistant wheat cultivar Frontana. *Canadian Journal of Plant Pathology*, *8*(2), 147–150. https://doi.org/10.1080/07060668609501818

De Bruyne, L., Höfte, M., and De Vleesschauwer, D. (2014). Connecting Growth and Defense: The Emerging Roles of Brassinosteroids and Gibberellins in Plant Innate Immunity. *Molecular Plant*, *7*(6), 943–959. https://doi.org/10.1093/mp/ssu050

de Torres Zabala, M., Littlejohn, G., Jayaraman, S., Studholme, D., Bailey, T., Lawson, T., Tillich, M., Licht, D., Bölter, B., Delfino, L., Truman, W., Mansfield, J., Smirnoff, N., and Grant, M. (2015). Chloroplasts play a central role in plant defence and are targeted by pathogen effectors. *Nature Plants*, *1*(6), 15074. https://doi.org/10.1038/nplants.2015.74

Dean, R., Van Kan, J. A. L., Pretorius, Z. A., Hammond-Kosack, K. E., Di Pietro, A., Spanu, P. D., Rudd, J. J., Dickman, M., Kahmann, R., Ellis, J., and Foster, G. D. (2012). The Top 10 fungal pathogens in molecular plant pathology. *Molecular Plant Pathology*, *13*(4), 414–430. https://doi.org/10.1111/j.1364-3703.2011.00783.x

Del Pozo-Insfran, D., Brenes, C. H., Serna Saldivar, S. O., and Talcott, S. T. (2006). Polyphenolic and antioxidant content of white and blue corn (*Zea mays* L.) products. *Food Research International*, *39*(6), 696–703. https://doi.org/10.1016/j.foodres.2006.01.014

Deng, G.-F., Xu, X.-R., Zhang, Y., Li, D., Gan, R.-Y., and Li, H.-B. (2013). Phenolic Compounds and Bioactivities of Pigmented Rice. *Critical Reviews in Food Science and Nutrition*, *53*(3), 296–306. https://doi.org/10.1080/10408398.2010.529624

Dhokane, D., Karre, S., Kushalappa, A. C., and McCartney, C. (2016). Integrated metabolo-transcriptomics reveals Fusarium head blight candidate resistance genes in wheat QTL-Fhb2. *PLoS ONE*, *11*(5), 1–27. https://doi.org/10.1371/journal.pone.0155851

Ding, L., Xu, H., Yi, H., Yang, L., Kong, Z., Zhang, L., Xue, S., Jia, H., and Ma, Z. (2011). Resistance to Hemi-Biotrophic *F. graminearum* Infection Is Associated with Coordinated and Ordered Expression of Diverse Defense Signaling Pathways. *PLOS ONE*, *6*(4), e19008. https://doi.org/10.1371/journal.pone.0019008

Dörmann, P., Kim, H., Ott, T., Schulze-Lefert, P., Trujillo, M., Wewer, V., and Hückelhoven, R. (2014). Cell-autonomous defense, re-organization and trafficking of membranes in plant-microbe interactions. *New Phytologist*, *204*(4), 815–822. https://doi.org/10.1111/nph.12978

Dubreuil-Maurizi, C., and Poinssot, B. (2012). Role of glutathione in plant signaling under biotic stress. *Plant Signaling and Behavior*, *7*(2). https://doi.org/10.4161/psb.18831

Ederli, L., Beccari, G., Tini, F., Bergamini, I., Bellezza, I., Romani, R., and Covarelli, L. (2021). Enniatin b and deoxynivalenol activity on bread wheat and on fusarium species development. *Toxins*, *13*(10), 1–17. https://doi.org/10.3390/toxins13100728

Ficco, D., De Simone, V., Colecchia, S. A., Pecorella, I., Platani, C., Nigro, F., Finocchiaro, F., Papa, R., and De Vita, P. (2014). Genetic variability in anthocyanin composition and nutritional properties of blue, purple, and red bread (Triticum aestivum L.) and durum (*Triticum turgidum* L. ssp. *turgidum* convar. *durum*) wheats. *Journal of Agricultural and Food Chemistry*, *62*(34), 8686–8695. https://doi.org/10.1021/jf5003683

Foroud, N A, Ouellet, T., Laroche, A., Oosterveen, B., Jordan, M. C., Ellis, B. E., and Eudes, F. (2012). Differential transcriptome analyses of three wheat genotypes reveal different host response pathways associated with Fusarium head blight and trichothecene resistance. *Plant Pathology*, *61*(2), 296–314. https://doi.org/10.1111/j.1365-3059.2011.02512.x

Foroud, Nora A, Pordel, R., Goyal, R. K., Ryabova, D., Eranthodi, A., Chatterton, S., and Kovalchuk, I. (2018). Chemical Activation of the Ethylene Signaling Pathway Promotes *Fusarium graminearum* Resistance in Detached Wheat Heads. *Phytopathology®*, *109*(5), 796–803. https://doi.org/10.1094/PHYTO-08-18-0286-R

Francesconi, S., and Balestra, G. M. (2020a). The modulation of stomatal conductance and photosynthetic parameters is involved in Fusarium head blight resistance in wheat. *PLoS ONE*, *15*(6 june), 1–21. https://doi.org/10.1371/journal.pone.0235482

Francesconi, S., Mazzaglia, A., and Balestra, G. M. (2019). Different inoculation methods affect components of

Fusarium head blight resistance in wheat. *Phytopathologia Mediterranea*, *58*(3), 679–691. https://doi.org/10.14601/Phyto-10942

Francesconi, S., Steiner, B., Buerstmayr, H., Lemmens, M., Sulyok, M., and Balestra, G. M. (2020b). Chitosan Hydrochloride Decreases *Fusarium graminearum* Growth and Virulence and Boosts Growth, Development and Systemic Acquired Resistance in Two Durum Wheat Genotypes. Molecules, 1–29. https://doi.org/10.3390/molecules25204752

Franke, R., Hemm, M. R., Denault, J. W., Ruegger, M. O., Humphreys, J. M., and Chapple, C. (2002). Changes in secondary metabolism and deposition of an unusual lignin in the ref8 mutant of *Arabidopsis*. *The Plant Journal*, *30*(1), 47–59. https://doi.org/10.1046/j.1365-313X.2002.01267.x

Funnell-Harris, D. L., Sattler, S. E., O'Neill, P. M., Gries, T., Tetreault, H. M., and Clemente, T. E. (2019). Response of Sorghum Enhanced in Monolignol Biosynthesis to Stalk Rot Pathogens. *Plant Disease*, *103*(9), 2277–2287. https://doi.org/10.1094/PDIS-09-18-1622-RE

Galindo-González, L., and Deyholos, M. K. (2016). RNA-seq Transcriptome Response of Flax (Linum usitatissimum L.) to the Pathogenic Fungus *Fusarium oxysporum* f. sp. *lini*. *Frontiers in Plant Science*, *7*. https://doi.org/10.3389/fpls.2016.01766

Gao, Xin-long, Li, F., Sun, Y., Jiang, J., Tian, X., Li, Q., Duan, K., Lin, J., Liu, H., and Wang, Q. (2023). Basal defense is enhanced in a wheat cultivar resistant to Fusarium head blight. *Journal of Integrative Agriculture*, *23*(4), 1238–1258. https://doi.org/10.1016/j.jia.2023.06.014

Gao, Xinlong, Li, F., Sun, Y., Jiang, J., Tian, X., Li, Q., Duan, K., Lin, J., Liu, H., and Wang, Q. (2024). Basal defense is enhanced in a wheat cultivar resistant to Fusarium head blight. *Journal of Integrative Agriculture*, *23*(4), 1238–1258. https://doi.org/10.1016/j.jia.2023.06.014

Gao, Y., Liu, X., Stebbing, J.-A., He, D., Laroche, A., Gaudet, D., and Xing, T. (2011). TaFLRS, a novel mitogen-activated protein kinase in wheat defence responses. *European Journal of Plant Pathology*, *131*(4), 643–651. https://doi.org/10.1007/s10658-011-9837-8

Gardiner, S. A., Boddu, J., Berthiller, F., Hametner, C., Stupar, R. M., Adam, G., and Muehlbauer, G. J. (2010). Transcriptome Analysis of the Barley–Deoxynivalenol Interaction: Evidence for a Role of Glutathione in Deoxynivalenol Detoxification. *Molecular Plant-Microbe Interactions®*, *23*(7), 962–976. https://doi.org/10.1094/MPMI-23-7-0962

Ge, S. X., Jung, D., and Yao, R. (2020). ShinyGO: a graphical gene-set enrichment tool for animals and plants. *Bioinformatics*, *36*(8), 2628–2629. https://doi.org/10.1093/bioinformatics/btz931

Ge, S. X., Son, E. W., and Yao, R. (2018). iDEP: an integrated web application for differential expression and pathway analysis of RNA-Seq data. *BMC Bioinformatics*, *19*(1), 534. https://doi.org/10.1186/s12859-018-2486-6

Glazebrook, J. (2005). Contrasting Mechanisms of Defense Against Biotrophic and Necrotrophic Pathogens. *Annual Review of Phytopathology*, *43*(Volume 43, 2005), 205–227. https://doi.org/10.1146/annurev.phyto.43.040204.135923

Gorash, A., Armonienė, R., and Kazan, K. (2021). Can effectoromics and loss-of-susceptibility be exploited for improving Fusarium head blight resistance in wheat? *The Crop Journal*, *9*(1), 1–16. https://doi.org/10.1016/j.cj.2020.06.012

Goujon, T., Sibout, R., Eudes, A., MacKay, J., and Jouanin, L. (2003). Genes involved in the biosynthesis of lignin precursors in *Arabidopsis thaliana*. *Plant Physiology and Biochemistry*, *41*(8), 677–687. https://doi.org/10.1016/S0981-9428(03)00095-0

Gozzi, M., Blandino, M., Dall'Asta, C., Martinek, P., Bruni, R., and Righetti, L. (2023). Anthocyanin Content and Fusarium Mycotoxins in Pigmented Wheat (*Triticum aestivum* L. spp. *aestivum*): An Open Field Evaluation. *Plants*, *12*(4). https://doi.org/10.3390/plants12040693

Gullner, G., Komives, T., Király, L., and Schröder, P. (2018). Glutathione S-Transferase Enzymes in Plant-Pathogen Interactions. *Frontiers in Plant Science*, *9*. https://doi.org/10.3389/fpls.2018.01836

Gunnaiah, R., and Kushalappa, A. C. (2014). Metabolomics deciphers the host resistance mechanisms in wheat cultivar

Sumai-3, against trichothecene producing and non-producing isolates of *Fusarium graminearum*. *Plant Physiology and Biochemistry*, *83*, 40–50. https://doi.org/10.1016/j.plaphy.2014.07.002

Gunnaiah, R., Kushalappa, A. C., Duggavathi, R., Fox, S., and Somers, D. J. (2012). Integrated metabolo-proteomic approach to decipher the mechanisms by which wheat qtl (Fhb1) contributes to resistance against *Fusarium graminearum*. *PLoS ONE*, *7*(7). https://doi.org/10.1371/journal.pone.0040695

Hammer, Ø., and Harper, D. A. T. (2005). Basic Statistical Methods. In *Paleontological Data Analysis* (pp. 8–60). https://doi.org/10.1002/9780470750711.ch2

Hölscher, D., Buerkert, A., and Schneider, B. (2016). Phenylphenalenones Accumulate in Plant Tissues of Two Banana Cultivars in Response to Herbivory by the Banana Weevil and Banana Stem Weevil. In *Plants* (Vol. 5, Issue 3). https://doi.org/10.3390/plants5030034

Huang, Y., Li, L., Smith, K. P., and Muehlbauer, G. J. (2016). Differential transcriptomic responses to *Fusarium graminearum* infection in two barley quantitative trait loci associated with Fusarium head blight resistance. *BMC Genomics*, *17*(1), 1–16. https://doi.org/10.1186/s12864-016-2716-0

Huot, B., Yao, J., Montgomery, B. L., and He, S. Y. (2014). Growth-defense tradeoffs in plants: A balancing act to optimize fitness. *Molecular Plant*, *7*(8), 1267–1287. https://doi.org/10.1093/mp/ssu049

Kang, Z., and Buchenauer, H. (2000). Ultrastructural and immunocytochemical investigation of pathogen development and host responses in resistant and susceptible wheat spikes infected by *Fusarium culmorum*. *Physiological and Molecular Plant Pathology*, *57*(6), 255–268. https://doi.org/10.1006/pmpp.2000.0305

Kangasjärvi, S., Neukermans, J., Li, S., Aro, E.-M., and Noctor, G. (2012). Photosynthesis, photorespiration, and light signalling in defence responses. *Journal of Experimental Botany*, *63*(4), 1619–1636. https://doi.org/10.1093/jxb/err402

Karre, S., Kumar, A., Dhokane, D., and Kushalappa, A. C. (2017). Metabolo-transcriptome profiling of barley reveals induction of chitin elicitor receptor kinase gene (HvCERK1) conferring resistance against *Fusarium graminearum*. *Plant Molecular Biology*, *93*(3), 247–267. https://doi.org/10.1007/s11103-016-0559-3

Karre, S., Kumar, A., Yogendra, K., Kage, U., Kushalappa, A., and Charron, J. B. (2019). HvWRKY23 regulates flavonoid glycoside and hydroxycinnamic acid amide biosynthetic genes in barley to combat Fusarium head blight. *Plant Molecular Biology*, *100*(6), 591–605. https://doi.org/10.1007/s11103-019-00882-2

Kazan, K., and Gardiner, D. M. (2018). Transcriptomics of cereal–*Fusarium graminearum* interactions: what we have learned so far. *Molecular Plant Pathology*, *19*(3), 764–778. https://doi.org/10.1111/mpp.12561

Kheiri, A., Moosawi Jorf, S. A., and Malihipour, A. (2019). Infection process and wheat response to Fusarium head blight caused by *Fusarium graminearum*. *European Journal of Plant Pathology*, *153*(2), 489–502. https://doi.org/10.1007/s10658-018-1576-7

Kikot, G. E., Hours, R. A., and Alconada, T. M. (2009). Contribution of cell wall degrading enzymes to pathogenesis of *Fusarium graminearum*: A review. *Journal of Basic Microbiology*, *49*(3), 231–241. https://doi.org/10.1002/jobm.200800231

Kim, B., Broeck, L. Van Den, Karre, S., Choi, H., Guan-, S. A. C., Wang, F., Jo, Y., Kyong, W., and Balint-, P. (2021). Analysis of the transcriptomic , metabolomic , and gene regulatory responses to *Puccinia sorghi* in maize. *Molecular Plant Pathology December 2020*, 465–479. https://doi.org/10.1111/mpp.13040

Kim, D., Paggi, J. M., Park, C., Bennett, C., and Salzberg, S. L. (2019). Graph-based genome alignment and genotyping with HISAT2 and HISAT-genotype. *Nature Biotechnology*, *37*(8), 907–915. https://doi.org/10.1038/s41587-019-0201-4

Knievel, D. C., Abdel-Aal, E.-S. M., Rabalski, I., Nakamura, T., and Hucl, P. (2009). Grain color development and the inheritance of high anthocyanin blue aleurone and purple pericarp in spring wheat (*Triticum aestivum* L.). *Journal of Cereal Science*, *50*(1), 113–120. https://doi.org/10.1016/j.jcs.2009.03.007

Knight, N. L., and Sutherland, M. W. (2015). Culm discolouration as an indicator of *Fusarium pseudograminearum* biomass. *Australasian Plant Pathology*, *44*(3), 319–326. https://doi.org/10.1007/s13313-015-0351-x

Kobayashi, I., and Kobayashi, Y. (2008). *Microtubules and Pathogen Defence BT - Plant Microtubules: Development and Flexibility* (P. Nick (ed.); pp. 121–140). Springer Berlin Heidelberg. https://doi.org/10.1007/7089_2007_144

Kumar, J., Rai, K. M., Pirseyedi, S., Elias, E. M., Xu, S., Dill-Macky, R., and Kianian, S. F. (2020). Epigenetic regulation of gene expression improves Fusarium head blight resistance in durum wheat. *Scientific Reports*, *10*(1), 1–15. https://doi.org/10.1038/s41598-020-73521-2

Kumar, J., Rai, K. M., Pirseyedi, S., Elias, E. M., Xu, S., Macky, R. D., and Kianian, S. F. (2020). Epigenetic regulation of gene expression improves Fusarium head blight resistance in durum wheat. *Scientific Reports*, *0123456789*, 1–15. https://doi.org/10.1038/s41598-020-73521-2

Leslie, J. F., and Summerell, B. A. (2006). *The Fusarium Laboratory Manual* (Vol. 66). Blackwell Publishing.

Li, G., and Yen, Y. (2008). Jasmonate and Ethylene Signaling Pathway May Mediate Fusarium Head Blight Resistance in Wheat. *Crop Science*, *48*(5), 1888–1896. https://doi.org/10.2135/cropsci2008.02.0097

Li, J., Wang, C., Yang, L., Qiu, F., Li, Y., Zheng, Y., Liu, S., Song, L., and Liang, W. (2023). Enhancing tomato resistance by exploring early defense events against Fusarium wilt disease. *Phytopathology Research*, *5*(1). https://doi.org/10.1186/s42483-023-00176-y

Li, K., Yu, D., Yan, Z., Liu, N., Fan, Y., Wang, C., and Wu, A. (2022). Exploration of Mycotoxin Accumulation and Transcriptomes of Different Wheat Cultivars during *Fusarium graminearum* Infection. *Toxin*, *14*(482), 1–15.

Li, T., Zhang, H., Huang, Y., Su, Z., Deng, Y., Liu, H., Mai, C., Yu, G., Li, H., Yu, L., Zhu, T., Yang, L., Li, H., and Zhou, Y. (2019). Effects of the Fhb1 gene on Fusarium head blight resistance and agronomic traits of winter wheat. *The Crop Journal*, *7*(6), 799–808. https://doi.org/10.1016/j.cj.2019.03.005

Li, X. Lan, Lü, X., Wang, X. Hong, Peng, Q., Zhang, M. Sheng, And Ren, M. Jian. (2020). Biotic and abiotic stress-responsive genes are stimulated to resist drought stress in purple wheat. *Journal of Integrative Agriculture*, *19*(1), 33–50. https://doi.org/10.1016/S2095-3119(19)62659-6

Liao, Y., Smyth, G. K., and Shi, W. (2014). featureCounts: an efficient general purpose program for assigning sequence reads to genomic features. *Bioinformatics*, *30*(7), 923–930. https://doi.org/10.1093/bioinformatics/btt656

Ligterink, W., Kroj, T., Nieden, U. zur, Hirt, H., and Scheel, D. (1997). Receptor-Mediated Activation of a MAP Kinase in Pathogen Defense of Plants. *Science*, *276*(5321), 2054–2057. https://doi.org/10.1126/science.276.5321.2054

Liu, Q., Qiu, Y., and Beta, T. (2010). Comparison of antioxidant activities of different colored wheat grains and analysis of phenolic compounds. *Journal of Agricultural and Food Chemistry*, *58*(16), 9235–9241. https://doi.org/10.1021/jf101700s

Liu, S., Jiang, J., Ma, Z., Xiao, M., Yang, L., Tian, B., Yu, Y., Bi, C., Fang, A., and Yang, Y. (2022). The Role of Hydroxycinnamic Acid Amide Pathway in Plant Immunity. *Frontiers in Plant Science*, *13*. https://doi.org/10.3389/fpls.2022.922119

Love, M. I., Huber, W., and Anders, S. (2014). Moderated estimation of fold change and dispersion for RNA-seq data with DESeq2. *Genome Biology*, *15*(12), 550. https://doi.org/10.1186/s13059-014-0550-8

Luo, K., Guo, J., He, D., Li, G., and Ouellet, T. (2023). Deoxynivalenol accumulation and detoxification in cereals and its potential role in wheat–*Fusarium graminearum* interactions. *ABIOTECH*, *4*(2), 155–171. https://doi.org/10.1007/s42994-023-00096-7

Ma, D., Li, Y., Zhang, J., Wang, C., Qin, H., Ding, H., Xie, Y., and Guo, T. (2016). Accumulation of phenolic compounds and expression profiles of phenolic acid biosynthesis-related genes in developing grains of white, purple, and red wheat. *Frontiers in Plant Science*, *7*(APR2016), 1–11. https://doi.org/10.3389/fpls.2016.00528

Mackintosh, C. A., Lewis, J., Radmer, L. E., Shin, S., Heinen, S. J., Smith, L. A., Wyckoff, M. N., Dill-Macky, R., Evans, C. K., Kravchenko, S., Baldridge, G. D., Zeyen, R. J., and Muehlbauer, G. J. (2007). Overexpression of defense response genes in transgenic wheat enhances resistance to Fusarium head blight. *Plant Cell Reports*, *26*(4), 479–488. https://doi.org/10.1007/s00299-006-0265-8

Macoy, D. M., Kim, W.-Y., Lee, S. Y., and Kim, M. G. (2015). Biotic stress related functions of hydroxycinnamic acid

amide in plants. *Journal of Plant Biology*, *58*(3), 156–163. https://doi.org/10.1007/s12374-015-0104-y

Mahajan, M., and Yadav, S. K. (2014). Overexpression of a tea flavanone 3-hydroxylase gene confers tolerance to salt stress and *Alternaria solani* in transgenic tobacco. *Plant Molecular Biology*, *85*(6), 551–573. https://doi.org/10.1007/s11103-014-0203-z

Mandalà, G., Ceoloni, C., Busato, I., Favaron, F., and Tundo, S. (2021). Transgene pyramiding in wheat: Combination of deoxynivalenol detoxification with inhibition of cell wall degrading enzymes to contrast Fusarium Head Blight and Crown Rot. *Plant Science*, *313*, 111059. https://doi.org/10.1016/j.plantsci.2021.111059

Martin, C., Schöneberg, T., Vogelgsang, S., Bertossa, M., Mauch-mani, B., Mascher, F., Mauch-mani, B., Mascher, F., Martin, C., Schöneberg, T., Vogelgsang, S., Vincenti, J., and Bertossa, M. (2017). Factors of wheat grain resistance to Fusarium head blight. *Phytopathologia Mediterranea*. https://doi.org/10.14601/Phytopathol_Mediterr-20292

Martinek, P., Škorpík, M., Chrpová, J., Fučík, P., and Schweiger, J. (2013). Development of the new winter wheat variety Skorpion with blue grain. *Czech Journal of Genetics and Plant Breeding*, *49*(2), 90–94. https://doi.org/10.17221/7/2013-cjgpb

Martínez-Moreno, F., Ammar, K., and Solís, I. (2022). Global Changes in Cultivated Area and Breeding Activities of Durum Wheat from 1800 to Date: A Historical Review. In *Agronomy* (Vol. 12, Issue 5). https://doi.org/10.3390/agronomy12051135

McMullen, M., Bergstrom, G., De Wolf, E., Dill-Macky, R., Hershman, D., Shaner, G., and Van Sanford, D. (2012). A Unified Effort to Fight an Enemy of Wheat and Barley: Fusarium Head Blight. *Plant Disease*, *96*(12), 1712–1728. https://doi.org/10.1094/PDIS-03-12-0291-FE

Medina-Puche, L., Tan, H., Dogra, V., Wu, M., Rosas-Diaz, T., Wang, L., Ding, X., Zhang, D., Fu, X., Kim, C., and Lozano-Duran, R. (2020). A Defense Pathway Linking Plasma Membrane and Chloroplasts and Co-opted by Pathogens. *Cell*, *182*(5), 1109-1124.e25. https://doi.org/10.1016/j.cell.2020.07.020

Meng, X., and Zhang, S. (2013). MAPK Cascades in Plant Disease Resistance Signaling. *Annual Review of Phytopathology*, *51*(Volume 51, 2013), 245–266. https://doi.org/10.1146/annurev-phyto-082712-102314

Mesterházy, A. (1995). Types and components of resistance to Fusarium head blight of wheat. *Plant Breeding*, *114*(5), 377–386. https://doi.org/10.1111/j.1439-0523.1995.tb00816.x

Oliveros, J. C. (2007). *Venny. An interactive tool for comparing lists with Venn's diagrams.* https://bioinfogp.cnb.csic.es/tools/venny/index.html

Pan, Y., Liu, Z., Rocheleau, H., Fauteux, F., Wang, Y., McCartney, C., and Ouellet, T. (2018). Transcriptome dynamics associated with resistance and susceptibility against fusarium head blight in four wheat genotypes. *BMC Genomics*, *19*(1), 1–26. https://doi.org/10.1186/s12864-018-5012-3

Perochon, A., and Doohan, F. M. (2024). Trichothecenes and Fumonisins: Key Players in *Fusarium*–Cereal Ecosystem Interactions. In *Toxins* (Vol. 16, Issue 2). https://doi.org/10.3390/toxins16020090

Pilu, R., Cassani, E., Sirizzotti, A., Petroni, K., and Tonelli, C. (2011). Effect of flavonoid pigments on the accumulation of fumonisin B1 in the maize kernel. *Journal of Applied Genetics*, *52*(2), 145–152. https://doi.org/10.1007/s13353-010-0014-0

Porter, K., and Day, B. (2016). From filaments to function: The role of the plant actin cytoskeleton in pathogen perception, signaling and immunity. *Journal of Integrative Plant Biology*, *58*(4), 299–311. https://doi.org/10.1111/jipb.12445

Ramaroson, M.-L., Koutouan, C., Helesbeux, J.-J., Le Clerc, V., Hamama, L., Geoffriau, E., and Briard, M. (2022). Role of Phenylpropanoids and Flavonoids in Plant Resistance to Pests and Diseases. In *Molecules* (Vol. 27, Issue 23). https://doi.org/10.3390/molecules27238371

Rawat, N., Pumphrey, M. O., Liu, S., Zhang, X., Tiwari, V. K., Ando, K., Trick, H. N., Bockus, W. W., Akhunov, E., Anderson, J. A., and Gill, B. S. (2016). Wheat Fhb1 encodes a chimeric lectin with agglutinin domains and a pore-forming toxin-like domain conferring resistance to Fusarium head blight. *Nature Genetics*, *48*(12), 1576–1580. https://doi.org/10.1038/ng.3706

Rudd, J. J., Keon, J., and Hammond-Kosack, K. E. (2008). The Wheat Mitogen-Activated Protein Kinases TaMPK3 and TaMPK6 Are Differentially Regulated at Multiple Levels during Compatible Disease Interactions with *Mycosphaerella graminicola* . *Plant Physiology*, *147*(2), 802–815. https://doi.org/10.1104/pp.108.119511

Saigo, T., Wang, T., Watanabe, M., and Tohge, T. (2020). Diversity of anthocyanin and proanthocyanin biosynthesis in land plants. *Current Opinion in Plant Biology*, *55*, 93–99. https://doi.org/10.1016/j.pbi.2020.04.001

Schenck, C. A., and Maeda, H. A. (2018). Tyrosine biosynthesis, metabolism, and catabolism in plants. *Phytochemistry*, *149*, 82–102. https://doi.org/10.1016/j.phytochem.2018.02.003

Schiavi, D., Ronchetti, R., Di Lorenzo, V., Salustri, M., Petrucci, C., Vivani, R., Giovagnoli, S., Camaioni, E., and Balestra, G. M. (2022). Circular Hazelnut Protection by Lignocellulosic Waste Valorization for Nanopesticides Development. *Applied Sciences (Switzerland)*, *12*(5). https://doi.org/10.3390/app12052604

Schroeder, H. W., and Christensen, J. J. (1963). Factors affecting resistance of wheat to scab caused by *Gibberella zeae*. *Phytopathology*, *53*(7, 1), 831–838.

Schweiger, W., Steiner, B., Ametz, C., Siegwart, G., Wiesenberger, G., Berthiller, F., Lemmens, M., Jia, H., Adam, G., Muehlbauer, G. J., Kreil, D. P., and Buerstmayr, H. (2013). Transcriptomic characterization of two major *Fusarium* resistance quantitative trait loci (QTLs), Fhb1 and Qfhs.ifa-5A, identifies novel candidate genes. *Molecular Plant Pathology*, *14*(8), 772–785. https://doi.org/10.1111/mpp.12048

Shumayla, Sharma, S., Kumar, R., Mendu, V., Singh, K., and Upadhyay, S. K. (2016). Genomic Dissection and Expression Profiling Revealed Functional Divergence in *Triticum aestivum* Leucine Rich Repeat Receptor Like Kinases (TaLRRKs). *Frontiers in Plant Science*, *7*. https://doi.org/10.3389/fpls.2016.01374

Singh, P., Singh, A., and Choudhary, K. K. (2023). Revisiting the role of phenylpropanoids in plant defense against UV-B stress. *Plant Stress*, *7*, 100143. https://doi.org/10.1016/j.stress.2023.100143

Singleton, V. L., and Rossi, J. A. (1965). Colorimetry of Total Phenolics with Phosphomolybdic-Phosphotungstic Acid Reagents. *American Journal of Enology and Viticulture*, *16*(3), 144 LP – 158. http://www.ajevonline.org/content/16/3/144.abstract

Soltabayeva, A., Dauletova, N., Serik, S., Sandybek, M., Omondi, J. O., Kurmanbayeva, A., and Srivastava, S. (2022). Receptor-like Kinases (LRR-RLKs) in Response of Plants to Biotic and Abiotic Stresses. In *Plants* (Vol. 11, Issue 19). https://doi.org/10.3390/plants11192660

Sompong, R., Siebenhandl-Ehn, S., Linsberger-Martin, G., and Berghofer, E. (2011). Physicochemical and antioxidative properties of red and black rice varieties from Thailand, China and Sri Lanka. *Food Chemistry*, *124*(1), 132–140. https://doi.org/10.1016/j.foodchem.2010.05.115

Sparks, A. H., Esker, P. D., Bates, M., Dall'Acqua, W., Guo, Z., Silwal, S. D., Tolos, S., and Garrett, K. A. (2008). Ecology and Epidemiology in R : Disease Progress over Time Nonlinear regression in R. *The Plant Health Instructor*. https://doi.org/10.1094/PHI-A-2008-0129-02

Stuper-Szablewska, K., Kurasiak-Popowska, D., Nawracała, J., and Perkowski, J. (2016). Study of metabolite profiles in winter wheat cultivars induced by *Fusarium* infection. *Cereal Research Communications*, *44*(4), 572–584. https://doi.org/10.1556/0806.44.2016.034

Su, X., Zhao, J., Gao, W., Zu, Q., Chen, Q., Li, C., and Qu, Y. (2022). Gb_ANR-47 Enhances the Resistance of Gossypium barbadense to *Fusarium oxysporum* f. sp. *vasinfectum* (FOV) by Regulating the Content of Proanthocyanidins. In *Plants* (Vol. 11, Issue 15). https://doi.org/10.3390/plants11151902

Su, Z., Bernardo, A., Tian, B., Chen, H., Wang, S., Ma, H., Cai, S., Liu, D., Zhang, D., Li, T., Trick, H., St. Amand, P., Yu, J., Zhang, Z., and Bai, G. (2019). A deletion mutation in TaHRC confers Fhb1 resistance to Fusarium head blight in wheat. *Nature Genetics*, *51*(7), 1099–1105. https://doi.org/10.1038/s41588-019-0425-8

Thapa, G., Gunupuru, L. R., Hehir, J. G., Kahla, A., Mullins, E., Doohan, F. M., Clark, S., and Gardiner, D. M. (2018). *A Pathogen-Responsive Leucine Rich Receptor Like Kinase Contributes to Fusarium Resistance in Cereals*. *9*(June), 1–15. https://doi.org/10.3389/fpls.2018.00867

Timoneda, A., Feng, T., Sheehan, H., Walker-Hale, N., Pucker, B., Lopez-Nieves, S., Guo, R., and Brockington, S. (2019). The evolution of betalain biosynthesis in *Caryophyllales*. *New Phytologist*, *224*(1), 71–85.

https://doi.org/10.1111/nph.15980

Tomassini, A., Sella, L., Raiola, A., D'Ovidio, R., and Favaron, F. (2009). Characterization and expression of *Fusarium graminearum* endo-polygalacturonases in vitro and during wheat infection. *Plant Pathology*, *58*(3), 556–564. https://doi.org/10.1111/j.1365-3059.2008.02019.x

Treutter, D. (2006). Significance of flavonoids in plant resistance: A review. *Environmental Chemistry Letters*, *4*(3), 147–157. https://doi.org/10.1007/s10311-006-0068-8

Tripathi, D., Raikhy, G., and Kumar, D. (2019). Chemical elicitors of systemic acquired resistance—Salicylic acid and its functional analogs. *Current Plant Biology*, *17*, 48–59. https://doi.org/10.1016/j.cpb.2019.03.002

Ullah, C., Unsicker, S. B., Fellenberg, C., Constabel, C. P., Schmidt, A., Gershenzon, J., and Hammerbacher, A. (2017). Flavan-3-ols Are an Effective Chemical Defense against Rust Infection . *Plant Physiology*, *175*(4), 1560–1578. https://doi.org/10.1104/pp.17.00842

Venturini, G., Toffolatti, S. L., Assante, G., Babazadeh, L., Campia, P., Fasoli, E., Salomoni, D., and Vercesi, A. (2015). The influence of flavonoids in maize pericarp on fusarium ear rot symptoms and fumonisin accumulation under field conditions. *Plant Pathology*, *64*(3), 671–679. https://doi.org/10.1111/ppa.12304

Venturini, Giovanni, Babazadeh, L., Casati, P., Pilu, R., Salomoni, D., and Toffolatti, S. L. (2016). Assessing pigmented pericarp of maize kernels as possible source of resistance to fusarium ear rot, *Fusarium* spp. infection and fumonisin accumulation. *International Journal of Food Microbiology*, *227*, 56–62. https://doi.org/10.1016/j.ijfoodmicro.2016.03.022

Wang, L., Li, Q., Liu, Z., Surendra, A., Pan, Y., Li, Y., Zaharia, L. I., Ouellet, T., and Fobert, P. R. (2018). Integrated transcriptome and hormone profiling highlight the role of multiple phytohormone pathways in wheat resistance against fusarium head blight. *PLOS ONE*, *13*(11), e0207036. https://doi.org/10.1371/journal.pone.0207036

Wang, X., Bi, W., Gao, J., Yu, X., Wang, H., And Liu, D. (2018). Systemic acquired resistance, NPR1, and pathogenesis-related genes in wheat and barley. *Journal of Integrative Agriculture*, *17*(11), 2468–2477. https://doi.org/10.1016/S2095-3119(17)61852-5

Weihmann, F., Eisermann, I., Becher, R., Krijger, J.-J., Hübner, K., Deising, H. B., and Wirsel, S. G. R. (2016). Correspondence between symptom development of *Colletotrichum graminicola* and fungal biomass, quantified by a newly developed qPCR assay, depends on the maize variety. *BMC Microbiology*, *16*(1), 94. https://doi.org/10.1186/s12866-016-0709-4

Whitney, K., Gracia-Gomez, G., Anderson, J. A., and Simsek, S. (2022). Time Course Metabolite Profiling of Fusarium Head Blight-Infected Hard Red Spring Wheat Using Ultra-High-Performance Liquid Chromatography Coupled with Quadrupole Time of Flight/MS. *Journal of Agricultural and Food Chemistry*, *70*(13), 4152–4163. https://doi.org/10.1021/acs.jafc.1c08374

Wu, F., Zhou, Y., Shen, Y., Sun, Z., Li, L., and Li, T. (2022). Linking Multi-Omics to Wheat Resistance Types to Fusarium Head Blight to Reveal the Underlying Mechanisms. *International Journal of Molecular Sciences*, *23*(4). https://doi.org/10.3390/ijms23042280

Xiao, J., Jin, X., Jia, X., Wang, H., Cao, A., Zhao, W., Pei, H., Xue, Z., He, L., Chen, Q., and Wang, X. (2013). Transcriptome-based discovery of pathways and genes related to resistance against Fusarium head blight in wheat landrace Wangshuibai. *BMC Genomics*, *14*(1), 197. https://doi.org/10.1186/1471-2164-14-197

Xing, F., Zhang, L., Ge, W., Fan, H., Tian, C., and Meng, F. (2024). Comparative transcriptome analysis reveals the importance of phenylpropanoid biosynthesis for the induced resistance of 84K poplar to anthracnose. *BMC Genomics*, *25*(1), 306. https://doi.org/10.1186/s12864-024-10209-1

Xu, Q., Tang, C., Wang, X., Sun, S., Zhao, J., Kang, Z., and Wang, X. (2019). An effector protein of the wheat stripe rust fungus targets chloroplasts and suppresses chloroplast function. *Nature Communications*, *10*(1), 5571. https://doi.org/10.1038/s41467-019-13487-6

Xue, R., Wu, J., Zhu, Z., Wang, L., Wang, X., Wang, S., and Blair, M. W. (2015). Differentially Expressed Genes in Resistant and Susceptible Common Bean (Phaseolus vulgaris L.) Genotypes in Response to *Fusarium oxysporum* f. sp. *phaseoli*. *PLOS ONE*, *10*(6), e0127698. https://doi.org/10.1371/journal.pone.0127698

Yang, F., Shen, H., Huang, T., Yao, Q., Hu, J., Tang, J., Zhang, R., Tong, H., Wu, Q., Zhang, Y., and Su, Q. (2023). Flavonoid production in tomato mediates both direct and indirect plant defences against whiteflies in tritrophic interactions. *Pest Management Science*, *79*(11), 4644–4654. https://doi.org/10.1002/ps.7667

Yang, Z., Ma, H., Hong, H., Yao, W., Xie, W., Xiao, J., Li, X., and Wang, S. (2015). Transcriptome-based analysis of mitogen-activated protein kinase cascades in the rice response to *Xanthomonas oryzae* infection. *Rice*, *8*(1), 4. https://doi.org/10.1186/s12284-014-0038-x

Yimer, H. Z., Nahar, K., Kyndt, T., Haeck, A., Van Meulebroek, L., Vanhaecke, L., Demeestere, K., Höfte, M., and Gheysen, G. (2018). Gibberellin antagonizes jasmonate-induced defense against *Meloidogyne graminicola* in rice. *New Phytologist*, *218*(2), 646–660. https://doi.org/10.1111/nph.15046

Zhang, W., Francis, T., Gao, P., Boyle, K., Jiang, F., Eudes, F., Cuthbert, R., Sharpe, A., and Fobert, P. R. (2018). Genetic characterization of type II Fusarium head blight resistance derived from transgressive segregation in a cross between Eastern and Western Canadian spring wheat. *Molecular Breeding*, *38*(1), 13. https://doi.org/10.1007/s11032-017-0761-2

Zhou, K., Hao, J., Griffey, C., Chung, H., O'Keefe, S. F., Chen, J., and Hogan, S. (2007). Antioxidant properties of Fusarium head blight-resistant and -susceptible soft red winter wheat grains grown in Virginia. *Journal of Agricultural and Food Chemistry*, *55*(9), 3729–3736. https://doi.org/10.1021/jf070147a

Zwart, R. S., Muylle, H., Van Bockstaele, E., and Roldán-Ruiz, I. (2008). Evaluation of genetic diversity of Fusarium head blight resistance in European winter wheat. *Theoretical and Applied Genetics*, *117*(5), 813–828. https://doi.org/10.1007/s00122-008-0822-3

6. General Conclusion

This work was an attempt to elucidate the role of anthocyanins in plant pathogen interaction, using a multidisciplinary approach, involving microbiology, biochemistry and plant pathology, and using the pathosystem *Fusarium* – wheat as a model. However, considering pigmented genotypes' physiology and phenology, anthocyanins could not play a direct role in wheat resistance against FHB. Indeed, as visible in Fig. S4.3.1, pigmentation starts to be observable after 10-14 days post anthesis, when infection is already underway. For this reason this work was not focused on the direct effect that flavonoids in the grains could have on grains infection, but rather it aimed to investigate if and how genotypes with peculiar flavonoids biosynthesis alteration could react to a fungal spike infection, considering preformed and inducible compounds.

Thus, most of this work was dedicated to the "plant side" (investigating its metabolism and physiological reaction) instead of the "pathogen side". Nevertheless, to date very little is known about the antifungal and/or anti-mycotoxins effect of anthocyanins and anthocyanidins. The chapter 2 tried to be a starting point to fill this knowledge gap. For the first time, the influence of anthocyanins on *F. avenaceum* growth and enniatins production was evaluated. Some important findings were highlighted. The analysis revealed that these flavonoids affect fungal growth depending on the glycosylation (where glycosides promote the fungal growth and the aglycon had no effect) end they may affect enniatins production by different mechanisms. While delphinidin and delphinidin 3-*O*-glucoside strongly affect regulation of key genes for enniatins biosynthesis, cyanidin 3-*O*-glucoside act in a different way, most likely involving post-translational regulation. Moreover, the pH-dependent mechanism of action of anthocyanins was supposed. This research raises new interesting research questions on a category of mycotoxins strongly under investigated. Even though the toxicity of enniatins is controversial, effect of plant metabolites on the synthesis of this important product on *F. avenaceum* may provide evidences about what may happen in the plant. Anthocyanins concentration in pigmented wheat grains may widely vary depending on the genotype. As explained in the introduction, other studies investigated anthocyanin concentration in mature grains, while a comprehensive time course quantification of anthocyanins from seed set to maturity is lacking. Considering our results (Supplementary file 4.4), at 2nd day post infection (which means 2 day post anthesis) cyanidin 3-*O*-glucoside in Purple durum was present at low concentration (10.29-12.53 ng/g, which means 0.01-0.012 ppm) in both infected and healthy spikes, while in chapter 2, anthocyanins concentrations lower than 1 ppm were found to be ineffective for both growth inhibition/promotion and mycotoxins reduction on *F. avenaceum*. This finding strengthens the hypothesis of an indirect role of flavonoids in wheat resistance. In this study, culture conditions (including fungal strain and compound concentrations) were selected considering the best experimental plan. Definitely, the use of only one species and one strain is an important limitation of this study. For future studies, *in planta* evaluations are strongly encouraged, considering different strains and involving other *Fusarium* species, producing other mycotoxins.

This knowledge about anti-mycotoxin effect could be considered in the framework of bio-based antimicrobials. Indeed, other phenolic compounds were proposed as antimicrobial against FHB, even if this application is subjected to certain limitations. Compared with other phenylpropanoids (ferulic acid, gallic acid, tannins…), anthocyanins extraction and purification procedures are more expensive and less standardized. Moreover, these compounds are very instable in non-acidic environment. However, anthocyanins extraction and stabilization are of great interest, especially in food industry, pushing research to innovative, sustainable and more performing strategies. Potentially, several food wastes could be

used as a source of anthocyanins, such as pigmented wheat bran (in the case of wheat) or fruit peels, providing interesting bio-molecules for crop protection in a framework of circular economy and waste valorization.

Results of Chapter 3 and 4 may appear contrasting, since in Chapter 3 an increased TAC due to the infection was recorded in mature spikes of DBC-480, but not in Purple durum, while in Chapter 4 an upregulation of *Ppm1* and an increase of some anthocyanins were underlined in Purple durum at 21 DPI. Comparing the results of these two studies, different time points and different analytical methods should be taken into account. Indeed, in Chapter 3 a rapid and easy-to-use (but less specific) method were employed to quantify anthocyanins in mature spikes, while in Chapter 4 HPLC-MS/MS was used for the specific quantification of some metabolites in an advanced stage of the infection in which, however, the spikes are still viable. Thus, putative explanations of our results may be the following: DBC-480 may accumulate flavonoids detected by TAC pH differential method, but not evaluated in the HPLC-MS/MS analysis; Purple durum, susceptible pigmented genotype, exhibited a more active flavonoid and anthocyanins biosynthesis due to the infection at late infection stage (21 DPI), but most likely the biosynthesis stopped after physiological maturity and the accumulated anthocyanins may be degraded, especially in infected spikes, causing a decrease in the resulting damaged kernels. Moreover, the consumption of anthocyanins by *Fusarium* has already been hypothesized in Chapter 2. However, further investigations, such as metabolomics analysis, may elucidate this point and confirm these speculations.

The study on the morphological and physiological traits associated to FHB in Purple Durum has been one of the first attempts to examine modification of this kind of traits due to FHB infection in a purple durum wheat genotype. Our results corroborate the importance of phenylpropanoids in FHB-wheat interaction and point the attention on anthocyanin metabolism, suggesting to further consider these compounds under-investigated for durum wheat resistance. Purple durum wheat accessions are an unexplored reservoir of diversity, potentially useful for durum wheat breeding, attempting the double breeding objective of biofortified staple food and FHB resistance. The contrasting research studies already present in literature regarding FHB resistance in pigmented wheat varieties encourage a more comprehensive screening for resistance in pigmented durum wheat, and the present research represents a starting point to achieve this important goal. Furthermore, our study highlighted that Purple durum is a susceptible genotype to *F. graminearum* infection, exhibiting high severity levels comparable to the susceptible genotype Svevo. Differential gene expression patterns were observed in the phenylpropanoids and flavonoid pathway genes across genotypes and infection stages. The genotype DBC-480 showed upregulation of several key genes involved in the phenylpropanoids pathway, particularly *PAL*, *C4H* and *DFR*, suggesting the involvement of these genes in the defense response. Notably, there was a substantial increase in metabolite content in infected Purple durum and Svevo compared to mock control plants, with *Fusarium* infection affecting the accumulation of some metabolites, particularly phenolic acids, in both soluble and cell wall bound fractions. The infection led to notable changes in metabolite composition, indicating a dynamic interaction between the pathogen and the host plant and suggesting a genotype-dependent response to infection. The soluble fraction exhibited increased antioxidant activity in response to infection, indicating a potential defense mechanism against oxidative stress induced by *Fusarium* infection. A positive correlation between phenolic acid content and antioxidant activity in the soluble fraction was observed, suggesting the contribution of phenylpropanoids to the antioxidant defense response in durum wheat spikes. This study highlights a dynamic interplay between genotype, gene expression, metabolite accumulation, and antioxidant activity in durum wheat spikes in response to *F. graminearum* infection. These findings contribute to the understanding of host-pathogen interactions for future breeding programs focused on improving FHB resistance in durum wheat varieties.

For plant resistance, type II resistance was predominantly considered, by the use of tip inoculation. Also in this case pigmented genotypes' physiology and phenology play a crucial role. Initial penetration (and type I resistance) could not be influenced by flavonoids found in external layers of the grains, because the initial penetration occur at flowering, when grains are not present yet. However, tip inoculation is the best choice for a simulated environment, while it could not be enough to explain what may happen in a real field environment. Moreover, although pigmentation is unlikely to be involved in type I resistance, the thesis did not provide data to exclude *a priori* this hypothesis. This is why some open field trials using different pigmented genotypes and natural inoculum has already been planned.

Last but not least, different pigmented bread wheat genotypes were evaluated for their resistance/susceptibility to FHB. Our results suggested that pigmentation and resistance are not directly related. However, an interesting reaction to the infection was demonstrated by the genotypes Skorpion, which need further investigation.

Additionally, a strong resistance to FHB was demonstrated by Vanilnoir and investigated through transcriptomics. Our results corroborate the importance of HCAAs in FHB resistance and raise the attention on growth – related hormones, such as cytokinins and gibberellins, which may have an unexpected role in regulating FHB resistance. Furthermore, including two pigmented genotypes in the trial underlined as purple genotypes may express a more active flavonoid biosynthetic pathway in response to *F. graminearum* infection than their equivalents (in terms of resistance) not-pigmented. While Sumai3 and Rosso favored the production of flavan-3-ols to the detriment of anthocyanins, infected Vanilnoir seems to stimulate the simultaneous production of anthocyanins and flavones, both potentially involved in its resistance mechanism. Hypothesis about resistance mechanism of Vanilnoir was discussed, suggesting the involvement of specific LRR-RLK participating to the specific cross-talk between plant and pathogen. However, further investigation including QTL mapping and metabolomics analysis may confirm the proposed theory, potentially enhancing knowledge about FHB resistance and providing new tools to improve wheat breading for resistance.